

Foraging behavior, neuroanatomy and  
neuroplasticity in cursorial and stationary hunting  
spiders

Inauguraldissertation

zur

Erlangung des akademischen Grades  
Dr. rer. nat. (Doctor rerum naturalium)

der

Mathematisch-Naturwissenschaftlichen Fakultät

der

Universität Greifswald

Vorgelegt von

Philip O. M. Steinhoff

Greifswald, 23.02.2023

Dekan: Prof. Dr. Gerald Kerth

1. Gutachterin: Prof. Dr. Gabriele Uhl

2. Gutachter\*in: Prof. Dr. Eileen Hebets; 3. Gutachterin: Prof. Dr. Ximena Nelson

Tag der Promotion: 11.09.2023

*Dedicated to all the individual spiders featured here:  
I know you had no choice, but thank you anyways.*

## List of publications included in this dissertation

---

### Published in peer-reviewed journals

**Steinhoff, P. O. M.**, Warfen, B., Voigt, S., Uhl, G., & Dammhahn, M. (2020). Individual differences in risk-taking affect foraging across different landscapes of fear. *Oikos*, 129 (12), 1891-1902.

**Steinhoff, P. O. M.**, Uhl, G., Harzsch, S., & Sombke, A. (2020). Visual pathways in the brain of the jumping spider *Marpissa muscosa*. *Journal of Comparative Neurology*, 528 (11), 1883-1902.

### Manuscript submitted for peer-review

**Steinhoff, P. O. M.**, Harzsch, S. & Uhl, G. (in review). Comparative neuroanatomy of the central nervous system in stationary and cursorial hunting spiders.

### Manuscript in preparation for publication

**Steinhoff, P. O. M.**, Mouginot, P. & Uhl, G. (in prep.). Neuroplasticity in response to sensory enrichment and deprivation in a cursorial and a stationary hunting spider.

---

**Table of Contents**

<b>Abstract</b>	<b>6</b>
<b>1. Summary</b>	<b>7</b>
<b>Background</b>	<b>7</b>
1.1.1 Foraging in landscapes of fear	7
1.1.2 Vision in (jumping) spiders	8
1.1.3 Neuroanatomy in spiders	9
1.1.4 Neuroplasticity	10
<b>Aims of the thesis</b>	<b>11</b>
<b>Results and discussion</b>	<b>13</b>
<b>Conclusions and perspectives</b>	<b>16</b>
<b>References</b>	<b>17</b>
<b>2. Publications</b>	<b>27</b>
<b>Chapter 1: Individual differences in risk-taking affect foraging across different landscapes of fear</b>	<b>27</b>
<b>Chapter 2: Visual pathways in the brain of the jumping spider <i>Marpissa muscosa</i></b>	<b>41</b>
<b>Chapter 3: Comparative neuroanatomy of the central nervous system in stationary and cursorial hunting spiders</b>	<b>63</b>
<b>Chapter 4: Neuroplasticity in response to sensory enrichment and deprivation in a cursorial and a stationary hunting spider</b>	<b>120</b>
<b>3. Eigenständigkeitserklärung</b>	<b>160</b>
<b>3.1 Anteile der Autoren an den zugrundeliegenden Publikationen</b>	<b>161</b>
<b>4. Curriculum Vitae</b>	<b>163</b>
<b>5. Acknowledgements</b>	<b>171</b>

## Abstract

The central nervous system (CNS) is the integration center for the coordination and regulation of all body activities of animals and the source of behavioral patterns, behavioral plasticity and personality. Understanding the anatomy and the potential for plastic changes of the CNS not only widens the knowledge on the biology of the respective species, but also enables a more fundamental understanding of behavioral and ecological patterns. The CNS of species with different sensory ecologies for example, will show specific differences in the wiring of their CNS, related to their lifestyle. Spiders are a group of mesopredators that include stationary hunting species that build webs for prey capture, and cursorial hunting species that do not build capture webs. These distinct lifestyles are associated with major differences in their sensory equipment, such as size of the different eyes.

In this thesis, I aimed to answer if a cursorial mesopredator would change its behavior due to different levels of perceived predation risk, and if this behavior would be influenced by individual differences (**chapter 1**); how the visual pathways in the brain of the cursorial hunting jumping spider *Marpissa muscosa* differs from that of the nocturnal cursorial hunting wandering spider *Cupiennius salei* (**chapter 2**); to what degree the visual systems of stationary and cursorial hunting spiders differ and whether CNS areas that process vibratory information show similar differences (**chapter 3**); and finally if the CNS in stationary and cursorial hunting spiders shows different patterns of neuroplasticity in response to sensory input and deprivation during development (**chapter 4**).

In **chapter 1**, I found that jumping spiders adjust their foraging behavior to the perceived level of risk. By favoring a dark over a light substrate, they displayed a background-matching strategy. Short pulses of acute risk, produced by simulated bird overflights, had only small effects on the behavior. Instead, a large degree of variation in behavior was due to among-individual differences in foraging intensity. These covaried with consistent among-individual differences in activity, forming a behavioral syndrome. Our findings highlight the importance of consistent among-individual differences in the behavior of animals that forage under risk. Future studies should address the mechanisms underlying these stable differences, as well as potential fitness consequences that may influence food-web dynamics.

In **chapter 2**, I found that the visual pathways in the brain of the jumping spider *M. muscosa* differ from that in the wandering spider *C. salei*. While the pathway of the principal eyes, which are responsible for object discrimination, is the same in both species, considerable differences occur in the pathway of the secondary eyes, which detect movement. Notably, *M. muscosa* possesses an additional second-order visual neuropil, which is integrating information from two different secondary eyes, and may enable faster movement decisions. I also showed that the tiny posterior median eye is connected to a first-order visual neuropil which in turn connects to the arcuate body (a higher-order neuropil), and is thus not vestigial as suggested before. Subsequent studies should focus on exploring the function of the posterior median eyes in different jumping spider species,

as they show considerable inter-specific size differences that may be correlated with a differing connectivity in the brain.

In **chapter 3**, I described all neuropils and major tracts in the CNS of two stationary (*Argiope bruennichi* and *Parasteatoda tepidariorum*) and two cursorial hunting spiders (*Pardosa amentata* and *M. muscosa*). I found major differences in the visual systems of the secondary eyes between cursorial and stationary hunting spiders, but also within the groups. *A. bruennichi* has specialized retinula cells in two of the secondary eyes, which connect to different higher-order neuropils. *P. tepidariorum* has only a single visual neuropil connected to all secondary eyes, and lacks recognizable mushroom bodies. The neuroanatomy of CNS areas that process mechanosensory information on the other hand, is remarkably similar between cursorial and stationary hunting species. This suggests that the same major circuits are used for the processing of mechanosensory information in both cursorial and stationary hunting spiders. Future studies on functional aspects of sensory processing in spiders can build on the findings of our study.

In **chapter 4**, I found that developmental neuroplasticity in response to sensory input differs between a cursorial (*M. muscosa*) and a stationary hunting spider (*P. tepidariorum*). While deprivation of sensory input leads to a volume increase in several visual and mechanosensory neuropils *M. muscosa*, neither sensory deprivation nor sensory enrichment had an effect on the volume of neuropils in *P. tepidariorum*. However, exposure to mechanical cues during development had an effect on the allometric scaling slope of the leg neuropils in both *M. muscosa* and *P. tepidariorum*. Future studies should focus on the genetic and cellular basis of developmental neuroplasticity in response to sensory input in order to explain the observed patterns.

## 1. Summary

### Background

#### 1.1.1 Foraging in landscapes of fear

When foraging, animals must weigh the potential rewards of finding food against the risk of encountering a predator (Lima, 1998; Lima & Dill, 1990). Foraging behavior is thus shaped to a large degree by the perceived predation risk, which is based on the animal's experience and imperfect understanding of its environment (Bouskila & Blumstein, 1992; Gaynor et al., 2019). The prey's perception of predation risk varies spatially and is referred to as landscape of fear (Gaynor et al., 2019; Laundré et al., 2001, 2010). The responses of animals to perceived risk are diverse and vary by species as well as by intensity, predictability, and distribution of predation risk, and the expected gain from foraging (Houston & McNamara, 1999; LaManna & Martin, 2016; Lima & Dill, 1990). Moreover, animals can adapt their behavior in response to changing risks through learning (Aguilar-Argüello et al., 2019; DePasquale et al., 2014; Palmer et al., 2017).

Studies over the last two decades have shown that population-wide optimal solutions to the tradeoff between foraging gain and predation avoidance are limited by individual differences in

behavior (Abbey-Lee & Dingemanse, 2019; Boone et al., 2022; Chang, Ng, et al., 2017; Harcourt et al., 2021; Réale et al., 2007; Sih, Bell, & Johnson, 2004). These differences, commonly referred to as animal personality or behavioral type, are exhibited in a variety of behavioral traits. When these traits are correlated, they are referred to as behavioral syndromes (Bell et al., 2009; Dingemanse et al., 2012; Sih, Bell, & Johnson, 2004; Sih, Bell, Johnson, et al., 2004). Behavioral types, such as shyness and boldness, can be measured through standardized tests and linked to behavior expressed in more ecologically relevant scenarios. For instance, aspects of foraging behavior differ consistently between individuals of different behavioral types (Chang, Teo, et al., 2017; Michalko et al., 2017, 2021; Toscano, 2017), and boldness can predict risk-taking during foraging and microhabitat use (Dammhahn & Almeling, 2012; Mella et al., 2015; Schirmer et al., 2020). Thus, an individual's tradeoff between foraging gain and risk should be related to its behavioral type.

### **1.1.2 Vision in (jumping) spiders**

The responses of animals to predation risk and the behaviors they exhibit strongly depend on what they are able to perceive, and the sensory ecology of a species thus defines the extent to which it can react (Gaynor et al., 2019; Jordan & Ryan, 2015). In many animals, vision is an important mediator of responses to predators. It allows animals to quickly detect and respond to potential threats, allowing them to make decisions about when to forage and when to hide or escape (Allen et al., 2010; Devereux et al., 2006; Fernández-Juricic et al., 2008; Jaitly et al., 2022; Martin, 2014; Smolka et al., 2011).

Some animal groups have evolved visual systems with multiple eyes and task differentiation between those eyes. Well-known examples are the compound eyes and ocelli of insects, the rhopalia in box jellyfishes and the principal and secondary eyes of spiders (Garm et al., 2007; Land, 1985b; N. Morehouse, 2020; O'Connor et al., 2009; Paulus, 1979). Most spiders possess one pair of principal eyes (or anterior median eyes, AME) and three pairs of secondary eyes (the posterior median, PME, anterior lateral, ALE, and posterior lateral, PLE eyes) (Land, 1985b; N. Morehouse, 2020). While the principal eyes are color-sensitive, have a movable retina and are used for object recognition, the secondary eyes are usually colorblind, have a non-movable retina and are specialized to detect motion (Blest, 1985; Land, 1985b; N. Morehouse, 2020; Schmid, 1998; Yamashita & Tateda, 1978).

Since sensing and sending of mechanosensory information (vibratory cues) is the major mode of communication and prey capture in spiders (Uetz & Roberts, 2002), it is perhaps unsurprising that most of the information available on the anatomy and function of spider eyes comes from research on the highly visual jumping spiders (Salticidae) (N. Morehouse, 2020; reviewed in N. I. Morehouse et al., 2017). Jumping spiders are well known for their elaborate courtship displays that include multimodal signaling with vibratory and visual elements being transmitted simultaneously (Elias et al., 2005, 2012; Elias, Hebets, & Hoy, 2006; Elias, Hebets, Hoy, et al., 2006). Visual signals often include flashing of colorful body parts such as legs and opisthosoma (Echeverri et al., 2017; Richman & Jackson, 1992; Taylor & McGraw, 2013). The large, forward-facing principal eyes are equipped with color-sensitive photoreceptors that enable spiders to see the displays of their potential mating partners and the movable retina tracks movements during courtship as well as while foraging (Jakob et al., 2018; Spano et al., 2012; Yamashita, 1985; Zurek & Nelson, 2012a, 2012b). Color-vision is superb in some species, with e.g. trichromatic vision in the genus



*Habronattus* (Zurek et al., 2015) and sex-specific ultra-violet and green signals in other species (Lim et al., 2007). The field of view of the secondary eyes allows the jumping spiders to almost see 360 degrees (Harland et al., 2012; Land, 1985a). One pair of secondary eyes however, the PME, are much reduced in size in most species (there are some exceptions in spartaeine and lyssomanine jumping spiders), and have been considered vestigial due to their tiny size (Homann, 1928; Land, 1972, 1985a).

### **1.1.3 Neuroanatomy in spiders**

Despite the rather large body of literature on eye anatomy and function in jumping spiders, relatively little is known about the structures in the brain that process the visual information, and about CNS anatomy in spiders in general. The CNS is the source of an animal's personality and behavioral plasticity, and it coordinates and regulates all functions of the body (Mery & Burns, 2010; Simmons & Young, 1999). Behavior ultimately reflects the architecture, connectivity and functions of the underlying CNS areas (Simmons & Young, 1999). Knowledge about the CNS can thus help to gain a better understanding of observed behavioral patterns and behavioral plasticity of animal species.

In spiders, the anatomy of the entire CNS has been studied in detail only in one species, the wandering spider *Cupiennius salei* (Keyserling, 1877) (Babu et al., 1985; Babu & Barth, 1984, 1989; Becherer & Schmid, 1999; Strausfeld et al., 1993; Strausfeld & Barth, 1993). Earlier studies by Saint-Rémy (1887) and Hanström (1921) focused exclusively on the brains and specifically the visual system of some spider species (see below). The CNS of spiders is a highly fused mass of nervous tissue that consists of segmental neuromeres: The protocerebrum, deutocerebrum and tritocerebrum (together termed the brain), four neuromeres associated with the walking legs and the opisthosomal neuromere (together termed ventral nerve cord) (Lehmann et al., 2016; Steinhoff et al., 2017). A distinct border between the different neuromeres is usually not discernable in the adult. In *C. salei*, the protocerebrum includes several distinct neuropils: the visual neuropils, the mushroom bodies and the arcuate body (Babu & Barth, 1984). Every eye serves its own first- and second-order visual neuropils, and while the second-order visual neuropils of the principal eyes are connected to the arcuate body, the second-order visual neuropils of the secondary eyes are connected to the mushroom bodies (Babu & Barth, 1984; Strausfeld et al., 1993; Strausfeld & Barth, 1993). Furthermore, the first-order visual neuropils of the secondary eyes are also connected to the arcuate body (Babu & Barth, 1984). The mushroom bodies (a large, paired neuropil in the center of the protocerebrum) and the arcuate body (an unpaired crescent-shaped neuropil at the posterior rim of the protocerebrum) can thus be considered higher-order visual neuropils (Babu & Barth, 1984; Strausfeld et al., 1993; Strausfeld & Barth, 1993). Further ventral in the brain and bordering the esophagus are the cheliceral neuropils, followed ventrally by the pedipalpal neuropils (Babu & Barth, 1984). The ventral nerve cord houses the leg neuropils, the opisthosomal neuropil and a central part that consists of a dense system of tracts (Babu et al., 1985; Babu & Barth, 1984, 1989). The tracts consist of ascending and descending neurites, connect the leg neuropils with each other and also extend upward into the brain (Babu & Barth, 1984). Mechanosensory, hygrosensory and thermosensory information gathered by the appendages is mostly processed by the respective appendage

neuropils and to a smaller degree within the central part of the ventral nerve cord (Anton & Tichy, 1994; Babu & Barth, 1984, 1989; Gronenberg, 1989).

While the general arrangement of neuropils is the same in *C. salei* and other spider species (Hanström, 1919; Steinhoff et al., 2017) studies on the visual systems of different spider species have revealed substantial differences with regard to the number and connectivity of visual neuropils (Hanström, 1921; Long, 2021; Steinhoff et al., 2020: part of this thesis, see details below; Weltzien & Barth, 1991). This is not surprising, giving the enormous range of different lifestyles in spiders, with species that hunt stationary using a capture web and others that hunt cursorial without the use of a capture web (Foelix, 2011). The large variety of sensory ecologies in spiders is probably best captured by the differences in size and arrangement of the different eyes (N. Morehouse, 2020). Differences in sensory structures that serve other senses (such as sensilla for mechanoreception) however, are less conspicuous and it remains unclear to date whether CNS neuropils that process this type of sensory information differ between species with different sensory ecologies.

#### **1.1.4 Neuroplasticity**

Already in the early days of modern neuroscience, it has been hypothesized that experience can modify the structure of the brain (Ramón y Cajal, 1928). Research in the last decades has started to explore in detail what kind of changes occur and why (Kolb & Gibb, 2014; reviewed in e.g. Kolb & Whishaw, 1998; Sweatt, 2016). Neuroplasticity can be studied at various levels, including large-scale volumetric changes, or changes in neural circuits and networks, changes in the structure and function of individual neurons and synaptic connections between neurons (Kolb & Gibb, 2014). However, what eventually elicits changes in behavior are synaptic reorganizations (including gain and loss of synapses within specific networks) (Caroni et al., 2012; Kolb & Gibb, 2014). Since neuroplasticity is closely linked to the functional role of the specific CNS areas affected by it, outcomes must be interpreted with regard to the function of CNS areas (Heisenberg, 1998; Menzel & Giurfa, 2001). While changes of neuronal circuits allow qualitative changes, such as additional behavioral traits or abilities, changes of the volume of sensory processing areas of the CNS lead to quantitative enhancements, e.g. a higher sensitivity or finer resolution of the sensory system (Chittka & Niven, 2009).

When comparing differences in CNS area volumes within and between species, scaling relationships have to be taken into account (Barton & Montgomery, 2019; Farnworth & Montgomery, 2022; Harvey & Pagel, 1988; Logan et al., 2018). The CNS, similar to many other morphological traits, scales allometrically with body size, resulting in the observation that smaller animals have relatively larger brains (Barton & Montgomery, 2019; Eberhard & Wcislo, 2011; Voje et al., 2014). This general trend in scaling is present not just between, but also within species (e.g. different body sizes due to different developmental stages) (Eberhard & Wcislo, 2011; Quesada et al., 2011). The allometric scaling relationship is typically given as a power function on the logarithmic scale:  $\log(y) = \beta \log(x) + \log(\alpha)$ , where  $y$  and  $x$  stand for the two structures of interest (e.g. brain size and body size),  $\beta$  describes the slope of the equation and  $\alpha$  is the  $y$ -axis intercept (Montgomery et al., 2016; Ott & Rogers, 2010; Stöckl et al., 2016; Tsuboi, 2021; Warton et al., 2006). When comparing volumes of CNS areas between species or between groups of individuals

within a species, true size differences would thus be visible by changes in  $\log(\alpha)$ , called elevation or grade-shift (Farnworth & Montgomery, 2022; Montgomery et al., 2016; Ott & Rogers, 2010; Stöckl et al., 2016; Warton et al., 2012). Shifts on the x axis on the other hand (termed major axis shift) indicate differences in size of the allometric control (typically a measure of total brain size) (Wainwright & Montgomery, 2022). Differences between groups in the slope  $\beta$  are more difficult to explain and are typically interpreted as a sign of differences in genetic and developmental constraints (Riska & Atchley, 1985; Tsuboi, 2021).

Although most studies on neuroplasticity were conducted in vertebrate taxa (Burns et al., 2009; Gogolla et al., 2007; Guay & Iwaniuk, 2008; Kihlslinger & Nevitt, 2006; e.g. Kolb & Elliott, 1987; Moser, 1999; Rosenzweig & Bennett, 1996), a diverse range of arthropods has been studied as well (cf. Fabian & Sachse, 2023 for a review on experience-dependent neuroplasticity in insects). Neuroplasticity due to learning, experience and formation of memory leads to volume changes of specific brain neuropils and increased density of microglomeruli in some species of social hymenopterans, the fruit fly *Drosophila* and locusts (reviewed with regard to olfactory plasticity in Anton & Rössler, 2020; Fahrbach et al., 1995, 2003; Falibene et al., 2015; Giurfa & Sandoz, 2012; Heisenberg et al., 1995; Meinertzhagen, 2001; Ott & Rogers, 2010; reviewed for desert ants in Rössler, 2019; Yilmaz et al., 2016). Neuroplasticity during development was found in honey bees and *Drosophila* (M. Barth et al., 1997; Groh et al., 2004, 2006; Heisenberg et al., 1995; Maleszka et al., 2009; Murphey, 1986; Withers et al., 1993).

In spiders, neuroplasticity was found in response to a marked change in lifestyle in the species *Deinopis spinosa*, where males stop foraging after the final molt, associated with a marked reduction in eye size and volume of associated brain neuropils (Stafstrom et al., 2017). It has furthermore been shown in a jumping spider that early environmental conditions affect the behavior (Liedtke & Schneider, 2017) and also the brain (Steinhoff et al., 2018). When spiders were reared under three different environmental conditions (physically enriched, socially enriched and deprived), individuals from the deprived group had smaller arcuate bodies, mushroom bodies and also total brain volumes (Steinhoff et al., 2018). Furthermore, spiders reared under all three experimental conditions had larger total brains, larger arcuate bodies and larger mushroom bodies than conspecifics that were caught in the wild, suggesting a nutritional tradeoff (Steinhoff et al., 2018). It remained unclear however, which aspect of the environment affected the CNS and led to the plastic changes. Further experimental studies on the effect of sensory input on CNS areas during development are thus needed.

### **Aims of the thesis**

This thesis is organized in four different chapters that represent the different studies conducted. Figure 1 gives a graphical abstract of this structure and highlights some of the major results. In **chapter 1** I asked whether, and if so how, the jumping spider *Marpissa muscosa* would adjust its foraging behavior to different levels of predation risk. I explored specifically, what effect visually perceived aspects such as color of the substrate and bird-dummy overflights would have, and to what extent among-individual differences could explain differences in foraging behavior. I predicted that jumping spiders would vary their foraging intensity according to both a constant

risk (light substrate color) and a variable risk (simulated bird overflights). I also expected foraging behavior to vary consistently among individuals and to covary with among-individual activity differences.

In **chapter 2** I aimed to elucidate the neuroanatomy of the visual system in the jumping spider *M. muscosa* and compare it to the visual system of the wandering spider *Cupiennius salei*, the only spider species in which the neuroanatomy has been described in detail before. Specific objectives of this study were the description of the number, sizes and shapes of the visual neuropils as well as the clarification of their interconnections and the tracing of their connections to the higher-order brain neuropils that combine the information from the different eyes. Based on the literature and the differences in sensory ecology between the species, I expected the visual systems to show substantial differences.

In **chapter 3** I compared the neuroanatomy of the entire CNS in four different spider species with different lifestyles (two cursorial hunting spiders, *Pardosa amentata* and *M. muscosa*, and two stationary hunting spiders, *Argiope bruennichi* and *Parasteatoda tepidariorum*) to assess if the differences in sensory ecology between the species correlate with differences in the neuroanatomy of the CNS. I specifically aimed to test whether the greater importance of visual information in foraging of the cursorial hunters would manifest in their brain, and vice-versa, whether the ventral nerve cord (which primarily receives mechanosensory information) would show any specializations in the stationary hunting spiders, which rely on vibratory cues for prey capture.

I further asked in **chapter 4**, which CNS areas would display neuroplastic changes in reaction to sensory deprivation (experimental group CON) or sensory enrichment by additional exposure to vibratory cues (experimental group VIB), visual cues (experimental group VIS) and a combination of both (experimental group VISVIB) during the postembryonic development of a cursorial (*M. muscosa*) and a stationary (*P. tepidariorum*) hunting spider. Our aim was to gain a better understanding of the functions of the different CNS areas in the two hunting type representatives and also study the neuroplasticity in response to sensory input. I predicted, that sensory information would affect the volume of the primary sensory processing neuropils, i.e. in the VIS group the first-order visual neuropils, in the VIB group the leg neuropils and in the VISVIB group both visual- and leg neuropils. I also expected the volumes of neuropils in the stationary hunting spider to be stronger influenced by the vibratory input and in the cursorial hunting spider by the visual input.

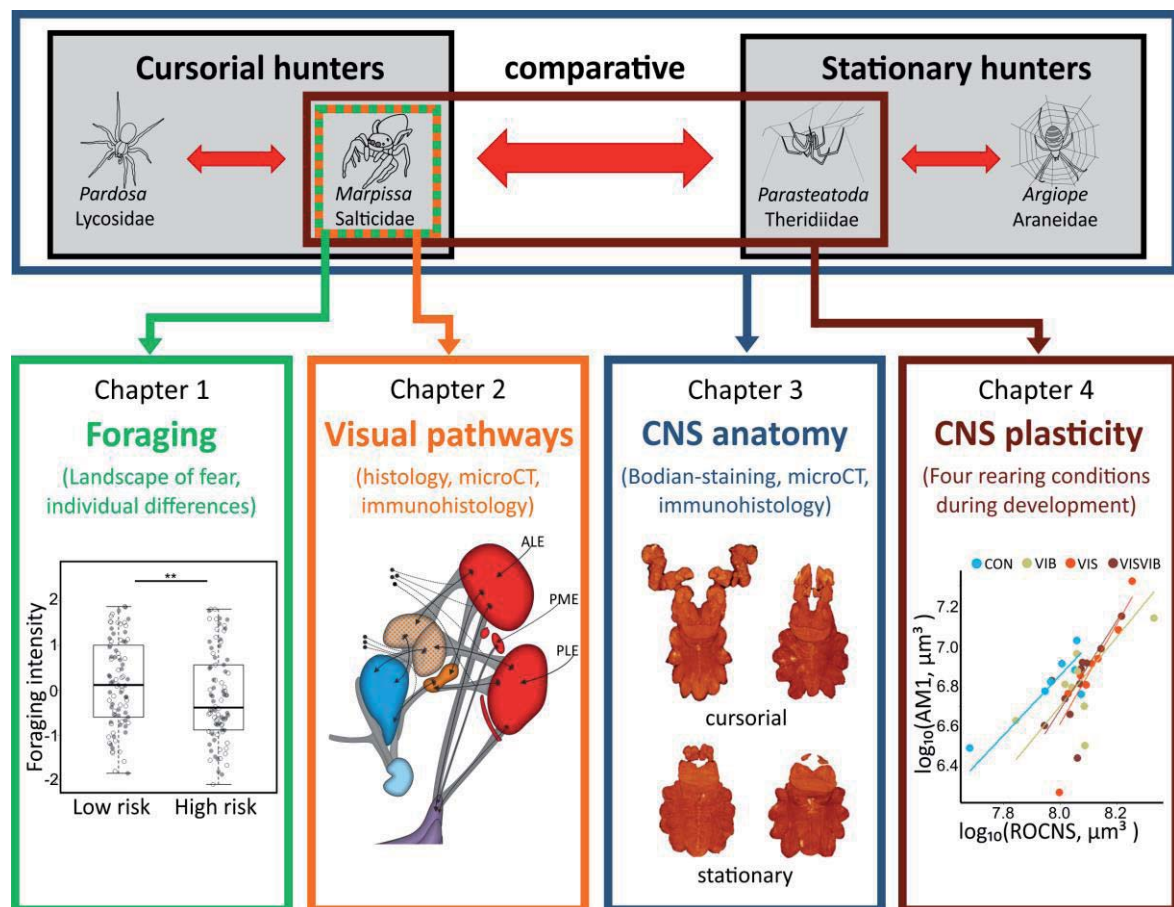


**Figure 1** Graphical abstract of the thesis structure and major results. (Chapter 1) The boxplots show that jumping spiders varied their foraging intensity depending on the level of risk. The individual data points illustrate the large variation; there were consistent individual differences in the perceived level of risk among individuals. (Chapter 2) The schematic drawing shows the secondary eye visual pathway in the jumping spider *M. muscosa*. The anterior lateral (ALE) and posterior lateral eyes (PLE) connect to two different second-order visual neuropils, of which one likely has an integrating function. The posterior median eye (PME) is connected to a visual neuropil, which connects to the arcuate body, and is thus not vestigial. (Chapter 3) MicroCT reconstructions of the CNS of two cursorial and two stationary hunting spiders. From left to right and top to bottom: The jumping spider *M. muscosa*, the wolf spider *P. amentata*, the orb-weaving spider *A. bruennichi*, and the cobweb spider *P. tepidariorum*. The differences in size and shape of the anteriorly located visual neuropils are very prominent. (Chapter 4) The graph shows an allometric scaling relationship between the first-order visual neuropil of the principal eyes (AM1) and the allometric control (rest of the CNS: ROCNS) in the jumping spider *M. muscosa*. There is a significant grade-shift in spiders from the deprived treatment (CON) compared to all other treatments (VIB, vibratory input; VIS, visual input; VISVIB, vibratory and visual input). This shows that an absence of sensory input during the development leads to a plastic response of sensory processing neuropils. Schematic spider drawings by Monica M. Sheffer.

## Results and discussion

I found in **chapter 1**, that jumping spiders adjust their foraging to different levels of risk. Especially when spiders were exposed to a white substrate, they reduced movement and foraging activity,

suggesting that camouflage is an important aspect of their foraging behavior. The body coloration of *M. muscosa* rather closely matches the color of the dead wood that they typically live on, and crypsis has been found to be a very common anti-predator strategy in spiders (Pekár, 2014; L. Robledo-Ospina & Rao, 2022). Consequently, the way in which jumping spiders foraged to avoid risk shows that they behave according to a background-matching strategy (L. E. Robledo-Ospina et al., 2017). Rather surprisingly however, short pulses of acute risk (simulated bird overflights) had only small effects on the foraging behavior. One possible explanation for this is that, because of the regular characteristics of the stimulus, response decrement occurred, which has been shown to be prevalent in jumping spiders (Humphrey et al., 2018; Melrose et al., 2019; Nelson et al., 2019). Instead of the risks themselves, a large part of the variation in foraging behavior was explained by among-individual differences in foraging behavior. Individuals of the jumping spider *M. muscosa* solve the tradeoff between resource gain and safety depending on their behavioral syndrome: highly active individuals also show higher foraging intensity and thus favor resource gain over safety, while less active individuals vice-versa favor safety over resource gain. The consistent among-individual differences in perceived predation risk could be due to differences in pace of life (Dammhahn et al., 2018; Pace-of-life syndrome: Réale et al., 2010). As spiders were collected in the wild, their life histories were unknown. However, since they were collected in the same general area, variation in pace of life can be expected to be small. Another likely explanation are differences in states, which can be certain characteristics of individuals that affect the tradeoff between costs and benefits of the behavior (Dammhahn et al., 2022; Houston & McNamara, 1999).

In **chapter 2** I found that the visual systems of the jumping spider *M. muscosa* and the wandering spider *C. salei* show remarkable differences. Although the available literature suggested that there are such differences (Duelli, 1980; Hanström, 1921; Hill, 1975), our study comprehensively investigated all parts of the visual system and found that while the visual pathway of the principal eye is the same in both species, major differences occur in the pathway of the secondary eyes. While in *C. salei* every eye serves its own first- and second-order visual neuropils, in *M. muscosa* the first-order visual neuropils of the ALE and the PLE are connected to two second-order visual neuropils, of which one is not glomerular. The latter suggests that information is already integrated at the level of the second-order visual neuropils in jumping spiders, which could potentially allow for faster movement decisions. The tiny PME is only connected to a single visual neuropil in *M. muscosa*, which further connects directly to the AB. The PME are thus not vestigial as suggested before. The finding that all first-order visual neuropils additionally connect to the arcuate body suggests that spiders may be able to perform some form of object recognition and differentiation with the secondary eyes as well. This has been suggested based on behavioral experiments before and recently, experimental evidence has shown that the secondary eyes are indeed able to differentiate biological motion from nonbiological motion (Agrò et al., 2021). Furthermore, gaze direction in jumping spiders has recently been found to be directed by both, principal and secondary eyes (Bruce et al., 2021), suggesting that these decisions are mediated by the arcuate body which I have shown to combine information from all eyes.

I found in **Chapter 3** that spiders with different sensory ecology differ considerably in terms of their central nervous system architecture. There are major differences in the secondary eye visual

system of cursorial and stationary hunting spiders, with the stationary hunters having fewer visual neuropils and different connectivity. While the visual system of the cursorial hunter *P. amentata* resembles that of the wandering spider *C. salei* with two successive visual neuropils serving each eye, the arrangement is very different in the two stationary hunting spiders. The orb-weaving spider *A. bruennichi* possesses no second order visual neuropils, which implies that the information sent to the higher-order neuropils is less processed and that the quality of motion vision may be reduced. However, the PLE and the PME each have two different first-order visual neuropils, of which one connects to the mushroom bodies and the other to the arcuate body. This is a unique case in spiders and suggests that *A. bruennichi* has specialized photoreceptor cells in the same eye, which either send information to the mushroom bodies or to the arcuate body (another, rather unlikely possibility is that a single photoreceptor cell connects to two different neuropils). Future studies should explore whether the different types of photoreceptor cells are spaced evenly over the retina, or whether they sample different fields of view. In the cobweb spider *P. tepidariorum*, all secondary eyes send their information into a single visual neuropil that is connected directly to the arcuate body. Since I did not detect a mushroom body in *P. tepidariorum*, it is likely that the ability of motion vision is much reduced or even absent in this species. In contrast to the visual system, the CNS areas that process mechanosensory information are remarkably similar between cursorial and stationary hunting spiders. While there were very few structural differences, the proportional volume of the leg neuropils and the opisthosomal neuropil was larger in stationary than in cursorial hunting spiders. The opisthosoma includes the spinnerets and various types of silk glands that are heavily involved in web building (Foelix, 2011; Kooor, 1987), which could explain the volumetric differences. I conclude that the importance of visual information is much reduced in stationary compared to cursorial hunting spiders, while the processing of mechanosensory information requires the same major circuits in both stationary and cursorial hunting spiders.

**Chapter 4** reveals that sensory input and deprivation during the development affects the CNS of a cursorial hunting spider stronger than that of a stationary hunting spider. Contrary to the expectations, volumes of primary sensory processing neuropils were not enlarged in the respective sensory enriched treatments (VIB, VIS and VISVIB) in both species tested (*M. muscosa* and *P. tepidariorum*). However, one first-order visual neuropil and two primarily mechanosensory processing neuropils showed a significant volume increase in the deprived treatment group (CON) in *M. muscosa*. These volume differences are also apparent as significant grade-shifts in allometric scaling analyses, indicating a potential effect of experience-expectant plasticity on the treatment group CON in *M. muscosa*. I furthermore found that the allometric scaling slope  $\beta$  of several mechanosensory neuropils (leg neuropils in both species, cheliceral and opisthosomal neuropils in *M. muscosa*) differs between the vibratory-enriched treatment group VIB and all other groups. This finding suggests that increased mechanosensory input during development affects the development of neuropils processing this information. While I generally found a stronger degree of neuroplasticity in the cursorial hunter *M. muscosa*, many neuropils in the stationary hunting *P. tepidariorum* were not significantly correlated with the allometric control measure (rest of CNS), suggesting that neuropils in this species are less constraint by total CNS size.

## Conclusions and perspectives

In this thesis, I compile four studies in which I explored aspects of foraging behavior, neuroanatomy and neuroplasticity in cursorial and stationary hunting spiders (Figure 1). Spiders comprise a large group of mesopredators that differ greatly in their sensory ecology. As such, spiders affect several trophic levels, as they are both predators and prey. A better understanding of the ecology and biology of spiders with different lifestyles will help to gain a more comprehensive picture of food-web dynamics and the role of spiders in their respective ecosystems in general. Since the CNS produces behavior, one important step towards the above mentioned goal is studying the anatomy and plasticity of their nervous systems. In the following, I will highlight the most important conclusions of our findings and outline future research avenues.

I found that a jumping spider adjusted its foraging behavior to different levels of risk in experimental landscapes of fear, just as predicted by theoretical models (Lima, 1998; Lima & Dill, 1990; McNamara & Houston, 1987). A large proportion of the variation that I found in risk-taking during foraging was due to among-individual differences in behavior and covaried with activity, demonstrating that activity is a personality trait in jumping spiders. The mechanisms that underlie constant differences in perceived predation risk are likely linked to different states (Dammhahn et al., 2022) and future research should try to explore which states are relevant and what the fitness consequences of risk-taking during foraging are.

In exploring the visual pathways in the brain of the jumping spider *M. muscosa* compared to the rather well known wandering spider *C. salei*, I found several differences that are likely linked to the highly visual lifestyle of the jumping spider. While the pathway of the principal eyes, which are used for object discrimination (N. Morehouse, 2020), is the same in both species, the jumping spider possesses an additional visual neuropil in the pathway of the secondary eyes, that likely combines information and may serve faster movement detection. I also find that the tiny posterior median eye (PME) of *M. muscosa* is not vestigial but serves its own visual neuropil that is directly connected to the arcuate body. Interestingly, a small number of other jumping spider species possess a large PME (Harland et al., 2012), and comparative neuroanatomical and neurophysiological research in the future should thus try to address what function the PME serves in different jumping spider species.

By executing the first comprehensive comparative study on the CNS anatomy of both cursorial and stationary hunting spiders, I have shown that the differences in lifestyle between the species are primarily mirrored by differences in the pathways of the brain that process visual information. These differences are diverse and future research should focus on elucidating whether spiders without recognizable mushroom bodies are capable of visual movement detection. It will furthermore be interesting to see, what functional roles the specialized photoreceptors of *A. bruennichi* play in its vision. Our map of the spider CNS and the connections between different neuropils will serve future studies on the functions of different sensory processing pathways, such as olfaction, which remain almost unexplored to date.



My analysis of the plastic responses of CNS neuropils in both a stationary and a cursorial hunter show, that the degree of plasticity varies between the two species. While the CNS of jumping spiders reacts to a deprivation of sensory input with a volume increase (grade-shift) in several neuropils, this is not the case in the investigated stationary hunting cobweb spider. In both species however, the development of the leg neuropils that receive mechanosensory information is affected by an increase in mechanical cues during development (shift in allometric slope  $\beta$ ). These findings are in line with our earlier study (chapter 3) on the nervous systems of cursorial and stationary hunting spiders, which implied that vibratory information is processed with the same CNS structures. It is however surprising, that instead of an expected grade-shift (i.e. increase in neuropil volume), leg neuropils reacted with a developmental shift in allometric slope to increased sensory input. Future studies should aim at disentangling nervous system plasticity in spiders by studying the effect of early environmental sensory input on genetic and cellular mechanisms.

## References

- Abbey-Lee, R. N., & Dingemanse, N. J. (2019). Adaptive individual variation in phenological responses to perceived predation levels. *Nature Communications*, *10*(1), 1601. <https://doi.org/10.1038/s41467-019-09138-5>
- Agrò, M. D., Rößler, D. C., Kim, K., & Shamble, P. S. (2021). Perception of biological motion by jumping spiders. *PLOS Biology*, *19*(7), e3001172. <https://doi.org/10.1371/journal.pbio.3001172>
- Aguilar-Argüello, S., Gerhard, D., & Nelson, X. J. (2019). Risk assessment and the use of novel shortcuts in spatial detouring tasks in jumping spiders. *Behavioral Ecology*, *30*(5), 1488–1498. <https://doi.org/10.1093/beheco/arz105>
- Allen, J. J., Mähnger, L. M., Buresch, K. C., Fetchko, T., Gardner, M., & Hanlon, R. T. (2010). Night vision by cuttlefish enables changeable camouflage. *Journal of Experimental Biology*, *213*(23), 3953–3960. <https://doi.org/10.1242/jeb.044750>
- Anton, S., & Rössler, W. (2020). Plasticity and modulation of olfactory circuits in insects. *Cell and Tissue Research*. <https://doi.org/10.1007/s00441-020-03329-z>
- Anton, S., & Tichy, H. (1994). Hygro- and thermoreceptors in tip-pore sensilla of the tarsal organ of the spider *Cupiennius salei*: Innervation and central projection. *Cell and Tissue Research*, *278*, 399–407.
- Babu, K. S., & Barth, F. G. (1984). Neuroanatomy of the central nervous system of the wandering spider, *Cupiennius salei* (Arachnida, Araneida). *Zoomorphology*, *104*(6), 344–359. <https://doi.org/10.1007/BF00312185>
- Babu, K. S., & Barth, F. G. (1989). Central nervous projections of mechanoreceptors in the spider *Cupiennius salei* Keys. *Cell and Tissue Research*, *258*(1). <https://doi.org/10.1007/BF00223146>
- Babu, K. S., Barth, F. G., & Strausfeld, N. J. (1985). Intersegmental sensory tracts and contralateral motor neurons in the leg ganglia of the spider *Cupiennius salei* Keys. *Cell and Tissue Research*, *241*(1), 53–57. <https://doi.org/10.1007/BF00214625>
- Barth, M., Hirsch, H. V., Meinertzhagen, I. A., & Heisenberg, M. (1997). Experience-dependent developmental plasticity in the optic lobe of *Drosophila melanogaster*. *The Journal of Neuroscience*, *17*(4), 1493–1504.

- Barton, R. A., & Montgomery, S. H. (2019). Proportional versus relative size as metrics in human brain evolution. *Proceedings of the National Academy of Sciences*, *116*(1), 3–4. <https://doi.org/10.1073/pnas.1817200116>
- Becherer, C., & Schmid, A. (1999). *Distribution of g-aminobutyric acid-, proctolin-, Periplaneta hypertrehalosaemic hormone- and FMRFamide-like immunoreactivity in the visual ganglia of the spider Cupiennius salei* Keys. 9.
- Bell, A. M., Hankison, S. J., & Laskowski, K. L. (2009). The repeatability of behaviour: A meta-analysis. *Animal Behaviour*, *77*(4), 771–783. <https://doi.org/10.1016/j.anbehav.2008.12.022>
- Blest, A. D. (1985). The Fine Structure of Spider Photoreceptors in Relation to Function. In F. G. Barth (Ed.), *Neurobiology of Arachnids* (pp. 79–102). Springer.
- Boone, S. R., Brehm, A. M., & Mortelliti, A. (2022). Seed predation and dispersal by small mammals in a landscape of fear: Effects of personality, predation risk and land-use change. *Oikos*, *2022*(2). <https://doi.org/10.1111/oik.08232>
- Bouskila, A., & Blumstein, D. T. (1992). Rules of thumb for predation hazard assessment: Predictions from a dynamic model. *The American Naturalist*, *139*(1), 161–176.
- Bruce, M., Daye, D., Long, S. M., Winsor, A. M., Menda, G., Hoy, R. R., & Jakob, E. M. (2021). Attention and distraction in the modular visual system of a jumping spider. *The Journal of Experimental Biology*, jeb.231035. <https://doi.org/10.1242/jeb.231035>
- Burns, J. G., Saravanan, A., & Rodd, F. H. (2009). Rearing environment affects the brain size of guppies: Lab-reared guppies have smaller brains than wild-caught guppies. *Ethology*, *115*(2), 122–133. <https://doi.org/10.1111/j.1439-0310.2008.01585.x>
- Caroni, P., Donato, F., & Muller, D. (2012). Structural plasticity upon learning: Regulation and functions. *Nature Reviews Neuroscience*, *13*(7), 478–490. <https://doi.org/10.1038/nrn3258>
- Chang, C., Ng, P. J., & Li, D. (2017). Aggressive jumping spiders make quicker decisions for preferred prey but not at the cost of accuracy. *Behavioral Ecology*, 479–484. <https://doi.org/10.1093/beheco/arw174>
- Chang, C., Teo, H. Y., Norma-Rashid, Y., & Li, D. (2017). Predator personality and prey behavioural predictability jointly determine foraging performance. *Scientific Reports*, *7*(1), 40734. <https://doi.org/10.1038/srep40734>
- Chittka, L., & Niven, J. (2009). Are Bigger Brains Better? *Current Biology*, *19*(21), R995–R1008. <https://doi.org/10.1016/j.cub.2009.08.023>
- Dammhahn, M., & Almeling, L. (2012). Is risk taking during foraging a personality trait? A field test for cross-context consistency in boldness. *Animal Behaviour*, *84*(5), 1131–1139. <https://doi.org/10.1016/j.anbehav.2012.08.014>
- Dammhahn, M., Dingemans, N. J., Niemelä, P. T., & Réale, D. (2018). Pace-of-life syndromes: A framework for the adaptive integration of behaviour, physiology and life history. *Behavioral Ecology and Sociobiology*, *72*(3), 62, s00265-018-2473-y. <https://doi.org/10.1007/s00265-018-2473-y>
- Dammhahn, M., Lange, P., & Eccard, J. A. (2022). The landscape of fear has individual layers: An experimental test of among-individual differences in perceived predation risk during foraging. *Oikos*, *2022*(6), e09124. <https://doi.org/10.1111/oik.09124>

- DePasquale, C., Wagner, T., Archard, G. A., Ferguson, B., & Braithwaite, V. A. (2014). Learning rate and temperament in a high predation risk environment. *Oecologia*, *176*(3), 661–667. <https://doi.org/10.1007/s00442-014-3099-z>
- Devereux, C. L., Whittingham, M. J., Fernández-Juricic, E., Vickery, J. A., & Krebs, J. R. (2006). Predator detection and avoidance by starlings under differing scenarios of predation risk. *Behavioral Ecology*, *17*(2), 303–309. <https://doi.org/10.1093/beheco/arj032>
- Dingemanse, N. J., Dochtermann, N. A., & Nakagawa, S. (2012). Defining behavioural syndromes and the role of ‘syndrome deviation’ in understanding their evolution. *Behavioral Ecology and Sociobiology*, *66*(11), 1543–1548. <https://doi.org/10.1007/s00265-012-1416-2>
- Duelli, P. (1980). The neuronal organization of the posterior lateral eyes of jumping spiders (Salticidae). *Zoologische Jahrbücher: Abteilung Für Anatomie Und Ontogenie Der Tiere*, *103*(1), 17–40.
- Eberhard, W. G., & Wcislo, W. T. (2011). Grade Changes in Brain–Body Allometry. In *Advances in Insect Physiology* (Vol. 40, pp. 155–214). Elsevier. <https://doi.org/10.1016/B978-0-12-387668-3.00004-0>
- Echeverri, S. A., Morehouse, N. I., & Zurek, D. B. (2017). Control of signaling alignment during the dynamic courtship display of a jumping spider. *Behavioral Ecology*, *28*(6), 1445–1453. <https://doi.org/10.1093/beheco/arx107>
- Elias, D. O., Hebets, E. A., & Hoy, R. R. (2006). Female preference for complex/novel signals in a spider. *Behavioral Ecology*, *17*(5), 765–771. <https://doi.org/10.1093/beheco/arl005>
- Elias, D. O., Hebets, E. A., Hoy, R. R., Maddison, W. P., & Mason, A. C. (2006). Regional seismic song differences in Sky Island populations of the jumping spider *Habronattus pugillis* Griswold (Araneae, Salticidae). *Journal of Arachnology*, *34*(3), 545–556. <https://doi.org/10.1636/S05-77.1>
- Elias, D. O., Hebets, E. A., Hoy, R. R., & Mason, A. C. (2005). Seismic signals are crucial for male mating success in a visual specialist jumping spider (Araneae: Salticidae). *Animal Behaviour*, *69*(4), 931–938. <https://doi.org/10.1016/j.anbehav.2004.06.024>
- Elias, D. O., Maddison, W. P., Peckmezian, C., Girard, M. B., & Mason, A. C. (2012). Orchestrating the score: Complex multimodal courtship in the *Habronattus coecatus* group of *Habronattus* jumping spiders (Araneae: Salticidae). *Biological Journal of the Linnean Society*, *105*(3), 522–547. <https://doi.org/10.1111/j.1095-8312.2011.01817.x>
- Fabian, B., & Sachse, S. (2023). Experience-dependent plasticity in the olfactory system of *Drosophila melanogaster* and other insects. *Frontiers in Cellular Neuroscience*, *17*, 1130091. <https://doi.org/10.3389/fncel.2023.1130091>
- Fahrbach, S. E., Farris, S. M., Sullivan, J. P., & Robinson, G. E. (2003). Limits on volume changes in the mushroom bodies of the honey bee brain. *Journal of Neurobiology*, *57*(2), 141–151. <https://doi.org/10.1002/neu.10256>
- Fahrbach, S. E., Strande, J. L., & Robinson, G. E. (1995). Neurogenesis is absent in the brains of adult honey bees and does not explain behavioral neuroplasticity. *Neuroscience Letters*, *197*(2), 145–148. [https://doi.org/10.1016/0304-3940\(95\)11913-H](https://doi.org/10.1016/0304-3940(95)11913-H)
- Falibene, A., Roces, F., & Rössler, W. (2015). Long-term avoidance memory formation is associated with a transient increase in mushroom body synaptic complexes in leaf-cutting ants. *Frontiers in Behavioral Neuroscience*, *9*(April), 1–13. <https://doi.org/10.3389/fnbeh.2015.00084>

- Farnworth, M. S., & Montgomery, S. H. (2022). Complexity of biological scaling suggests an absence of systematic trade-offs between sensory modalities in *Drosophila*. *Nature Communications*, *13*(1), 2944. <https://doi.org/10.1038/s41467-022-30579-y>
- Fernández-Juricic, E., Gall, M. D., Dolan, T., Tisdale, V., & Martin, G. R. (2008). The visual fields of two ground-foraging birds, House Finches and House Sparrows, allow for simultaneous foraging and anti-predator vigilance. *Ibis*, *150*(4), 779–787. <https://doi.org/10.1111/j.1474-919X.2008.00860.x>
- Foelix, R. (2011). *Biology of Spiders*. Oxford University Press, USA.
- Garm, A., O'Connor, M., Parkefelt, L., & Nilsson, D.-E. (2007). Visually guided obstacle avoidance in the box jellyfish *Tripedalia cystophora* and *Chiropsella bronzie*. *Journal of Experimental Biology*, *210*(20), 3616–3623. <https://doi.org/10.1242/jeb.004044>
- Gaynor, K. M., Brown, J. S., Middleton, A. D., Power, M. E., & Brashares, J. S. (2019). Landscapes of fear: Spatial patterns of risk perception and response. *Trends in Ecology & Evolution*, *34*(4), 355–368. <https://doi.org/10.1016/j.tree.2019.01.004>
- Giurfa, M., & Sandoz, J.-C. (2012). Invertebrate learning and memory: Fifty years of olfactory conditioning of the proboscis extension response in honeybees. *Learning & Memory*, *19*(2), 54–66. <https://doi.org/10.1101/lm.024711.111>
- Gogolla, N., Galimberti, I., & Caroni, P. (2007). Structural plasticity of axon terminals in the adult. *Current Opinion in Neurobiology*, *17*(5), 516–524. <https://doi.org/10.1016/j.conb.2007.09.002>
- Groh, C., Ahrens, D., & Rössler, W. (2006). Environment- and age-dependent plasticity of synaptic complexes in the mushroom bodies of honeybee queens. *Brain, Behavior and Evolution*, *68*(1), 1–14. <https://doi.org/10.1159/000092309>
- Groh, C., Tautz, J., & Rössler, W. (2004). Synaptic organization in the adult honey bee brain is influenced by brood-temperature control during pupal development. *Proceedings of the National Academy of Sciences of the United States of America*, *101*(12), 4268–4273. <https://doi.org/10.1073/pnas.0400773101>
- Gronenberg, W. (1989). Anatomical and physiological observations on the organization of mechanoreceptors and local interneurons in the central nervous system of the wandering spider *Cupiennius salei*. *Cell and Tissue Research*, *258*(1). <https://doi.org/10.1007/BF00223155>
- Guay, P.-J., & Iwaniuk, A. N. (2008). Captive breeding reduces brain volume in waterfowl (Anseriformes). *The Condor*, *110*(2), 276–284. <https://doi.org/10.1525/cond.2008.8424>
- Hanström, B. (1919). *Zur Kenntnis des Zentralen Nervensystems der Arachnoiden und Pantopoden*.
- Hanström, B. (1921). Über die Histologie und vergleichende Anatomie der Sehganglien und Globuli der Araneen. *Kungliga Svenska Vetenskapsakademiens Handlingar*, *61*(12), 1–39.
- Harcourt, R., Hindell, M. A., McMahon, C. R., Goetz, K. T., Charrassin, J.-B., Heerah, K., Holser, R., Jonsen, I. D., Shero, M. R., Hoenner, X., Foster, R., Lenting, B., Tarszisz, E., & Pinkerton, M. H. (2021). Regional Variation in Winter Foraging Strategies by Weddell Seals in Eastern Antarctica and the Ross Sea. *Frontiers in Marine Science*, *8*. <https://www.frontiersin.org/articles/10.3389/fmars.2021.720335>
- Harland, D. P., Li, D., & Jackson, R. R. (2012). How jumping spiders see the world. In *How animals see the world: Comparative behavior, biology, and evolution of vision* (pp. 133–163). Oxford University Press. <https://doi.org/10.1093/acprof:oso/9780195334654.003.0010>

- Harvey, P. H., & Pagel, M. D. (1988). The allometric approach to species differences in brain size. *Human Evolution*, 3(6), 461–472. <https://doi.org/10.1007/BF02436332>
- Heisenberg, M. (1998). What do the mushroom bodies do for the insect brain? An introduction. *Learning & Memory*, 5, 1–10.
- Heisenberg, M., Heusipp, M., & Wanke, C. (1995). Structural plasticity in the *Drosophila* brain. *The Journal of Neuroscience*, 15(3), 1951–1960.
- Hill, D. E. (1975). *The structure of the central nervous system of jumping spiders of the genus Phidippus (Araneae: Salticidae)* [M.Sc. thesis]. Oregon State University.
- Homann, H. (1928). Beiträge zur Physiologie der Spinnenaugen. *Zeitschrift für vergleichende Physiologie*, 7(2), 201–268. <https://doi.org/10.1007/BF00339163>
- Houston, A. I., & McNamara, J. M. (1999). *Models of adaptive behaviour: An approach based on state*. Cambridge University Press.
- Humphrey, B., Helton, W. S., Bedoya, C., Dolev, Y., & Nelson, X. J. (2018). Psychophysical investigation of vigilance decrement in jumping spiders: Overstimulation or understimulation? *Animal Cognition*, 21(6), 787–794. <https://doi.org/10.1007/s10071-018-1210-2>
- Jaitly, R., Ehrnsten, E., Hedlund, J., Cant, M., Lehmann, P., & Hayward, A. (2022). The evolution of predator avoidance in cephalopods: A case of brain over brawn? *Frontiers in Marine Science*, 9. <https://www.frontiersin.org/articles/10.3389/fmars.2022.909192>
- Jakob, E. M., Long, S. M., Harland, D. P., Jackson, R. R., Carey, A., Searles, M. E., Porter, A. H., Canavesi, C., & Rolland, J. P. (2018). Lateral eyes direct principal eyes as jumping spiders track objects. *Current Biology*, 28(18), R1092–R1093. <https://doi.org/10.1016/j.cub.2018.07.065>
- Jordan, L. A., & Ryan, M. J. (2015). The sensory ecology of adaptive landscapes. *Biology Letters*, 11(5), 20141054. <https://doi.org/10.1098/rsbl.2014.1054>
- Kihlslinger, R. L., & Nevitt, G. A. (2006). Early rearing environment impacts cerebellar growth in juvenile salmon. *The Journal of Experimental Biology*, 209(Pt 3), 504–509. <https://doi.org/10.1242/jeb.02019>
- Kolb, B., & Elliott, W. (1987). Recovery from early cortical damage in rats. II. Effects of experience on anatomy and behavior following frontal lesions at 1 or 5 days of age. *Behavioural Brain Research*, 26(1), 47–56. [https://doi.org/10.1016/0166-4328\(87\)90015-5](https://doi.org/10.1016/0166-4328(87)90015-5)
- Kolb, B., & Gibb, R. (2014). Searching for the principles of brain plasticity and behavior. *Cortex*, 58, 251–260. <https://doi.org/10.1016/j.cortex.2013.11.012>
- Kolb, B., & Whishaw, I. Q. I. (1998). Brain plasticity and behavior. *Annual Review of Psychology*, 49, 43–64. <https://doi.org/10.1146/annurev.psych.49.1.43>
- Kovoor, J. (1987). Comparative Structure and Histochemistry of Silk-Producing Organs in Arachnids. In W. Nentwig (Ed.), *Ecophysiology of Spiders* (pp. 160–186). Springer Berlin Heidelberg.
- LaManna, J. A., & Martin, T. E. (2016). Costs of fear: Behavioural and life-history responses to risk and their demographic consequences vary across species. *Ecology Letters*, 19(4), 403–413. <https://doi.org/10.1111/ele.12573>
- Land, M. F. (1972). Mechanisms of Orientation and Pattern Recognition by Jumping Spiders (Salticidae). In R. Wehner (Ed.), *Information Processing in the Visual Systems of*

- Anthropods* (pp. 231–247). Springer Berlin Heidelberg. [https://doi.org/10.1007/978-3-642-65477-0\\_34](https://doi.org/10.1007/978-3-642-65477-0_34)
- Land, M. F. (1985a). Fields of view of the eyes of primitive jumping spiders. *Journal of Experimental Biology*, *119*, 381–384.
- Land, M. F. (1985b). The morphology and optics of spider eyes. In F. G. Barth (Ed.), *Neurobiology of arachnids* (pp. 53–76). Springer.
- Laundré, J. W., Hernández, L., & Altendorf, K. B. (2001). Wolves, elk, and bison: Reestablishing the “landscape of fear” in Yellowstone National Park, U.S.A. *Canadian Journal of Zoology*, *79*(8), 1401–1409. <https://doi.org/10.1139/z01-094>
- Laundré, J. W., Hernandez, L., & Ripple, W. J. (2010). The landscape of fear: Ecological implications of being afraid. *The Open Ecology Journal*, *3*(3), 1–7. <https://doi.org/10.2174/1874213001003030001>
- Lehmann, T., Melzer, R., Hörnig, M. K., Michalik, P., Sombke, A., & Harzsch, S. (2016). Arachnida (excluding Scorpiones). In A. Schmidt-Rhaesa, S. Harzsch, & G. Purschke (Eds.), *Structure and Evolution of Invertebrate Nervous Systems*. Oxford University Press. <https://doi.org/10.1093/acprof:oso/9780199682201.001.0001>
- Liedtke, J., & Schneider, J. M. (2017). Social makes smart: Rearing conditions affect learning and social behaviour in jumping spiders. *Animal Cognition*, *20*(6), 1093–1106. <https://doi.org/10.1007/s10071-017-1125-3>
- Lim, M. L. M., Land, M. F., & Li, D. (2007). Sex-Specific UV and Fluorescence Signals in Jumping Spiders. *Science*, *315*(5811), 481–481. <https://doi.org/10.1126/science.1134254>
- Lima, S. L. (1998). Nonlethal effects in the ecology of predator-prey interactions. *BioScience*, *48*(1), 25–34. <https://doi.org/10.2307/1313225>
- Lima, S. L., & Dill, L. M. (1990). Behavioral decisions made under the risk of predation: A review and prospectus. *Canadian Journal of Zoology*, *68*(4), 619–640. <https://doi.org/10.1139/z90-092>
- Logan, C. J., Avin, S., Boogert, N., Buskell, A., Cross, F. R., Currie, A., Jelbert, S., Lukas, D., Mares, R., Navarrete, A. F., Shigeno, S., & Montgomery, S. H. (2018). Beyond brain size: Uncovering the neural correlates of behavioral and cognitive specialization. *Comparative Cognition & Behavior Reviews*, *13*, 55–89. <https://doi.org/10.3819/CCBR.2018.130008>
- Long, S. M. (2021). Variations on a theme: Morphological variation in the secondary eye visual pathway across the order of Araneae. *Journal of Comparative Neurology*, *529*(2), 259–280. <https://doi.org/10.1002/cne.24945>
- Maleszka, J., Barron, A. B., Helliwell, P. G., & Maleszka, R. (2009). Effect of age, behaviour and social environment on honey bee brain plasticity. *Journal of Comparative Physiology A*, *195*(8), 733–740. <https://doi.org/10.1007/s00359-009-0449-0>
- Martin, G. R. (2014). The subtlety of simple eyes: The tuning of visual fields to perceptual challenges in birds. *Philosophical Transactions of the Royal Society B: Biological Sciences*, *369*(1636), 20130040. <https://doi.org/10.1098/rstb.2013.0040>
- McNamara, J. M., & Houston, A. I. (1987). Starvation and predation as factors limiting population size. *Ecology*, *68*(5), 1515–1519. <https://doi.org/10.2307/1939235>
- Meinertzhagen, I. a. (2001). Plasticity in the insect nervous system. *Advances in Insect Physiology*, *28*, 84–167. [https://doi.org/10.1016/S0065-2806\(01\)28009-6](https://doi.org/10.1016/S0065-2806(01)28009-6)

- Mella, V. S. A., Ward, A. J. W., Banks, P. B., & McArthur, C. (2015). Personality affects the foraging response of a mammalian herbivore to the dual costs of food and fear. *Oecologia*, *177*(1), 293–303. <https://doi.org/10.1007/s00442-014-3110-8>
- Melrose, A., Nelson, X. J., Dolev, Y., & Helton, W. S. (2019). Vigilance all the way down: Vigilance decrement in jumping spiders resembles that of humans. *Quarterly Journal of Experimental Psychology*, *72*(6), 1530–1538. <https://doi.org/10.1177/1747021818798743>
- Menzel, R., & Giurfa, M. (2001). Cognitive architecture of a mini-brain: The honeybee. In *Trends in Cognitive Sciences* (Vol. 5, Issue 2, pp. 62–71). [https://doi.org/10.1016/S1364-6613\(00\)01601-6](https://doi.org/10.1016/S1364-6613(00)01601-6)
- Mery, F., & Burns, J. G. (2010). Behavioural plasticity: An interaction between evolution and experience. *Evolutionary Ecology*, *24*(3), 571–583. <https://doi.org/10.1007/s10682-009-9336-y>
- Michalko, R., Gibbons, A. T., Goodacre, S. L., & Pekár, S. (2021). Foraging aggressiveness determines trophic niche in a generalist biological control species. *Behavioral Ecology*, *32*(2), 257–264. <https://doi.org/10.1093/beheco/araa123>
- Michalko, R., Košulič, O., & Řežucha, R. (2017). Link between aggressiveness and shyness in the spider *Philodromus albidus* (Araneae, Philodromidae): State dependency over stability. *Journal of Insect Behavior*, *30*(1), 48–59. <https://doi.org/10.1007/s10905-017-9596-2>
- Montgomery, S. H., Merrill, R. M., & Ott, S. R. (2016). Brain composition in *Heliconius* butterflies, posteclosion growth and experience-dependent neuropil plasticity: Anatomy and plasticity of *heliconius* brains. *Journal of Comparative Neurology*, *524*(9), 1747–1769. <https://doi.org/10.1002/cne.23993>
- Morehouse, N. (2020). Spider vision. *Current Biology*, *30*(17), R975–R980. <https://doi.org/10.1016/j.cub.2020.07.042>
- Morehouse, N. I., Buschbeck, E. K., Zurek, D. B., Steck, M., & Porter, M. L. (2017). Molecular Evolution of Spider Vision: New Opportunities, Familiar Players. *The Biological Bulletin*, *233*(1), 21–38. <https://doi.org/10.1086/693977>
- Moser, M. B. (1999). Making more synapses: A way to store information? *Cellular and Molecular Life Sciences*, *55*(4), 593–600. <https://doi.org/10.1007/s000180050317>
- Murphey, R. K. (1986). The myth of the inflexible invertebrate: Competition and synaptic remodelling in the development of invertebrate nervous systems. *Journal of Neurobiology*, *17*(6), 585–591. <https://doi.org/10.1002/neu.480170603>
- Nelson, X. J., Helton, W. S., & Melrose, A. (2019). The effect of stimulus encounter rate on response decrement in jumping spiders. *Behavioural Processes*, *159*, 57–59. <https://doi.org/10.1016/j.beproc.2018.12.020>
- O'Connor, M., Garm, A., & Nilsson, D.-E. (2009). Structure and optics of the eyes of the box jellyfish *Chiropsella bronzie*. *Journal of Comparative Physiology A*, *195*(6), 557–569. <https://doi.org/10.1007/s00359-009-0431-x>
- Ott, S. R., & Rogers, S. M. (2010). Gregarious desert locusts have substantially larger brains with altered proportions compared with the solitary phase. *Proceedings of the Royal Society B*, *277*(1697), 3087–3096. <https://doi.org/10.1098/rspb.2010.0694>

- Palmer, M. S., Fieberg, J., Swanson, A., Kosmala, M., & Packer, C. (2017). A 'dynamic' landscape of fear: Prey responses to spatiotemporal variations in predation risk across the lunar cycle. *Ecology Letters*, *20*(11), 1364–1373. <https://doi.org/10.1111/ele.12832>
- Paulus, H. (1979). Eye structure and the monophyly of the Arthropoda. In *Arthropod phylogeny*. Vam Nostrand Reinhold Company.
- Pekár, S. (2014). Comparative analysis of passive defences in spiders (Araneae). *Journal of Animal Ecology*, *83*(4), 779–790. <https://doi.org/10.1111/1365-2656.12177>
- Quesada, R., Triana, E., Vargas, G., Douglass, J. K., Seid, M. A., Niven, J. E., Eberhard, W. G., & Wcislo, W. T. (2011). The allometry of CNS size and consequences of miniaturization in orb-weaving and cleptoparasitic spiders. *Arthropod Structure & Development*, *40*(6), 521–529. <https://doi.org/10.1016/j.asd.2011.07.002>
- Ramón y Cajal, S. (1928). *Degeneration & Regeneration of the Nervous System* (R. M. May., Ed.). Oxford University Press, Humphrey Milford.
- Réale, D., Garant, D., Humphries, M. M., Bergeron, P., Careau, V., & Montiglio, P.-O. (2010). Personality and the emergence of the pace-of-life syndrome concept at the population level. *Philosophical Transactions of the Royal Society B: Biological Sciences*, *365*(1560), 4051–4063. <https://doi.org/10.1098/rstb.2010.0208>
- Réale, D., Reader, S. M., Sol, D., McDougall, P. T., & Dingemanse, N. J. (2007). Integrating animal temperament within ecology and evolution. *Biological Reviews*, *82*(2), 291–318. <https://doi.org/10.1111/j.1469-185X.2007.00010.x>
- Richman, D. B., & Jackson, R. R. (1992). A review of the ethology of jumping spiders (Araneae, Salticidae). *Bulletin of the British Arachnological Society*, *9*(2).
- Riska, B., & Atchley, W. R. (1985). Genetics of Growth Predict Patterns of Brain-Size Evolution. *Science*, *229*(4714), 668–671. <https://doi.org/10.1126/science.229.4714.668>
- Robledo-Ospina, L. E., Escobar-Sarria, F., Troscianko, J., & Rao, D. (2017). Two ways to hide: Predator and prey perspectives of disruptive coloration and background matching in jumping spiders. *Biological Journal of the Linnean Society*, *122*(4), 752–764. <https://doi.org/10.1093/biolinnean/blx108>
- Robledo-Ospina, L., & Rao, D. (2022). Dangerous visions: A review of visual antipredator strategies in spiders. *Evolutionary Ecology*, *36*. <https://doi.org/10.1007/s10682-022-10156-x>
- Rosenzweig, M. R., & Bennett, E. L. (1996). Psychobiology of plasticity: Effects of training and experience on brain and behavior. *Behavioural Brain Research*, *78*(1), 57–65. [https://doi.org/10.1016/0166-4328\(95\)00216-2](https://doi.org/10.1016/0166-4328(95)00216-2)
- Rössler, W. (2019). *Neuroplasticity in desert ants (Hymenoptera: Formicidae) – importance for the ontogeny of navigation*. [https://doi.org/10.25849/MYRMECOL.NEWS\\_029:001](https://doi.org/10.25849/MYRMECOL.NEWS_029:001)
- Saint-Rémy, G. (1887). Contribution à l'étude du cerveau chez les Arthropodes trachéates. *Archives de Zoologie Experimentale et Générale*.
- Schirmer, A., Hoffmann, J., Eccard, J. A., & Dammhahn, M. (2020). My niche: Individual spatial niche specialization affects within- and between-species interactions. *Proceedings of the Royal Society B: Biological Sciences*, *287*(1918), 20192211. <https://doi.org/10.1098/rspb.2019.2211>
- Schmid, A. (1998). Different functions of different eye types in the spider *Cupiennius salei*. *Journal of Experimental Biology*, *201*, 221–225.



- Sih, A., Bell, A., & Johnson, J. C. (2004). Behavioral syndromes: An ecological and evolutionary overview. *Trends in Ecology & Evolution*, *19*(7), 372–378. <https://doi.org/10.1016/j.tree.2004.04.009>
- Sih, A., Bell, A. M., Johnson, J. C., & Ziemba, R. E. (2004). Behavioral Syndromes: An Integrative Overview. *The Quarterly Review of Biology*, *79*(3), 241–277. <https://doi.org/10.1086/422893>
- Simmons, P. J., & Young, D. (1999). *Nerve cells and animal behaviour* (2nd ed). Cambridge University Press.
- Smolka, J., Zeil, J., & Hemmi, J. M. (2011). Natural visual cues eliciting predator avoidance in fiddler crabs. *Proceedings of the Royal Society B: Biological Sciences*, *278*(1724), 3584–3592. <https://doi.org/10.1098/rspb.2010.2746>
- Spano, L., Long, S. M., & Jakob, E. M. (2012). Secondary eyes mediate the response to looming objects in jumping spiders (*Phidippus audax*, Salticidae). *Biology Letters*, *8*(6), 949–951. <https://doi.org/10.1098/rsbl.2012.0716>
- Stafstrom, J. A., Michalik, P., & Hebets, E. A. (2017). Sensory system plasticity in a visually specialized, nocturnal spider. *Scientific Reports*, *7*(1), 46627. <https://doi.org/10.1038/srep46627>
- Steinhoff, P. O. M., Liedtke, J., Sombke, A., Schneider, J. M., & Uhl, G. (2018). Early environmental conditions affect the volume of higher-order brain centers in a jumping spider. *Journal of Zoology*, *304*(3), 182–192. <https://doi.org/10.1111/jzo.12512>
- Steinhoff, P. O. M., Sombke, A., Liedtke, J., Schneider, J. M., Harzsch, S., & Uhl, G. (2017). The synganglion of the jumping spider *Marpissa muscosa* (Arachnida: Salticidae): Insights from histology, immunohistochemistry and microCT analysis. *Arthropod Structure & Development*, *46*(2), 156–170. <https://doi.org/10.1016/j.asd.2016.11.003>
- Steinhoff, P. O. M., Uhl, G., Harzsch, S., & Sombke, A. (2020). Visual pathways in the brain of the jumping spider *Marpissa muscosa*. *Journal of Comparative Neurology*, *528*(11), 1883–1902. <https://doi.org/10.1002/cne.24861>
- Stöckl, A., Heinze, S., Charalabidis, A., el Jundi, B., Warrant, E., & Kelber, A. (2016). Differential investment in visual and olfactory brain areas reflects behavioural choices in hawk moths. *Scientific Reports*, *6*(1), 26041. <https://doi.org/10.1038/srep26041>
- Strausfeld, N. J., & Barth, F. G. (1993). Two visual systems in one brain: Neuropils serving the secondary eyes of the spider *Cupiennius salei*. *The Journal of Comparative Neurology*, *328*(1), 43–62. <https://doi.org/10.1002/cne.903280104>
- Strausfeld, N. J., Weltzien, P., & Barth, F. G. (1993). Two visual systems in one brain: Neuropils serving the principal eyes of the spider *Cupiennius salei*. *The Journal of Comparative Neurology*, *328*(1), 63–75. <https://doi.org/10.1002/cne.903280105>
- Sweatt, J. D. (2016). Neural plasticity and behavior – sixty years of conceptual advances. *Journal of Neurochemistry*, *139*, 179–199. <https://doi.org/10.1111/jnc.13580>
- Taylor, L. A., & McGraw, K. J. (2013). Male ornamental coloration improves courtship success in a jumping spider, but only in the sun. *Behavioral Ecology*, *24*(4), 955–967. <https://doi.org/10.1093/beheco/art011>
- Toscano, B. J. (2017). Prey behavioural reaction norms: Response to threat predicts susceptibility to predation. *Animal Behaviour*, *132*, 147–153. <https://doi.org/10.1016/j.anbehav.2017.08.014>

- Tsuboi, M. (2021). Exceptionally Steep Brain-Body Evolutionary Allometry Underlies the Unique Encephalization of Osteoglossiformes. *Brain, Behavior and Evolution*, 96(2), 49–63. <https://doi.org/10.1159/000519067>
- Uetz, G. W., & Roberts, J. A. (2002). Multisensory Cues and Multimodal Communication in Spiders: Insights from Video/Audio Playback Studies. *Brain, Behavior and Evolution*, 59(4), 222–230. <https://doi.org/10.1159/000064909>
- Voje, K. L., Hansen, T. F., Egset, C. K., Bolstad, G. H., & Pélabon, C. (2014). Allometric Constraints and the Evolution of Allometry. *Evolution*, 68(3), 866–885. <https://doi.org/10.1111/evo.12312>
- Wainwright, J. B., & Montgomery, S. H. (2022). Neuroanatomical shifts mirror patterns of ecological divergence in three diverse clades of mimetic butterflies. *Evolution*, 76(8), 1806–1820. <https://doi.org/10.1111/evo.14547>
- Warton, D. I., Duursma, R. A., Falster, D. S., & Taskinen, S. (2012). Smatr 3— an R package for estimation and inference about allometric lines. *Methods in Ecology and Evolution*, 3(2), 257–259. <https://doi.org/10.1111/j.2041-210X.2011.00153.x>
- Warton, D. I., Wright, I. J., Falster, D. S., & Westoby, M. (2006). Bivariate line-fitting methods for allometry. *Biological Reviews*, 81(2), 259–291. <https://doi.org/10.1017/S1464793106007007>
- Weltzien, P., & Barth, F. G. (1991). Volumetric measurements do not demonstrate that the spider brain “central body” has a special role in web building. *Journal of Morphology*, 208(1), 91–98. <https://doi.org/10.1002/jmor.1052080104>
- Withers, G. S., Fahrbach, S. E., & Robinson, G. E. (1993). Selective neuroanatomical plasticity and division of labour in the honeybee. *Nature*, 364(6434), 238–240. <https://doi.org/10.1038/364238a0>
- Yamashita, S. (1985). Photoreceptor Cells in the Spider Eye: Spectral Sensitivity and Efferent Control. In F. G. Barth (Ed.), *Neurobiology of Arachnids* (p. 15). Springer.
- Yamashita, S., & Tateda, H. (1978). Spectral sensitivities of the anterior median eyes of the orb web spiders, *Argiope bruennichi* and *A. amoena*. *Journal of Experimental Biology*, 74, 12.
- Yilmaz, A., Lindenberg, A., Albert, S., Grübel, K., Spaethe, J., Rössler, W., & Groh, C. (2016). Age-related and light-induced plasticity in opsin gene expression and in primary and secondary visual centers of the nectar-feeding ant *Camponotus rufipes*. *Developmental Neurobiology*, 76(9), 1041–1057. <https://doi.org/10.1002/dneu.22374>
- Zurek, D. B., Cronin, T. W., Taylor, L. A., Byrne, K., Sullivan, M. L. G., & Morehouse, N. I. (2015). Spectral filtering enables trichromatic vision in colorful jumping spiders. *Current Biology*, 25(10), R403–R404. <https://doi.org/10.1016/j.cub.2015.03.033>
- Zurek, D. B., & Nelson, X. J. (2012a). Saccadic tracking of targets mediated by the anterior-lateral eyes of jumping spiders. *Journal of Comparative Physiology A*, 198(6), 411–417. <https://doi.org/10.1007/s00359-012-0719-0>
- Zurek, D. B., & Nelson, X. J. (2012b). Hyperacute motion detection by the lateral eyes of jumping spiders. *Vision Research*, 66, 26–30. <https://doi.org/10.1016/j.visres.2012.06.011>

## 2. Publications

### **Chapter 1: Individual differences in risk-taking affect foraging across different landscapes of fear**

Philip O. M. Steinhoff<sup>1</sup>, Bennet Warfen<sup>1</sup>, Sissy Voigt<sup>1</sup>, Gabriele Uhl<sup>1</sup> and Melanie Dammhahn<sup>2#</sup>

<sup>1</sup> Zoological Institute and Museum, General and Systematic Zoology, University of Greifswald, Loitzer Straße 26, Greifswald, Germany.

<sup>2</sup>Animal Ecology, Institute for Biochemistry and Biology, University of Potsdam, Potsdam, Germany.

<sup>#</sup>Current affiliation: Institute for Neuro- and Behavioural Biology (INVB), University of Münster, Hüfferstraße 1a, Münster, Germany.

*\*Corresponding Author. E-Mail: philipsteinhoff@gmail.com*

*Manuscript published in Oikos 129; doi: 10.1111/oik.07508*



## Research

### Individual differences in risk-taking affect foraging across different landscapes of fear

Philip O. M. Steinhoff, Bennet Warfen, Sissy Voigt, Gabriele Uhl and Melanie Dammhahn

P. O. M. Steinhoff (<https://orcid.org/0000-0003-1676-8105>) ✉ ([philipsteinhoff@gmail.com](mailto:philipsteinhoff@gmail.com)), B. Warfen, S. Voigt and G. Uhl, Zoological Inst. and Museum, General and Systematic Zoology, Univ. of Greifswald, Loitzer Straße 26, DE-17489 Greifswald, Germany. – M. Dammhahn (<http://orcid.org/0000-0003-0557-740X>), Animal Ecology, Inst. for Biochemistry and Biology, Univ. of Potsdam, Potsdam, Germany.

#### Oikos

129: 1891–1902, 2020

doi: 10.1111/oik.07508

Subject Editor: Allan Edelsparre

Editor-in-Chief: Pedro Perez-Neto

Accepted 31 August 2020



One of the strongest determinants of behavioural variation is the tradeoff between resource gain and safety. Although classical theory predicts optimal foraging under risk, empirical studies report large unexplained variation in behaviour. Intrinsic individual differences in risk-taking behaviour might contribute to this variation. By repeatedly exposing individuals of a small mesopredator to different experimental landscapes of risks and resources, we tested 1) whether individuals adjust their foraging behaviour according to predictions of the general tradeoff between energy gain and predation avoidance and 2) whether individuals differ consistently and predictably from each other in how they solve this tradeoff. Wild-caught individuals ( $n = 42$ ) of the jumping spider *Marpissa muscosa*, were subjected to repeated release and open-field tests to quantify among-individual variation in boldness and activity. Subsequently, individuals were tested in four foraging tests that differed in risk level (white/dark background colour) and risk variation (constant risk/variable risk simulated by bird dummy overflights) and contained inaccessible but visually perceivable food patches. When exposed to a white background, individuals reduced some aspects of movement and foraging intensity, suggesting that the degree of camouflage serves as a proxy of perceived risk in these predators. Short pulses of acute predation risk, simulated by bird overflights, had only small effects on aspects of foraging behaviour. Notably, a significant part of variation in foraging was due to among-individual differences across risk landscapes that are linked to consistent individual variation in activity, forming a behavioural syndrome. Our results demonstrate the importance of among-individual differences in behaviour of animals that forage under different levels of perceived risk. Since these differences likely affect food-web dynamics and have fitness consequences, future studies should explore the mechanisms that maintain the observed variation in natural populations.

Keywords: animal personality, behavioural syndrome, foraging, jumping spider, landscape of fear, risk–reward tradeoff



[www.oikosjournal.org](http://www.oikosjournal.org)

© 2020 The Authors. Oikos published by John Wiley & Sons Ltd on behalf of Nordic Society Oikos  
This is an open access article under the terms of the Creative Commons Attribution License, which permits use, distribution and reproduction in any medium, provided the original work is properly cited.

## Introduction

The risk of predation is a strong selective force for most animals. Predation risk affects behavioural decisions aimed at reducing immediate individual risk (Lima 1998). These behavioural adjustments involve anti-predator behaviour and energetic tradeoffs, and thus affect prey fitness directly and indirectly. One of the best described and studied examples is the tradeoff between foraging gain and predation risk (Lima and Dill 1990, Lima 1998) with animals adjusting foraging behaviour to avoid a direct predator attack but also react to the mere presence of a predator, i.e. indirect predation risk. Indirect (non-consumptive) effects rely on perceived predation risk, i.e. the individual's assessment of the likelihood of a predator attack, which is based on experience and imperfect knowledge of the environment (Bouskila and Blumstein 1992, Gaynor et al. 2019). Behavioural responses of animals to perceived risk are manifold; they vary between species, with intensity, spatial and temporal distribution and predictability of predation risk, and with the expected gain from foraging (Lima and Dill 1990, Houston and McNamara 1999, LaManna and Martin 2016). Moreover, animals can learn to adjust their behaviour in response to changing risks (DePasquale et al. 2014, Palmer et al. 2017, Aguilar-Argüello et al. 2019).

As revealed by a wealth of studies over the last two decades (Sih et al. 2004a, Réale et al. 2007, Chang et al. 2017b, Abbey-Lee and Dingemanse 2019), population-wide optimal solutions to the tradeoff between foraging gain and predation avoidance are constrained by intrinsic individual differences in behaviour. Consistent among-individual differences in behaviour – commonly termed animal personality or temperament – are exhibited in a variety of traits and when these are correlated, they are termed behavioural syndromes (Sih et al. 2004a, b, Bell et al. 2009, Dingemanse et al. 2012). Individual phenotypic expressions of behavioural traits (behavioural types; e.g. shyness/boldness) can be measured in standardized tests and correlated with behaviours expressed in ecologically more relevant experimental scenarios. For example aspects of foraging behaviour vary consistently between individuals of different behavioural types (Toscano et al. 2016, Chang et al. 2017b, Michalko et al. 2017) and risk-taking during foraging and microhabitat use can be predicted by boldness (Dammhahn and Almeling 2012, Mella et al. 2015, Schirmer et al. 2020). Thus, how an individual trades off between foraging gain and risk should be linked to its behavioural type. Indeed, young salmonids exhibit consistent foraging tactics that are linked to their willingness to take risks (Farwell and McLaughlin 2009). Similarly, in an apex predator, the pike *Esox lucius*, behaviour under different levels of risk was associated with the individual's behavioural type (Nyqvist et al. 2012). Since apex predators affect the structure of lower trophic levels (Crooks and Soulé 1999, Ritchie and Johnson 2009, Shores et al. 2019), such among-individual variation in foraging under risk should modify cascading effects in trophic chains (Moran et al. 2017). A particular case

are mesopredators, which are under risk of predation by other (often larger) predators while they are pursuing their prey. Therefore, mesopredators might provide an important link in multi-layered landscapes of fear (Brown 1999, Laundre et al. 2010), because among-individual variation in their risk-taking could create both indirect bottom-up and top-down effects in food webs. However, much less is known about the effects that behaviour of mesopredators can have on both its predators and its prey (but see Welch et al. 2017). As a first step towards filling this gap, we aimed to test whether aspects of foraging behaviour of a mesopredator, the jumping spider *Marpissa muscosa*, differ depending on the levels of risk and whether consistent individual differences in behaviour (measured in the functional context of satiated exploration) covary with risk-taking during foraging (measured in the functional context of hungry foraging).

Jumping spiders (Salticidae) are visually hunting predators, that are preyed upon mainly by birds, lizards and parasitic wasps (Edmunds 1993, Foelix 1996, Gunnarsson 2007, Piovio-Scott et al. 2017). From the araneophagic jumping spider, *Portia labiata*, we know that the behavioural type affects the speed at which individuals make a prey-choice and the performance at cognitively demanding tasks (Chang et al. 2017a, 2018). Furthermore, an individual's behavioural type and the predictability of prey individuals (in terms of reaction towards a predator) both affected the foraging success in *Portia labiata* (Chang et al. 2017b). *Marpissa muscosa*, one of the largest jumping spiders in Europe (total body size roughly 1 cm), shows consistent among-individual differences in activity- and boldness-related traits (Liedtke et al. 2015). In order to create landscapes of fear that are perceived as such by the study organism, the ecology and sensory capacities of an animal need to be considered (Jordan and Ryan 2015). *Marpissa muscosa* builds nests under the bark of dead wood and hunts on the surface of the bark by stalking prey. The spider is well camouflaged due to its brown-grey mottled coloration pattern (appearance) on brown-grey dead wood. Consequently, we used a brown versus white background as low and high-risk level. Our reasoning behind this is that we assume that exposure without cover incurs some risk for a small mesopredator and individuals therefore perceive a low level of risk even when no simulated predator is present. To mimic a predator, we additionally introduced a visual temporal high-risk stimulus (fast moving shadow). Hence, we aimed to manipulate perceived predation risk or 'fear', defined as 'conscious or unconscious risk perception' (Gaynor et al. 2019, p. 356). We used a fully-crossed factorial design, varied risk level (uniformly high and low) and risk variation (constant and variable) to test the following hypotheses and predictions: H1) jumping spiders adjust foraging behaviour to the level and variation of risk in a landscape. Specifically, we expected reduced foraging behaviour 1) under higher risk (white background compared to brown background) and 2) under variable as compared to constant risk (i.e. recurrent presence of simulated predator overflight or the absence thereof). Further, we expected 3) spiders to reduce foraging

behaviour more in reaction to a simulated predator when foraging on a white background as compared to foraging on a brown background. H2) Aspects of foraging behaviour under risk vary among individuals. We expected 4) foraging behaviour to be repeatable across different landscapes of risk. H3) Among-individual differences in hungry foraging under risk are associated with individual differences in boldness and activity (measured in the context of satiated exploration). 5) We expected positive among-individual covariances between foraging under risk and consistent behavioural traits (boldness, activity).

## Methods

### Study subjects and housing conditions

Adult female *Marpissa muscosa* (n=42) were collected in Greifswald (Germany) and kept for 6–8 weeks in the laboratory prior to the experiment. Prosoma width was measured using a stereo microscope with a camera and Axiovision 4.8 software. Spiders were fed on *Drosophila hydei* weekly and kept individually in plastic boxes of 145 × 110 × 68 mm size. Boxes were enriched with paper tissue and an Eppendorf-tube filled with wet cotton wool to keep some humidity. During open-field tests, spiders were fed ad libitum whereas they were starved three days prior to testing their foraging behaviour in risk landscapes.

### Behavioural tests for among-individual differences in behaviour

We quantified among-individual differences in behaviour with a combined emergence and open-field test (functional context of satiated exploration) (Archer 1973). The test setup was adapted from Schirmer et al. (2019) and consisted of a round white PVC arena (diameter 50 cm) with a 30 cm high wall and an attached small opaque tube (7 cm length, 1 cm diameter; syringe, 10 ml BD covered with dark tape). The arena was under a direct spotlight (ca 60 cm above arena floor) and its wall was covered with Vaseline to prevent individuals from climbing. We virtually divided the arena into an edge zone of 2 cm width along the wall and a centre zone because we assumed that individuals perceive the edge zone as safer than the open exposed center of the arena. With the emergence test, we quantified the propensity of an individual to enter an unknown and potentially risky area. We assumed that spiders perceived the dark and closed tube as safer than the open arena (compare also to the setup used by Jakob et al. 2007). For this test, individual spiders were gently transferred from their home boxes into the tube. The tube was closed with a foam plug and attached to the arena. After three minutes of acclimatisation, we opened the tube by removing the plug. We recorded the time (in s) until the individual entered the open arena with its full body (latency). If a spider did not enter into the arena during the course of 20 min, the latency was set to 20 min and it was gently pushed with the syringe's

piston into the arena. Upon entering the arena, a re-entering of the tube was prevented by pushing the syringe's piston plane with the arena wall and the open-field test started. During the open-field test, the observer was not present in the test room. Over 30 min, we video-recorded the individual's behaviour in the arena with a digital camera. Using EthoVisionXT (ver. 14.0), we quantified from the videos the following variables related to movement, activity and spatial exploration behaviours: 1) cumulative duration moving (in s) defined as any state in which the velocity is higher than start velocity (no movement), 2) frequency of entering the centre zone of the arena, 3) the cumulative duration in edge zone of the arena, 4) average distance to the wall of the arena and 5) average mobility (in percent) defined as the amount of pixel change between two images. The test was repeated three times per individual with one day between tests.

### Foraging test in risk landscapes

We quantified foraging and risk-taking behaviour in landscapes of risks and resources (in the functional context of hungry foraging), set-up in the round arenas used for open-field tests. The landscape contained a 5 × 5 cm plastic lid in the centre of the arena that served as a retreat for the spider. The lid was covered with tape to ensure that it was dark below and glued on small sticks of 1.5 cm that allowed the spider to freely enter and exit under the lid. Four food patches were placed in seven cm distance to the retreat along cardinal axes. These food patches were transparent plastic containers (5 × 5 cm) each containing six living *Drosophila hydei*. There was constant movement in the containers since the flies disturbed each other. The spiders reacted to the flies' movements but could not prey upon them. We used a fully-crossed experimental design with two levels of risk with two risk variations each. First, we used 1) a high-risk level composed of a white arena (brightness value 282 lux) with spiders being clearly distinct from the background colour and 2) a low-risk level composed of an arena with a dark brown background (brightness value 164 lux) with spiders being well camouflaged. In a forced choice test in an arena with a bi-coloured floor, spiders preferred the dark brown background over the white one (placed in the center 18 out of 21 individuals moved first in the dark part, binomial test:  $p = 0.001$ ). For each of these risk levels we used two risk variations: 1) constant risk (open arena without simulated predator) and 2) variable risk (open arena with the recurrent presence of a simulated predator overflight passing over the arena). Using a small servomotor glued onto the spotlight above the arena, we moved a wooden skewer (2 mm diameter) with a paper bird silhouette (size 6 × 6.5 cm) attached to it across the arena under the spotlight once every two minutes. The shadow appeared for less than a second at the arena ground and was large enough to darken the entire arena. A moving shadow has previously been shown to elicit antipredator responses in a wolf spider (Lohrey et al. 2009).

To increase the motivation to forage, we starved the spiders for three days prior to first testing and did not feed them during the whole experiment that lasted eight days.

Each spider was tested in each of the four treatments, with a break of one day between tests. The order of treatments was randomized across individuals. Spider handling was executed with small brushes. We gently transferred the individuals from their home cage to the retreat, slowly turned it upside down and placed it into the centre of the arena. We thereby ensured that each individual started the trial from the same position. In case the spider jumped out of the lid before it could be positioned, we gently removed the spider from the arena and placed it back into its home cage to repeat the procedure some minutes later. Once the individual was placed in the arena in the retreat, the experimenter left the room. We video-recorded the individuals' behaviour in the arena with a digital camera over 60 min. After each test, the individual was transferred back to its home box, and food patches and arena were cleaned with soap and water to remove chemical traces from previous tests.

Using EthoVisionXT (ver. 14.0), we quantified from the videos the following variables related to movement, activity and foraging: 1) cumulative duration in the arena outside of the retreat, 2) frequency of entering the arena with the full body, 3) cumulative duration moving defined as any state in which the velocity is higher than start velocity (no movement), 4) latency to first approach a food patch (i.e. enter with its full body into a zone of 2 cm around a food patch), 5) the cumulative duration of food patch visits (i.e. time spent in zones around food patches), 6) total frequency of patch visits, 7) mean duration of food patch visits and, 8) coefficient of variation (CV) of patch visit durations as a measure of unevenness of food patch visits. A small CV indicates a more equal foraging effort across the landscape (independent of total foraging effort) and a large CV indicates unequal foraging effort. In addition, we recorded the latency to enter the area, i.e. emerge with the full body from the retreat. This variable was zero-inflated and highly skewed; in 22% (38/172) of tests the spiders emerged immediately from the retreat (in 52% corresponding to 89/172 tests the spiders emerged within 20 s), probably due to handling of subjects prior to the test and latency to emerge mainly reflecting motivation. Therefore, we first treated this variable as binomial (0 for immediate emergence and 1 for latencies > 0 s) in statistical analyses. Since latency to emerge did not vary by risk treatments (interaction between risk modalities:  $\chi^2 = 3.00$ ,  $df = 1$ ,  $p = 0.08$ ) and was not repeatable ( $R = 0$ ,  $p = 0.50$ , 95%-CI: 0, 0.115), we discarded it from all further analyses.

## Statistical analyses

To test whether aspects of behaviour expressed in the open-field and in the foraging test were repeatable over time (open-field test) and across risk treatments (foraging test), we estimated repeatability of behavioural variables using the R package *rptR* (Nakagawa and Schielzeth 2010, Stoffel et al. 2017). For each dependent variable, we specified the underlying error distribution (Poisson for all frequencies and Gaussian for all other variables); latencies and cumulative duration moving in the open-field test as well as duration

moving in the foraging test were log-transformed. We used 1000 simulations to estimate confidence intervals and 1000 permutations to estimate p-values.

To condense repeatable behavioural variables into meaningful composite variables, we performed principal component analyses (PCA) for open-field tests and foraging tests separately. Variables in these data sets conformed to the assumptions of PCAs, such as pairwise correlations < 0.9, Kaiser–Meyer–Olkin criterion > 0.5, significant Bartlett's test, and correlation determinant < 1. We retained PCA components with Eigenvalues > 1 and used oblimin rotation to increase interpretability of the components. Subsequently, we estimated repeatability of the PCA components via methods specified above and used PCA components as dependent variables in multivariate models.

To test for effects of risk treatments on variation in foraging behaviours, we ran generalized or linear mixed effects models (G/LMMs) using the R package *lme4* and modelled the error structure of the data via the underlying distribution families of the response variables (Poisson for all frequencies and Gaussian for all other variables). As fixed effects, we entered as our test predictors the two risk treatments, risk level (high or low) and risk variation (constant or variable), and their interaction. Additionally, we initially entered as control predictors the variables order of treatment presentations and arena identity to control for potential order effects and variation between the two experimental arenas used. Further, we entered the fixed effect prosoma width to control for variation in foraging behaviour due to body size. As random effect, we included spider identity, specified as random intercept. Using stepwise backward model selection, we compared nested models via log-likelihood ratio tests with and without control predictors and with and without the interaction and retained more parsimonious models (Zuur et al. 2009). Test predictors (risk treatments), for which we had specific predictions, were always retained in the model. If the interaction between risk modalities improved model fit, we ran post hoc analyses for simple effects of one treatment (e.g. high-risk level) within one level of the respective other treatment (e.g. constant risk) and vice versa. We assessed model fit based on residual distribution using qqplots. We estimated the proportion of explained variance by the fixed factors alone (marginal  $R^2$ ) and by fixed and random factors together (conditional  $R^2$ ) using the R package *MuMIn* (Burnham and Anderson 2002, Nakagawa and Schielzeth 2013); for GLMMs we report lognormal  $R^2$ .

To test for covariance between behavioural dimensions (i.e. composite behaviours), we run a set of bivariate Bayesian mixed-effects models using the R package *MCMCglmm* (Hadfield 2010). For open-field behaviour, we set no fixed effect. For behaviours from the foraging test, we entered risk level and risk variation as fixed effects, as well as the order of treatments. Individual identity was entered as a random effect, specified as random intercept. We used slightly informative priors by dividing the total variance in the data by the number of estimated random effects and set a low degree of belief ( $\nu = 1$ ), since we do



not have much information regarding the posterior distribution of the dependent variable (Hadfield 2010). Since behaviours in the open-field tests and in foraging tests were not obtained at the same time, we fixed the within-individual covariance to zero (Dingemanse and Dochtermann 2013). Error structures of the data were modelled via the underlying distribution families of the response variables. We used 101 000 iterations, a thinning interval of 100 and a burnin of 1000, which resulted in low temporal autocorrelation between estimates of subsequent models. Based on the posterior distributions, we extracted covariances between pairs of response variables and their credibility intervals. Covariances were interpreted significant if the credibility intervals did not include zero (Houslay and Wilson 2017). All statistical analyses were performed with

the program R (ver. 3.3.0, <www.r-project.org>) using the specified packages. The level of significance was set at  $\alpha < 0.05$ .

## Results

### Among-individual differences in behaviour in open-field and foraging tests

All behavioural variables quantified in both open-field and foraging tests, except the cumulative duration in edge zone in the open-field test, were repeatable over time or across contexts (all  $R > 0.15$ , all  $p < 0.05$ ; Fig. 1, Supplementary material Appendix 1 Table A1). For the open-field test, the PCA

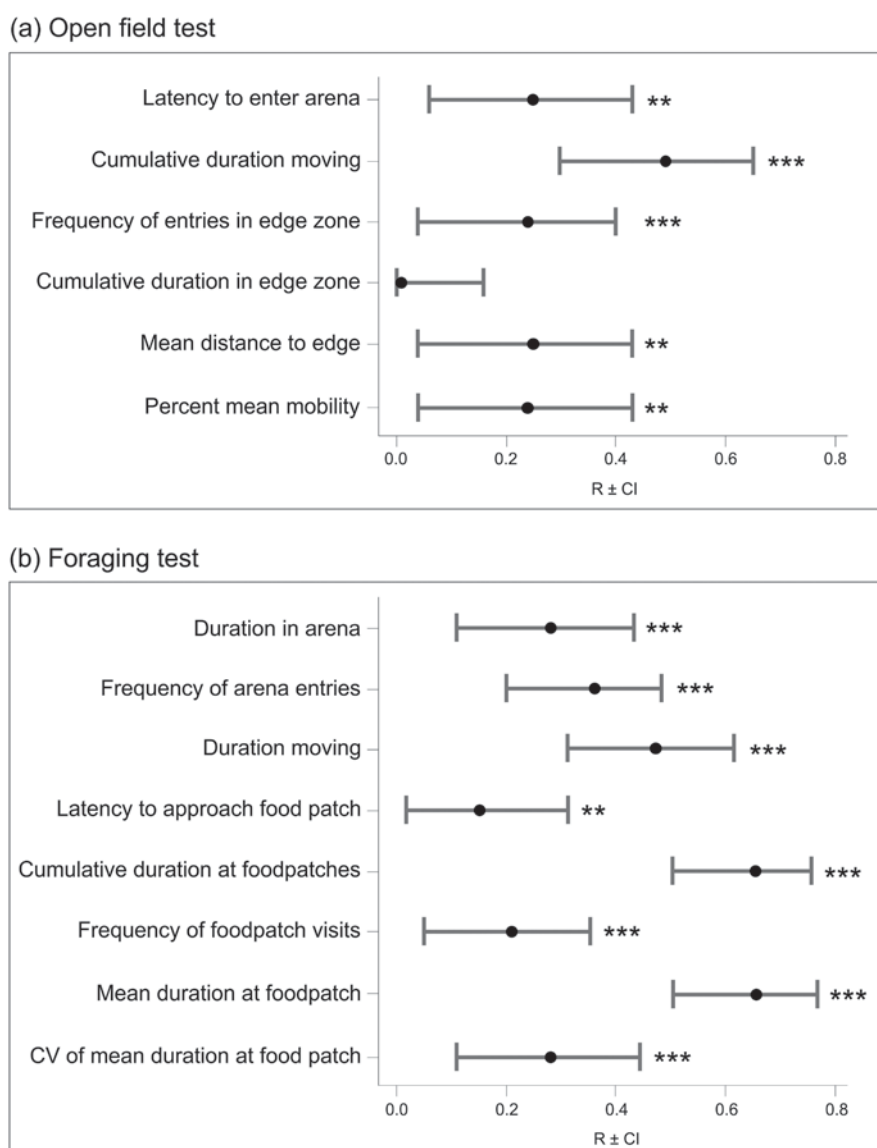


Figure 1. Repeatability estimates of behavioural variables from (a) the combined emergence and open-field test and (b) the foraging test. Spiders were fed ad libitum during the open field test and starved for 3–9 days over the course of the foraging test. Black dots give the repeatability estimate; whiskers show the 95%-confidence intervals. Stars indicate the significance levels with \*  $p < 0.05$  and \*\*  $p < 0.001$ .

yielded two meaningful components, cumulatively explaining 70% of the variance. We consider the first component (Eigenvalue = 1.57, explained variance: 49%, Supplementary material Appendix 1 Table A2) to represent boldness. Boldness was high if individuals entered the arena fast, kept a distance to the edge (i.e. stayed more in the exposed centre of the arena), and had a high percentage of moving (all loadings > 0.61, all |correlations| > 0.60 after oblimin rotation, Supplementary material Appendix 1 Table A2). We consider the second component (Eigenvalue = 1.02, explained variance = 21%, Supplementary material Appendix 1 Table A2) to represent activity. Activity was high if individuals moved for longer durations and changed often between the centre of the arena and the edge zone (all loadings > 0.65, all |correlations| > 0.75 after oblimin rotation, Supplementary material Appendix 1 Table A2). For the foraging test, the PCA yielded two meaningful components, cumulatively explaining 65% of the variance. We consider the first component (Eigenvalue = 1.82, explained variance: 41%, Supplementary material Appendix 1 Table A3) to represent foraging intensity. This foraging intensity was high if individuals started foraging fast, retreated less often (low frequency of arena entries), spent much time in the arena (high cumulative duration in the arena), spent much time visiting food patches (high cumulative duration close to food patch), and had long average food patch visits (all loadings > 0.54, all |correlations| > 0.53 after oblimin rotation, Supplementary material Appendix 1 Table A3). We consider the second component (Eigenvalue = 1.39, explained variance = 24%, Supplementary material Appendix 1 Table A3) to represent foraging movements. This component was high if individuals moved for longer durations, changed often between food patches and had a low variation in the duration of food patch visits (all loadings > 0.65, all |correlations| > 0.63 after oblimin rotation, Supplementary material Appendix 1 Table A3). Both composite variables from the open-field test were repeatable over time (boldness:  $R = 0.20 \pm 0.09$ , [0.01, 0.39],  $p = 0.017$ ; activity:  $R = 0.37 \pm 0.10$ , [0.16, 0.54],  $p < 0.001$ ). Likewise, both composite variables from the foraging test were repeatable across contexts (foraging intensity:  $R = 0.61 \pm 0.07$ , [0.47, 0.72],  $p < 0.001$ ; foraging movement:  $R = 0.38 \pm 0.09$ , [0.20, 0.43],  $p < 0.001$ ).

### Variation in foraging behaviour across risk treatments

When fully exposed against a white background, i.e. under high risk, jumping spiders reduced their foraging intensity compared to the lower risk while being camouflaged against a brown background (Table 1a, Fig. 2). Risk variation (recurrent presentation of a predator silhouette or absence thereof) had no effect on foraging intensity and the interaction between risk level and risk variation was not significant (Table 1a, Fig. 2). Larger jumping spiders had higher foraging intensity and with increasing experience with the test set-up individuals reduced foraging intensity (despite the simultaneous increase in starvation duration). Overall, the model explained 66% of the variation ( $R^2_{\text{conditional}}$ ) in foraging

Table 1a. Results of (generalized) linear mixed effects models of composite variables quantifying foraging intensity and foraging movements during the foraging test of individual foragers of *Marpissa muscosa* in resource landscapes varying in risk. Risk level refers to high-risk (white background) or low-risk (brown background) treatment, risk variation refers to constant risk (no simulated predator overflights) and variable risk (simulated predator overflights). Shown are effects ( $\beta$ ) and their standard error (SE) as well as p-values from model comparisons based on LR-tests, proportion of variance explained by the random effect individual, proportion of variance explained by the fixed effects ( $R^2_{\text{marginal}}$ ) and by fixed and random effects ( $R^2_{\text{conditional}}$ ). Significant effects are marked in bold. Non-significant control variables and interactions were removed from models, indicated by empty cells. The reference levels are 'low risk' and 'constant risk'.

Variable	Foraging intensity		Foraging movements	
	$\beta \pm \text{SE}$	p	$\beta \pm \text{SE}$	p
Intercept	-2.97 $\pm$ 1.74		0.11 $\pm$ 0.14	
Prosoma width	1.24 $\pm$ 0.61	<b>0.042</b>		
Order	-0.15 $\pm$ 0.04	<b>&lt;0.001</b>		
Risk level	-0.29 $\pm$ 0.09	<b>0.001</b>	-0.17 $\pm$ 0.12	0.169
Risk variation	-0.05 $\pm$ 0.09	0.605	-0.06 $\pm$ 0.12	0.639
Risk level $\times$ Risk variation				
$R^2_{\text{marginal}}$		0.10		0.01
$R^2_{\text{conditional}}$		0.66		0.38
Random effect variance		0.63		0.38

intensity; however, only 10% of the variation was explained by the fixed effects alone ( $R^2_{\text{marginal}}$ ) (Supplementary material Appendix 1 Fig. A3). Foraging movements neither varied with risk level nor with risk variation nor was the interaction of risk level and variation significant. Only the random effect contributed to the explained variation (Table 1a).

Analysing risk effects for specific behavioural variables alone revealed that jumping spiders varied many behaviours according to risk level and risk variation (Table 1b–1c). Specifically, under high risk level they reduced the duration spent in the arena, the duration spent foraging, the mean duration per feeding patch visit and the duration moving, but they entered the arena more frequently compared to low risk, camouflaged conditions. If exposed to recurrent simulated predator overflights, individuals entered the arena later and reduced the duration spent in the arena, but they increased the entries into the arena. The interaction between risk level and variation was only significant for the frequency of patch changes. Post hoc tests revealed, if risk was constant, individuals changed more often between food patches under high as compared to low risk ( $\beta = 0.16 \pm 0.03$ ,  $z = 4.99$ ,  $p < 0.001$ ), but if exposed to recurrent simulated predator overflights (variable risk) there was no difference between risk level treatments ( $\beta = -0.01 \pm 0.03$ ,  $z = 0.23$ ,  $p = 0.817$ ). If risk was high (white background), individuals changed less often if risk varied over time (silhouette present recurrently) as compared to constant risk (no silhouette present) ( $\beta = -0.12 \pm 0.03$ ,  $z = 4.19$ ,  $p < 0.001$ ). If risk was low, there was no difference between risk-variation treatments ( $\beta = 0.03 \pm 0.03$ ,  $z = 1.00$ ,  $p = 0.317$ ). For all behavioural variables, models explained between 16

Table 1b. Results of (generalized) linear mixed effects models of variables quantifying foraging intensity during the foraging test of individual foragers of *Marpissa muscosa* in resource landscapes varying in risk. Risk level refers to high-risk (white background) or low-risk (brown background) treatment, risk variation refers to constant risk (no simulated predator overflights) and variable risk (simulated predator overflights). Shown are effects ( $\beta$ ) and their standard error (SE) as well as p-values from model comparisons based on LR-tests, proportion of variance explained by the random effect individual, proportion of variance explained by the fixed effects ( $R^2_{\text{marginal}}$ ) and by fixed and random effects ( $R^2_{\text{conditional}}$ ). Significant effects are marked in bold. Non-significant control variables and interactions were removed from models, indicated by empty cells. The reference levels are 'low risk' and 'constant risk'.

Variable	Duration in arena (min)		Frequency of entries		Latency foraging (log-transformed, min)		Duration foraging (min)		Mean duration per visit	
	$\beta \pm \text{SE}$	p	$\beta \pm \text{SE}$	p	$\beta \pm \text{SE}$	p	$\beta \pm \text{SE}$	p	$\beta \pm \text{SE}$	p
Intercept	23.40 $\pm$ 14.58		6.30 $\pm$ 1.39		4.60 $\pm$ 0.17		-24.51 $\pm$ 32.36		-6.13 $\pm$ 8.08	
Prosoma width	10.73 $\pm$ 5.08	<b>0.035</b>	-1.57 $\pm$ 0.48	<b>0.001</b>			21.09 $\pm$ 11.29	0.062	5.27 $\pm$ 2.82	0.062
Order			0.15 $\pm$ 0.02	<b>&lt;0.001</b>			-2.39 $\pm$ 0.69	<b>&lt;0.001</b>	-0.60 $\pm$ 0.17	<b>&lt;0.001</b>
Risk level	-3.56 $\pm$ 1.30	<b>0.006</b>	0.16 $\pm$ 0.04	<b>&lt;0.001</b>	0.14 $\pm$ 0.18	0.412	-4.87 $\pm$ 1.55	<b>0.002</b>	-1.22 $\pm$ 0.39	<b>0.002</b>
Risk variation	-2.68 $\pm$ 1.30	<b>0.039</b>	0.27 $\pm$ 0.04	<b>&lt;0.001</b>	-0.38 $\pm$ 0.18	<b>0.029</b>	-0.47 $\pm$ 1.55	0.761	-0.11 $\pm$ 0.39	0.761
Risk level $\times$ Risk variation										
$R^2_{\text{marginal}}$		0.09		0.20		0.03		0.09		0.09
$R^2_{\text{conditional}}$		0.33		0.91		0.18		0.71		0.71
Random effect variance		0.27		0.42		0.16		0.68		0.68

and 91% of the variation ( $R^2_{\text{conditional}}$ ), but the explained variance was mainly due to the random effects.

### Among-individual covariation of behaviours: foraging behaviour syndromes

Activity in the open-field covaried positively with foraging intensity in the foraging test (Cov = 0.36, [0.01, 0.69]; Supplementary material Appendix 1 Table A4, Fig. 3). None of the other pairs of composite variables covaried significantly across tests (Supplementary material Appendix 1 Table A4).

## Discussion

In experimental landscapes of risks and resources, jumping spiders adjusted their foraging behaviour according to predictions of the general tradeoff between energy gain and predation avoidance (McNamara and Houston 1987, Lima

and Dill 1990, Lima 1998). Being more exposed to a background, individuals reduced some aspects of movement and foraging intensity, suggesting that the strength of camouflage serves as a proxy of perceived risk in these small cursorial predators. Short pulses of acute predation risk, simulated by bird overflights, had no general effects on foraging intensity and movement but modified some specific aspects of foraging behaviour. Notably, a significant part of variation in foraging was due to among-individual differences across different risk landscapes. These among-individual differences in foraging intensity covary with consistent individual variation in activity at the among-individual level, forming a behavioural syndrome. Below we discuss these findings in more detail.

### Jumping spiders adjusted foraging behaviour to the level of perceived risk

Animals that perceive predation risk, adjust their behaviour to balance resource intake with becoming a resource

Table 1c. Results of (generalized) linear mixed effects models of variables quantifying foraging movements during the foraging test of individual foragers of *Marpissa muscosa* in resource landscapes varying in risk. Risk level refers to high-risk (white background) or low-risk (brown background) treatment, risk variation refers to constant risk (no simulated predator overflights) and variable risk (simulated predator overflights). Shown are effects ( $\beta$ ) and their standard error (SE) as well as p-values from model comparisons based on LR-tests, proportion of variance explained by the random effect individual, proportion of variance explained by the fixed effects ( $R^2_{\text{marginal}}$ ) and by fixed and random effects ( $R^2_{\text{conditional}}$ ). Significant effects are marked in bold. Non-significant control variables and interactions were removed from models, indicated by empty cells. The reference levels are 'low risk' and 'constant risk'.

Variable	Duration moving (log-transformed, min)		Frequency of patch changes		CV of mean visit duration	
	$\beta \pm \text{SE}$	p	$\beta \pm \text{SE}$	p	$\beta \pm \text{SE}$	p
Intercept						
Prosoma width					1.10 $\pm$ 0.08	
Order			-0.04 $\pm$ 0.01	<b>&lt;0.001</b>		
Risk level	-0.24 $\pm$ 0.11	<b>0.037</b>	0.17 $\pm$ 0.03	<b>&lt;0.001</b>	-0.11 $\pm$ 0.07	0.117
Risk variation	-0.13 $\pm$ 0.11	0.243	0.04 $\pm$ 0.03	0.154	0.12 $\pm$ 0.07	0.099
Risk level $\times$ Risk variation			-0.18 $\pm$ 0.04	<b>&lt;0.001</b>		
$R^2_{\text{marginal}}$		0.02		0.04		0.02
$R^2_{\text{conditional}}$		0.49		0.88		0.31
Random effect variance		0.48		0.27		0.29

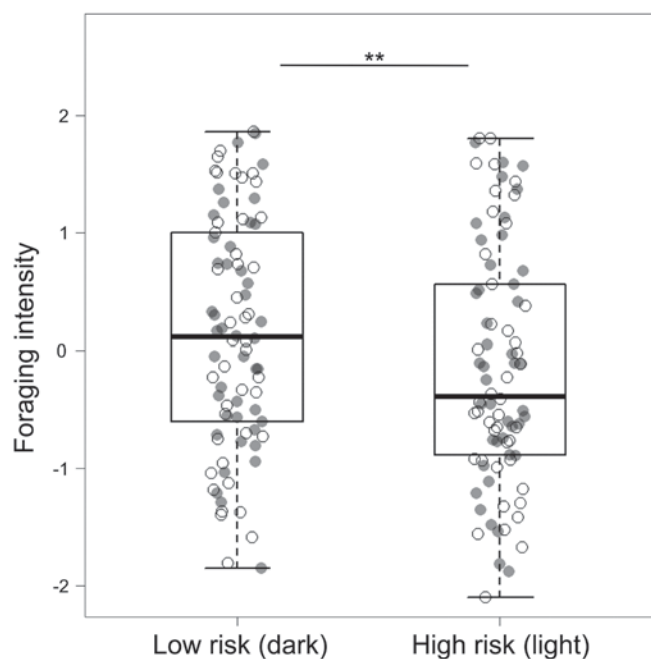


Figure 2. Foraging intensity in the low-risk and the high-risk treatment. Distribution of data indicated by dots (dark dots: constant risk; light dots: variable high risk, recurrent simulated bird overflights).

for others (Brown and Kotler 2004, Gaynor et al. 2019). The perception and subsequent behavioural response of an animal to a specific landscape of fear will depend to a large degree on the sensory and cognitive capabilities of the animal (Gaynor et al. 2019). Outstanding visual capabilities

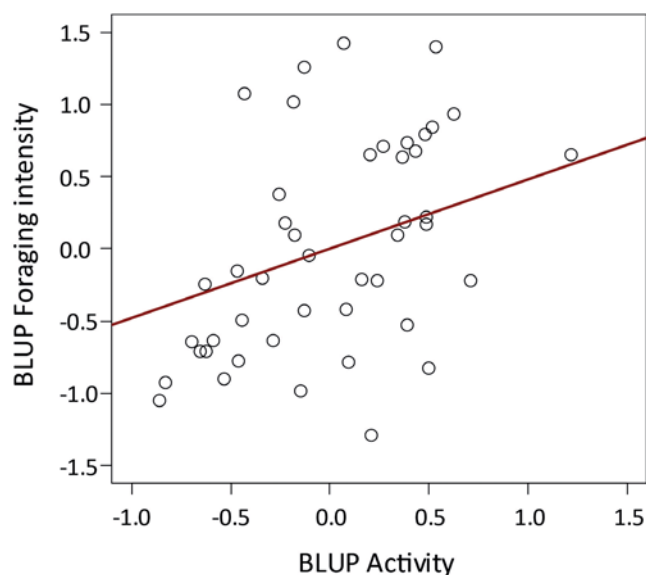


Figure 3. Among-individual correlation between activity in the open-field test and foraging intensity in the foraging test. Dots are best unbiased predictors (BLUPs), which indicate an individuals' mean behaviour across repeats (open-field test) or across foraging tests, estimated from the bivariate Bayesian mixed effects model.

for example, might enable an animal to plan ahead and better avoid predators (Mugan and MacIver 2020). Studies on a variety of animal taxa showed that prey and mesopredator individuals forage longer in safer habitats, i.e. those without predator cues, in the darkness or with more vegetation cover (Verdolin 2006, Mukherjee et al. 2009). When camouflaged against a brown background, jumping spiders in our experiment expressed higher foraging intensity, spent more time at food patches, and returned less often to the hide as compared to an environment where they were clearly exposed against a white background. This variation in foraging behaviour suggests that jumping spiders behave according to a background-matching strategy (Robledo-Ospina et al. 2017). Background-matching, or crypsis, is the most common anti-predator strategy in spiders (Pekár 2014). Spiders using this strategy have been shown to be less detectable by predators (Théry and Casas 2002, Defrize et al. 2010, Rubi et al. 2019). Interestingly, detectability of walking wolf spiders depended on how well they were camouflaged against the background, whereas background coloration had no influence on the detectability of stationary or courting wolf spiders (Rubi et al. 2019). Habitat selection is a complex process and probably always involves assessment and integration of a suite of different types of sensory information (e.g. in the jumping spider *Lyssomanes viridis*, Tedore and Johnsen 2015, 2016). Thus, by varying aspects of the physical landscape, namely the degree of visual camouflage, we created an experimental landscape that elicited changes in foraging behaviour. These results suggest that predation risk between treatments was perceived differently by the spiders, as different landscapes of fear (Gaynor et al. 2019). Measuring perceived risk more directly, i.e. in energetic costs of foraging via giving-up density (Brown 1999), is difficult in predators such as spiders that feed very infrequently. However, respirometry during foraging under risk, as used by Okuyama (2015) for the jumping spider *Hasarius adansoni*, might allow to quantify among-individual differences in energetic costs of perceived predation risk in future studies.

### Simulated bird overflights did not elicit a clear anti-predator reaction

In contrast to our predictions, recurrent simulated bird overflights had only small effects on foraging behaviour in the jumping spider. While it might seem counter-intuitive at first, simulated short pulses of acute risk had a weaker effect on spider behaviour than constant risk. This finding is in line with results from a meta-analysis by Verdolin (2006), which revealed that habitat characteristics elicit stronger behavioural adjustments in prey organisms than cues of live predators; albeit most of the data included in this analysis is based on rodents and vegetation cover (Verdolin 2006). Since crypsis is the most common passive defence in spiders (Pekár 2014), habitat characteristics should help to predict spatial variation of predation risk. Although birds are key predators of cursorial hunting spiders (Gunnarsson and Wiklander 2015), individuals in our tests responded to simulated bird overflights

only by starting to forage later and by spending more time under the hide. Similarly, wolf spiders sought shelter more often, but also increased locomotion, in response to simulated bird overflights (Lohrey et al. 2009). While spiders in our tests did not increase movement or mobility, we observed in pre-tests with individuals not used in the experiment that they jumped or ran backwards when the shadow passed over them. This behaviour, which could tentatively be interpreted as a startle response, also occurred during the experiments, but was only shown by some individuals and never in a consistent way. Given the excellent camouflage of *M. muscosa* in its natural environment, it is likely that the spiders freeze in response to an approaching predator and only flee in the very last moment – a typical anti-predator response of other jumping spider species (Stankowich 2009, Shamble et al. 2016). However, we did not observe a consistent freezing reaction towards the variable high-risk stimulus, and movement duration was not affected by it (Table 1c). Possibly, spiders habituated quickly to the regular (every 2 min) predator risk stimulus as they also reduced foraging intensity with increasing experience. Response decrement is prevalent in jumping spiders (Humphrey et al. 2018, Melrose et al. 2019, Nelson et al. 2019), but since individuals probably got hungrier over the test phases (three days without food during the first test, nine days during the last test), the response decrement might have been dampened.

### Individuals differed in behaviour over time and across contexts

Activity and boldness are consistent among-individual behavioural traits in various taxa (Bell et al. 2009), including jumping spiders (Royauté et al. 2014). A previous study, using a (differently staged) open-field test with *M. muscosa*, also reports repeatability of activity – and boldness-related behaviours (Liedtke et al. 2015). We show here that *M. muscosa* expresses especially high repeatability when trying to forage (mean time spent at a food patch and duration spent at the food patches; Table 1), indicating that some individuals showed consistently higher foraging intensity than others, in addition to the effects of the different risk levels. These findings support the idea that risk-taking during foraging is a personality trait (Dammhahn and Almeling 2012, Mella et al. 2015). Risk-taking during foraging is moderately heritable; as for example, the latency to resume feeding after a startling stimulus in great tits *Parus major* (van Oers et al. 2004). Moreover, as demonstrated experimentally in the field for *Anolis sagrei* lizards, selection on risk-taking varies with microhabitat use and the presence of predators (Lapiedra et al. 2018). How an individual trades off food rewards over safety likely has implications for both components of fitness. Risk-averse individuals that do not use foraging opportunities to avoid predation ought to have lower resource gain, while foregoing safety to access food might reduce survival prospects of risk-taking individuals. Since individuals of different behavioural types pick microhabitats according to their risk-taking propensity (Schirmer et al. 2019) or invest differently

into resource exploration and exploitation (Patrick et al. 2017), their fitness costs could be even under natural conditions (Patrick et al. 2017).

### Activity and foraging under risk represent a behavioural syndrome

Although individuals adjusted foraging to the different risk levels and risk variation in our experiment, the effect sizes were small. There was considerable variation in expressed behaviours and body size also significantly influenced foraging intensity (larger individuals had a higher foraging intensity and spent more time foraging). However, among-individual differences explained a prominent part of variation in all aspects of foraging behaviour under all risk levels and risk variation. Similarly, individual differences were the only predictor of anti-predator behaviour in wild-caught Arnhem rock rats, *Zygomys maini* (Cremona et al. 2015). As summarized in Toscano et al. (2016) and Moran et al. (2017), many aspects of foraging are associated with consistent behavioural traits, but only few studies experimentally disentangled intrinsic among-individual differences in general behaviour (e.g. boldness and spatial exploration) and in risk-taking during foraging and even less repeatedly assess foraging in different risk conditions (Dammhahn and Almeling 2012, Mella et al. 2015). Repeatedly testing individuals of jumping spiders in two functional contexts, i.e. satiated spatial exploration (open-field test) and hungry foraging (risk-landscape test), allowed us to estimate among-individual covariation between independently assessed behaviours. How active a satiated individual explores a novel environment is functionally linked to, and thus predictive for, how intensively this individual forages under risk. This behavioural integration into a behavioural syndrome provides an ecological validation of activity/exploration (sensu Réale et al. 2007) and should have consequences for fitness and for trophic interactions between species (Toscano et al. 2016, Moran et al. 2017). Thus, our results strongly suggest that individuals solve the tradeoff between food reward and safety differently with highly active individuals favouring resource gain over safety, whereas less active individuals favour safety over resource gain. Future studies should test whether and how these intrinsic individual differences along the safety-reward tradeoff are functionally integrated with pace-of-life syndromes (Réale et al. 2010, Dammhahn et al. 2018), stabilize variation in behavioural types in the population (Abbey-Lee and Dingemanse 2019), and affect ecological interactions along the food chain (Toscano et al. 2016, Moran et al. 2017).

### Conclusions

As predicted by theoretical models (McNamara and Houston 1987, Lima and Dill 1990, Lima 1998), a small mesopredator adjusted foraging behaviour to risk level and risk variation in artificial landscapes of fear. Notably, a large proportion of variation in risk-taking during foraging was due to among-individual differences and functionally integrated with

activity at the among-individual level. These results suggest that standardized experimental measures of activity predict individual variation in highly ecologically relevant behaviours such as foraging, providing an ecological validation of the personality trait activity for jumping spiders (Réale et al. 2007). The way an individual trades off perceived risk and resource gain, likely has implications for survival and reproductive success. Fascinating areas of future research will be to illuminate fitness consequences of risk-taking during foraging, as well as studying the mechanisms maintaining variation in risk-taking in populations. Small mesopredators with high among-individual variation in foraging under risk, such as *Marpissa muscosa*, will be suitable systems to explore potential cascading effects of this variation on trophic interactions and on modulation of food-web dynamics.

### Data availability statement

Data are available from the Dryad Digital Repository: <<http://dx.doi.org/10.5061/dryad.zpc866t73>> (Steinhoff et al. 2020).

**Acknowledgements** – The authors wish to thank Michaël Beaulieu and Peter Michalik for granting access to the EthoVision program and Rita Fragueira for an expert introduction into the program. We are indebted to Brian Schulze for help with programming and setting up the simulated bird stimulus. We thank Ingo Arnstedt, Elisabeth Böttcher, Tim M. Dederichs, Rebecca Meth and Felix Wrana for helping with pilot experiments. Open Access funding enabled and organized by Project DEAL.

**Funding** – This study was supported by a Bogislaw Scholarship from the University of Greifswald (to POMS) and by the German Science Foundation DFG UH 87/11-1 (to GU) and DA 1377/4-1 (to MD).

**Author contributions** – All authors had full access to all the data in the study and take responsibility for the integrity of the data and the accuracy of data analyses. MD and POMS conceived and designed the study. POMS, SV and BW performed the behavioural tests and the video analysis. MD and POMS analysed the data, all authors interpreted the results. MD and POMS wrote the first draft. All authors contributed to the writing of the final manuscript. POMS, GU and MD obtained funding.

**Conflicts of interest** – The authors have no conflicts of interest.

### References

- Abbey-Lee, R. N. and Dingemanse, N. J. 2019. Adaptive individual variation in phenological responses to perceived predation levels. – *Nat. Commun.* 10: 1601.
- Aguilar-Argüello, S. et al. 2019. Risk assessment and the use of novel shortcuts in spatial detouring tasks in jumping spiders. – *Behav. Ecol.* 30: 1488–1498.
- Archer, J. 1973. Tests for emotionality in rats and mice: a review. – *Anim. Behav.* 21: 205–235.
- Bell, A. M. et al. 2009. The repeatability of behaviour: a meta-analysis. – *Anim. Behav.* 77: 771–783.
- Bouskila, A. and Blumstein, D. T. 1992. Rules of thumb for predation hazard assessment: predictions from a dynamic model. – *Am. Nat.* 139: 161–176.
- Brown, J. S. 1999. Vigilance, patch use and habitat selection: foraging under predation risk. – *Evol. Ecol. Res.* 1: 49–71.
- Brown, J. S. and Kotler, B. P. 2004. Hazardous duty pay and the foraging cost of predation: foraging cost of predation. – *Ecol. Lett.* 7: 999–1014.
- Burnham, K. P. and Anderson, D. R. 2002. Model selection and multimodel inference: a practical information-theoretic approach. – Springer.
- Chang, C. et al. 2017a. Aggressive jumping spiders make quicker decisions for preferred prey but not at the cost of accuracy. – *Behav. Ecol.* 28: 479–484.
- Chang, C. et al. 2017b. Predator personality and prey behavioural predictability jointly determine foraging performance. – *Sci. Rep.* 7: 40734.
- Chang, C. et al. 2018. Aggressive spiders make the wrong decision in a difficult task. – *Behav. Ecol.* 29: 848–854.
- Cremona, T. et al. 2015. Do individual differences in behavior influence wild rodents more than predation risk? – *J. Mammal.* 96: 1337–1343.
- Crooks, K. R. and Soulé, M. E. 1999. Mesopredator release and avifaunal extinctions in a fragmented system. – *Nature* 400: 563–566.
- Dammhahn, M. and Almeling, L. 2012. Is risk taking during foraging a personality trait? A field test for cross-context consistency in boldness. – *Anim. Behav.* 84: 1131–1139.
- Dammhahn, M. et al. 2018. Pace-of-life syndromes: a framework for the adaptive integration of behaviour, physiology and life history. – *Behav. Ecol. Sociobiol.* 72: 62.
- Defrize, J. et al. 2010. Background colour matching by a crab spider in the field: a community sensory ecology perspective. – *J. Exp. Biol.* 213: 1425–1435.
- DePasquale, C. et al. 2014. Learning rate and temperament in a high predation risk environment. – *Oecologia* 176: 661–667.
- Dingemanse, N. J. and Dochtermann, N. A. 2013. Quantifying individual variation in behaviour: mixed-effect modelling approaches. – *J. Anim. Ecol.* 82: 39–54.
- Dingemanse, N. J. et al. 2012. Defining behavioural syndromes and the role of ‘syndrome deviation’ in understanding their evolution. – *Behav. Ecol. Sociobiol.* 66: 1543–1548.
- Edmunds, M. 1993. Does mimicry of ants reduce predation by wasps on salticid spiders? – *Mem. Queensl. Mus.* 33: 507–512.
- Farwell, M. and McLaughlin, R. L. 2009. Alternative foraging tactics and risk taking in brook charr (*Salvelinus fontinalis*). – *Behav. Ecol.* 20: 913–921.
- Foelix, R. 1996. *Biology of spiders*. – Oxford Univ. Press.
- Gaynor, K. M. et al. 2019. Landscapes of fear: spatial patterns of risk perception and response. – *Trends Ecol. Evol.* 34: 355–368.
- Gunnarsson, B. 2007. Bird predation on spiders: ecological mechanisms and evolutionary consequences. – *J. Arachnol.* 35: 509–529.
- Gunnarsson, B. and Wiklander, K. 2015. Foraging mode of spiders affects risk of predation by birds: predation risk in spiders. – *Biol. J. Linn. Soc.* 115: 58–68.
- Hadfield, J. D. 2010. MCMC methods for multi-response generalized linear mixed models: the MCMCglmm R package. – *J. Stat. Softw.* 33: 1–22.
- Houslay, T. M. and Wilson, A. J. 2017. Avoiding the misuse of BLUP in behavioural ecology. – *Behav. Ecol.* 28: 948–952.

- Houston, A. I. and McNamara, J. M. 1999. Models of adaptive behaviour: an approach based on state. – Cambridge Univ. Press.
- Humphrey, B. et al. 2018. Psychophysical investigation of vigilance decrement in jumping spiders: overstimulation or understimulation? – *Anim. Cogn.* 21: 787–794.
- Jakob, E. M. et al. 2007. Jumping spiders associate food with color cues in a T-maze. – *J. Arachnol.* 35: 487–492.
- Jordan, L. A. and Ryan, M. J. 2015. The sensory ecology of adaptive landscapes. – *Biol. Lett.* 11: 20141054.
- LaManna, J. A. and Martin, T. E. 2016. Costs of fear: behavioural and life-history responses to risk and their demographic consequences vary across species. – *Ecol. Lett.* 19: 403–413.
- Lapiedra, O. et al. 2018. Predator-driven natural selection on risk-taking behavior in anole lizards. – *Science* 360: 1017–1020.
- Laundre, J. W. et al. 2010. The landscape of fear: ecological implications of being afraid. – *Open Ecol. J.* 3: 1–7.
- Liedtke, J. et al. 2015. Early environmental conditions shape personality types in a jumping spider. – *Front. Ecol. Evol.* 3: 134.
- Lima, S. L. 1998. Nonlethal effects in the ecology of predator–prey interactions. – *BioScience* 48: 25–34.
- Lima, S. L. and Dill, L. M. 1990. Behavioral decisions made under the risk of predation: a review and prospectus. – *Can. J. Zool.* 68: 619–640.
- Lohrey, A. K. et al. 2009. Antipredator responses of wolf spiders (Araneae: Lycosidae) to sensory cues representing an avian predator. – *Anim. Behav.* 77: 813–821.
- McNamara, J. M. and Houston, A. I. 1987. Starvation and predation as factors limiting population size. – *Ecology* 68: 1515–1519.
- Mella, V. S. A. et al. 2015. Personality affects the foraging response of a mammalian herbivore to the dual costs of food and fear. – *Oecologia* 177: 293–303.
- Melrose, A. et al. 2019. Vigilance all the way down: vigilance decrement in jumping spiders resembles that of humans. – *Q. J. Exp. Psychol.* 72: 1530–1538.
- Michalko, R. et al. 2017. Link between aggressiveness and shyness in the spider *Philodromus albidus* (Araneae, Philodromidae): state dependency over stability. – *J. Insect. Behav.* 30: 48–59.
- Moran, N. P. et al. 2017. Weaving animal temperament into food webs: implications for biodiversity. – *Oikos* 126: 917–930.
- Mugan, U. and MacIver, M. A. 2020. Spatial planning with long visual range benefits escape from visual predators in complex naturalistic environments. – *Nat. Commun.* 11: 3057.
- Mukherjee, S. et al. 2009. Patch use in time and space for a mesopredator in a risky world. – *Oecologia* 159: 661–668.
- Nakagawa, S. and Schielzeth, H. 2010. Repeatability for gaussian and non-gaussian data: a practical guide for biologists. – *Biol. Rev.* 85: 935–956.
- Nakagawa, S. and Schielzeth, H. 2013. A general and simple method for obtaining  $R^2$  from generalized linear mixed-effects models. – *Methods Ecol. Evol.* 4: 133–142.
- Nelson, X. J. et al. 2019. The effect of stimulus encounter rate on response decrement in jumping spiders. – *Behav. Processes* 159: 57–59.
- Nyqvist, M. J. et al. 2012. Behavioural syndrome in a solitary predator is independent of body size and growth rate. – *PLoS One* 7: e31619.
- Okuyama, T. 2015. Metabolic responses to predation risk in a jumping spider: metabolic responses to threat. – *J. Zool.* 297: 9–14.
- Palmer, M. S. et al. 2017. A ‘dynamic’ landscape of fear: prey responses to spatiotemporal variations in predation risk across the lunar cycle. – *Ecol. Lett.* 20: 1364–1373.
- Patrick, S. C. et al. 2017. Boldness predicts an individual’s position along an exploration–exploitation foraging tradeoff. – *J. Anim. Ecol.* 86: 1257–1268.
- Pekár, S. 2014. Comparative analysis of passive defences in spiders (Araneae). – *J. Anim. Ecol.* 83: 779–790.
- Piovia-Scott, J. et al. 2017. The effect of lizards on spiders and wasps: variation with island size and marine subsidy. – *Ecosphere* 8: e01909.
- Réale, D. et al. 2007. Integrating animal temperament within ecology and evolution. – *Biol. Rev.* 82: 291–318.
- Réale, D. et al. 2010. Personality and the emergence of the pace-of-life syndrome concept at the population level. – *Phil. Trans. R. Soc. B* 365: 4051–4063.
- Ritchie, E. G. and Johnson, C. N. 2009. Predator interactions, mesopredator release and biodiversity conservation. – *Ecol. Lett.* 12: 982–998.
- Robledo-Ospina, L. E. et al. 2017. Two ways to hide: predator and prey perspectives of disruptive coloration and background matching in jumping spiders. – *Biol. J. Linn. Soc.* 122: 752–764.
- Royauté, R. et al. 2014. Interpopulation variations in behavioral syndromes of a jumping spider from insecticide-treated and insecticide-free orchards. – *Ethology* 120: 127–139.
- Rubi, T. L. et al. 2019. Courtship behavior and coloration influence conspicuousness of wolf spiders (*Schizocosa ocreata* (Hentz)) to avian predators. – *Behav. Processes* 162: 215–220.
- Schirmer, A. et al. 2019. Individuals in space: personality-dependent space use, movement and microhabitat use facilitate individual spatial niche specialization. – *Oecologia* 189: 647–660.
- Schirmer, A. et al. 2020. My niche: individual spatial niche specialization affects within- and between-species interactions. – *Proc. R. Soc. B* 287: 20192211.
- Shamble, P. S. et al. 2016. Airborne acoustic perception by a jumping spider. – *Curr. Biol.* 26: 2913–2920.
- Shores, C. R. et al. 2019. Mesopredators change temporal activity in response to a recolonizing apex predator. – *Behav. Ecol.* 30: 1324–1335.
- Sih, A. et al. 2004a. Behavioral syndromes: an ecological and evolutionary overview. – *Trends Ecol. Evol.* 19: 372–378.
- Sih, A. et al. 2004b. Behavioral syndromes: an integrative overview. – *Q. Rev. Biol.* 79: 241–277.
- Stankowich, T. 2009. When predators become prey: flight decisions in jumping spiders. – *Behav. Ecol.* 20: 318–327.
- Steinhoff, P. O. M. et al. 2020. Data from: Individual differences in risk-taking affect foraging across different landscapes of fear. – Dryad Digital Repository, <<http://dx.doi.org/10.5061/dryad.zpc866t73>>.
- Stoffel, M. A. et al. 2017. rptR: repeatability estimation and variance decomposition by generalized linear mixed-effects models. – *Methods Ecol. Evol.* 8: 1639–1644.
- Tedore, C. and Johnsen, S. 2015. Immunological dependence of plant-dwelling animals on the medicinal properties of their plant substrates: a preliminary test of a novel evolutionary hypothesis. – *Arthropod–Plant Interact.* 9: 437–446.
- Tedore, C. and Johnsen, S. 2016. Disentangling the visual cues used by a jumping spider to locate its microhabitat. – *J. Exp. Biol.* 219: 2396–2401.
- Théry, M. and Casas, J. 2002. Predator and prey views of spider camouflage. – *Nature* 415: 133–133.

- Toscano, B. J. et al. 2016. Personality, foraging behavior and specialization: integrating behavioral and food web ecology at the individual level. – *Oecologia* 182: 55–69.
- van Oers, K. et al. 2004. A genetic analysis of avian personality traits: correlated, response to artificial selection. – *Behav. Genet.* 34: 611–619.
- Verdolin, J. L. 2006. Meta-analysis of foraging and predation risk trade-offs in terrestrial systems. – *Behav. Ecol. Sociobiol.* 60: 457–464.
- Welch, R. J. et al. 2017. Hunter or hunted? Perceptions of risk and reward in a small mesopredator. – *J. Mammal.* 98: 1531–1537.
- Zuur, A. et al. 2009. Mixed effects models and extensions in ecology with R. – Springer Science & Business Media.



**Chapter 2: Visual pathways in the brain of the jumping spider *Marpissa muscosa***

Philip O.M. Steinhoff<sup>1\*</sup>, Gabriele Uhl<sup>1</sup>, Steffen Harzsch<sup>2</sup> & Andy Sombke<sup>3</sup>

<sup>1</sup> Zoological Institute and Museum, General and Systematic Zoology, University of Greifswald, Loitzer Straße 26, 17489 Greifswald, Germany.

<sup>2</sup> Zoological Institute and Museum, Cytology and Evolutionary Biology, University of Greifswald, Soldmannstraße 23, 17489 Greifswald, Germany

<sup>3</sup> Department of Integrative Zoology, University of Vienna, Althanstraße 14, 1090 Vienna, Austria



*\*Corresponding Author. E-Mail: philipsteinhoff@gmail.com*

*Manuscript published in the Journal of Comparative Neurology 528(11); doi: 10.1002/cne.24861*



## RESEARCH ARTICLE

# Visual pathways in the brain of the jumping spider *Marpissa muscosa*

Philip O. M. Steinhoff<sup>1</sup>  | Gabriele Uhl<sup>1</sup> | Steffen Harzsch<sup>2</sup> | Andy Sombke<sup>3</sup> 

<sup>1</sup>General and Systematic Zoology, Zoological Institute and Museum, University of Greifswald, Greifswald, Germany

<sup>2</sup>Cytology and Evolutionary Biology, Zoological Institute and Museum, University of Greifswald, Greifswald, Germany

<sup>3</sup>Department of Integrative Zoology, University of Vienna, Vienna, Austria

## Correspondence

Philip O. M. Steinhoff, General and Systematic Zoology, Zoological Institute and Museum, University of Greifswald, Loitzer Straße 26, 17489 Greifswald, Germany.  
Email: philipsteinhoff@gmail.com

## Funding information

Deutsche Forschungsgemeinschaft, Grant/Award Numbers: DFG INST 292/119-1 FUGG, DFG INST 292/120-1 FUGG, DFG UH 87/11-1; Laudier Histology Cooperation Travel Grant; Bogislaw scholarship, University of Greifswald

## Peer Review

The peer review history for this article is available at <https://publons.com/publon/10.1002/cne.24861>.

## Abstract

Some animals have evolved task differentiation among their eyes. A particular example is spiders, where most species have eight eyes, of which two (the principal eyes) are used for object discrimination, whereas the other three pairs (secondary eyes) detect movement. In the ctenid spider *Cupiennius salei*, these two eye types correspond to two visual pathways in the brain. Each eye is associated with its own first- and second-order visual neuropil. The second-order neuropils of the principal eyes are connected to the arcuate body, whereas the second-order neuropils of the secondary eyes are linked to the mushroom body. We explored the principal- and secondary eye visual pathways of the jumping spider *Marpissa muscosa*, in which size and visual fields of the two eye types are considerably different. We found that the connectivity of the principal eye pathway is the same as in *C. salei*, while there are differences in the secondary eye pathways. In *M. muscosa*, all secondary eyes are connected to their own first-order visual neuropils. The first-order visual neuropils of the anterior lateral and posterior lateral eyes are connected with a second-order visual neuropil each and an additional shared one (L2). In the posterior median eyes, the axons of their first-order visual neuropils project directly to the arcuate body, suggesting that the posterior median eyes do not detect movement. The L2 might function as an upstream integration center enabling faster movement decisions.

## KEYWORDS

brain, jumping spider, *Marpissa muscosa*, principal eyes, secondary eyes, visual neuropils, visual pathway, RRID AB\_1541510, RRID AB\_2315147, RRID AB\_2338680, RRID AB\_2534074, RRID AB\_2637882, RRID AB\_477585, RRID AB\_528479

**Abbreviations:** AB, arcuate body; ALE, anterior lateral eyes; AL1, first-order visual neuropils of ALE; AL2/PL2, second-order visual neuropils of ALE and PLE; AL1x, neuropilar subunit of the AL1; AME, anterior median eyes; AM1, first-order visual neuropils of AME; AM2, second-order visual neuropils of AME; L2, second-order visual neuropils of anterior and posterior lateral eyes; MB, mushroom bodies (neuropil with attributes of a mushroom body-like organization); MBbr, mushroom body bridge; MBn, neurites between pedunculus and AL2/PL2; MBh, mushroom body haft; MBp, pedunculus of the mushroom body; MBs, mushroom body shaft; PLE, posterior lateral eyes; PL1, first-order visual neuropils of the PLE; PL1x, neuropilar subunit of the PL1; PME, posterior median eyes; PM1, first-order visual neuropils of the PME; PM2, second-order visual neuropils of the PME; SC1-3, protocerebral soma cluster 1-3.

## 1 | INTRODUCTION

In some animal species with multiple eyes, different eyes serve different specific tasks, such as compound eyes and ocelli in insects or the rhopalia in box jellyfishes (Garm, O'Connor, Parkefeld, & Nilsson, 2007; O'Connor, Garm, & Nilsson, 2009; Paulus, 1979). Spiders vary strongly in their visual abilities, as well as in number, arrangement, and size of their eyes (reviewed in Morehouse, Buschbeck, Zurek,

This is an open access article under the terms of the Creative Commons Attribution-NonCommercial-NoDerivs License, which permits use and distribution in any medium, provided the original work is properly cited, the use is non-commercial and no modifications or adaptations are made.

© 2020 The Authors. *The Journal of Comparative Neurology* published by Wiley Periodicals, Inc.

Steck, & Porter, 2017). Most species possess four pairs of eyes, of which one pair differs from the three other pairs in its anatomy and developmental origin (Land, 1985b; Morehouse et al., 2017). The principal eyes (or anterior median eyes [AME]) possess a movable retina and their spectral sensitivities allow for color vision (Barth, Nakagawa, & Eguchi, 1993; Land, 1985a; Schmid, 1998; Yamashita & Tateda, 1976, 1978). The other three pairs of eyes are the so-called secondary eyes (posterior median, anterior lateral, and posterior lateral eyes). Their morphology and anatomy differs considerably among spider families (Homann, 1950, 1952), but they generally do not have a movable retina. In several groups of cursorial hunting spiders, the secondary eyes are used for movement detection (Land, 1985b; Morehouse et al., 2017; Schmid, 1998). Most secondary eyes possess a light-reflecting tapetum (but absent in e.g., jumping spiders), which led to the assumption that they play a major role for night or dim light vision (Foelix, 1996).

Jumping spiders (Salticidae) are cursorial hunters with excellent vision. Their eyes have been studied in much greater detail compared to any other spider group (e.g., Harland, Li, & Jackson, 2012; Land, 1985b; Morehouse et al., 2017). The principal eyes of jumping spiders are large and face forward; their field of view is small, but their spatial acuity is one of the highest among invertebrate eyes (Harland et al., 2012; Land, 1985a; Morehouse et al., 2017). The secondary eyes of salticids possess only one photoreceptor type and thus cannot discriminate colors (Yamashita & Tateda, 1976). Among the secondary eyes, the anterior lateral eyes (ALE) and posterior lateral eyes (PLE) are large, able to detect motion, and elicit an orienting response of the principal eyes toward the moving object (Duelli, 1978; Jakob et al., 2018; Spano, Long, & Jakob, 2012; Zurek & Nelson, 2012a, 2012b; Zurek, Taylor, Evans, & Nelson, 2010). The posterior median eyes (PME) of most salticids (except for the non-salticoids) are very small and positioned between ALE and PLE (Land, 1985a; Maddison & Hedin, 2003). Since the fields of view of ALE and PLE overlap, the PME do not have an exclusive field of view (Land, 1985a).

Although the eyes of jumping spiders have been studied in detail, less is known about the brain structures that process visual information (but see Duelli, 1980; Hanström, 1921; Hill, 1975; Nagata, Arikawa, & Kinoshita, 2019; Steinhoff et al., 2017; Strausfeld, 2012). Our knowledge on the visual processing pathways in the brain of spiders is mostly based on investigations of the ctenid spider species *Cupiennius salei* (Keyserling, 1877) (Babu & Barth, 1984; Becherer & Schmid, 1999; Schmid & Duncker, 1993; Strausfeld & Barth, 1993; Strausfeld, Weltzien, & Barth, 1993). *C. salei* possesses two separate visual pathways, one for the principal eyes and one for all secondary eyes (Strausfeld et al., 1993; Strausfeld & Barth, 1993). In *C. salei*, every eye is connected to its own first- and second-order visual neuropil (Barth, 2002). Although the second-order visual neuropils of the principal eyes are connected to the arcuate body (AB; Strausfeld et al., 1993), the second-order visual neuropils of the secondary eyes are associated with the mushroom bodies (Strausfeld & Barth, 1993). Additionally, the first-order visual neuropils of the secondary eyes are directly connected to the AB (Babu & Barth, 1984).

In *C. salei*, similar to salticids, the principal eyes are used for object recognition, while the secondary eyes serve the purpose of movement

detection (Fenk, Hoinkes, & Schmid, 2010; Schmid, 1998). The secondary eyes of *C. salei* have a high spectral sensitivity, similar to their principal eyes (Barth et al., 1993) and similar to jumping spiders are capable of acute motion detection (Fenk & Schmid, 2010; Zurek & Nelson, 2012a). However, they are unable to detect color in moving objects (Orlando & Schmid, 2011) and the relative size of different eyes and thus fields of view in *C. salei* differ considerably from jumping spiders (Land, 1985a; Land & Barth, 1992). Furthermore, Steinhoff et al. (2017) showed that the structure and arrangement of the secondary eye visual neuropils in the jumping spider *Marpissa muscosa* (Clerck, 1757) differ from those in *C. salei*. We thus hypothesize, that the secondary eye visual pathways of jumping spiders also differ from that in the ctenid spider species *C. salei*. Here, we describe the principal and secondary eye visual pathways in the brain of the jumping spider *M. muscosa*. We use paraffin histology, immunohistochemistry, and microCT analysis to visualize tracts in the visual system. We compare our findings in *M. muscosa* with results of earlier studies and new immunohistochemical data on the principal and secondary eye pathways in the brain of *C. salei*. We discuss the similarities and differences in the principal and secondary eye pathways of these two spider species in the light of different functional roles of their eyes.

## 2 | MATERIAL AND METHODS

### 2.1 | Animals

Adult female *M. muscosa* were collected in and near Greifswald (Germany). Spiders were fed on *Drosophila* sp. weekly and kept individually in plastic boxes of 145 x 110 x 68 mm size that were enriched with paper tissue.

### 2.2 | Paraffin-histology

The prosomata of two females of *M. muscosa* were fixed in Gregory's artificially aged Bouin solution (Gregory, 1980). After 4 days in fixative, the prosomata were dehydrated through a graded ethanol series (80, 90, and 3x 96% ethanol for 20 min each) and were then transferred for 2 hr into a 1:1 solution of 96% ethanol:tetrahydrofuran (Carl Roth, CP82.1) at room temperature. Samples were kept for 24 hr in pure tetrahydrofuran followed by 24 hr in a solution of 1:1 tetrahydrofuran and paraffin (Carl Roth, 6643.1) at 60°C. Afterward, samples were transferred to 100% paraffin at 60°C for 48 hr and then embedded in fresh paraffin. Sagittal and transversal sections (5 µm) were cut with a motorized rotary microtome (Microm HM 360). Sections were stained with Azan according to Geidies (Schulze & Graupner, 1960), and mounted in Roti-Histokitt II (Carl Roth, T160.1).

### 2.3 | MicroCT analysis

Prosomata of two individuals of *M. muscosa* and one individual of *C. salei* were fixed in Dubosq-Brazil solution (1 g saturated

**TABLE 1** Primary and secondary antibodies

Labeling reagent	Dilution and specifications
<i>Primary</i>	
Monoclonal anti-synapsin antibody produced in mouse (RRID AB_528479)	1:1,000, DSHB 3C11 (Steinhoff et al., 2017; this study)
Polyclonal anti $\alpha$ -tubulin antibody produced in rabbit (RRID AB_2637882)	1:1,000 or 1:250, ThermoFisher PA5-58711
Monoclonal anti-acetylated $\alpha$ -tubulin antibody produced in mouse (RRID AB_477585)	1:1000, Sigma Aldrich T6793
Monoclonal anti-histamine antibody produced in rabbit (RRID AB_1541510)	1:1,000, Progen 16043 (Harzsch, Wildt, Battelle, & Waloszek, 2005; Sombke & Harzsch, 2015)
<i>Secondary</i>	
Polyclonal Cy3 anti-mouse IgG secondary antibody produced in goat (RRID AB_2338680)	1:500, Jackson Immuno Research, 115-165-003
Polyclonal Alexa 488 anti-rabbit IgG secondary antibody produced in goat (RRID AB_2534074)	1:500, Invitrogen, A11006
Alexa Fluor 488 phalloidin (RRID AB_2315147)	1:50, Molecular Probes A-12379
Hoechst 33258	1:1000, Sigma 14530
YOYO 1491	Molecular Probes Y-3601

**TABLE 2** Methods and antisera combinations

Methods	Antisera combinations/staining	Coupled with	Specimens
Wholemout	Anti-synapsin	Cy3 anti-mouse (goat)	5
Vibratome sections (50 $\mu$ m; 80 $\mu$ m)	Anti-synapsin (mouse)	Cy3 anti-mouse (goat)	16
	Anti- $\alpha$ -tubulin (rabbit)	Alexa Fluor 488 anti-rabbit (goat) Nuclear labeling: Hoechst 33258	
	Anti-acetylated- $\alpha$ -tubulin (mouse)	Nuclear labeling: YOYO	6
	Anti-histamine (rabbit)	Alexa Fluor 488 anti-rabbit (goat)	4
	Anti-synapsin (mouse)	Cy3 anti-mouse (goat) Phalloidin	5
Paraffin sections (5 $\mu$ m)	Azan-novum	/	2
microCT scans	1% iodine (in 99% ethanol)	/	4

alcoholic picric acid, 150 ml 80% ethanol, 15 ml pure acetic acid, and 60 ml 37% formaldehyde). Prior to fixation, legs and opisthosomata were cut off and cuticle and musculature were removed from the dorsocaudal part of the prosomata to allow faster penetration of the fixative. After 4 days in fixative, samples were washed six times for 20 min in 0.1M phosphate buffered saline (PBS, pH 7.4) followed by dehydration in a graded ethanol series (80, 90, 96, and 3x 99.8% ethanol for 20 min each). Samples were then transferred to an 1% iodine solution (iodine, resublimated [Carl Roth, X864.1] in 99.8% ethanol) over 48 hr to enhance tissue contrast (Sombke, Lipke, Michalik, Uhl, & Harzsch, 2015) and subsequently critical point dried with an automated dryer (Leica EM CPD300). The protocol applied was: slow CO<sub>2</sub> admittance with a delay of 120 s, 30 exchange cycles, followed by a slow heating process and slow gas discharge. Dried prosomata were mounted using a conventional glue gun onto aluminum rods, so that the AME were oriented upward.

MicroCT scans were performed using a Zeiss XradiaXCT-200 (Sombke et al., 2015). Scans were performed with a macro-, a 4x-, and a 20x objective lens unit and the following settings: 40 kV and 8 W or 30 kV and 6 W, 200  $\mu$ A, exposure times between 2 and 4 s. Tomographic projections were reconstructed with the XMRReconstructor software (Zeiss), resulting in image stacks (TIFF format). Scans were performed using Binning 2 for noise reduction and were reconstructed with full resolution (using Binning 1).

## 2.4 | Immunohistochemistry

Four different combinations of markers were used to visualize neuropils and connecting neurites in the visual system (see Table 1 for a list of marker combinations used, and Table 2 for specifications of labeling reagents).

After anaesthetization with CO<sub>2</sub>, brains of 31 females of *M. muscosa* (details Table 2) and four females of *C. salei* were

dissected in PBS and fixed in 4% paraformaldehyde over night at room temperature. Specimens for histamine immunohistochemistry were prefixed overnight at 4°C in 4% *N*-(3-dimethylaminopropyl)-*N'*-ethylcarbodiimide hydrochloride (EDAC, Sigma-Aldrich E6383). Brains were washed six times for 15 min each in PBS and subsequently immersed in poly-L-lysine (Sigma-Aldrich, P4707) for 1 min. Samples were then embedded in 10% or 4% agarose (Sigma-Aldrich, A9414) and sectioned (50 or 80 μm) with a Microm HM 650V vibratome. After permeabilization in PBS-TX (PBS, 0.3% Triton X-100 [Sigma-Aldrich, X100], 1% bovine serum albumin [Sigma-Aldrich, A2153], 0.05% Na-acide; or alternatively PBS, 0.5% Triton, 1.5% DMSO) for 1 hr at room temperature, incubation in primary antibodies took place over night at 4°C or room temperature. Sections were washed in several changes of PBS-TX after the incubation. Incubation in secondary antibodies or counterstains took place overnight at 4°C or room temperature. After washing in several changes of PBS, sections were mounted in Mowiol (Merck 475904).

The brains of five additional females of *M. muscosa* were processed as whole-mounts, using an adjusted protocol after Ott (2008; see also Steinhoff et al., 2017). Brains were dissected in TRIS buffer (0.1M, pH 7.4 [Carl Roth, 4855]), and fixed in zinc-formaldehyde at room temperature under soft agitation for several days. Afterward, brains were washed in TRIS buffer three times for 15 min each and incubated in a 4:1 mixture of methanol and DMSO (dimethylsulfoxide [Carl Roth, 4720]) for 2 hr. After incubation in 100% methanol for 1 hr, brains were rehydrated in a graded series of methanol (90, 70, 50, and 30%) for 10 min each and washed in TRIS buffer. This was followed by permeabilization in PBS-DMSO (PBS, 5% bovine serum albumin, 1% DMSO, 0.05% Na-acide) for 2 hr at room temperature and incubation in primary antibody for 4 days at 4°C. Brains were then washed several times for 2 hr in PBS-DMSO and incubated in secondary antibody for 4 days at 4°C, and transferred to a graded series of glycerol, with 1, 2, and 4% (for 2 hr each) and 8, 15, 30, 50, 60, 70, and 80% (for 1 hr each) glycerol in TRIS buffer and 1% DMSO. After five changes in pure ethanol for 30 min each, brains were mounted in fresh methyl salicylate (Sigma, 76631). In control experiments, in which we replaced the primary antibodies with PBS-TX, no neuronal labeling was detected.

## 2.5 | Western blot

In western blots of *Drosophila melanogaster* Meigen, 1830 head homogenates (Klagges et al., 1996), the monoclonal antibody mouse anti-*Drosophila* synapsin "Synorf 1" (provided by E. Buchner, Universität Würzburg, Germany; raised against a *Drosophila* Glutathione S-Transferase[GST]-synapsin fusion protein) recognizes at least 4 synapsin isoforms (ca. 70, 74, 80, and 143 kDa). In western blot analyses in Crustacea (Harzsch & Hansson, 2008; Sullivan, Benton, Sandeman, & Beltz, 2007) and Chilopoda (Sombke, Harzsch, & Hansson, 2011), isoforms in the same range (75–90 kDa) were recognized. Furthermore, the Synorf 1 antibody labels synaptic neuropil in taxa as diverse as Araneae (Fabian-Fine, Volkandt, & Seyfarth, 1999; Nagata

et al., 2019; Steinhoff et al., 2017; Widmer, Höger, Meisner, French, & Torkkeli, 2005), Chaetognatha (Harzsch & Müller, 2007) and Plathelminthes (Cebrià, 2008), suggesting that the epitope that this antiserum recognizes is highly conserved. To test this, we conducted a western blot analysis as well, in which we compared brain tissue of *D. melanogaster* and *M. muscosa*. The antibody provided similar results for both species, staining one strong band around 70 kDa, and in *M. muscosa* another weak band around 60 kDa. This result suggests that the epitope that Synorf 1 recognizes is conserved between *D. melanogaster* and *M. muscosa*.

## 2.6 | Microscopy, image processing, and nomenclature

Immunohistochemically labeled sections and whole-mounts were examined and photographed with a Leica SP5 II confocal microscope (cLSM). Paraffin sections were examined and photographed with a customized Visionary Digital BK Plus Lab System (duninc.com/bk-plus-lab-system.html). 3D-visualization of microCT image stacks was prepared in AMIRA 6.0.0 (ThermoFisher). An interactive 3D-visualization of the microCT reconstructions was created using ImageJ 1.51n and Adobe Acrobat Pro 9.0 (see Figure S1). Images were processed in Corel PaintShop Pro using global contrast and brightness adjustment features as well as black and white inversion. Schematic drawings were generated using Corel Draw 20.1 and figure plates were assembled in Corel PaintShop Pro 21.0. A color code for all depicted structures, as used in Loesel, Wolf, Kenning, Harzsch, and Sombke (2013) and Steinhoff et al. (2017), was used for 3D visualizations and the schematic drawings. The terminology used for brain structures follows Richter et al. (2010). For structures specific to spiders, we use terms according to Lehmann et al. (2016), Strausfeld et al. (1993), and Strausfeld and Barth (1993). Positional information is given with respect to the body axis. We are referring to results from immunohistochemical experiments as immunoreactivity, for example, synapsin-immunoreactivity.

## 3 | RESULTS

### 3.1 | General organization of the protocerebrum

In *M. muscosa*, the protocerebrum comprises bilaterally paired neuropils of the visual system and the mushroom body as well as the unpaired AB and the protocerebral neuropil (Figures 1 and 2; for details see Steinhoff et al., 2017). All neuropils of the visual system are recognizable in paraffin sections (Figure 3) and microCT analysis (Figure 4; Figure S1), and are also characterized by a strong synapsin-immunoreactivity (Figures 1, 5, 6, and 7a,b). Tracts and individual neurites exhibit prominent tubulin-immunoreactivity (Figures 1, 2, and 5–7). Furthermore, the optic nerves (between retinae and first-order visual neuropils) and the corresponding first-order visual neuropils display histamine-immunoreactivity (Figure 8), which is known to

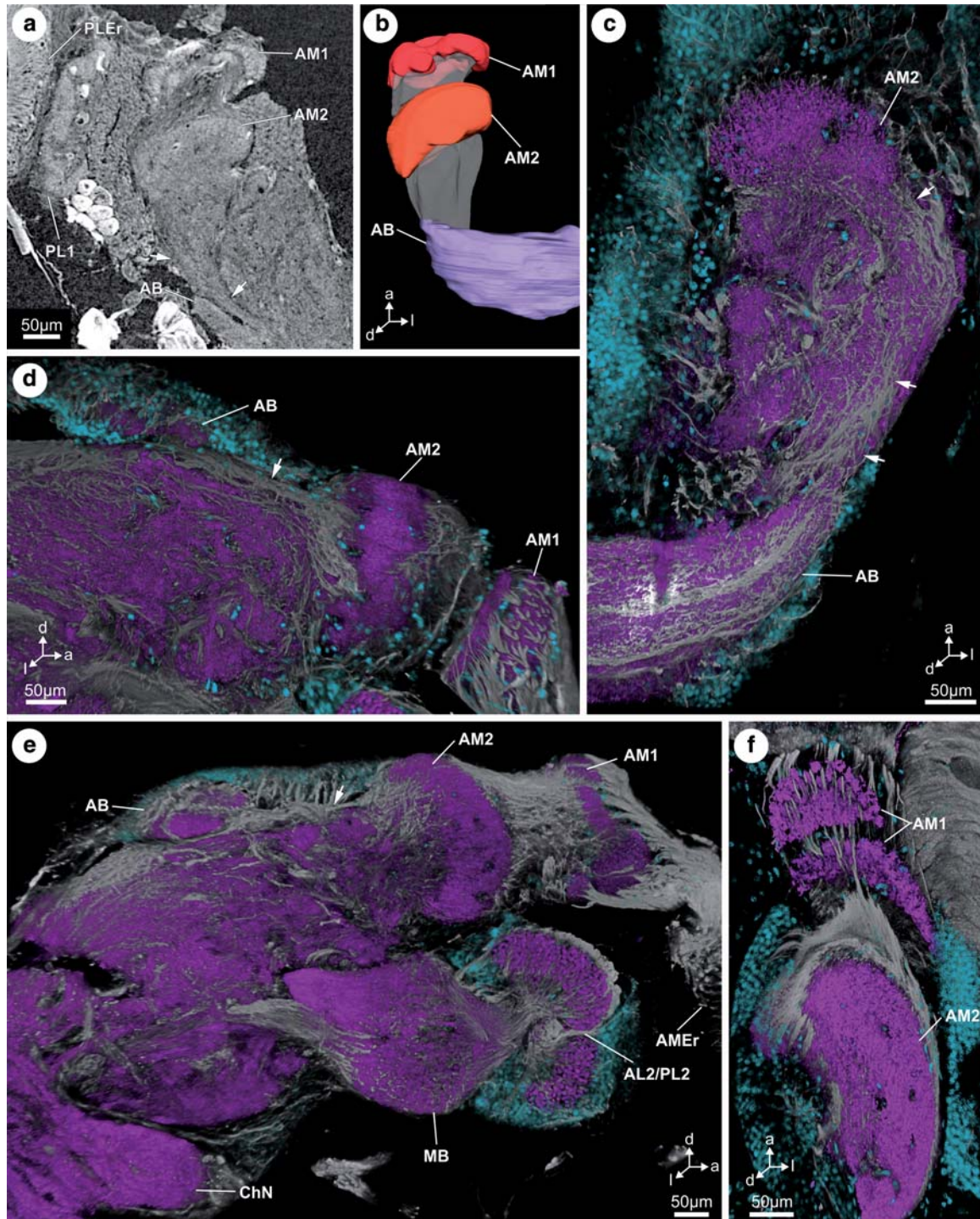


**FIGURE 1** The principal eye pathway in *Maripissa muscosa*. (a) Virtual horizontal section of the dorsal protocerebrum, obtained by microCT analysis, shows the connections between the AM1, AM2 and the AB. (b) Three-dimensional reconstruction based on a microCT image stack shows the same connections as in (a). (c–f) Maximum projection of image stacks (clsm), show tubulin-immunoreactivity (gray), and somata (blue) in the protocerebrum of *M. muscosa*. (c) Horizontal section showing the AM2, the AB, and connecting neurites (arrows). (d) Sagittal section through the AM1, AM2, and the AB showing the connecting neurites between AM2 and AB (arrow). (e) Sagittal section showing at least two lobes of the AM1, the thick tract to the AM2, and the thinner connection to the AB (arrow). AL2/PL2 and MB are also visible. (f) Horizontal section showing two lobes of the AM1, retinula cell axons terminating in those and interneurons connecting AM1 with AM2. Abbreviations: a, anterior; AB, arcuate body; AL2/PL2, second-order visual neuropil of anterior lateral and posterior lateral eyes; AM1, first-order visual neuropil of the anterior median eyes; AM2, second-order visual neuropil of the anterior median eyes; AMEr, retina of the anterior median eyes; ChN, cheliceral neuropil; d, dorsal; l, lateral; MB, mushroom body; PL1, first-order visual neuropil of the posterior lateral eyes; PLer, retina of the posterior lateral eyes; PM1, first-order visual neuropil of the posterior median eyes [Color figure can be viewed at [wileyonlinelibrary.com](http://wileyonlinelibrary.com)]



**FIGURE 2** Maximum projection of an image stack (clsm), showing tubulin-immunoreactivity (gray) and somata (blue) in the protocerebrum of *Marpissa muscosa*. The AL1 and PL1 are connected to both, the AL2/PL2 and the L2. The neurites forming these connections originate in SC1. The AL2/PL2 and the L2 are connected to the MBp via neurites, which originate in the SC2. The two MBp are connected with each other via the mushroom body bridge, which is formed by long neurites that project along the periphery of the MBp and seem to originate in the SC2. Some of these long neurites also connect the MBp with the MBh. Other neurites originate in SC3 and enter the protocerebrum medially. Abbreviations: a, anterior; AL1, first-order visual neuropil of the anterior lateral eyes; AL2/PL2, second-order visual neuropil of ALE and PLE; d, dorsal; l, lateral; L2, shared second-order visual neuropil of the anterior lateral and posterior lateral eyes; MBh, mushroom body haft; MBp, mushroom body pedunculus; SC1-3, soma cluster 1-3 [Color figure can be viewed at [wileyonlinelibrary.com](http://wileyonlinelibrary.com)]

consistently label retinula cell axons and their terminals in the visual systems of arthropods (Battelle et al., 1991; Harzsch et al., 2005, 2006; Nässel, 1999; Schmid & Duncker, 1993; Sombke & Harzsch, 2015). A soma cortex including three discernable protocerebral clusters surrounds most of the central nervous system

(Figures 2, 5, 6a,b,d, and 7a-d). Soma cluster 1 (SC1) is located between the first-order visual neuropils of the lateral eyes and their second-order visual neuropil (AL2/PL2), cluster 2 (SC2) medially to the AL2/PL2, and cluster 3 (SC3) anteromedially to the mushroom body bridge (MBp; Figure 2).



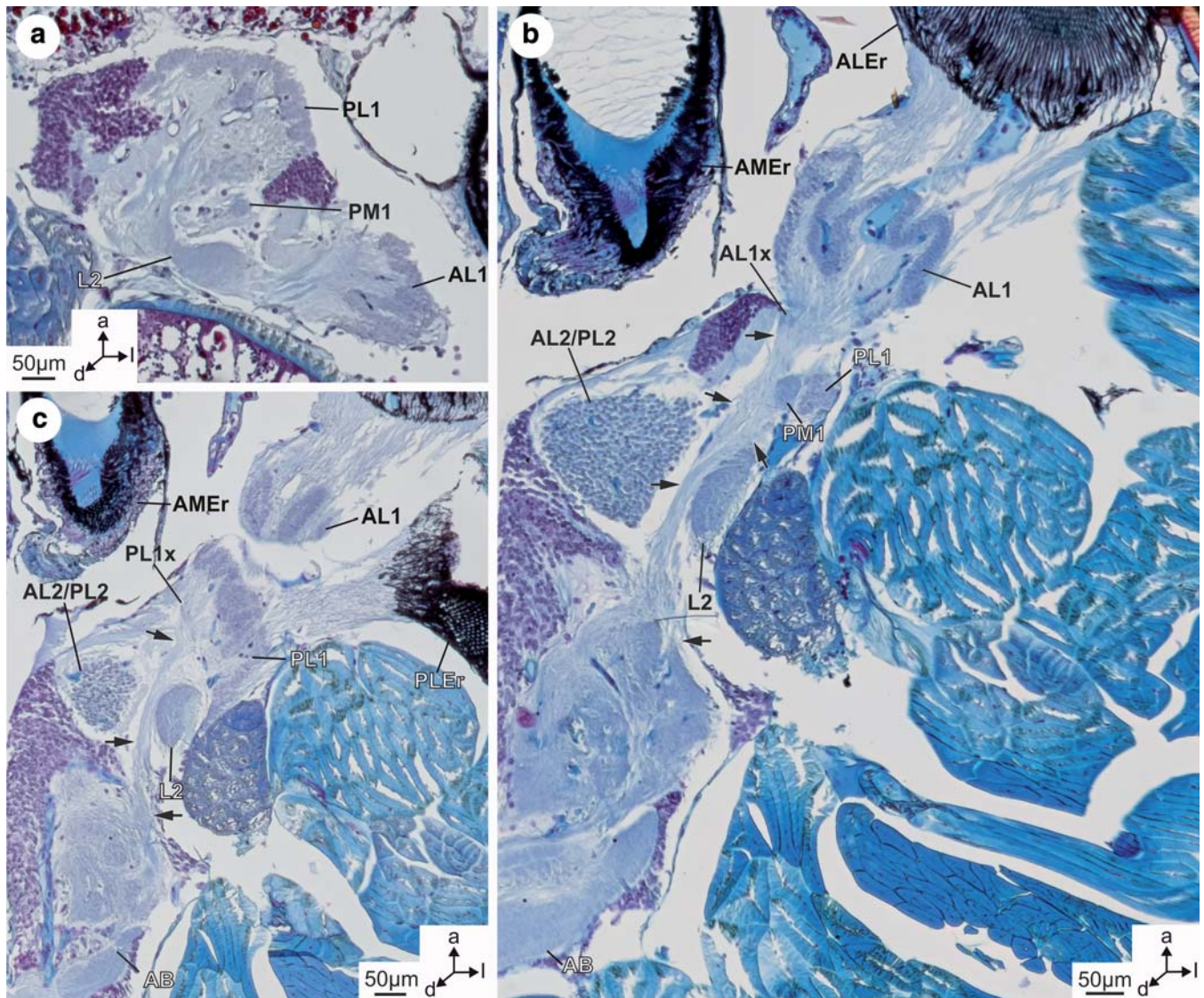


**FIGURE 3** Paraffin sections through the anterior protocerebrum of *Maripissa muscosa*. (a) Sagittal section showing the conspicuous tracts that connect the AL1 and PL1 with the L2. (b) Horizontal section showing the convoluted and columnar structure of the AL1. Neurites that connect the AL1 with the AB probably synapse in the AL1x. Long neurites connecting the PL1 with the AB are visible curving around L2. Other long neurites contributing to the tract to the AB synapse in PM1. Arrows point to neurites contributing to the tract between first-order visual neuropils of the secondary eyes and the arcuate body. (c) Horizontal section showing several neurites that connect the PL1 with the AL2/PL2, as well as the neurites contributing to the tract between the PL1 and the AB (highlighted by arrows). Abbreviations: a, anterior; AB, arcuate body; AL1, first-order visual neuropil of the anterior lateral eyes; AL1x, neuropilar subunit of the AL1; AL2/PL2, second-order visual neuropil of anterior lateral and posterior lateral eyes; ALEr, retina of the anterior lateral eyes; AMEr, retina of the anterior median eyes; d, dorsal; l, lateral; L2, shared second-order visual neuropil of the anterior lateral and posterior lateral eyes; PL1, first-order visual neuropil of the posterior lateral eyes; PLEr, retina of the anterior lateral eyes; PL1x, neuropilar subunit of the PL1; PM1, first-order visual neuropil of the posterior median eyes [Color figure can be viewed at [wileyonlinelibrary.com](http://wileyonlinelibrary.com)]

### 3.2 | The principal eye pathway

The retina of the AME is connected to its first-order visual neuropil (AM1), which consists of at least two, but most likely four tightly adjoining subunits (Figure 1a,e,f). The AM1 is situated close to the second-order visual neuropil of the AME (AM2) and connected to it

via parallel neurites (Figure 1e,f). The AM2 is large, oval shaped and its posterior margin within the protocerebral neuropil is not clearly recognizable in anti-synapsin labeling (Figure 1). Anti-tubulin labeling reveals a tract of neurites that connects the AM2 with the lateral flanges of the AB, as well as some neurites with unclear termination that penetrate the protocerebral neuropil (Figure 1c–e).

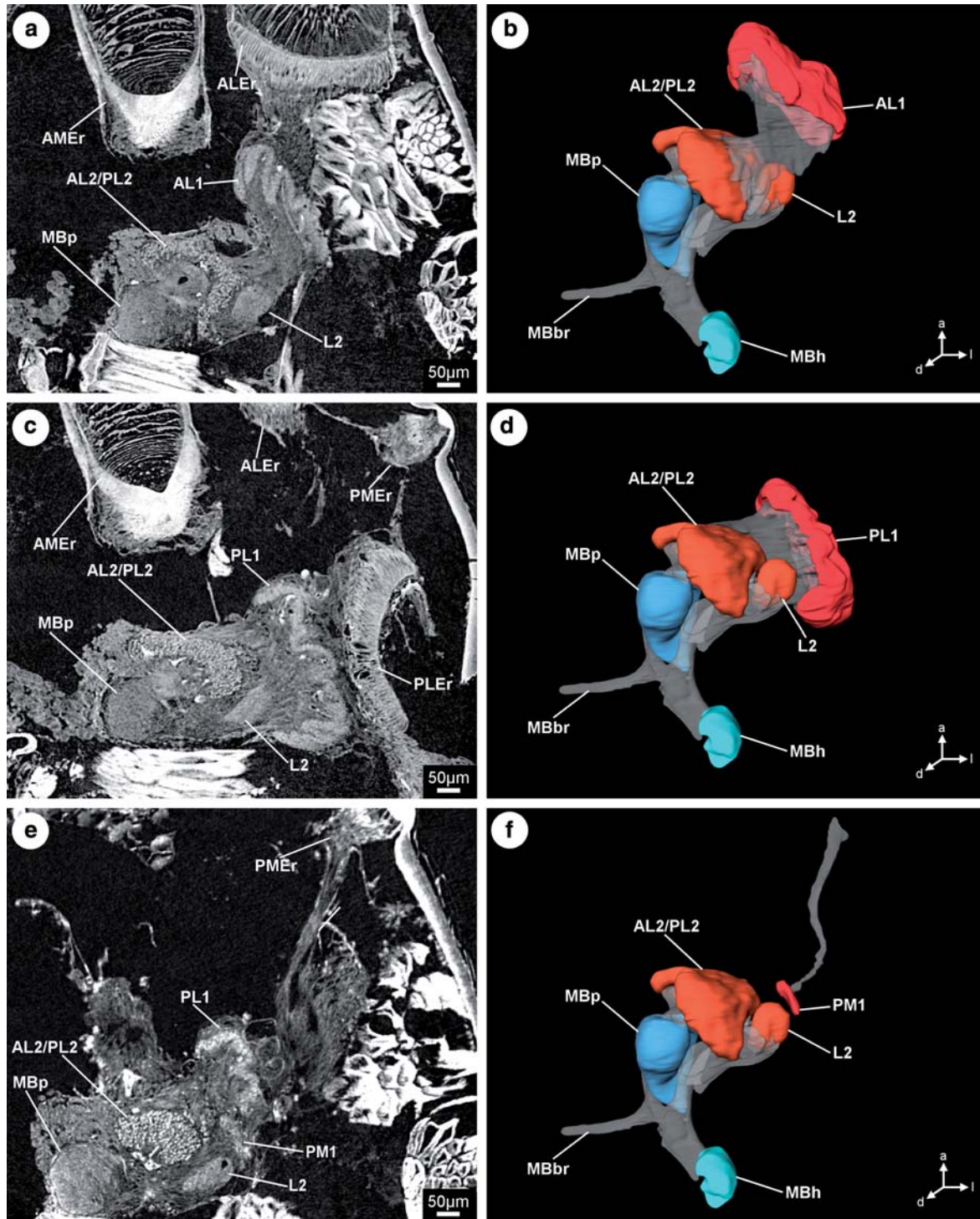


**FIGURE 4** Protocerebral neuropils depicted in different virtual horizontal sections obtained by microCT analysis (a, c, e) and three-dimensional reconstructions based on microCT image stacks (b, d, f). (a and b) The retina of the ALE is located very closely to its first-order visual neuropil, the AL1. The AL1 has a convoluted surface and is connected to the AL2/PL2 and the L2. (c and d) The retina of the PLE almost comes in contact with its first-order visual neuropil, the PL1. The PL1 has a convoluted surface and is connected to the MB and the L2. (e and f) A comparatively long optic nerve connects the retina of the PME with its first-order visual neuropil, the PM1. See Supporting Information for an interactive 3D-visualization of the microCT reconstruction. Abbreviations: a, anterior; AL1, first-order visual neuropil of the anterior lateral eyes; AL2/PL2, second-order visual neuropil of anterior lateral and posterior lateral eyes; ALEr, retina of the anterior lateral eyes; AMEr, retina of the anterior median eyes; d, dorsal; l, lateral; L2, shared second-order visual neuropil of the anterior lateral and posterior lateral eyes; MBbr, mushroom body bridge; MBh, mushroom body haft; MBp, mushroom body pedunculus; PL1, first-order visual neuropil of the posterior lateral eyes; PLEr, retina of the posterior lateral eyes; PM1, first-order visual neuropil of the posterior median eyes; PME, retina of the posterior median eyes [Color figure can be viewed at [wileyonlinelibrary.com](http://wileyonlinelibrary.com)]

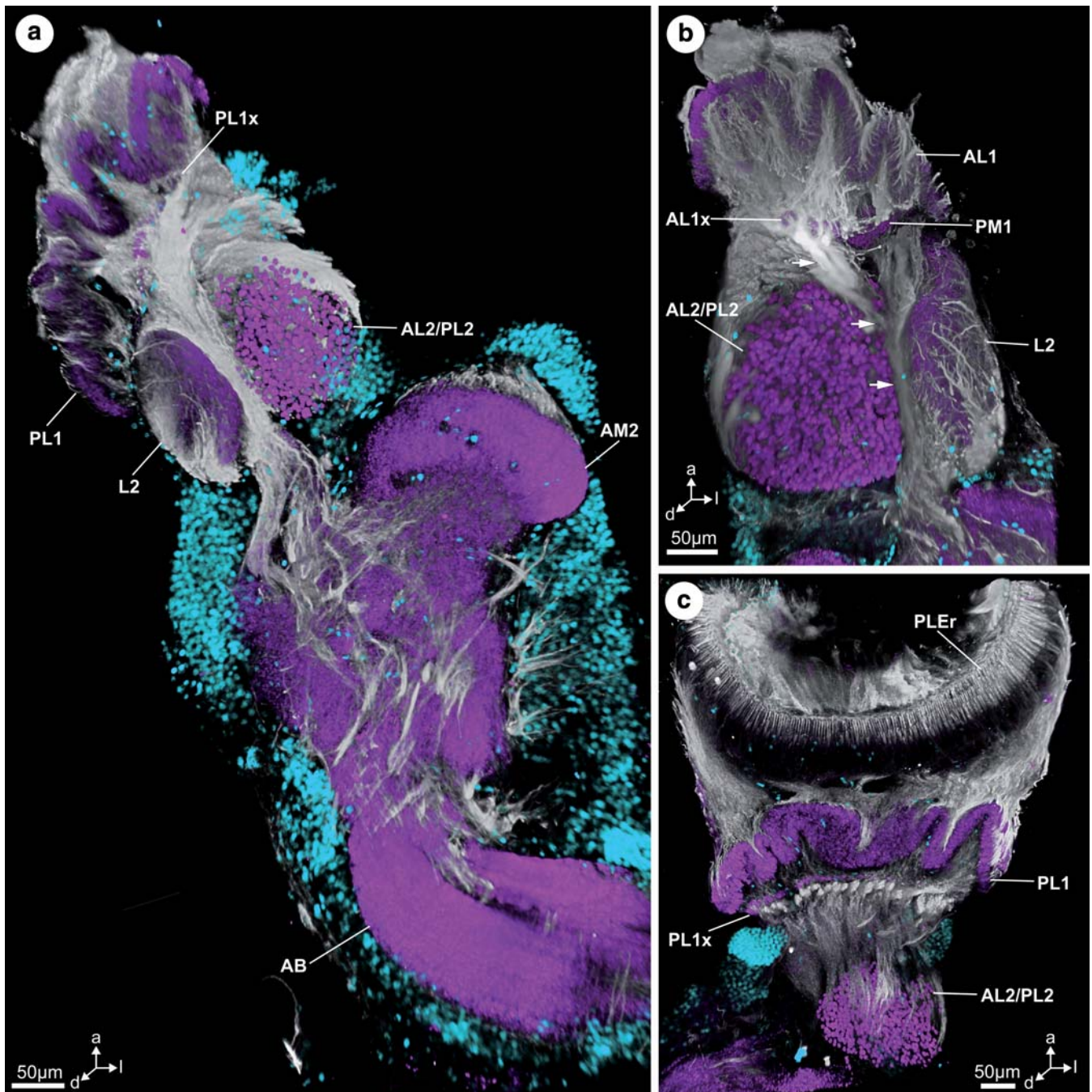


**FIGURE 5** Maximum projections of image stacks (clsm) showing tubulin-immunoreactivity (gray), synapsin-immunoreactivity (magenta), and somata (blue) in the secondary eye visual pathway of *Maripissa muscosa*. (a) Neurites from the PL1 pass between AL2/PL2 and L2 toward the AB. (b) Neurites from AL1x join the tract from the PM1 that passes through between AL2/PL2 and L2 (highlighted by arrows). (c) The PL1 is in close spatial relationship to the PLEr. Parallel neurites connect the PL1 and PL1x with the AL2/PL2. Abbreviations: a, anterior; AB, arcuate body; AL1, first-order visual neuropil of the anterior lateral eyes; AL1x, neuropilar subunit of the AL1; AL2/PL2, second-order visual neuropil of anterior lateral and posterior lateral eyes; AM2, second-order visual neuropil of the anterior median eyes; d, dorsal; l, lateral; L2, shared second-order visual neuropil of the anterior lateral and posterior lateral eyes; MBp, mushroom body pedunculus; PL1, first-order visual neuropil of the posterior lateral eyes; PL1x, neuropilar subunit of the PL1; PLEr, retina of the posterior lateral eyes; PM1, first-order visual neuropil of the posterior median eyes [Color figure can be viewed at [wileyonlinelibrary.com](http://wileyonlinelibrary.com)]

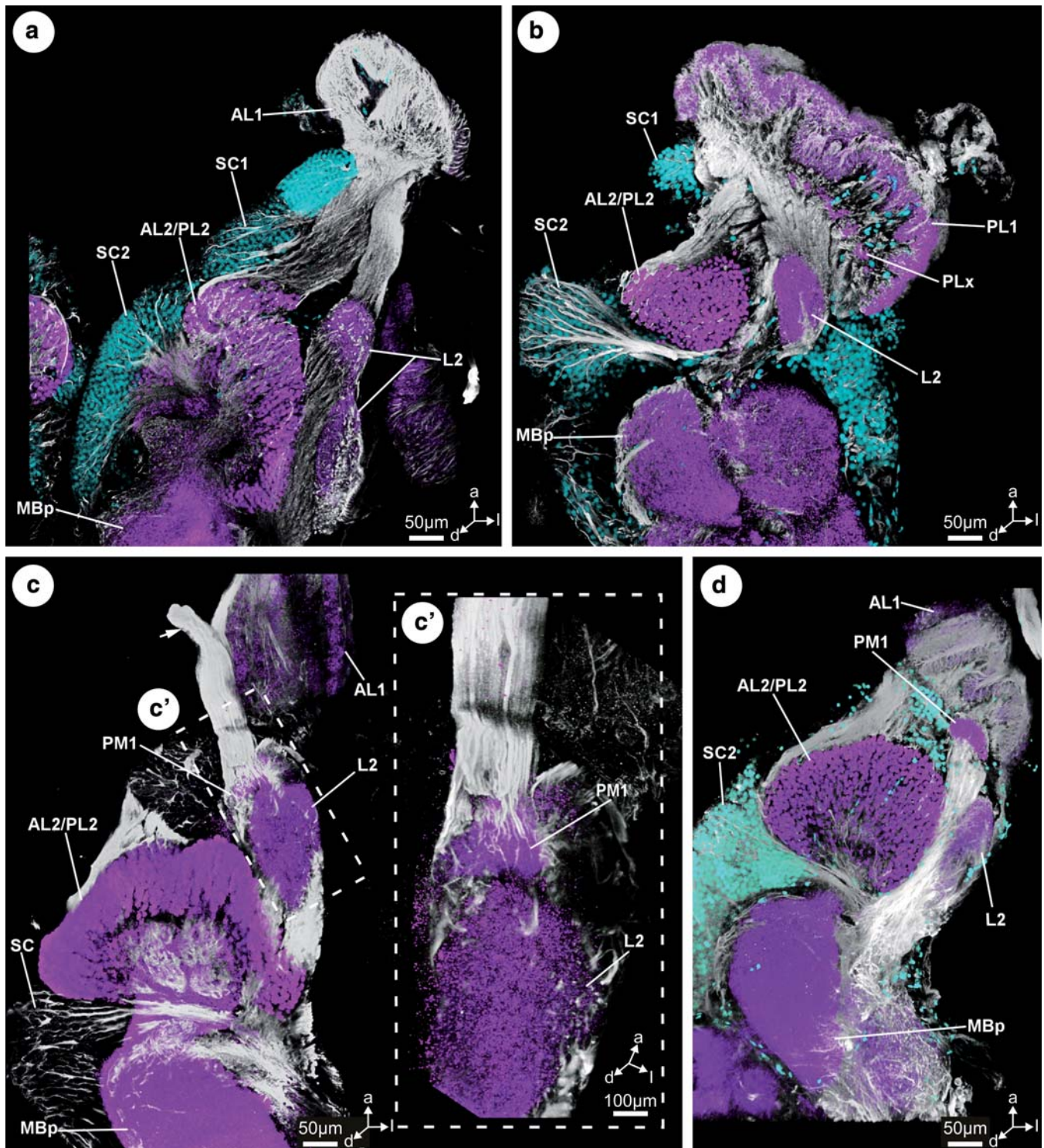
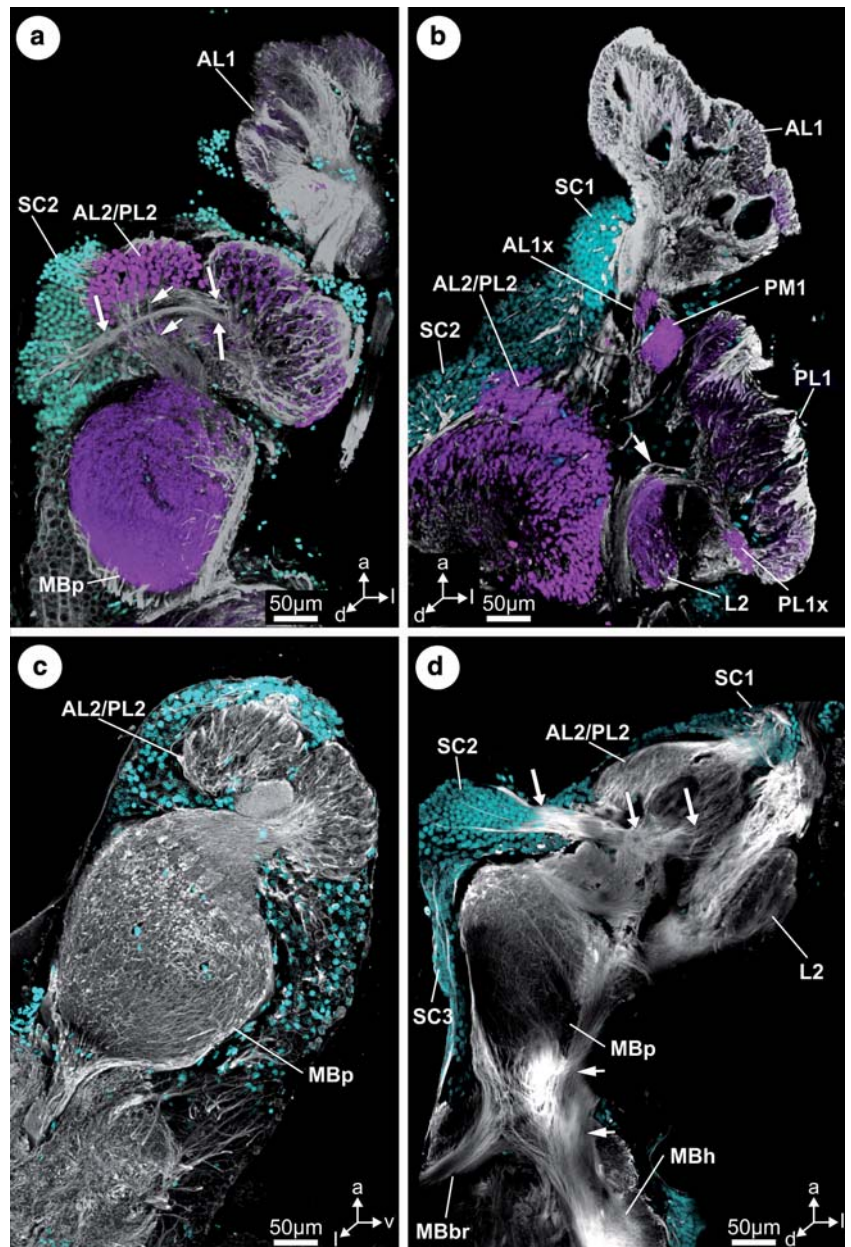


**FIGURE 6** Maximum projections of image stacks (clsm) showing tubulin-immunoreactivity (gray), synapsin-immunoreactivity (magenta), and somata (blue) in the secondary eye visual pathway of *Maripissa muscosa*. (a) The AL1 is connected to the AL2/PL2 and the L2 via two prominent neurite tracts. Some of the neurites contributing to these tracts originate in SC1. Neurites connecting the AL2/PL2 with the MBp originate in SC2. (b) The PL1 is connected to the AL2/PL2 and the L2 via two prominent neurite tracts. Some neurites that arise in SC2 pass between AL2/PL2 and MBp toward the L2. (c) The optic nerve of the PME (highlighted by arrow) terminates in the PM1. (c') Higher magnification of c, showing the termination site of the PME optic nerve in the PM1. (d) Neurites from the PM1 pass between AL2/PL2 and L2. Abbreviations: a, anterior; AL1, first-order visual neuropil of the anterior lateral eyes; AL2/PL2, second-order visual neuropil of anterior lateral and posterior lateral eyes; MBp, mushroom body pedunculus; PL1, first-order visual neuropil of the posterior lateral eyes; PL1x, neuropilar subunit of the PL1; PM1, first-order visual neuropil of the posterior median eyes; SC1-2, soma cluster 1-2 [Color figure can be viewed at [wileyonlinelibrary.com](http://wileyonlinelibrary.com)]

**FIGURE 7** Maximum projections of image stacks (clsm) showing tubulin-immunoreactivity (gray), synapsin-immunoreactivity (magenta), and somata (blue) in the secondary eye visual pathway of *Marpissa muscosa*. (a) Horizontal section through AL1, MBp and AL2/PL2. The AL1 connects to one of the two tightly adjoining clusters of AL2/PL2. Arrows point to primary neurites connecting SC2 and AL2/PL2. Arrowheads point to neurites connecting the AL2/PL2 with the MBp. (b) Horizontal section through visual neuropils. The PM1 is situated between AL1 and PL1, AL2/PL2 appear as a uniform array. The arrowhead points to neurites connecting PL1 with AB, neurites probably synapse in the PL1x. (c) A sagittal section through AL2/PL2 and MBp reveals two distinct clusters of AL2/PL2 and the chiasm formed by neurites that connect AL2/PL2 with the MBp. (d) Tubulin-immunoreactivity shows long peripheral neurites contributing to the MBbr and connecting the MBp with the MBh. Arrows point to primary neurites connecting SC2 with the AL2/PL2. Arrowheads point to neurites connecting the MBp with the MBh. Abbreviations: a, anterior; AL1, first-order visual neuropil of the anterior lateral eyes; AL1x, neuropilar subunit of the AL1; AL2/PL2, second-order visual neuropil of anterior lateral and posterior lateral eyes; d, dorsal; l, lateral; L2, shared second-order visual neuropil of the anterior lateral and posterior lateral eyes; MBbr, mushroom body bridge; MBh, mushroom body haft; MBp, mushroom body pedunculus; PL1, first-order visual neuropil of the posterior lateral eyes; PL1x, neuropilar subunit of the PL1; PM1, first-order visual neuropil of the posterior median eyes; SC1-3, soma cluster 1-3 [Color figure can be viewed at [wileyonlinelibrary.com](http://wileyonlinelibrary.com)]



### 3.3 | Connectivity of the first-order visual neuropils of the anterior and posterior lateral eyes

The retinae of the ALE and PLE are connected with their respective first-order visual neuropils (AL1 and PL1) via short, thick optic nerves (Figure 3b,c, 4a,b, and 5c). A subpopulation of histaminergic neurites, which are interpreted here as retinula cell axons, terminates in distinct distal layers of these neuropils (AL1x and PL1x; Figure 8a–c). Both the AL1 and PL1 are connected to the second-order visual neuropil of the lateral eyes (L2) and the AL2/PL2 via prominent tracts of parallel ordered neurites that exhibit strong tubulin-immunoreactivity (Figures 2, 5, 6a,b,d, and 7a,b). This connectivity is also evident in both, histological sections (Figure 3) and microCT analysis (Figure 4). The tracts are predominantly formed by neurites that originate in SC1, which surrounds this region of the anterior protocerebrum

laterally, dorsally, and medially (Figures 2, 6, and 7b,d). The L2 and the AL2/PL2 are bi-lobed, which corresponds to the separate inputs from AL1 and PL1 (Figures 3a, 3b,d, 5a, 6a,c, and 8a,b). In histological sections, a thin but conspicuous tract is detectable that passes between L2 and AL2/PL2 and likely terminates in the AB (Figures 3b,c, 5a,b, 6d, and 7b). The neurites forming this tract might originate in SC1 and further innervate the AL1x and PL1x, as well as the PM1 (see below; Figures 3, 5, and 6d).

### 3.4 | Connectivity of the first-order visual neuropils of the posterior median eyes

The PME are much smaller than all three other pairs of secondary eyes, and so is their retina (Figure 4c,e). Because of the small retina,

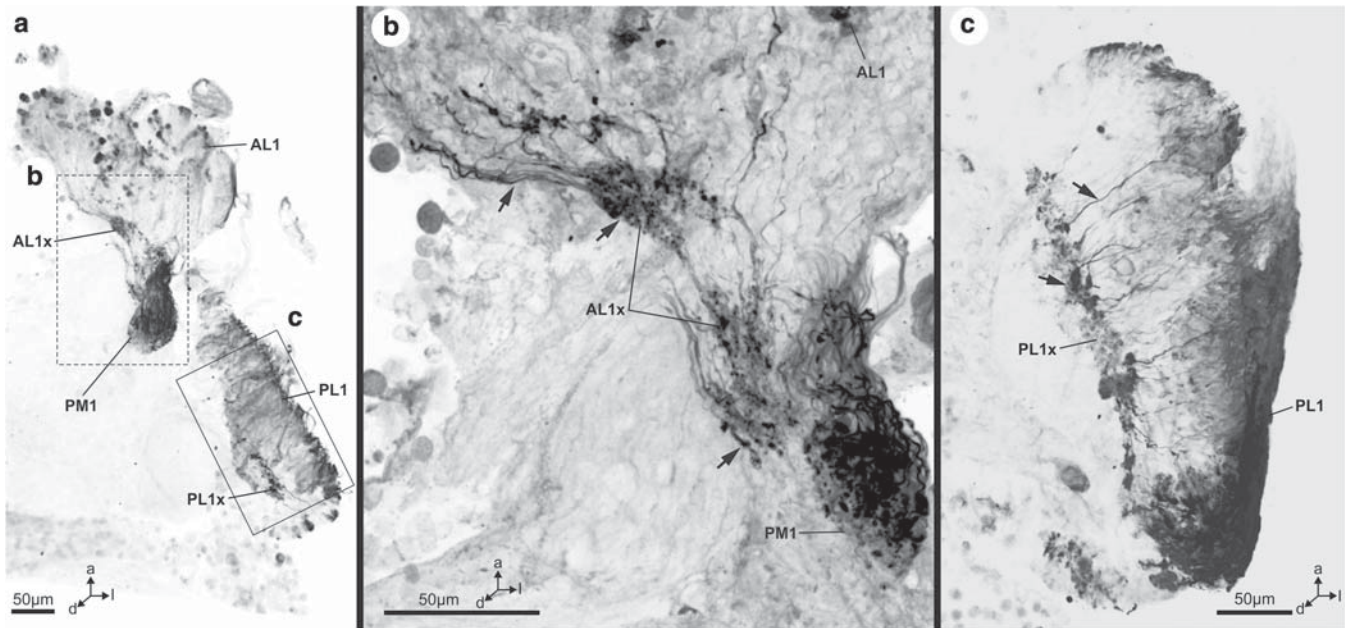


**FIGURE 8** Maximum projections of image stacks (clsm), showing histamine-immunoreactivity in horizontal sections through the anteriormost protocerebrum of *Marpissa muscosa*. (a) Overview shows strong histamine-immunoreactivity of retinula cell axon terminals in the AL1 and its substructure the AL1x, as well as in the PL1 and its substructure the PL1x. Retinula cell axons of the PME and their terminals in the PM1 exhibit strong histamine-immunoreactivity. (b) Magnification showing histamine-immunoreactive retinula cell axons and their terminals in the AL1x and PM1. Note the close spatial association of AL1x and PM1; AL1x is somewhat distorted due to sectioning. Arrows point to histamine-immunoreactive retinula cell axons and their terminals. (c) Magnification showing histamine-immunoreactive retinula cell axons and their terminals in the PL1 and PL1x. Arrows point to a retinula cell axon and a large terminal in the PL1x. Abbreviations: a, anterior; AL1, first-order visual neuropil of the anterior lateral eyes; AL1x, neuropilar subunit of the AL1; d, dorsal; l, lateral; PL1, first-order visual neuropil of the posterior lateral eyes; PL1x, neuropilar subunit of the PL1; PM1, first-order visual neuropil of the posterior median eyes

only a thin but long nerve, which enters the protocerebrum between the AL1 and PL1, connects the PME to its first-order visual neuropil (PM1; Figures 4e and 6c,c'). The PM1 is situated between AL1 and PL1 (Figures 3a,b, 4e, 5b, 6c,d, 7b, and 8a). A prominent tract projects from the PM1 to the dorsoventral part of the protocerebrum and seems to terminate in the anterolateral apices of the AB (Figure 3b, 5b, and 6d).

### 3.5 | The second-order visual neuropil of anterior lateral eyes, posterior lateral eyes and the mushroom body

The second-order visual neuropil of ALE and PLE (AL2/PL2) is of glomerular organization and composed of two lobes that tightly adjoin dorsally and are fused in their ventral part (Figures 7a,c,d and 9a,b). Thus, only an uniform array of glomeruli is visible in most sections (Figures 3b, 4a,c,e, 5, and 6). Each glomerulus is composed of a high number of synaptic complexes (Figure 9c–e). These synaptic complexes can be visualized by anti-synapsin labeling and phalloidin-labeling (Figure 9d,e). Co-localization of synapsin and f-actin is almost absent (Figure 9). Individual glomeruli are innervated by neurites originating in the AL1 and PL1 (Figures 5c, 6a,b,d, and 7d). Anti-tubulin labeling reveals that neurites interweave the array of glomeruli mostly

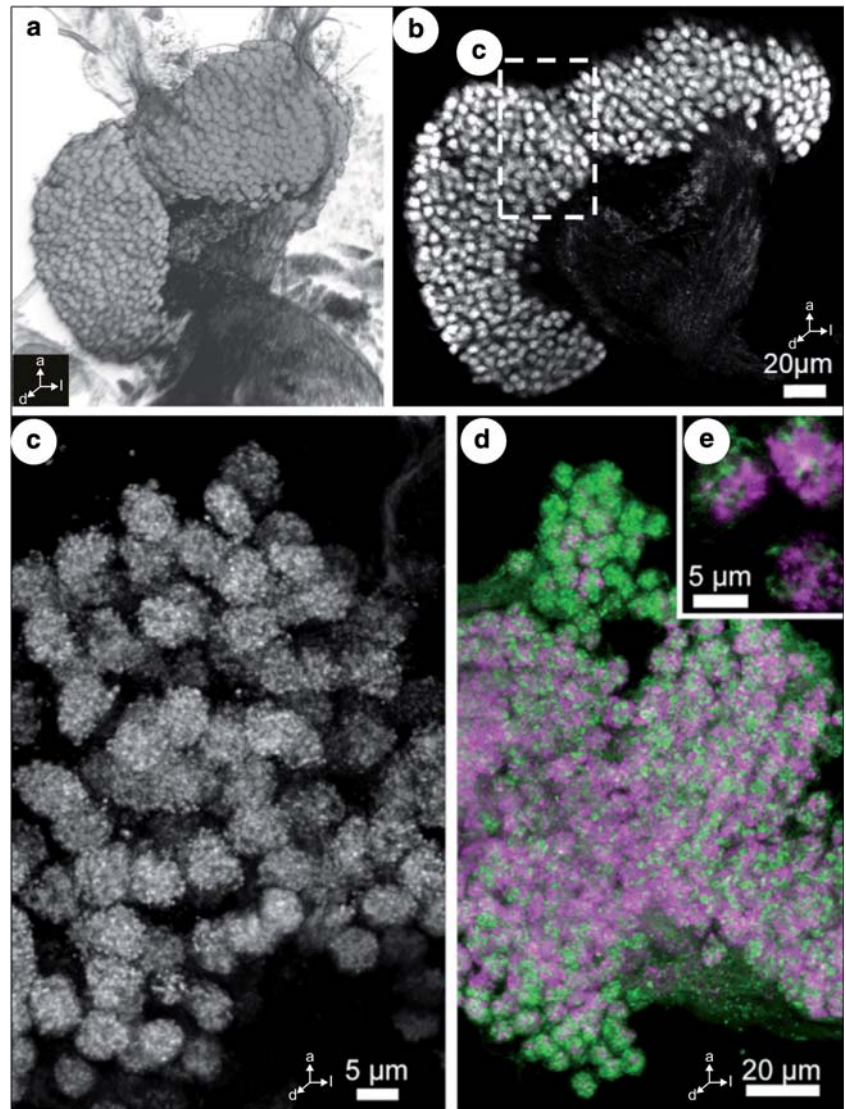
in parallel from proximal to distal (Figures 5c and 6a). Within the core-region of the AL2/PL2, tubulin-immunoreactive neurites are more abundant (Figure 6a,c). Two neurite bundles (MBn) connect the AL2/PL2 and the mushroom body pedunculus (MBp) and form a complete chiasm close to the AL2/PL2 (Figures 7a,c,d and 9a). Neurites from the medial SC2 contribute to these bundles by projecting into the AL2/PL2 and into the MBp (Figures 2, 6–2, 6, and 7a,d). Other neurites from SC2 pass between AL2/PL2 and MBp toward the L2 (Figure 6b,d). Thus, a large number of interweaving neurites characterizes the region of the MBn, which makes tracing of individual trajectories difficult (Figure 7a,d).

Some long neurites that appear to originate in SC2 project along the periphery of the MBp and join with neurites arising from the mushroom body haft (MBh). Together they form the mushroom body bridge (MBbr) (Figures 2, 6, and 7a,c,d). Other peripheral neurites from SC2 enter the MBh, where they seem to terminate (Figures 2, 4, and 7d).

### 3.6 | Visual neuropils and the mushroom body in *Cupiennius salei*

The dorsal-most neuropils in the protocerebrum of *C. salei* are the AM1 and AM2, which are connected by numerous

**FIGURE 9** The second-order visual neuropil of anterior lateral and posterior lateral eyes in the secondary eye visual pathway of *Marpissa muscosa*. (a) Three-dimensional volume rendering of an anti-synapsin labeled whole-mount, view from posterodorsal. Note the two distinct clusters of glomeruli that adjoin closely and coat the MBp anteriorly. (b) Single optical section of the AL2/PL2 within an anti-synapsin labeled whole-mount shows two distinct clusters of glomeruli and a chiasm of neurites connecting them to the MBp. (c) Stack of optical sections through the AL2/PL2 (maximum intensity projection), showing synapsin-immunoreactivity. The glomerular subunits within each individual glomeruli may represent synaptic boutons. (d) Anti-synapsin (magenta) and phalloidin (green) double-labeling reveals glomerular substructures (boutons) of the glomeruli. (e) Three individual glomeruli with glomerular substructures (boutons) labeled by anti-synapsin and phalloidin [Color figure can be viewed at [wileyonlinelibrary.com](http://wileyonlinelibrary.com)]



intertwining neurites (Figure 10a). The AM2 is connected to the AB via a thin tract (Figure 10a). Located ventrally and somewhat anterior to the AM1 is the PM1, which is large and spans over one hemisphere of the protocerebrum at its broadest part (Figure 10a,b,e). Its shape is cup-like, but somewhat irregular (Figure 10e). The PL1 is situated anteroventral of the PM1, is similar in size, but horseshoe shaped (Figure 10b). Both the PM1 and the PL1 are subdivided into an upper, strongly synapsin-immunoreactive part where the retinula cell axons terminate and a lower part where the synapsin-immunoreactivity is more patchily distributed (PM1x and PL1x; Figure 10b,e). Tubulin-immunoreactivity is strongest in the lower part, where the neurites that connect the PM1 and PM2 with their respective second-order neuropils bundle together. The AL1 is the smallest first-order neuropil and located close to the midline, between PM1 and PL1 (Figure 10b). Each first-order visual neuropil is connected to its second-order visual neuropil. These are of glomerular organization and situated close to each other (Figure 10b,c).

Although the AL2 is horseshoe shaped, the PL2 and PM2 are more elongate in shape and also larger (Figure 10b,c).

The mushroom body is characterized by strong synapsin-immunoreactivity and consists of a pedunculus (MBp), a shaft (MBs), and a haft (MBh; Figure 10b). The MBs and the MBh are fused with the MBp, and together form one continuous synapsin-immunoreactive domain (Figure 10b).

#### 4 | DISCUSSION

Comparative neuroanatomical studies on different spider species show that while general brain anatomy is similar, the structure of different neuropils especially within the protocerebrum varies (Hanström, 1921; Long, 2016; Steinhoff et al., 2017; Weltzien & Barth, 1991). The previous investigation by Steinhoff et al. (2017) on the general brain anatomy of *M. muscosa* suggested that the brains of jumping spiders and the spider species *C. salei*

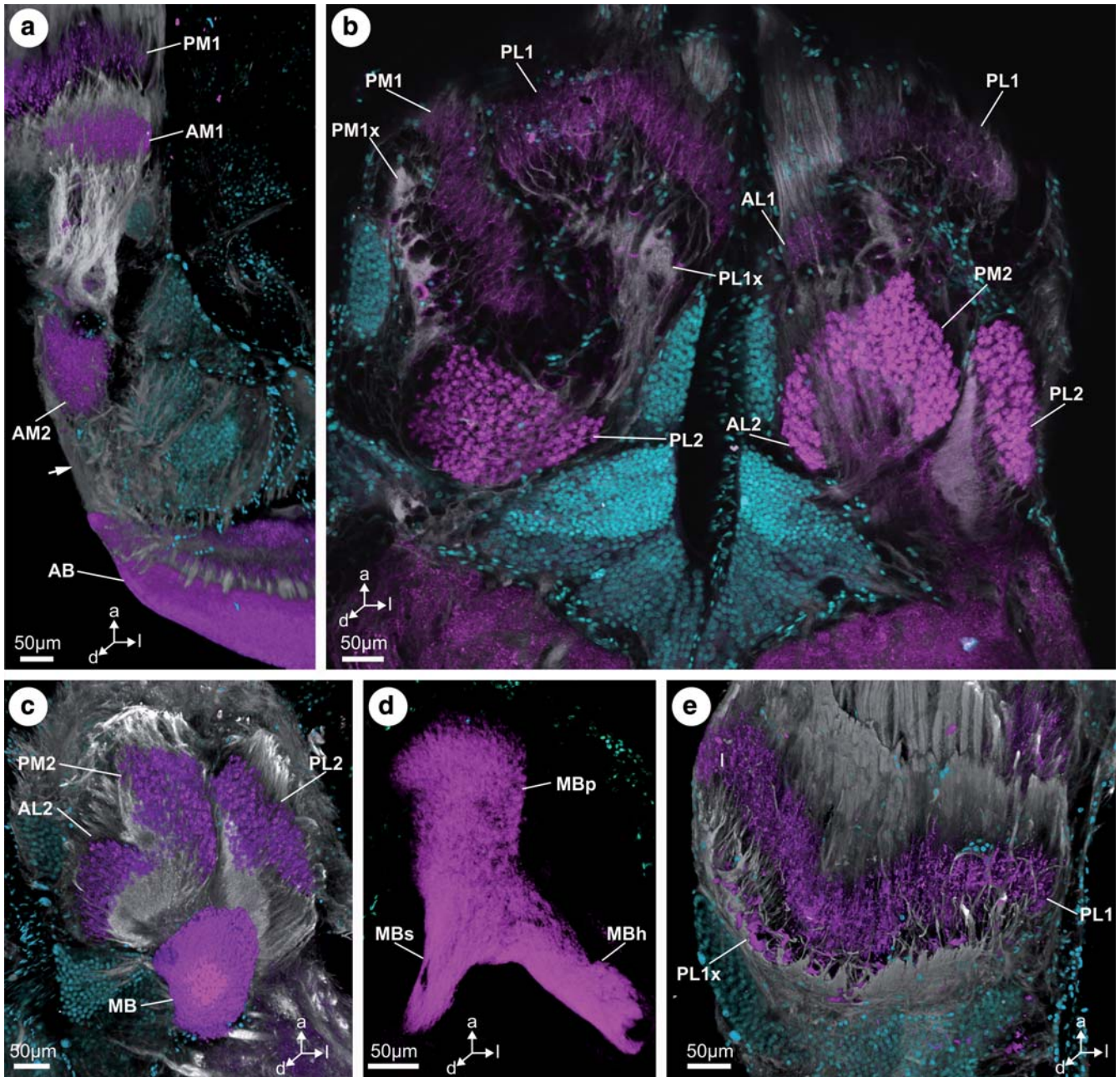


**FIGURE 10** Maximum projections of image stacks (clsm; a, c–e) and single optical section (clsm) showing synapsin-immunoreactivity (magenta), tubulin-immunoreactivity (gray), and somata (cyan) in the secondary eye visual system of *Cupiennius salei*. (a) In the principal eye visual pathway, the AM1 is connected to the AM2 via a thick tract. Connecting neurites between AM2 and the AB are also visible (arrow). (b) Within the secondary eye visual pathways, every eye is associated with its own first-order visual neuropil (AL1, PM1, and PL2); the PM1 and PL1 appear to have a substructure (PM1x and PL1x). All three second-order visual neuropils are substructured into glomeruli. (c) The AL2, PM2, and PL2 are all connected to the MB. (d) The MB of *C. salei* consists of a MBp, MBh, and MBs. All three substructures form a continuous synapsin-rich neuropil. (e) Horizontal section showing the PM1 and the PM1x. Abbreviations: a, anterior; AB, arcuate body; AL1, first-order visual neuropil of the anterior lateral eyes; AL2, second-order visual neuropil of the anterior lateral eyes; AM1, first-order visual neuropil of the anterior median eyes; AM2, second-order visual neuropil of the anterior median eyes; d, dorsal; l, lateral; MBh, mushroom body haft; MBp, mushroom body pedunculus; MBs, mushroom body shaft; PL1, first-order visual neuropil of the posterior lateral eyes; PL1x, neuropilar subunit of the PL1; PL2, second-order visual neuropil of the posterior lateral eyes; PM1, first-order visual neuropil of the posterior median eyes; PM1x, neuropilar subunit of the PM1; PM2, second-order visual neuropil of the posterior median eyes [Color figure can be viewed at [wileyonlinelibrary.com](http://wileyonlinelibrary.com)]

differ in structure and arrangement of neuropils. Although the general architecture is similar, we have shown here that the connectivity of neuropils in the secondary eye pathways differ

between these two species, which suggests differences in information processing and function of secondary eye visual neuropils.



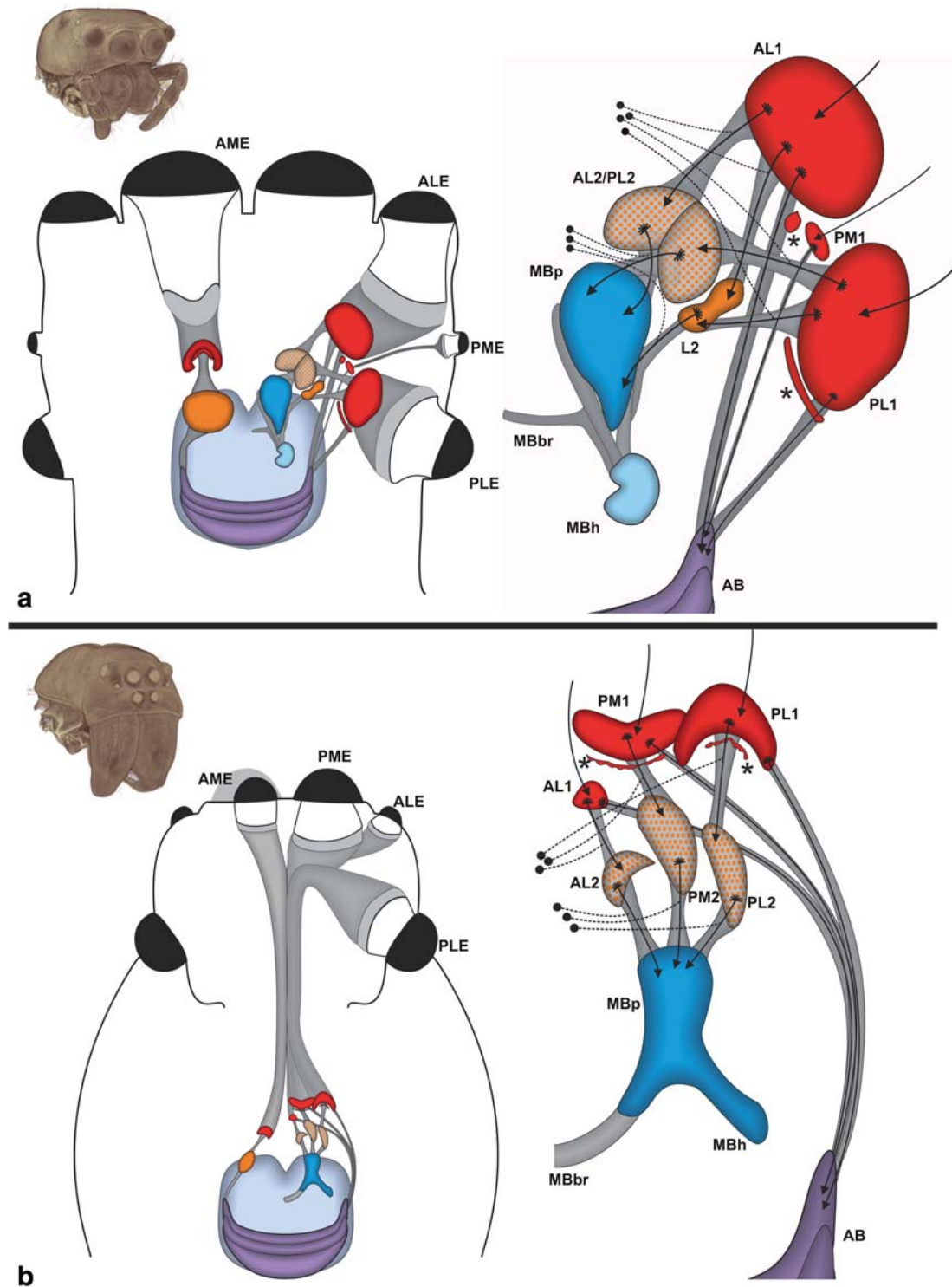


**FIGURE 11** Schematic representations of the principal and secondary eye visual pathways in the brains of (a) *Marpissa muscosa* and (b) *Cupiennius salei*. Insets top left: 3D volume rendering of the prosomata of (a) *M. muscosa* and (b) *C. salei*, based on microCT analysis. (b) Left anterior median eye concealed by posterior median eye. Abbreviations: AB, arcuate body; AL1, first-order visual neuropil of the anterior lateral eyes; AL2, second-order visual neuropil of the anterior lateral eyes; AL2/PL2, second-order visual neuropil of anterior lateral and posterior lateral eyes; ALE, anterior lateral eye; AME, anterior median eye; L2, shared second-order visual neuropil of the anterior lateral and posterior lateral eyes; MBbr, mushroom body bridge; MBh, mushroom body haft; MBp, mushroom body pedunculus; PL1, first-order visual neuropil of the posterior lateral eyes; PL2, second-order visual neuropil of the posterior lateral eyes; PLE, posterior lateral eye; PME, posterior median eye; PM1, first-order visual neuropil of the posterior median eyes; PM2, second-order visual neuropil of the posterior median eyes. Filled black circles indicate somata with known positions, dotted lines represent primary neurites, and arrows indicate the assumed direction of information flow. Asterisks mark neuropilar subregions of first-order neuropils (AL1x and PL1x in *M. muscosa*, PM1x and PL1x in *C. salei*) [Color figure can be viewed at [wileyonlinelibrary.com](http://wileyonlinelibrary.com)]

The relative size and position of the secondary eyes differs between *M. muscosa* and *C. salei*. Although in *M. muscosa* the PME is very small and oriented sideways, it is the largest eye in *C. salei* and oriented forward (Morehouse et al., 2017; Figure 11). The PLE are similar in relative size and position, but the ALE are considerably smaller in *C. salei*, albeit also oriented forward (Figure 11). The relative size of the retinae as well as the brain is smaller in *C. salei*, which is why the optic nerves associated with the eyes are much longer in *C. salei* (Figure 11).

#### 4.1 | Connectivity of neuropils in the principal eye pathway

The connection of the AME retinula cell axons to the AM1 has recently been described in detail by Nagata et al. (2019) for the jumping spider *Hasarius adansoni* (Audouin, 1826). These authors revealed that there are four photoreceptor layers in the retina, which each connect to one of four subregions in the AM1 (Nagata et al., 2019). We show here that in *M. muscosa* the AM1 is further connected to the AM2, which is the same as described for *C. salei* (Strausfeld et al., 1993). In *C. salei*, two types of neurons have been identified whose axons connect the AM2 with the flanges and the inner part of the AB (Strausfeld et al., 1993). In *M. muscosa* this pattern is likely the same, although we were only able to unambiguously detect neurites that connect the AM2 with the flanges of the AB. There are, however, neurites that project from the AM2 into the protocerebral neuropil and some of those may well proceed toward the inner part of the AB.

#### 4.2 | Connectivity of the first-order visual neuropils of the anterior and posterior lateral eyes

In *M. muscosa*, all retinula cell axons from ALE, PLE, and PME seem to terminate in their associated first-order visual neuropils (Figure 8). This is in accordance to what has been found in other Araneae (Becherer & Schmid, 1999; Duelli, 1980; Schmid & Duncker, 1993; Strausfeld & Barth, 1993; Strausfeld et al., 1993). Nevertheless, this pattern is different in all other investigated taxa of Chelicerata (e.g., Scorpiones, Xiphosura, or Pycnogonida), where a subset of retinula cell axons also projects into the second-order visual neuropils (Battelle, Sombke, & Harzsch, 2016; Lehmann & Melzer, 2013, 2018). It should be noted, however, that this discrepancy between spiders and all other arachnids still needs to be scrutinized using cobalt fills, which have not been employed in spiders yet (Lehmann & Melzer, 2018). In *C. salei*, a few histaminergic neurites terminate in all second-order visual neuropils, and have been interpreted as interneurons (Schmid & Duncker, 1993). However, as long as no neuronal tracings have been carried out, it cannot be ruled out that these neurites might instead represent retinula cell axons. In *M. muscosa*, we did not detect any histaminergic neurites that terminate in the second-order visual neuropils. There are, however, numerous histaminergic neurites that terminate in AL1x and PL1x. These neurites seem to originate at the

very distal part of the neuropil or even outside of it (Figure 8). Therefore, we propose that the AL1x and PL1x are innervated by histaminergic retinula cell axons.

In our histological sections, it appears as if some neurites that contribute to the tract between AL1, PL1 and the AB arise in AL1x and PL1x, respectively (Figure 3b,c and 5a,b). Hill (1975) described in *Phidippus* sp. that neurites from the AL1x domain contribute to a tract projecting towards the posterior protocerebrum. However, Hill (1975) did not mention terminations of retinula cell axons in the AL1x and PL1x, but detected neurites connecting the AL1 with the AL1x. Thus, it is possible that Hill (1975) either misinterpreted retinula cell axons as interneurons, or that we missed connecting neurites between AL1 and AL1x. In our immunohistological investigations, we found that synapsin-immunoreactive substructures of first-order visual neuropils are also present in *C. salei*, the PM1x and the PL1x. In both, *M. muscosa* and *C. salei*, this region is additionally characterized by strong tubulin-immunoreactivity. This can be explained by the tight packing of neurites that converge at the level of the AL1x and PL1x in *M. muscosa* and the PM1x and PL1x in *C. salei* to form the tracts to the respective second-order visual neuropils. A subdivision of PM1 and PL1 is also visible in histamine-immunolabeled material from the study by Schmid and Duncker (1993; compare Figures 2c,d and 3a,b), although not discussed by the authors. It remains open whether retinula cell axons or interneurons terminate at the synapsin immunoreactive part of the PL1x and PM1x in *C. salei* and the AL1x and PL1x in *M. muscosa*.

In *M. muscosa*, the convoluted first-order visual neuropils of the ALE and the PLE are both connected with the AL2/PL2 and the L2, as well as with the AB, which is only partially consistent with Hill's (1975) study on the nervous system in *Phidippus* spp., where he found that axons of the AL1, and not the PL1, join the tract that projects toward the AB. Duelli (1980) did not detect connections between PL1 and L2 in the salticids *Evarcha arcuata* (Clerck, 1757) and *Pseudamycus validus* (Thorell, 1877). He described "large field horizontal neurons," closely bypassing the AL2/PL2 and L2 and connecting the PL1 with the posterior protocerebrum (Duelli, 1980). Judging from their structure and position, these neurons might be identical to the neurites described in our study that contribute to the tract which connects the first-order visual neuropils of the secondary eyes with the AB. This discrepancy might be due to incomplete staining in the earlier studies where reduced-silver staining was employed. Our approach combines specific and broader markers with specific staining techniques. It should also be noted that the studies on the secondary eye pathways in jumping spiders were conducted on different species. However, it seems unlikely that the secondary eye pathways differ considerably within salticoid jumping spiders (Maddison & Hedin, 2003; Morehouse et al., 2017).

Based on our results, AL2/PL2 and L2 are shared second-order visual neuropils of both AL1 and PL1 in *M. muscosa*. The situation in *C. salei* is, however, different. Here, the first-order visual neuropils of all three secondary eyes are connected to individual second-order visual neuropils (Figure 11a,b; Strausfeld & Barth,

1993). Each of these second-order visual neuropils (AL2, PL2, PM2) is composed of small neuropilar glomeruli (Figure 11). An unstructured second-order visual neuropil (without glomeruli), such as the L2, is absent in *C. salei* (Strausfeld & Barth, 1993). Similar to the “giant interneurons” described for jumping spiders by Duelli (1980), Strausfeld and Barth (1993) detected “lamina wide-field neurons” that connect all first-order visual neuropils with a region close to the AB. It is very likely that these neurons correspond to the axons forming the tract between first-order visual neuropils and the AB that we described in *M. muscosa*.

### 4.3 | First-order visual neuropils of the posterior median eyes

The PM1 is by far the smallest first-order visual neuropil of all secondary eyes in *M. muscosa*. This correlates with the much smaller overall size of the PME (compared to ALE and PLE). The PME have previously been considered vestigial (Land, 1972, 1985b), but since there is an optic nerve and a corresponding first-order visual neuropil, we conclude that these eyes are functional. Previously, Steinhoff et al. (2017) considered the PM1 to be a second-order visual neuropil (“PM2”), based on its close spatial relationship with the AL1x. However, we now demonstrate that the PM1 is innervated only by retinula cell axons originating in the PME, and connections between PM1 and AL1x seem to be absent. This coincides with Hill's (1975) description for *Phidippus* spp., although he described additional neurites connecting PL1 and PM1. It is likely that these neurites contribute to the tract that connects the first-order visual neuropils with the AB (Figure 11a), instead of actually forming synapses in the PM1. Our data suggests that the PM1 differs from all other eyes by being connected to the AB only. Consequently, the pathway of the PME lacks a second-order visual neuropil. Information from this eye is not processed within the mushroom bodies, but exclusively in the AB.

### 4.4 | Second-order visual neuropils of the anterior and posterior lateral eyes

Visual neuropils with a glomerular structure have been found in the protocerebrum of several spider species (e.g., Long, 2016). They have been termed “lame glomérulée” by Saint Rémy (1887), “glomeruli” by Hanström (1921) and Babu and Barth (1984), “spherules” by Strausfeld and Barth (1993), and “microglomeruli” by Steinhoff et al. (2017). The presence and arrangement of these glomerular neuropils differs between spider species (Hanström, 1921; Long, 2016) and some authors have considered them as a substructure of the MB (Babu & Barth, 1984; Hill, 1975), whereas others have considered them to be separate second-order visual neuropils (Long, 2016; discussed in Steinhoff et al., 2017; Strausfeld & Barth, 1993). Our results demonstrate that in *M. muscosa*, the AL2/PL2 represents two closely adjoining second-

order visual neuropils of the ALE and PLE, respectively. In *M. muscosa*, the AL2/PL2 was also found to react less plastically to different environmental conditions than the MBp (Steinhoff, Liedtke, Sombke, Schneider, & Uhl, 2018), which was interpreted as further evidence for their function as discrete visual neuropils. Within the AL2/PL2, each glomerulus seems to consist of numerous synaptic complexes and Duelli (1980) estimated roughly 400 synapses per glomerulus in the jumping spider *Evarcha arcuata*. Studies in insects used anti-synapsin labeling to detect presynaptic sites, and phalloidin (which labels f-actin) to highlight postsynaptic sites of synaptic complexes (Groh & Rössler, 2011). To investigate the AL2/PL2 of *M. muscosa*, we have employed the same double-labeling approach (Figure 9d,e), but the anti-synapsin and phalloidin labeled areas in each synaptic complex were not clearly differentiated, as is the case in social hymenopterans (Groh & Rössler, 2011), despite co-localization being minimal. This might indicate that phalloidin does not consistently label postsynaptic sites in *M. muscosa*, or that the organization of the presynaptic and postsynaptic sites within the AL2/PL2 of *M. muscosa* differs compared to the glomeruli in mushroom body calyces of investigated insect species. To clarify synaptic connectivity within the AL2/PL2 in *M. muscosa* and spiders in general, a detailed transmission electron microscopic study is needed.

### 4.5 | Mushroom body pedunculus, haft, and bridge

The somata within SC2 of the neurons that connect the second-order visual neuropils to the MBp have been referred to as “globuli cells” (Hanström, 1921; Steinhoff et al., 2017) and the neurons including these somata as “T-cells” (Strausfeld & Barth, 1993). In *C. salei*, globuli cells have a smaller diameter of the soma and nucleus than other cell bodies in the protocerebrum (Babu & Barth, 1984). We could not find such size differences in *M. muscosa*. In fact, all three nuclear markers revealed that somata of the three identified clusters as well the somata of the surrounding cortex exhibit a similar size (Figures 2, 3, 5, 6, and 7). Thus, according to their definition (Kenyon, 1896; Richter et al., 2010), somata of SC2 are no globuli cells in *M. muscosa*. The long neurites that connect the SC2 with the AL2/PL2 and the L2 are probably primary neurites (Richter et al., 2010), from which dendrites branch into the AL2/PL2 and L2 respectively, and axons project into the MBp, MBh, and MBbr. A similar arrangement has been described by Babu and Barth (1984) for *C. salei* and by Hill (1975) for two *Phidippus* species.

The structure and organization of the MB differs between *M. muscosa* and *C. salei*, as already reported by Steinhoff et al. (2017). The MBh is a separate structure of the mushroom body in *M. muscosa*, connected to the MBp by neurites (Steinhoff et al., 2017), whereas in *C. salei*, it is fused with the MBp (Strausfeld & Barth, 1993). Furthermore, the mushroom body shaft, which in *C. salei* gives rise to the MBbr (Strausfeld & Barth, 1993) is absent or fused with the MBp in *M. muscosa*.

## 4.6 | Functional considerations

The jumping spider *M. muscosa* and the wandering spider *C. salei* differ strongly in their lifestyle. While *M. muscosa* is a diurnal hunter that actively pursues its prey and relies on vision for prey capture, *C. salei* is an exclusively nocturnal sit-and-wait predator, which detects its prey based on vibratory cues (Barth & Seyfarth, 1979). Although attack behavior of *C. salei* can be elicited by visual cues under experimental conditions (Fenk et al., 2010), mechanosensing is the major modality for hunting prey, since *C. salei* also captures prey when its eyes are occluded (Hergenröder & Barth, 1983). Given these obvious differences in lifestyle and relative importance of sensory modalities, it is surprising how similar the general brain anatomy of *M. muscosa* and *C. salei* is. Apart from differences in size and structure of neuropils, the visual pathway of the principal eyes is identical in *C. salei* and *M. muscosa*. Parts of the visual pathways of the secondary eyes in the jumping spider *M. muscosa* differ, however, from those in the wandering spider *C. salei*. These differences might reflect the differences in the visual fields and corresponding functions of their secondary eyes (Land, 1985a; Land & Barth, 1992). The most conspicuous difference between the visual systems in the brains of *M. muscosa* and *C. salei* is the pathway of the PME. While the two larger secondary eyes (ALE and PLE) are connected to the mushroom bodies in *M. muscosa*, the PME are not (Figure 11). This suggests that the PME do not play a role in motion detection (Duelli, 1978; Land, 1971; Zurek et al., 2010). In *C. salei*, however, the PME are important movement detectors (Schmid, 1998) connected to the mushroom bodies (Strausfeld & Barth, 1993).

Another interesting difference between the two species is the presence of the L2 in *M. muscosa* (Steinhoff et al., 2017), which is absent in *C. salei*. The structure of this neuropil differs from the AL2/PL2 and all second-order visual neuropils in *C. salei*, since the L2 in *M. muscosa* lacks a glomerular organization. Glomeruli might ensure a retinotopic organization of neurites within the second-order visual neuropils. This has been hypothesized for both *C. salei* (Strausfeld & Barth, 1993) and for the PLE pathway of jumping spiders (Duelli, 1980), where no lateral connections between individual glomeruli of the AL2/PL2 were found. We hypothesize that while a retinotopic organization is kept in the AL2/PL2, it is lost in the L2. Information from the movement-detecting ALE and PLE in *M. muscosa* might be integrated not only in the MB, but also in the L2, and enable faster movement decisions. Alternatively, a glomerular organization might be the most space-saving structure for the processing of input from differentially tuned groups of axons (Eisthen, 2002; Hildebrand & Shepherd, 1997), and although the L2 is not composed of glomeruli, information might still be processed in parallel without lateral connections. This would also indicate that a higher number of neurites synapse in the AL2/PL2 than in the L2 in *M. muscosa*.

Some early branched off salticid species possess a large PME that has its own field of view (e.g., *Portia*; Land, 1985a; Maddison & Hedin, 2003). Land (1985a) suggested that in jumping spiders with a small PME, such as *M. muscosa*, the fields of view of ALE and PLE have expanded to fill the space not covered by the PME. The evolutionary

transformation to a smaller PME and larger ALE and PLE might have led to visual pathways that also incorporated the L2. Future studies will focus on the visual pathways in the brains of early branched off jumping spider species with large PME, to identify possible ancestral arrangements of the PME pathway.

### ACKNOWLEDGMENTS

The authors wish to thank Georg Brenneis and Matthes Kenning (University of Greifswald), Nicholas J. Strausfeld (University of Arizona, Tucson), Wolfgang Rössler (University of Würzburg) and Friedrich G. Barth (University of Vienna) for helpful discussions. The authors are grateful to Kerstin Stejskal and Thomas Hummel (Department of Neurobiology, University of Vienna) for providing *Cupiennius salei* and Elvira Lutjanov, Christian Müller, Sabine Ziesemer, and Jan-Peter Hildebrandt (all University of Greifswald) for help with western blot analysis. Tim M. Dederichs and Peter Michalik (both University of Greifswald) helped to obtain pictures with the Visionary Digital camera system. Monica M. Sheffer provided helpful linguistic comments that improved the manuscript. This study was financially supported by the German Research Foundation DFG UH 87/11-1 and DFG INST 292/119-1 FUGG, DFG INST 292/120-1 FUGG. POMS was additionally supported by a Bogislaw Scholarship from the University of Greifswald and a Laudier Histology Cooperation & Travel Grant.

### CONFLICT OF INTEREST

The authors have no conflicts of interests.

### AUTHOR CONTRIBUTIONS

All authors had full access to all the data in the study and take responsibility for the integrity of the data and the accuracy of data analysis. P.O.M.S., A.S., and G.U. study concept and design. P.O.M.S. acquisition of data. P.O.M.S. and A.S. analysis and interpretation of data. P.O.M.S. and A.S. wrote the manuscript. G.U. and S.H. contributed to the writing of the manuscript. G.U., S.H., and P.O.M.S. obtained funding.

### DATA AVAILABILITY STATEMENT

The data that support the findings of this study are available from the corresponding author upon reasonable request.

### ORCID

Philip O. M. Steinhoff  <https://orcid.org/0000-0003-1676-8105>

Andy Sombke  <https://orcid.org/0000-0001-7383-440X>

### REFERENCES

- Babu, K. S., & Barth, F. G. (1984). Neuroanatomy of the central nervous system of the wandering spider, *Cupiennius salei* (Arachnida, Araneida). *Zoomorphology*, 104, 344–359. <https://doi.org/10.1007/BF00312185>
- Barth, F., & Seyfarth, E.-A. (1979). *Cupiennius salei* keys (Araneae) in the highlands of Central Guatemala. *Journal of Arachnology*, 7, 255–263.
- Barth, F. G. (2002). The central nervous system. In F. G. Barth (Ed.), *A spider's world; senses and behavior* (pp. 161–174). Berlin Heidelberg: Springer.

- Barth, F. G., Nakagawa, T., & Eguchi, E. (1993). Vision in the ctenid spider *Cupiennius salei*: Spectral range and absolute sensitivity. *Journal of Experimental Biology*, 79, 63–79. <https://doi.org/ghijagsj>
- Battelle, B. A., Calman, B. G., Andrews, A. W., Grieco, F. D., Mleziva, M. B., Callaway, J. C., & Stuart, A. E. (1991). Histamine: A putative afferent neurotransmitter in *Limulus* eyes. *Journal of Comparative Neurology*, 305(4), 527–542. <https://doi.org/10.1002/cne.903050402>
- Battelle, B. A., Sombke, A., & Harzsch, S. (2016). Xiphosura. In A. Schmidt-Rhaesa, S. Harzsch, & G. Purschke (Eds.), *Structure and evolution of invertebrate nervous systems* (pp. 428–442). Oxford: Oxford University Press.
- Becherer, C., & Schmid, A. (1999). Distribution of g-aminobutyric acid-, proctolin-, *Periplaneta* hypertrehalosaemic hormone- and FMRFamide-like immunoreactivity in the visual ganglia of the spider *Cupiennius salei* keys. *Comparative Biochemistry and Physiology Part A*, 122, 267–275.
- Cebrià, F. (2008). Organization of the nervous system in the model planarian *Schmidtea mediterranea*: An immunocytochemical study. *Neuroscience Research*, 61(4), 375–384. <https://doi.org/10.1016/j.neures.2008.04.005>
- Duelli, P. (1978). Movement detection in the posterolateral eyes of jumping spiders (*Evarcha arcuata*, Salticidae). *Journal of Comparative Physiology A*, 124(1), 15–26. <https://doi.org/10.1007/BF00656387>
- Duelli, P. (1980). The neuronal organization of the posterior lateral eyes of jumping spiders (Salticidae). *Zoologische Jahrbücher: Abteilung für Anatomie und Ontogenie der Tiere*, 103(1), 17–40.
- Eisthen, H. L. (2002). Why are olfactory systems of different animals so similar? *Brain, Behavior and Evolution*, 59(5–6), 273–293. <https://doi.org/10.1159/000063564>
- Fabian-Fine, R., Volkmandt, W., & Seyfarth, E.-A. (1999). Peripheral synapses at identifiable mechanosensory neurons in the spider *Cupiennius salei*: Synapsin-like immunoreactivity. *Cell and Tissue Research*, 295(1), 13–19.
- Fenk, L. M., Hoinkes, T., & Schmid, A. (2010). Vision as a third sensory modality to elicit attack behavior in a nocturnal spider. *Journal of Comparative Physiology A*, 196(12), 957–961. <https://doi.org/10.1007/s00359-010-0575-8>
- Fenk, L. M., & Schmid, A. (2010). The orientation-dependent visual spatial cut-off frequency in a spider. *The Journal of Experimental Biology*, 213(18), 3111–3117. <https://doi.org/10.1242/jeb.041939>
- Foelix, R. F. (1996). *Biology of spiders*. New York: Oxford University Press.
- Garm, A., O'Connor, M., Parkefeld, L., & Nilsson, D.-E. (2007). Visually guided obstacle avoidance in the box jellyfish *Tripedalia cystophora* and *Chiropsella bronzie*. *Journal of Experimental Biology*, 210(20), 3616–3623. <https://doi.org/10.1242/jeb.004044>
- Gregory, G. E. (1980). The Bodian Protargol technique. In N. J. Strausfeld & T. A. Miller (Eds.), *Neuroanatomical techniques insect nervous system* (pp. 75–95). Berlin Heidelberg: Springer.
- Groh, C., & Rössler, W. (2011). Comparison of microglomerular structures in the mushroom body calyx of neopteran insects. *Arthropod Structure and Development*, 40(4), 358–367. <https://doi.org/10.1016/j.asd.2010.12.002>
- Hanström, B. (1921). Über die Histologie und vergleichende Anatomie der Sehganglien und Globuli der Araneen. *Kungliga Svenska Vetenskapsakademiens Handlingar*, 61(12), 1–39.
- Harland, D. P., Li, D., & Jackson, R. R. (2012). How jumping spiders see the world. In O. F. Lazareva, T. Shimizu, & E. A. Wasserman (Eds.), *How animals see the world: Comparative behavior, biology, and evolution of vision* (pp. 133–164). New York: Oxford University Press.
- Harzsch, S., & Hansson, B. S. (2008). Brain architecture in the terrestrial hermit crab *Coenobita clypeatus* (Anomura, Coenobitidae), a crustacean with a good aerial sense of smell. *BMC Neuroscience*, 9(1), 1–35. <https://doi.org/10.1186/1471-2202-9-58>
- Harzsch, S., & Müller, C. H. (2007). A new look at the ventral nerve centre of *Sagitta*: Implications for the phylogenetic position of Chaetognatha (arrow worms) and the evolution of the bilaterian nervous system. *Frontiers in Zoology*, 4(1), 14.
- Harzsch, S., Vilpoux, K., Blackburn, D. C., Platchetki, D., Brown, N. L., Melzer, R., ... Battelle, B. A. (2006). Evolution of arthropod visual systems: Development of the eyes and central visual pathways in the horseshoe crab *Limulus polyphemus* Linnaeus, 1758 (Chelicerata, Xiphosura). *Developmental Dynamics*, 235(10), 2641–2655. <https://doi.org/10.1002/dvdy.20866>
- Harzsch, S., Wildt, M., Battelle, B., & Waloszek, D. (2005). Immunohistochemical localization of neurotransmitters in the nervous system of larval *Limulus polyphemus* (Chelicerata, Xiphosura): Evidence for a conserved protocerebral architecture in Euarthropoda. *Arthropod Structure and Development*, 34(3), 327–342. <https://doi.org/10.1016/j.asd.2005.01.006>
- Hergenröder, R., & Barth, F. G. (1983). Vibratory signals and spider behavior: How do the sensory inputs from the eight legs interact in orientation? *Journal of Comparative Physiology A*, 152(3), 361–371. <https://doi.org/10.1007/BF00606241>
- Hildebrand, J. G., & Shepherd, G. M. (1997). Mechanisms of olfactory discrimination: Converging evidence for common principles across phyla. *Annual Review of Neuroscience*, 20(1), 595–631. <https://doi.org/10.1146/annurev.neuro.20.1.595>
- Hill, D. E. (1975). *The structure of the central nervous system of jumping spiders of the genus Phidippus (Araneae: Salticidae)* (MSc thesis). Oregon State University.
- Homann, H. (1950). Die Nebenaugen der Araneen. *Zoologische Jahrbücher: Abteilung für Anatomie und Ontogenie der Tiere*, 71, 56–144.
- Homann, H. (1952). Die Nebenaugen der Araneen. *Zweite Mitteilung. Zoologische Jahrbücher: Abteilung für Anatomie und Ontogenie der Tiere*, 72, 345–364.
- Jakob, E. M., Long, S. M., Harland, D. P., Jackson, R. R., Carey, A., Searles, M. E., ... Rolland, J. P. (2018). Lateral eyes direct principal eyes as jumping spiders track objects. *Current Biology*, 28(18), R1092–R1093. <https://doi.org/10.1016/j.cub.2018.07.065>
- Kenyon, F. C. (1896). The meaning and structure of the so-called “mushroom bodies” of the hexapod brain. *The American Naturalist*, 30, 643–650.
- Klagges, B. R. E., Heimbeck, G., Godenschwege, T. A., Hofbauer, A., Pflugfelder, G. O., Reifegerste, R., ... Buchner, E. (1996). Invertebrate synapsins: A single gene codes for several isoforms in *Drosophila*. *Journal of Neuroscience*, 16, 3145–3165.
- Land, M. F. (1971). Orientation by jumping spiders in the absence of visual feedback. *The Journal of Experimental Biology*, 54(1), 119–139.
- Land, M. F. (1972). Mechanisms of orientation and pattern recognition by jumping spiders (Salticidae). In R. Wehner (Ed.), *Information processing in the visual systems of arthropods* (pp. 231–247). Berlin Heidelberg: Springer.
- Land, M. F. (1985a). Fields of view of the eyes of primitive jumping spiders. *Journal of Experimental Biology*, 119, 381–384.
- Land, M. F. (1985b). The morphology and optics of spider eyes. In F. G. Barth (Ed.), *Neurobiology of arachnids* (pp. 53–76). Berlin: Springer.
- Land, M. F., & Barth, F. G. (1992). The quality of vision in the ctenid spider *Cupiennius salei*. *Journal of Experimental Biology*, 164, 227–242.
- Lehmann, T., & Melzer, R. R. (2013). Looking like *Limulus*?—Retinula axons and visual neuropils of the median and lateral eyes of scorpions. *Frontiers in Zoology*, 10(1), 40. <https://doi.org/10.1186/1742-9994-10-40>
- Lehmann, T., & Melzer, R. R. (2018). Also looking like *Limulus*?—Retinula axons and visual neuropils of Amblypygi (whip spiders). *Frontiers in Zoology*, 15(1), 52. <https://doi.org/10.1186/s12983-018-0293-6>
- Lehmann, T., Melzer, R. R., Hörnig, M. K., Michalik, P., Sombke, A., & Harzsch, S. (2016). Arachnida (excluding scorpiones). In A. Schmidt-Rhaesa, S. Harzsch, & G. Purschke (Eds.), *Structure and evolution of invertebrate nervous systems* (pp. 453–477). Oxford, England: Oxford University Press.
- Loesel, R., Wolf, H., Kenning, M., Harzsch, S., & Sombke, A. (2013). Architectural principles and evolution of the arthropod central nervous system. In A. Minelli (Ed.), *Arthropod biology and evolution* (pp. 299–342).

- Berlin Heidelberg: Springer-Verlag. <https://doi.org/10.1007/978-3-642-36160-9>
- Long, S. M. (2016). *Spider brain morphology & behavior* (PhD thesis). University of Massachusetts, Amherst.
- Maddison, W. P., & Hedin, M. C. (2003). Jumping spider phylogeny (Araneae: Salticidae). *Invertebrate Systematics*, 17(4), 529. <https://doi.org/10.1071/is02044>
- Morehouse, N. I., Buschbeck, E. K., Zurek, D. B., Steck, M., & Porter, M. L. (2017). Molecular evolution of spider vision: New opportunities, familiar players. *Biological Bulletin*, 233(1), 21–38. <https://doi.org/10.1086/693977>
- Nagata, T., Arikawa, K., & Kinoshita, M. (2019). Photoreceptor projection from a four-tiered retina to four distinct regions of the first optic ganglion in a jumping spider. *Journal of Comparative Neurology*, 527, 1–14. <https://doi.org/10.1002/cne.24584>
- Nässel, D. R. (1999). Histamine in the brain of insects: A review. *Microscopy Research and Technique*, 44(2–3), 121–136.
- O'Connor, M., Garm, A., & Nilsson, D. E. (2009). Structure and optics of the eyes of the box jellyfish *Chiropsella bronzie*. *Journal of Comparative Physiology A*, 195(6), 557–569. <https://doi.org/10.1007/s00359-009-0431-x>
- Orlando, E., & Schmid, A. (2011). Colour blindness of the movement-detecting system of the spider *Cupiennius salei*. *Journal of Experimental Biology*, 214(4), 546–550. <https://doi.org/10.1242/jeb.051672>
- Ott, S. R. (2008). Confocal microscopy in large insect brains: Zinc-formaldehyde fixation improves synapsin immunostaining and preservation of morphology in whole-mounts. *Journal of Neuroscience Methods*, 172(2), 220–230. <https://doi.org/10.1016/j.jneumeth.2008.04.031>
- Paulus, H. (1979). Eye structure and the monophyly of the Arthropoda. In G. AP (Ed.), *Arthropod phylogeny* (pp. 299–383). New York, NY: Van Nostrand Reinhold Company.
- Richter, S., Loesel, R., Purschke, G., Schmidt-Rhaesa, A., Scholtz, G., Stach, T., ... Harzsch, S. (2010). Invertebrate neurophylogeny: Suggested terms and definitions for a neuroanatomical glossary. *Frontiers in Zoology*, 7, 29. <https://doi.org/10.1186/1742-9994-7-29>
- Saint Rémy, G. (1887). Contribution à l'étude du cerveau chez les arthropodes trachéates. *Archives de Zoologie Experimentale et Générale*, 2, 1–274.
- Schmid, A. (1998). Different functions of different eye types in the spider *Cupiennius salei*. *The Journal of Experimental Biology*, 201, 221–225.
- Schmid, A., & Duncker, M. (1993). Histamine immunoreactivity in the central nervous system of the spider *Cupiennius salei*. *Cell & Tissue Research*, 273(3), 533–545. <https://doi.org/10.1007/BF00333707>
- Schulze, E., & Graupner, H. (1960). *Anleitung zum mikroskopisch-technischen Arbeiten in Biologie und Medizin* (Vol. 1). Akademische Verlagsgesellschaft.
- Sombke, A., & Harzsch, S. (2015). Immunolocalization of histamine in the optic neuropils of *Scutigera coleoptrata* (Myriapoda: Chilopoda) reveals the basal organization of visual systems in Mandibulata. *Neuroscience Letters*, 594, 111–116. <https://doi.org/10.1016/j.neulet.2015.03.029>
- Sombke, A., Harzsch, S., & Hansson, B. S. (2011). Organization of deutocerebral neuropils and olfactory behavior in the centipede *Scutigera coleoptrata* (Linnaeus, 1758) (Myriapoda: Chilopoda). *Chemical Senses*, 36(1), 43–61. <https://doi.org/10.1093/chemse/bjq096>
- Sombke, A., Lipke, E., Michalik, P., Uhl, G., & Harzsch, S. (2015). Potential and limitations of x-ray micro-computed tomography in arthropod neuroanatomy: A methodological and comparative survey. *Journal of Comparative Neurology*, 523(8), 1281–1295. <https://doi.org/10.1002/cne.23741>
- Spano, L., Long, S. M., & Jakob, E. M. (2012). Secondary eyes mediate the response to looming objects in jumping spiders (*Phidippus audax*, Salticidae). *Biology Letters*, 8(6), 949–951. <https://doi.org/10.1098/rsbl.2012.0716>
- Steinhoff, P. O. M., Liedtke, J., Sombke, A., Schneider, J. M., & Uhl, G. (2018). Early environmental conditions affect the volume of higher-order brain centers in a jumping spider. *Journal of Zoology*, 304(3), 182–192. <https://doi.org/10.1111/jzo.12512>
- Steinhoff, P. O. M., Sombke, A., Liedtke, J., Schneider, J. M., Harzsch, S., & Uhl, G. (2017). The synganglion of the jumping spider *Marpissa muscosa* (Arachnida: Salticidae): Insights from histology, immunohistochemistry and microCT analysis. *Arthropod Structure and Development*, 46(2), 156–170. <https://doi.org/10.1016/j.asd.2016.11.003>
- Strausfeld, N. J. (2012). *Arthropod brains: Evolution, functional elegance, and historical significance*. Cambridge, MA: Belknap Press of Harvard University Press.
- Strausfeld, N. J., & Barth, F. G. (1993). Two visual systems in one brain: Neuropils serving the secondary eyes of the spider *Cupiennius salei*. *The Journal of Comparative Neurology*, 328(1), 43–62. <https://doi.org/10.1002/cne.903280105>
- Strausfeld, N. J., Weltzien, P., & Barth, F. G. (1993). Two visual systems in one brain: Neuropils serving the principal eyes of the spider *Cupiennius salei*. *The Journal of Comparative Neurology*, 328(1), 63–75. <https://doi.org/10.1002/cne.903280105>
- Sullivan, J. M., Benton, J. L., Sandeman, D. C., & Beltz, B. S. (2007). Adult neurogenesis: A common strategy across diverse species. *Journal of Comparative Neurology*, 500(3), 574–584. <https://doi.org/10.1002/cne.21187>
- Weltzien, P., & Barth, F. G. (1991). Volumetric measurements do not demonstrate that the spider brain “central body” has a special role in web building. *Journal of Morphology*, 208(1), 91–98. <https://doi.org/10.1002/jmor.1052080104>
- Widmer, A., Höger, U., Meisner, S., French, A. S., & Torkkeli, P. H. (2005). Spider peripheral mechanosensory neurons are directly innervated and modulated by octopaminergic efferents. *Journal of Neuroscience*, 25(6), 1588–1598. <https://doi.org/10.1523/jneurosci.4505-04.2005>
- Yamashita, S., & Tateda, H. (1976). Spectral sensitivities of jumping spider eyes. *Journal of Comparative Physiology A*, 105(1), 29–41. <https://doi.org/10.1007/BF01380051>
- Yamashita, S., & Tateda, H. (1978). Spectral sensitivities of the anterior median eyes of the orb web spiders, *Argiope bruennichii* and *A. amoena*. *Journal of Experimental Biology*, 74(1), 47–57.
- Zurek, D. B., & Nelson, X. J. (2012a). Hyperacute motion detection by the lateral eyes of jumping spiders. *Vision Research*, 66, 26–30. <https://doi.org/10.1016/j.visres.2012.06.011>
- Zurek, D. B., & Nelson, X. J. (2012b). Saccadic tracking of targets mediated by the anterior-lateral eyes of jumping spiders. *Journal of Comparative Physiology A*, 198(6), 411–417. <https://doi.org/10.1007/s00359-012-0719-0>
- Zurek, D. B., Taylor, A. J., Evans, C. S., & Nelson, X. J. (2010). The role of the anterior lateral eyes in the vision-based behaviour of jumping spiders. *The Journal of Experimental Biology*, 213, 2372–2378. <https://doi.org/10.1242/jeb.042382>

## SUPPORTING INFORMATION

Additional supporting information may be found online in the Supporting Information section at the end of this article.

**How to cite this article:** Steinhoff POM, Uhl G, Harzsch S, Sombke A. Visual pathways in the brain of the jumping spider *Marpissa muscosa*. *J Comp Neurol*. 2020;528:1883–1902. <https://doi.org/10.1002/cne.24861>

### **Chapter 3: Comparative neuroanatomy of the central nervous system in stationary and cursorial hunting spiders**

Philip O.M. Steinhoff<sup>1\*</sup>, Steffen Harzsch<sup>2</sup> & Gabriele Uhl<sup>1</sup>

<sup>1</sup> Zoological Institute and Museum, General and Systematic Zoology, University of Greifswald, Loitzer Straße 26, 17489 Greifswald, Germany. *E-Mail: gabriele.uhl@uni-greifswald.de*

<sup>2</sup> Zoological Institute and Museum, Cytology and Evolutionary Biology, University of Greifswald, Soldmannstraße 23, 17487 Greifswald, Germany

*\*Corresponding Author. E-Mail: philipsteinhoff@gmail.com*

*Manuscript submitted to the Journal of Comparative Neurology on January 30th 2023.*





# Comparative neuroanatomy of the central nervous system in stationary and cursorial hunting spiders

Philip O.M. Steinhoff<sup>1\*</sup>, Steffen Harzsch<sup>2</sup> & Gabriele Uhl<sup>1</sup>

<sup>1</sup> Zoological Institute and Museum, General and Systematic Zoology, University of Greifswald, Loitzer Straße 26, 17489 Greifswald, Germany. *E-Mail: gabriele.uhl@uni-greifswald.de*

<sup>2</sup> Zoological Institute and Museum, Cytology and Evolutionary Biology, University of Greifswald, Soldmannstraße 23, 17487 Greifswald, Germany

*\*Corresponding Author. E-Mail: philipsteinhoff@gmail.com*

## ACKNOWLEDGEMENTS

We thank Nick Strausfeld and Gabriella Wolff for invaluable tips on the Bodian-staining method. Ingrid Handt granted access to the greenhouses of the botanical garden and Shou-Wang Lin assisted with microCT reconstructions. We thank Heidi Land for helpful discussions on details of the histology. We thank Georg Brenneis and Jakob Krieger for critical discussions that helped to improve the manuscript. This study was financially supported by the German Research Foundation DFG UH 87/11-1 and DFG INST 292/119-1 FUGG, DFG INST 292/120-1 FUGG. POMS was additionally supported by a Bogislaw Scholarship from the University of Greifswald and a Laudier Histology Cooperation & Travel Grant.

## DATA AVAILABILITY STATEMENT

All serial Bodian-stained sections used to identify and reconstruct central nervous system structures are available at MorphDBase (URL will be added shortly before publication). 3D PDFs of all reconstructed nervous systems are available from Morphobank (morphobank.org) and can be accessed by the reviewers using the project number 4539 in the field "Email address" and the password SpiderBrains. The 3D PDFs as well as a list with all reconstructed CNS volumes is stored under "Documents".

## Abstract

Spiders (Araneae) include cursorial species that stalk their prey and stationary species that build webs for prey capture. While many cursorial hunting spiders rely on visual cues for prey capture, stationary hunting spiders use vibratory cues (mechanosensation). We predicted that the differences in primary sensory input between the species are mirrored by differences in the central nervous system (CNS). We investigated the CNS anatomy of four spider species, two cursorial hunters *Pardosa amentata* (Lycosidae) and *Marpissa muscosa* (Salticidae), and two stationary hunters *Argiope bruennichi* (Araneidae) and *Parasteatoda tepidariorum* (Theridiidae). The CNS was analyzed using Bodian silver impregnations, immunohistochemistry, and microCT analysis. We found that there are major differences in the secondary eye pathway of the brain that pertain to first order, second order and higher order brain centers (mushroom bodies). While *P. amentata* and *M. muscosa* have prominent visual neuropils and mushroom bodies, these are much reduced in the two stationary species. *A. bruennichi* is missing second order visual neuropils but has specialized photoreceptors that project to two distinct visual neuropils, and *P. tepidariorum* has no mushroom bodies, indicating that motion vision might be absent in this species. Interestingly, differences in the ventral nerve cord are much less pronounced. We found that the stationary spiders had proportionally larger leg neuropils than the cursorial spiders. Our findings suggest that the importance of visual information is much reduced in stationary compared to cursorial spiders, while processing of mechanosensory information requires the same major circuits in both stationary and cursorial hunting spiders.

## Keywords

Neuroanatomy, Arachnida, visual neuropils, Bodian-staining, volumes, lifestyle, sensory ecology

## 1 Introduction

Differences in the specific lifestyle of closely related animal species are mirrored in the relative size and wiring of different central nervous system (CNS) areas. This is particularly evident when lifestyles rely on specific sensory modalities, such as vision in whirligig beetles (Strausfeld et al., 2009), visual and olfactory cues in butterflies that use different food sources (Couto et al., 2020; Montgomery et al., 2021), or differences in feeding ecology in primates (Louail et al., 2019). Spiders (Araneae) represent a group of predators that have evolved a wide range of lifestyles, particularly with regard to foraging strategies that depend strongly on vision or vibration (Foelix, 2011). Such lifestyle-specific sensory input is likely reflected in the structure of the CNS. However, while sensory systems in spiders have been well studied (reviewed in Barth, 2002), our knowledge of spider CNS-anatomy is mainly derived from one species with a cursorial lifestyle, the wandering spider *Cupiennius salei* (Keyserling,

1877) (Anton & Tichy, 1994; Babu & Barth, 1984, 1989; Loesel et al., 2011; Schmid & Becherer, 1999; Schmid & Duncker, 1993; Strausfeld et al., 1993; Strausfeld & Barth, 1993). Studies on the brains of other spider species have specifically focussed on details of the visual system (Hanström, 1921; Kovoor et al., 2005; Long, 2021; Steinhoff et al., 2020).

The CNS of spider species studied so far is composed of highly fused ganglia: The ventral nerve cord (VNC), which consists of the posterior opisthosomal neuropil (OpN), four paired leg neuropils (LN 1-4) and a central area with different neuropilar structures that receive primary sensory input from sensilla located on the legs and pedipalps (Anton & Tichy, 1994; Babu & Barth, 1984, 1989). The brain, which is located antero-dorsal of, and fused with the VNC, is composed of the three neuromeres tritocerebrum, deuto- and protocerebrum (Lehmann et al., 2015; Scholtz & Edgecombe, 2006; Steinhoff et al., 2017). The tritocerebrum is largely made up by the pedipalpal neuropil (PdN) and situated just below the esophagus, while the deutocerebrum contains the cheliceral neuropil (ChN) and is situated lateral and dorsal of the esophagus (Babu & Barth, 1984; Lehmann et al., 2015; Steinhoff et al., 2017). The protocerebrum is the dorsalmost neuromere of the brain and is composed of a central neuropilar area (protocerebral neuropil, PN), the higher order integration neuropils arcuate body (AB) and mushroom bodies (MB), as well as the visual neuropils (Babu & Barth, 1984; Steinhoff et al., 2020).

Most spiders possess four pairs of eyes, one of which distinctively differs from the others in anatomy and development (Land, 1985; Morehouse et al., 2017). The principal eyes (or anterior median eyes, AME) have a movable retina, are able to detect colors and are used for object recognition (Barth et al., 1993; Land, 1985; Schmid, 1998; Yamashita & Tateda, 1976, 1978). The secondary eyes (composed of anterior lateral eyes, ALE, posterior lateral eyes, PLE and posterior median eyes, PME), differ considerably between spider families (Homann, 1950, 1952), but have a retina that is not movable, cannot distinguish colors and are used for motion detection (Land, 1985; Morehouse et al., 2017; Schmid, 1998). The principal eye pathway in the brain is similar in all spider species investigated so far and consists of a first order (AM1), second order (AM2) and higher order (arcuate body, AB) neuropil (Steinhoff et al., 2020; Strausfeld et al., 1993). The secondary eye pathway shows pronounced variation between different spider species (Hanström, 1921; Long, 2021; Steinhoff et al., 2020). While in *C. salei* every secondary eye serves its own first and second order visual neuropil (Babu & Barth, 1984; Strausfeld & Barth, 1993), this is not the case in jumping spiders, in which two shared second order visual neuropils exist and the PME is only connected to a single visual neuropil (Steinhoff et al., 2020). Hanström (1921) compared the visual systems of the secondary eyes of three families of stationary hunting spiders with 2 families of cursorial hunting spiders. He found only a single visual neuropil for all secondary eyes in the stationary hunting spiders, in contrast to large first- and second order visual neuropils in wolf spiders and jumping spiders (Hanström, 1921). Long (2021) investigated the secondary eye visual neuropils of species of 19 different families across the spider tree of life and, based on presence and size of neuropils, categorized them in 4 groups: (1) spiders with a single visual neuropil, (2) spiders with a single visual neuropil and mushroom bodies, (3) spiders with a first order visual neuropil, a small second order visual neuropil and mushroom bodies and (4) spiders with large first- and second order visual neuropils and large mushroom bodies. Perhaps not surprisingly, these differences in neuropil number in the secondary eye visual pathway also result in volumetric

differences in visual and higher order protocerebral neuropils of different spider species, as shown by Weltzien and Barth (1991) and Long (2021).

To date, it remains unclear whether the differences in spider brain anatomy are restricted to visual brain areas. This study therefore investigates, whether other central nervous system regions show similar differences that can be related to the sensory ecology of the species studied. We compare the two cursorial hunters *Marpissa muscosa* (Clerck, 1757) and *Pardosa amentata* (Clerck, 1757) with two stationary, web building hunters *Argiope bruennichi* (Scopoli, 1772) and *Parasteatoda tepidariorum* (C. L. Koch, 1841). We compare our findings with the CNS of *C. salei*, (Babu & Barth, 1984, 1989; Strausfeld et al., 1993; Strausfeld & Barth, 1993). We discuss the functional implications of our findings with regard to the sensory ecology of the species studied here.

## 2 Material and Methods

### Experimental animals

Adult females of the following species: *Argiope bruennichi*, *Marpissa muscosa* and *Pardosa amentata*, were collected in and near Greifswald (Germany) and processed for histology and microCT immediately. Individuals of the species *Parasteatoda tepidariorum* were collected in the greenhouses of the botanical garden of the University Greifswald and reared in climate chambers (26°C, 80% humidity, 12/12 hrs light cycle). *P. tepidariorum* individuals were kept individually in plastic boxes of 145 x 110 x 68 mm size that were enriched with paper tissue.

### MicroCT analysis and volume calculation

Prosomata were fixed in fresh acetic alcohol formalin solution (AAF; 10 ml 16% paraformaldehyde, 2.5 ml glacial acetic acid, 42 ml 80% ethanol) at room temperature for 4 hours. Samples were dehydrated in a graded ethanol series (70%, 80%, 90%, 96% and 3x 99.8% ethanol for 30 minutes each) and then transferred to an 1% iodine solution (iodine, resublimated [Carl Roth, X864.1] in 99.8% ethanol) for 48 h to enhance tissue contrast. Samples were subsequently washed three times in 99.8% ethanol, mounted in fresh 99.8% ethanol and scanned once (overview scan of the entire prosoma). Afterwards, samples were critical point dried with an automated dryer (Leica EM CPD300) using slow CO<sub>2</sub> admittance with a delay of 120 seconds, 30 exchange cycles (CO<sub>2</sub> : 99.8% ethanol), followed by a slow heating process and slow gas discharge. Dried prosomata were mounted using a conventional glue gun onto plastic rods, so that the anterior median eyes were oriented upwards.

MicroCT scans were carried out with an optical laboratory-scale X-ray microscope (Zeiss XradiaXCT-200). Scans were performed with a 4x or a 10x objective lens unit using the following settings: 40 kV, 8 W, 200 µA and exposure times between 0.5 and 3s. Scans took between 1 and 2 h and resulted in pixel sizes between 1.7 µm and 5.5 µm. Reconstruction of tomographic projections was done using the XMReconstructor software (Zeiss), resulting in image stacks (TIFF format). All scans

were performed using Binning 2 for noise reduction (summarizing 4 pixels) and were reconstructed with full resolution (using Binning 1).

The volumes of the different neuropilar structures were calculated using AMIRA 5.4.5 and 6.0.0 (Visualization Science Group, FEI). Since we are comparing different species with different body sizes, it was necessary to calculate the amount of shrinkage of the tissue for each specimen (Rivera Quiroz & Miller, 2022). To do this, the CNS volume in both the wet and the dried condition and the factor by which the two differed was calculated. This factor was later used to adjust the volumes of the different brain regions, which were reconstructed and calculated from the dried scans. In order to account for individual variation, we reconstructed the CNS structures of 3 specimen per species and used the mean for comparison (given in percent of total CNS neuropil volume). A full table of all calculated volumes is available from Morphobank (see data availability statement).

### **Bodian reduced silver staining**

Following anesthetization with CO<sub>2</sub> and removal of the opisthosoma and legs (without coxae), the prosomata of several individuals of the four focal species were fixed in AAF solution (42 ml 80% ethanol, 10 ml 16% paraformaldehyde (PFA), 2.5 ml acetic acid). After four hours in fixative, the prosoma was dehydrated through a graded ethanol series (70%, 80%, 90%, 96%) and was then transferred for two hours into a 1:1 solution of 96% ethanol:tetrahydrofuran [Carl Roth, CP82.1]. Samples were kept for 24 hours in 100% tetrahydrofuran followed by 24 hours in a solution of 1:1 tetrahydrofuran and paraffin (Carl Roth, 6643.1). Afterwards, samples were embedded in pure paraffin. Horizontal, frontal and sagittal sections (15 µm) were made with a motorized rotary microtome (Microm HM 360) and subsequently stained according to the original Bodian method (Bodian, 1936). Sections were rehydrated through an ethanol series (Roti Histokit, terpeneol, 100%, 90%, 70%, 50% ethanol) and incubated overnight at 60°C in a 2% protargol solution. Protargol was synthesized according to the recipe by Pan et al. (2013). To achieve an ideal staining result, the pH was set to 8.0. No copper was added to the solution, as we found that even a small amount (0.25%) increased the selectivity of the stain to an undesired degree. In the morning, the staining jar was allowed to cool to room temperature, sections were briefly rinsed in ddH<sub>2</sub>O and then developed in a 1% hydroquinone/ 2% sodium sulfite mixture in ddH<sub>2</sub>O for 5 min. Afterwards, sections were rinsed under running tap water for 3 min and then placed in a solution of 1% gold chloride in ddH<sub>2</sub>O for 10 min. Sections were then rinsed in two changes of ddH<sub>2</sub>O for 15 sec each and placed in a 4% oxalic acid solution for 8 min. Following two additional rinses in ddH<sub>2</sub>O for 15 sec each, sections were placed in 10% sodium thiosulfate for 5 min. Finally, sections were washed two times in ddH<sub>2</sub>O for 8 min, dehydrated through an ethanol series (the inverse of the series above) and mounted in Roti-Histokitt II (Carl Roth, T160.1) under glass slides. The protocol described above consistently yielded very good staining of *P. amentata*, *M. muscosa* and *P. tepidariorum* sections. However, no consistent results were obtained for *A. bruennichi*, as often only a few neurites were recognizable. In some series, individual sections stained well, while in other series only parts of sections or none at all showed the desired degree of selectivity. We tried variations of the above protocol following the

recommendations of Gregory (1980) but none of them produced results comparable to those we obtained in the other species studied here. Interestingly, attempts in related species (*Argiope lobata*, *Araneus cornutus*) did not work either, which raises the question whether some specific tissue property present in orb-weavers is responsible for the partial failure of the Bodian method.

### **Anterograde tracing of retinula cells**

To clarify the identity of the visual neuropils, the axons of retinula cells (rca) of the different secondary eyes were traced in *A. bruennichi* and *P. tepidariorum*. The spiders were anaesthetized with CO<sub>2</sub> and immobilized on a dissection dish filled with plasticine, using insect pins and a piece of fine mesh. A tiny hole was pierced into one of the eyes using a custom made manual micromanipulator and a minutia. Using thin forceps, a crystal of micro-emerald (dextran fluorescein with biotin, 3000 MW, D7156; ThermoFisher) was inserted through the hole in the eye. The hole was then sealed with Vaseline. The preparations were stored overnight at 4°C so that the dye had sufficient time to reach the termination sites of the retinula cell axons. The next morning, the spiders were dissected, the CNS with eye nerve and retinae attached isolated and fixed overnight in 2% PFA. After several washing steps in PBS, the brains were immunostained with anti-synapsin (see details of below; Table 1 & 2). Finally, the tissue was cleared in RapiClear (SunJin Lab) and imaged with a Leica SP5 II confocal microscope.

### **Immunohistochemistry**

Three different combinations of markers were used to visualize neuropils and connecting neurites in the central nervous system of the four focal spider species (see Table 1 for a list of marker combinations used, and Table 2 for specifications of labeling reagents).

Individuals of the four species (details Table 2) were anaesthetized with CO<sub>2</sub> and then their brains were dissected out in PBS and fixed overnight at 4°C in 2% PFA. The brains were washed six times in PBS for 15 minutes each and then immersed in Poly-L-Lysin (Sigma-Aldrich, P4707) for one minute. Samples were then embedded in 4% agarose (Sigma-Aldrich, A9414) and sectioned (50 or 80 µm) using a Microm HM 650 V vibratome. After permeabilization in PBS-TX (PBS, 0.3% Triton X-100 [Sigma-Aldrich, X100], 1 % bovine serum albumin [Sigma-Aldrich, A2153], 0.05% Na-acide; or alternatively PBS, 0.5% Triton, 1.5% DMSO) for 1 h at room temperature, incubation in primary antibodies was performed overnight at 4°C or room temperature. The sections were washed several times with PBS-TX after incubation. Incubation in secondary antibodies or counterstains was done overnight at 4°C or room temperature. After repeated washing in PBS, the sections were mounted in Mowiol (Merck 475904).

Two individuals of *Parasteatoda tepidariorum* were processed as whole-mounts, according to an adapted protocol after Ott (2008; see also Steinhoff et al., 2017). Brains were dissected in TRIS buffer (0.1M, pH 7.4 [Carl Roth, 4855]), and fixed in zincformaldehyde at room temperature with gentle shaking for several days. The brains were then washed three times for 15 min each in TRIS buffer and

incubated for two hours in a 4:1 mixture of methanol and DMSO (dimethylsulfoxide [Carl Roth, 4720]). After incubation in 100% methanol for 1 hr, the brains were rehydrated in a graded series of methanol (90, 70, 50, and 30%) for 10 min each and washed in TRIS buffer. The brains were then permeabilized in PBS-DMSO (PBS, 5% bovine serum albumin, 1% DMSO, 0.05% Na-acide) for 2 hrs at room temperature and incubated in primary antibody at 4°C for 4 days. The brains were then washed several times in PBS-DMSO for 2 hr and incubated in secondary antibody for 4 days at 4°C. They were then transferred to a graded glycerol series containing 1, 2, and 4% (each for 2 hrs) and 8, 15, 30, 50, 60, 70, and 80% (each for 1 hr) glycerol in TRIS buffer and 1% DMSO. After five changes in pure ethanol for 30 min each, the brains were mounted in fresh methyl salicylate (Sigma, 76631). We replaced the primary antibodies with PBSTX in control experiments and did not detect any neuronal labeling.

### **Microscopy, image processing and nomenclature**

Immunohistochemically labelled sections and whole-mounts were examined with a Nikon eclipse 90i microscope and imaged with a Leica SP5 II confocal microscope (cLSM). Serial Bodian-stained paraffin sections were examined and photographed with a Nikon eclipse 90i microscope at 20x magnification. Alignment of images from Bodian-stained sections was carried out using the TrakEM2 module in ImageJ 1.52i and the AlignSlices module in AMIRA 5.4.5. Three-dimensional visualizations of Bodian and microCT image stacks was performed using AMIRA 5.4.5 and 6.0.0 (Visualization Science Group, FEI). Drawings and figure plates were created using, Corel PaintShop Pro 21.0 and CorelDRAW 20.1. The images were processed in Corel Paint Shop Pro with global contrast and brightness adjustment functions. The terminology used for CNS structures is consistent with Richter et al. (2010). For spider-specific CNS structures, we follow the terminology of Steinhoff et al. (2020), Strausfeld et al. (1993), Strausfeld and Barth (1993) and (specifically with regard to tracts in the VNC) Babu and Barth (1984, 1989). Positional data are given in relation to the body axis. We refer to results from immunohistochemical experiments as immunoreactivity, for example synapsin-immunoreactivity.

### **Abbreviations**

<b>AB</b>	Arcuate body
<b>ABd</b>	Dorsal lobe of the arcuate body
<b>ABv</b>	Ventral lobe of the arcuate body
<b>ALE</b>	Anterior lateral eyes
<b>AL1</b>	First order visual neuropils of ALE
<b>AL2/PL2</b>	Second order visual neuropils of ALE and PLE
<b>AME</b>	Anterior median eyes
<b>AM1</b>	First order visual neuropils of AME

<b>AM2</b>	Second order visual neuropils of AME
<b>ASc</b>	Anterior stomodeal commissure
<b>Bc3-5</b>	Brain commissure 3-5
<b>BN</b>	Blumenthal neuropil
<b>BVT</b>	Brain vertical tract
<b>Cc</b>	Central commissure
<b>Chc</b>	Cheliceral commissure
<b>Chc2</b>	Cheliceral commissure 2
<b>ChN</b>	Cheliceral neuropil
<b>CL</b>	Centro-lateral tract
<b>CT</b>	Central tract
<b>cVNC</b>	central part of the ventral nerve cord
<b>Dc</b>	Dorsal commissure
<b>Dcb</b>	Deutocerebrum
<b>ES</b>	Esophagus
<b>GC</b>	Globuli cells
<b>L2</b>	Second order visual neuropils of anterior and posterior lateral eyes
<b>LCT</b>	Lateral cerebral tract
<b>LN 1-4</b>	Leg neuropils 1-4
<b>LSAT</b>	Lateral sensory association tract
<b>MB</b>	Mushroom bodies
<b>MBb</b>	Mushroom body bridge
<b>MBb2</b>	Mushroom body bridge 2
<b>MBd</b>	Mushroom body head
<b>MBh</b>	Mushroom body haft
<b>MBp</b>	Pedunculus of the mushroom body
<b>MC</b>	Mid-central tract
<b>MDc</b>	Mid-central commissure



<b>MCT</b>	Median-cerebral tract
<b>MD</b>	Mid-dorsal tract
<b>MDc</b>	Mid-dorsal commissure
<b>MV</b>	Mid-ventral tract
<b>oe</b>	oesophagus
<b>OpN</b>	Opisthosomal neuropil
<b>PCC</b>	Protocerebral commissure
<b>PCDT</b>	Protocerebro-dorsal tract
<b>PCMT</b>	Protocerebro-median tract
<b>PCVT</b>	Protocerebro-ventral tract
<b>PdN</b>	Pedipalpal neuropil
<b>Pdp</b>	Pedipalpal projection
<b>Pdc</b>	Pedipalpal commissure
<b>Pdc2</b>	Pedipalpal commissure
<b>PH</b>	Pharynx
<b>PHd</b>	Dilator muscle of pharynx
<b>PLE</b>	Posterior lateral eyes
<b>PL1</b>	First order visual neuropils of the PLE
<b>PL2</b>	Second order visual neuropils of the PLE
<b>PME</b>	Posterior median eyes
<b>PM1</b>	First order visual neuropils of the PME
<b>PM2</b>	Second order visual neuropils of the PME
<b>PN</b>	Protocerebral neuropil
<b>Princ_VN1</b>	First order visual neuropil of the principal eyes
<b>Princ_VN2</b>	Second order visual neuropil of the principal eyes
<b>PrincVis</b>	Visual neuropils of the principal eyes
<b>PSc</b>	Posterior stomodeal commissure
<b>rca</b>	retinula cell axons

<b>SC</b>	Soma cortex
<b>Sec_VN1</b>	First order visual neuropil of the secondary eyes
<b>Sec_VN2</b>	Second order visual neuropil of the secondary eyes
<b>SecVis</b>	Visual neuropil(s) of the secondary eyes
<b>SLT</b>	Sensory longitudinal tract
<b>ST</b>	Sucking stomach
<b>STb</b>	Stomodaeal bridge
<b>Tcb</b>	Tritocerebrum
<b>VC</b>	Ventral commissure
<b>VisN</b>	Visual neuropils
<b>VL</b>	Ventro-lateral tract
<b>VMT</b>	Ventral median tract
<b>VNC</b>	Ventral nerve cord

### 3 Results

#### General organization of the central nervous system

The CNS comprises a fused ventral nerve cord (VNC) and the brain. The VNC consists of a central neuropil rich in tracts (cVNC, see details below), four paired leg neuropils and a posterior opisthosomal neuropil. The brain is composed of three neuromeres, the trito-, deuto- and protocerebrum. The tritocerebrum is situated below the esophagus and formed by the pedipalpal neuropil, while the deutocerebrum borders the esophagus laterally, extends slightly above it and consists of the cheliceral neuropil. The protocerebrum is the dorsalmost neuromere of the brain and consist of a central neuropil with many tracts, the arcuate body and visual neuropils. The entire CNS is surrounded by a soma cortex, which is thickest ventral of the VNC, while only a thin layer of very few somata can be observed dorsal of the VNC (Figures 13a). We could distinguish two different cell types: Giant somata, which are found in small numbers and only ventral of the VNC (Figures 7d, 13a) and regular somata that are most densely packed anterior of the protocerebral neuropil (PN) (Figures 1a,d, 3a-b,e,f, 6a,c,e, 7a-d, 8b-c,d, 9a-e, 10a-d, 13a-b). In the following, we give a detailed description of each CNS area. We always describe *P. amentata* first, because its CNS is most similar to that of *C. salei* and then highlight the differences in the other three species, *M. muscosa*, *A. bruennichi* and *P. tepidariorum*. We will be brief in describing the visual system in *M. muscosa*, as we described it in great detail in an earlier study (Steinhoff et al., 2020). 3D PDFs with all reconstructed neuropils and tracts for all species are available at Morphobank (see data availability statement).

## The principal eye pathway

In *P. amentata*, the retina of the principal eyes is connected to its first-order neuropil (AM1) by long retinula cell axons. The AM1 is cup-shaped and situated posterior to the first order visual neuropils of the secondary eyes (see section below), embedded in the anterior soma cluster (Figures 1b-b'). It is connected to the second-order visual neuropil (AM2) by a neurite bundle (Figures 1b-b'). The AM2 is of oval shape and a neurite tract projects from it into the posterior brain region and connects to the arcuate body (AB) (Figures 1b-b'). This general arrangement is the same in all four species studied, although in *M. muscosa* the AM1 is clearly subdivided into distinct regions (Figures 1a and compare Steinhoff et al., 2020). The AM1 in *A. bruennichi* is the dorsalmost neuropil and situated anterior of the dorsal soma cluster (Figures 1c-c'). The AM2 is located at the outer rim of the brain, has weak synapsin-immunoreactivity and its shape is less well distinguishable from the surrounding neuropil than in *P. amentata* (Figures 1c). In *P. tepidariorum*, the AM1 is roundish instead of cup-shaped and situated more anterior than in *P. amentata* (Figures 1d-d'). The AM2 has a slender oval shape and is less clearly distinguishable from the surrounding protocerebral neuropil (Figures 1d).

## The secondary eye pathway

In *P. amentata*, each eye supplies its own first order visual neuropil via long retinula cell axons that extend in a single bundle through the anterior prosoma along with the nerve of the principal eyes (Figures 4a). The first order visual neuropil of the PME (PM1) is the largest and most dorsally located visual neuropil. The first order visual neuropil of the PLE (PLE1) is only slightly smaller and similarly shaped, lying just below the PM1 (Figures 2a,c, 4a). The first order visual neuropil of the ALE (AL1) is much smaller than the PM1 and PL1 and nested within the visual neuropils posterior of the ventralmost part of the PL1 (Figures 2a,c, 4a). All first order visual neuropils send long conspicuous axons along the brain margin into the region immediately anterior and ventral of the AB, where they form an arch and probably terminate (Figures 2c, 4a). In addition, each first order visual neuropil supplies its own second order visual neuropil (PM2, PL2 and AL2), which are glomerular in structure and located directly posterior of their first order visual neuropil (Figures 2a,c, 4a). While PM2 and PL2 are both slightly smaller than PM1 and PL1 respectively, AL2 is similar in size to AL1 (Figures 2a,c, 4a). All three second order visual neuropils send most of their axons to the anterior part of the MB, the mushroom body head (MBd) (Figures 2a,c, 4a). This arrangement found in *P. amentata* contrasts with the situation in *M. muscosa*, where the first order visual neuropils of the AL1 and PL1 are connected to two second order visual neuropils (AL2/PL2 and L2) and the small PM1 is only connected to the AB (Figures 2b,d, 4b). While AL1 and PL1 are also connected to the AB, AL2/PL2 and L2 are all connected to the MB in *M. muscosa* (Figures 2b,d, 4b) (compare also Steinhoff et al., 2020).

In *A. bruennichi*, anti-synapsin labelling and Bodian-staining show that the retinula cell axons of the secondary eyes terminate in two closely adjacent, anterior cauliflower shaped neuropils and a smaller, tripartite finger-shaped neuropil, which is located just posterior of the cauliflower-shaped neuropils (Figures 3a-c). Dye-backfills from the different secondary eyes reveal that the posterior-median eyes send retinula cell axons only into the more medial cauliflower-shaped neuropil (PM1a) and the left (closest to the midline of the brain) "finger" of the tripartite neuropil (PM1b) (Figures 3a). The retinula

cell axons of the posterior-lateral eyes, on the other hand, terminate in the more lateral cauliflower-shaped neuropil (PL1a) and the medial “finger” of the tripartite neuropil (PL1b) (Figures 3b, 5a). The smaller anterior-lateral eye (ALE) sends retinula cell axons only into the right (lateralmost) “finger” of the tripartite neuropil (AL1) (Figures 3c, 5a), but some axons terminate posterior of the AL1 (Figures 3c', 5a). Crossing of retinula cell axons from the different eyes was not observed, implying that each eye strictly serves its own visual neuropils (Figures 3a-c, 5a). Thus, PME and PLE send axons into two first order visual neuropils, PM1a, PM1b, PL1a and PL1b, while the ALE only sends axons into one first order visual neuropil, the AL1 (Figures 3a-c). While PM1b, PL1b and AL1 are connected to the region just anterior and ventral of the AB via long neurites that run along the outer rim of the protocerebrum, PM1a and PL1a are connected to the anterior MB via thick neurite tracts (Figures 2f-f',h, 5a).

In *P. tepidariorum*, there is only one pair of first order visual neuropils of the secondary eyes (SecVis), supplied by retinula cell axons of all secondary eyes as shown by Bodian stains and dye backfills (Figures 2e-e', 3d-e'). While the retinula cell axons of the ALE terminate mostly anterior-medially in the SecVis, the termination sites of the PME rca are distributed more throughout the neuropil and some terminate posteriorly and outside of the SecVis (Figures 3d-e', 5b). Due to the small size of the secondary eyes, we were not able to trace the PLE rca, but these likely terminate in the most lateral part of the SecVis (Figures 3e, 5b). A thin tract of neurites connects the SecVis directly to the AB, similar to the other species studied (Figures 2e-e', 5b). Tubulin-immunostaining shows that further neurites originating from the SecVis run ventrally into the protocerebral neuropil (Figures 2g-g'). Their exact termination site or origin (if they are ascending neurites) could not be determined.

### **Arcuate body**

In all four species investigated, the AB is a distinct crescent-shaped neuropil in the dorso-posterior region of the brain, directly adjacent to the soma cortex (Figures 1, 2c-d,e'-f', 7a, 8, 13a). It consists of three distinct layers and contains an intricate arrangement of fine neurites that cross each other in a regular pattern (Figures 7a, 8b,d). In sagittal sections using Bodian stains or anti-tubulin immunolabeling, a group of neurites (likely primary neurites) arises in the soma cluster dorsal of the AB, passes through the AB and projects into the central part of the PN (Figure 13). In all species examined, the AB is the termination site of neurites from the visual neuropils AM2, PL1, AL1 and PM1 (PL1b and PM1b in *A. bruennichi*, see above) (Figures 1b-d', 2c-f'). The AB is further connected to the PN and the VNC via the protocerebro-dorsal tract (PCDT; see details below) (Figures 8a,c,f). We did not detect any significant differences between the four species in the structure and connectivity of the AB.

### **Mushroom bodies**

*P. amentata* possesses prominent, bilaterally paired mushroom bodies (MB), that can be subdivided into 3 structures: The cup-shaped mushroom body head (MBd) the mushroom body pedunculus (MBp) and the mushroom body haft (MBh) (Figures 2a,c, 4a, 6a,b, 13a). The MB are connected to each other by a thick commissure (mushroom body bridge, MBb) that forms an arch across the midline of

the brain and enters the MBp from posterior (Figures 2c, 4a, 6a-b). A second, much thinner commissure consisting of a few long neurites (MBb2) is situated posterior-ventrally of the MB, embedded within the PN (Figures 7b, 8a,e). The neurites that compose the MBb2 are part of the MCT (see below) and enter the MBp from ventrally (Figures 8a,e). The MBb2 could only be detected in frontal Bodian-stained sections, likely due to the fact that it is very thin. In *M. muscosa*, however, the MBb2 is composed of more neurites and can be distinguished in both horizontal and frontal Bodian-stained sections (Figures 6d). A MBd is not detectable in *M. muscosa* and the MBh does not form a continuous neuropil with the MBp as was found for *P. amentata* (Figures 6c-d) (compare also Steinhoff et al., 2020).

The MB in *A. bruennichi* consist of a drop-shaped MBp that shows strong synapsin-immunoreactivity, a thick MBb containing large neurites, and the MBh located in the center of the bridge on the midline of the brain, forming a single roundish neuropilar structure (Figures 2f',h, 5a, 6e-f). We did not detect a MBb2, but there are a few thin, long neurites projecting from the MBh into the central PN (Figures 6f). In *P. tepidariorum*, no MB-like neuropil could be detected by either immunostaining or Bodian staining. However, there is a thin commissure crossing the brains midline, which we putatively interpret as MBb (Figures 2g', 12b). A MBb2 is not present in *P. tepidariorum*.

### **Protocerebral tracts**

Apart from the visual neuropils, the protocerebrum in all species investigated consists of a central neuropil (protocerebral neuropil, PN), traversed by commissures that connect the different neuropils with each other, as well as prominent longitudinal tracts connecting the higher order neuropils AB and MB with the VNC. While several of the longitudinal tracts could be reconstructed from Bodian-stained serial sections, the exact connections of the commissures are not always clear. They are characterized here and synonymized between the different species based on their position and relative size. In *P. amentata*, we detected four brain commissures, which are: The anterior and posterior stomodeal commissures (ASc and PSc), two commissures similar in size, both situated posterior to the stomodeal bridge neuropil (Stb) and bordering the PN dorsally and the esophagus ventrally (Figures 8a,d-f, 11a-c). The Stb is located just dorsally of the esophagus, enveloping it laterally and thus forming a horseshoe-shape (Figures 7c, 8a,e, 9d, 11a-c). The ASc consists of neurites that curve downward and form two thick tracts that reach the ventral part of the VNC and connect to the centro-lateral tract (CL tract, see below) (Figures 8a,e, 11b). The neurites making up the PSc, on the other hand, curve upward where they split up into individual neurites that reach both the lateral- and dorsalmost parts of the PN and connect the PSc directly to the AB (Figures 8d,f, 11b). Dorsal of the PSc are the Bc3 and Bc4, both of which are considerably smaller than the ASc and PSc (Figures 6a-b, 8f, 11a). While the Bc4 is composed of neurites directed towards the dorsal PN, the Bc3 consists of neurites directed towards the ventral PN (Figures 8f). The dorsalmost commissure in the PN is the PCC, which consists of thin neurites embedded in a neuropilar structure and is situated immediately posterior of the MBb (Figures 7a-c, 8f, 11a). A prominent tract (median cerebral tract, MCT) connects the PCC directly with the ventral nerve cord and joins the sensory longitudinal tract (SLT, see below) (Figures 7c, 8e, 13a). The MCT also extends to a region dorsal of the PCC, showing that it consists not only of neurites involved in the PCC, but also of neurites originating dorsolaterally of the PCC (Figures

7c). Anteriolateral of the MCT is the brain vertical tract (BVT), a conspicuous bundle of neurites originating in the dorsal somata cluster and extending ventrally into the SLT (Figures 8a,e). Anterior of the PCC is the protocerebro-ventral tract (PCVT), which forms two bilaterally paired arches below the MB that extend into the central PN (Figures 6b, 7b, 11a). The ventral median tract (VMT) is formed by neurites that pass below the PCC and the MBb and cross over the latter, where they enter the dorsal PN (Figures 6b, 7a). The lateral cerebral tract (LCT) is the most laterally located tract in the protocerebrum and connects the MB to the VNC (Figures 2c, 6b, ). In *P. amentata* the LCT divides into four different tracts, one of which connects to the MBh, one into the MBp and two into the MBd (Figures 6b). The protocerebro-dorsal tract (PCDT) is located just below the AB and forms an arch anterior of the neurites from the secondary eye visual neuropils (Figures 7b, 8a,c-d,f, 11a). The PCDT also has branches that connect it to the AB, the VNC and the central PN (Figures 7b, 8a,c-d,f, 11a). The brain commissures in *M. muscosa* are very similar in size and shape to those of *P. amentata* (Figures 6d, 11d-f). However, there is an additional commissure not found in *P. amentata* (brain commissure five, Bc5), which is situated dorsal of the PSc, has a downward curved shape and consists of thin, tightly adjoining neurites (Figures 6d). In *M. muscosa*, the LCT splits into three individual tracts instead of four (as in *P. amentata*), two of which are connected to the MBp and one of which contributes to the MBb, while none appears to be directly connected to the MBh (Figures 6c-d). In *A. bruennichi*, the LCT arises from the mid-central tract of the VNC (MC, see below), does not split up in the protocerebrum and connects to the MBp (Figures 6f). There are a number of neurites that extend from the MBh towards the LCT and might contribute to the formation of the LCT, but we did not observe a direct connection (Figures 6f). We did not detect Bc4 in *A. bruennichi*. While the general architecture of the protocerebral tract system in *P. tepidariorum* resembles that of *P. amentata*, we did not detect a LCT as in all other investigated species.

### **Cheliceral and pedipalpal neuropils**

The cheliceral neuropils border and extend above the esophagus, while the pedipalpal neuropils are entirely situated below the esophagus in all investigated species. Both the cheliceral and pedipalpal neuropils are connected by commissures. There are two pedipalpal commissures in all species examined (Figures 9b-c, 10b, 11, 12). There is a single cheliceral commissures in *A. bruennichi* and *P. tepidariorum* (Figures 12), whereas *P. amentata* and *M. muscosa* possess two cheliceral commissures located above and below the esophagus (Figures 9d, 11b-c,e-f). In addition to the pedipalpal commissures and ventrally situated, every species has a bundle of neurites projecting from the pedipalpal neuropil into the VNC (Pdp) and terminating within the sensory longitudinal tract (SLT, see below) (Figures 9a,e, 10c, 11a-d, f).

### **The ventral nerve cord**

The anatomy of the VNC is remarkably similar in the investigated species. The central neuropil is dominated by six major longitudinal tracts and contralateral commissures between the leg neuropils, which are embedded in a central association area (Figures 10, 11, 12, 13). This general layout is fairly consistent with the description of the VNC in *Cupiennius salei* (Babu & Barth, 1984). There are six longitudinal tracts that traverse the VNC from the posterior opisthosomal neuropil to the brain, where

they enter the PN and then split up into smaller tracts (described above; Figures 7d, 8a,c-f, 9e). The Mid-dorsal tract (MD) is the most dorsal one. This tract occupies most of the dorsal VNC (Figures 8a,f, 9e, 10a, 11, 12). The Mid-central tract (MC) is situated just below the Dc and flanks the midline of the VNC (Figures 8f, 10a-b, 11a-b,d-e, 12, 13a). It has a distinct, almost triangular shape, with the widest part oriented towards and extending into the brain (Figures 10b). Ventral of the MC follow three similarly sized tracts that form the core of the VNC: The Centro-lateral tract (CL) followed by/dorsal of the slightly more medial central tract (CT), which is dorsal of the Ventro-lateral tract (VL) (Figures 8a,c,e-f, 9e, 10b-d, 11, 12). The most ventrally located tract is the Mid-ventral tract, which is situated just dorsally of the ventral somata cluster (Figures 11c,f, 12c,f). In addition to these major longitudinal tracts, we identified a large tract (sensory longitudinal tract, SLT; known to receive sensory input in *C. saiei*), located in the centralmost area of the VNC, anteriorly connecting to the protocerebrum, where it splits into smaller tracts (see above, Figures 7d, 8a,d-e, 10a-b,d, 11, 12, 13a). The SLT is characterized by mostly small neurites, which in Bodian preparations are darker in color than the neurites of the other six longitudinal tracts (Figures 7d, 8d, 10d, 13a). In addition to the longitudinal tracts, there is a longitudinal neuropilar structure, the lateral sensory association tract (LSAT), which shows strong anti-synapsin immunoreactivity in all investigated species (Figure 13c). While it is easy to distinguish the different longitudinal tracts, it is more difficult to tell apart the different groups of commissures, which are often stacked in close proximity and connect the bilaterally paired leg neuropils and longitudinal tracts. We identified four distinct commissures (dorsal commissure: Dc, mid-dorsal commissure: MDc, central commissure: Cc and ventral commissure: Vc; Figures 8e-f, 9a,e, 10a-b, 11, 12) in all four species and an additional fifth commissure (mid-central commissure: Mcc; Figures 8f, 11c) in *P. amentata* and *M. muscosa*. In all four species, the Dc and MDc are closely adjacent without longitudinal tracts in between (Figures 10a, 11b,d-e, 12a-b,d-e), while the other commissures are more clearly separated (Figures 8f, 9e, 11c,f, 12c,f). In *P. amentata* and *M. muscosa*, we detected a somewhat columnar shaped neuropilar structure just below the esophagus and bordering the midline of the brain. This structure stains darker than the surrounding tissue in the Bodian preparations (Figure 9c). We tentatively interpret this structure as Blumenthals neuropil (BN). However, we could not confirm its presence in anti-synapsin immunolabeling of *P. amentata* and *M. muscosa*, nor find it at all in *A. bruennichi* and *P. tepidariorum*.

### **Comparative volumetric analysis of the central nervous system neuropils**

The spider species investigated here differ in their relative investment in different neuropils (see pie charts in Fig. 14 for information on comparative brain volumes). In all four species, the VNC makes up more than half of the CNS volume, but it is much larger in the stationary hunting spiders than in the cursorial hunting spiders (73.3% in *A. bruennichi* and 76.5% in *P. tepidariorum* compared to 63.8% in *P. amentata* and 55% in *M. muscosa*). While the central VNC (cVNC) has a similar proportional volume in all 4 species, the LN and the OpN are proportionally larger in the stationary hunters *A. bruennichi* and *P. tepidariorum* than in the cursorial hunting spiders *P. amentata* and *M. muscosa*. The LN is also considerably larger in *P. amentata* than in *M. muscosa*. Within the brain, the largest differences in proportional investment are found between cursorial and stationary hunting spiders, with *P. amentata* and *M. muscosa* having much more nervous tissue dedicated to visual processing (visual

neuropils and mushroom bodies) than *A. bruennichi* and *P. tepidariorum*. However, there are also clear differences between the two cursorial hunters (*M. muscosa* has much larger proportional visual brain area than *P. amentata*) and the two stationary hunters (*A. bruennichi* has more nervous tissue dedicated to visual processing than *P. tepidariorum*). Furthermore, the visual neuropils of the principal eyes (PrincVis) have the same proportional volume in *P. amentata* and in *A. bruennichi*. We also found that the relative volumes of the PN are somewhat larger in the cursorial hunting spiders than in the stationary hunting spiders, while the PdN is largest in *P. amentata*, followed by *A. bruennichi*, *M. muscosa* and *P. tepidariorum*. There seems to be no difference in the proportional volume of the AB and the ChN.

## 4 Discussion

Comparative studies on the neuroanatomy of spiders have so far focused on the visual system, particularly the neuropils in the secondary eye visual pathway (Hanström, 1921; Long, 2021; Steinhoff et al., 2020). Stationary hunting spiders were reported to have fewer and smaller visual neuropils than cursorial hunting spiders, however, this aspect displayed a high level of variability (Hanström, 1921; Long, 2021; Steinhoff et al., 2020). Here, we have extended the scope of comparative neuroanatomical studies in spiders by performing a detailed analysis of all parts of the CNS. While we confirm that the most striking differences occur in the secondary eye visual pathway, we also find additional differences in the connectivity and relative volume of neuropils in the brain and show that the anatomy of the VNC is remarkably conserved among spider species with different sensory ecologies (Figures 4, 5, 10, 12, 15; Table 3).

### Soma cortex and cell types

Babu and Barth (1984) distinguished four distinct cell types in *C. salei*: Type A, which had the smallest diameter and were termed “globuli cells” because of the association with the mushroom bodies. However, Steinhoff et al. (2020) reported that in *M. muscosa* the somata in the corresponding cell cluster were not smaller than other somata. We can now confirm this finding using Bodian stains for all four species investigated here. We found that the somata in the anterior part of the brain are more densely packed (Figure 13a), but we did not find a cluster of distinctly smaller somata as described for *C. salei* (Babu & Barth, 1984; Strausfeld & Barth, 1993). Either an anterior protocerebral cluster of smaller somata is specific to *C. salei*, or there is not any real size difference between “type A” and “type B” cells. Instead, the differences may only be in packing density. Type B cells were described as small somata that make up the majority of the cortex (Babu & Barth, 1984). They correspond to the regular somata described in this study. Type C cells in *C. salei* were described as neurosecretory cells that are intermediate in size between regular (“type B”) and giant (“type D”) somata; few in number and occur in the protocerebrum (Babu & Barth, 1984). We did not find any candidates for such cells in any of the four species studied here. However, it is possible that the staining methods employed here did not make them visible. Unfortunately, no images of type C cells in *C. salei* are available, so



that it remains somewhat unclear what to look for. Type D cells have been described as large motor- or interneurons (Babu & Barth, 1984) and correspond to the giant somata described here (Figure 7d).

## Visual system

The number of neuropils in the visual system and their connectivity in the principal eye-pathway is the same in all spider species studied to date (Long, 2021; Steinhoff et al., 2020; Strausfeld et al., 1993). Considering the variation within the visual pathway of the secondary eyes, this is remarkable and suggests that the AME serve a similar function in all spider species that possess them. In Salticids and in *C. salei*, the AME are used for object recognition (Fenk et al., 2010; Land, 1972; Schmid, 1998). However, whether stationary hunting spiders such as *A. bruennichi* and *P. tepidariorum* are capable of such behavioral performance remains to be tested.

The visual system of the secondary eyes in *P. amentata* is very similar in anatomy and connectivity to that of *C. salei* (Steinhoff et al., 2020; Strausfeld & Barth, 1993). In both species, all secondary eyes serve their own first and second order visual neuropils, before the information is sent on to the MB. All first order visual neuropils are furthermore connected to the AB. Aside from the similarities, the AL1, PL1 and PM1 appear to be much more convoluted in *P. amentata* than in *C. salei* (this study, compare with Babu & Barth, 1984; Steinhoff et al., 2020; Strausfeld & Barth, 1993), which probably increases the surface area of these neuropils. This aspect coincides with the fact that *C. salei* is strictly nocturnal and hunts prey mainly through vibratory cues (Barth & Seyfarth, 1979), while *P. amentata* hunts its prey during the day, when more visual information is available. The secondary eye visual system of the stationary hunter *A. bruennichi* is very different from all other visual systems described so far in spiders. While *A. bruennichi* has no second-order visual neuropils, the PME and the PLE have specialized retinula cells that project either into a neuropil that is linked to the MB (PM1a, PL1a) or another neuropil that connects to the AB (PM1b, PL1b). The ALE, on the other hand, only connects to a single neuropil, which is linked to the AB (AL1), but some retinula cell axons project further into the PN and could potentially connect the ALE to the MB as well. Long (2021) reported the absence of second-order visual neuropils in the species *Argiope trifasciata*, but misinterpreted the identity of the different first-order visual neuropils as three different structures, each serving one eye. It would be interesting to explore how the distinct photoreceptors are arranged in the retina and whether they sample the entire field of view or only part of it. The lack of a second-order visual neuropil implies that less intensely processed information is sent to the MB in this species. The quality of motion vision might thus be reduced compared to spiders with second-order visual neuropils. In *P. tepidariorum*, all secondary eyes extend their retinula cell axons into a single visual neuropil (SecVis) that is directly connected to the AB. We found that some PME rca terminate posterior of the SecVis, and these may connect further to other brain regions than the AB. We also discovered a potential MBb, indicating the possibility that the MB circuit is present in *P. tepidariorum* but reduced to such a degree that no neuropils are visible.

## The spider mushroom body

The mushroom body of spiders is clearly a higher-order visual neuropil, as it receives input mainly from the second-order visual neuropils of the secondary eyes (Babu & Barth, 1984; Long, 2021;

Steinhoff et al., 2020; Strausfeld & Barth, 1993 and cf. this study). Furthermore, we have shown here that *P. tepidariorum* does not possess any conspicuous mushroom-body-like neuropils, which is also the case in other spider species and seems to be related to poor visual abilities and a stationary lifestyle (Long, 2021). The obvious question that arises from these findings is whether the mushroom bodies of spiders should be termed differently as has been done earlier (termed optical neuropil 3, ON3 in Strausfeld & Barth, 1993). This would avoid confusion with mushroom bodies in insects that primarily process olfactory input. Wolff and Strausfeld (2015) regarded the MB to be lost in spiders but to be present in other arachnids. Unfortunately, this suggestion was not discussed or explained further by the authors, but likely is based on the absence of expression of the DCO and leo proteins in the MB of the spiders they investigated. These markers, in contrast, are expressed in the MB of other arachnids such as amblypygids (Wolff & Strausfeld, 2015). However, earlier studies suggested, based on gene expression similarities, that the MB of insects and spiders are homologous (Doeffinger et al., 2010). Strausfeld (2012) argued that a switch in modality from olfaction to vision might have occurred. Developmental and gene expression studies might help to clarify this question. In the meantime, it seems appropriate to refer to the MB in spiders as “spider mushroom body” and point out that it differs at least functionally, from the mushroom body of most insects and other arachnids.

### Tracts in the protocerebrum

While the MBb and the PCC were described by Babu & Barth (1984) for *C. salei*, the other brain commissures discovered in this study (MBb2, Asc, Psc, Bc3, Bc4, Bc5) had not been detected in *C. salei* (Table 3). It is likely that these commissures contribute to smaller circuits that were not analyzed in the CNS of *C. salei* (Babu & Barth, 1984), since it seems unlikely that they are not also present in this species. The VMT was described as connecting to the MBp after crossing over the MBb in *C. salei* (Babu & Barth, 1984). We could not confirm this in any of the four species studied here. It rather seems as if the VMT connects to the dorsal PN after crossing over the MBb (Fig. 6, 15). The PCDT was described as “entering the hafts” in *C. salei* (Babu & Barth, 1984), a pattern we could not observe in the species studied here. In horizontal sections, it is obvious that it projects into the central PN (Figures 7b), and it is therefore possible that it also sends some neurites to the MB. If these connections exist, they must be rather inconspicuous. We did not detect an equivalent to Bc4 in *A. bruennichi*, but this could be due to the lower selectivity of the Bodian stain in this species compared to the three other species. However, anti-tubulin labelling also failed to detect Bc4, leading us to assume that it either belongs to a circuit that is not present in *A. bruennichi*, or that the neurites that comprise it are too thin to be detected with the methods used here. Babu & Barth (1984) described a protocerebro-median tract (PCMT) in *C. salei*, formed by the union of MC, CT, CL and VL tracts before splitting up again into the protocerebral tracts LCT, MCT and VMT. We could not confirm the presence of this tract (Table 3). Instead, we were able to follow the course of each longitudinal tract into the PN, where they appear to taper but not merge (Fig. 8a,e-f). While we reported that LCT and MCT both join the SLT near the esophagus, we could not find any connections of the VMT to the VNC (Fig. 6, 15). It should be noted that all longitudinal tracts from the VNC tightly adjoin as they pass the esophageal connective, and although this was not observed here, it is quite possible that neurites cross over into different tracts. Tracking individual neurons is desirable for greater clarity.

## Tracts in the VNC

Babu & Barth (1984) identified four commissures: DC, MDC, CC and VC in *C. salei*. Babu & Barth (1989) also mention four commissures, but they are termed DC, MDC, MCC and CC. It is unclear whether MCC constitutes a newly identified fifth commissure and VC was omitted, or whether CC from the earlier study was renamed MCC and VC from the earlier paper was renamed CC. Later, Becherer & Schmid (1999) redrew the figure from Babu & Barth (1989) and added the VC as fifth commissure without justifying this or indicating that they significantly altered the original drawing. In the four spider species investigated here, we found that Dc and MDc tightly adjoin and a separation is not possible with the methods used here. We also did not detect an Mcc in the studied stationary hunters *A. bruennichi* and *P. tepidariorum*, but were able to detect it in *P. amentata* and *M. muscosa*. It seems unlikely that the stationary hunters would lack this fifth commissure, and it is well possible that it is tightly adjoining one of the neighboring commissures (much like Dc and MDc).

Babu and Barth (1984, 1989) identified and described five “sensory longitudinal tracts (SLT)” in the central VNC of *C. salei*. They termed them “sensory” because they found that many sensory neurons from the legs terminate in the tracts. Because these sensory neurons project both into the posterior and the anterior direction, they concluded that the SLTs must consist of both descending and ascending neurons (Babu & Barth, 1984) (Fig. 15). In the species studied here, we could not distinguish five different SLTs, but only a single, large SLT occupying the most central part of the VNC (Figure 13a, 15). This could be partially due to the methods employed here, as we were unable to identify the termination sites of the sensory neurons, which might reveal a patterning not visible in Bodian stains and anti-tubulin immunolabelled material. However, the position, color and thickness of neurites that make up the SLT (Figures 10d, 13a), clearly shows that it is identical to the SLTs described in *C. salei* (Babu & Barth, 1984). We can therefore assume that the arrangement of afferent sensory neurons is similar to the one in *C. salei* in the four species described here.

While the central VNC is characterized by the six prominent longitudinal tracts, it also houses several neuropilar structures that receive direct sensory input (Babu & Barth, 1989). In addition to the LN, sensory neurons also project directly to the SLT's, the LSAT and even onto some of the longitudinal tracts (Babu & Barth, 1989; Gronenberg, 1990). A third termination site of sensory neurons within the central VNC is the Blumenthals neuropil, which receives input from hygro- and thermoreceptors and has so far only been found in *C. salei* (Anton & Tichy, 1994) (Figure 15). We found a candidate structure in *P. amentata* and *M. muscosa* that very likely is the BN (Figure 9c). However, anterograde tracing of sensilla is required to explore this assumption. Such testing could also show whether the BN is truly absent or only less conspicuous in *A. bruennichi* and *P. tepidariorum*.

## Volumetric differences

Differences in sensory ecology often correlate with differences in the volume of CNS areas (Chittka & Niven, 2009). Larger volumes typically occur especially in sensory processing areas of the CNS and allow quantitative enhancements, such as a finer resolution or higher sensitivity of the sensory system (Chittka & Niven, 2009). We can thus expect the largest volume differences between stationary and cursorial hunting spiders in the CNS areas that process sensory information, whereas differences in

CNS areas that mostly consist of tracts should be less pronounced. Indeed, this is what we found in the four species studied here (Figure 14). The differences in proportional volume of CNS areas clearly reflect the differences in lifestyle: Neuropils that mostly process visual information are proportionally much larger in the cursorial hunting spiders, while the opposite is true for the LN that process mechanosensory information. We found very little differences in the central VNC (cVNC) and the PN, which both consist to a large degree of tracts. It should be noted, that the proportional volume of the neuropils associated with the principal eyes is the same in *P. amentata* and *A. bruennichi*, suggesting a similar importance of the visual information gathered by these eyes. The volume differences observed in the OpN might be related to the fact that *A. bruennichi* and *P. tepidariorum* spin webs, a complicated task that involves specific movements and the precise use of various silk glands (Foelix, 2011; Koor, 1987). *P. amentata* has the proportionally largest PdN, about twice that of *P. tepidariorum*, while the other two species have volumes in between. These species-specific differences possibly indicate behavioral differences in the use of the pedipalps, which would need to be explored in future studies. It is interesting that the ChN has a similar size in all species, although it processes primary sensory information. Likely, the amount and quality of information gathered by the sensilla on the chelicerae is similar in all species. The similarity in proportional volume of the AB supports the notion that it is not (in contrast to the MB) primarily a higher order visual neuropil, but of overarching importance (see functional discussion below).

### Functional considerations

With the additional information on spider CNS anatomy and connectivity provided here, a picture emerges of the functional relationships of CNS areas and variation among different groups of spiders (Table 3; Figure 15). While the LN1-4, ChN and PdN process sensory information from their respective appendages (Anton & Tichy, 1994; Babu & Barth, 1989; Gronenberg, 1989) they also house a “motor region” consisting of efferent neurites (Babu & Barth, 1989; Schmid & Becherer, 1999). More proximal neuropil regions such as the LSAT, SLT, BN and to some extent the longitudinal tracts also receive direct sensory information and, in addition, are innervated by interneurons from various CNS regions, potentially serving as higher-order integration centers within the VNC (Figure 15). Apart from being processed within the VNC, sensory information is also sent to various regions in the brain (Gronenberg, 1990) and likely processed in the PN and the AB. The present study shows that the arrangement of tracts and neuropil regions is similar in spider species that differ greatly in lifestyle (Table 3; Figure 15) and it is therefore reasonable to assume that these similarities also extend to functionality.

The brain receives direct sensory information from the eyes, and the visual pathways, particularly of the secondary eyes, vary greatly in spiders (Hanström, 1921; Long, 2021; Steinhoff et al., 2020; this study). These anatomical differences most likely result in different functionality. Cursorial hunting spiders detect motion with their secondary eyes (Schmid, 1998; Zurek et al., 2010; Zurek & Nelson, 2012), which send information to the MB. At least one type of neuron originating at the MB innervates the motor region of the LN (Gronenberg, 1990), which suggests that the MB play a role in vision-guided motion control. Visual motion detection is thus likely to be much less well developed or even absent in stationary hunting spiders that do not possess mushroom bodies such as *P. tepidariorum*.

The evolution of three-dimensional webs, such as those build by *P. tepidariorum*, was likely largely driven by avoidance of predators (Blackledge et al., 2002), which in turn might allow for smaller eyes and reduced visual processing in the brain.

While MB differ strongly in different spider species (Long, 2021; Steinhoff et al., 2020; this study), the AB is very similar and always present, even in spiders that lack eyes (personal observation, unpublished). This, and the fact that the AB is well connected to both the VNC and the brain, suggests that it plays a major role in the integration of sensory information and potentially motor control. To further study the functions of the various CNS regions described here, electrophysiological recordings from individual neurons in combination with dye backfills are needed (cf. Gronenberg, 1990). The findings of this study can provide the basis for such explorations. Promising avenues are for example the central processing of olfactory information in spiders, which remains almost completely unexplored to date.

## References

- Anton, S., & Tichy, H. (1994). Hygro- and thermoreceptors in tip-pore sensilla of the tarsal organ of the spider *Cupiennius salei*: Innervation and central projection. *Cell and Tissue Research*, *278*, 399–407.
- Babu, K. S., & Barth, F. G. (1984). Neuroanatomy of the central nervous system of the wandering spider, *Cupiennius salei* (Arachnida, Araneida). *Zoomorphology*, *104*(6), 344–359. <https://doi.org/10.1007/BF00312185>
- Babu, K. S., & Barth, F. G. (1989). Central nervous projections of mechanoreceptors in the spider *Cupiennius salei* Keys. *Cell and Tissue Research*, *258*(1). <https://doi.org/10.1007/BF00223146>
- Barth, F. G. (2002). *A spider's world: Senses and behavior*. Springer-Verlag.
- Barth, F. G., Nakagawa, T., & Eguchi, E. (1993). Vision in the ctenid spider *Cupiennius salei*: Spectral range and absolute sensitivity. *Journal of Experimental Biology*, *79*, 63–79. <https://doi.org/ghjjagsj>
- Barth, F. G., & Seyfarth, E.-A. (1979). *Cupiennius salei* Keys. (Araneae) in the Highlands of Central Guatemala. *The Journal of Arachnology*, *7*(3), 255–263.
- Blackledge, T. A., Coddington, J. A., & Gillespie, R. G. (2002). Are three-dimensional spider webs defensive adaptations? Spider webs as predator defences. *Ecology Letters*, *6*(1), 13–18. <https://doi.org/10.1046/j.1461-0248.2003.00384.x>
- Bodian, D. (1936). A new method for staining nerve fibers and nerve endings in mounted paraffin sections. *The Anatomical Record*, *65*(1), 89–97. <https://doi.org/10.1002/ar.1090650110>
- Chittka, L., & Niven, J. (2009). Are Bigger Brains Better? *Current Biology*, *19*(21), R995–R1008. <https://doi.org/10.1016/j.cub.2009.08.023>
- Couto, A., Wainwright, J. B., Morris, B. J., & Montgomery, S. H. (2020). Linking ecological specialisation to adaptations in butterfly brains and sensory systems. *Current Opinion in Insect Science*, *42*, 55–60. <https://doi.org/10.1016/j.cois.2020.09.002>

- Doeffinger, C., Hartenstein, V., & Stollewerk, A. (2010). Compartmentalisation of the precheliceral neuroectoderm in the spider *Cupiennius salei*: Development of the arcuate body, the optic ganglia and the mushroom body. *The Journal of Comparative Neurology*, NA-NA. <https://doi.org/10.1002/cne.22355>
- Fenk, L. M., Hoinkes, T., & Schmid, A. (2010). Vision as a third sensory modality to elicit attack behavior in a nocturnal spider. *Journal of Comparative Physiology A*, 196(12), 957–961. <https://doi.org/10.1007/s00359-010-0575-8>
- Foelix, R. (2011). *Biology of Spiders*. Oxford University Press, USA.
- Gregory, G. E. (1980). The Bodian Protargol Technique. In N. J. Strausfeld & T. A. Miller (Eds.), *Neuroanatomical Techniques* (pp. 75–95). Springer.
- Gronenberg, W. (1989). Anatomical and physiological observations on the organization of mechanoreceptors and local interneurons in the central nervous system of the wandering spider *Cupiennius salei*. *Cell and Tissue Research*, 258(1). <https://doi.org/10.1007/BF00223155>
- Gronenberg, W. (1990). The organization of plurisegmental mechanosensitive interneurons in the central nervous system of the wandering spider *Cupiennius salei*. *Cell and Tissue Research*, 260, 49–61.
- Hanström, B. (1921). Über die Histologie und vergleichende Anatomie der Sehganglien und Globuli der Araneen. *Kungliga Svenska Vetenskapsakademiens Handlingar*, 61(12), 1–39.
- Homann, H. (1950). Die Nebenaugen der Araneen. *Zoologische Jahrbücher: Abteilung Für Anatomie Und Ontogenie Der Tiere*, 71, 56–144.
- Homann, H. (1952). Die Nebenaugen der Araneen. 2. Mitteilung. *Zoologische Jahrbücher: Abteilung Für Anatomie Und Ontogenie Der Tiere*, 72, 345–364.
- Kovoor, J. (1987). Comparative Structure and Histochemistry of Silk-Producing Organs in Arachnids. In W. Nentwig (Ed.), *Ecophysiology of Spiders* (pp. 160–186). Springer Berlin Heidelberg.
- Kovoor, J., Muñoz-Cuevas, A., & Ortega-Escobar, J. (2005). The visual system of *Lycosa tarentula* (Araneae, Lycosidae): Microscopic anatomy of the protocerebral optic centres. *Italian Journal of Zoology*, 72(3), 205–216. <https://doi.org/10.1080/11250000509356673>
- Land, M. F. (1972). Mechanisms of Orientation and Pattern Recognition by Jumping Spiders (Salticidae). In R. Wehner (Ed.), *Information Processing in the Visual Systems of Anthropods* (pp. 231–247). Springer Berlin Heidelberg. [https://doi.org/10.1007/978-3-642-65477-0\\_34](https://doi.org/10.1007/978-3-642-65477-0_34)
- Land, M. F. (1985). The morphology and optics of spider eyes. In F. G. Barth (Ed.), *Neurobiology of Arachnids* (pp. 53–76). Springer. [https://doi.org/10.1007/978-3-642-70348-5\\_4](https://doi.org/10.1007/978-3-642-70348-5_4)
- Lehmann, T., Melzer, R., Hörnig, M. K., Michalik, P., Sombke, A., & Harzsch, S. (2015). Arachnida (excluding Scorpiones). In *Structure and Evolution of Invertebrate Nervous Systems*. Oxford University Press. <https://doi.org/10.1093/acprof:oso/9780199682201.001.0001>
- Loesel, R., Seyfarth, E.-A., Bräunig, P., & Agricola, H.-J. (2011). Neuroarchitecture of the arcuate body in the brain of the spider *Cupiennius salei* (Araneae, Chelicerata) revealed by allatostatin-, proctolin-, and CCAP-immunocytochemistry and its evolutionary implications. *Arthropod Structure & Development*, 40(3), 210–220. <https://doi.org/10.1016/j.asd.2011.01.002>

- Long, S. M. (2021). Variations on a theme: Morphological variation in the secondary eye visual pathway across the order of Araneae. *Journal of Comparative Neurology*, 529(2), 259–280. <https://doi.org/10.1002/cne.24945>
- Louail, M., Gilissen, E., Prat, S., Garcia, C., & Bouret, S. (2019). Refining the ecological brain: Strong relation between the ventromedial prefrontal cortex and feeding ecology in five primate species. *Cortex; a Journal Devoted to the Study of the Nervous System and Behavior*, 118, 262–274. <https://doi.org/10.1016/j.cortex.2019.03.019>
- Montgomery, S. H., Rossi, M., McMillan, W. O., & Merrill, R. M. (2021). Neural divergence and hybrid disruption between ecologically isolated *Heliconius* butterflies. *Proceedings of the National Academy of Sciences*, 118(6), e2015102118. <https://doi.org/10.1073/pnas.2015102118>
- Morehouse, N. I., Buschbeck, E. K., Zurek, D. B., Steck, M., & Porter, M. L. (2017). Molecular evolution of spider vision: New opportunities, familiar players. *Biological Bulletin*, 233(1), 21–38. <https://doi.org/10.1086/693977>
- Pan, X., Bourland, W. A., & Song, W. (2013). Protargol Synthesis: An In-house Protocol. *Journal of Eukaryotic Microbiology*, 60(6), 609–614. <https://doi.org/10.1111/jeu.12067>
- Rivera Quiroz, F. A., & Miller, J. (2022). Micro-CT visualization of the CNS: Performance of different contrast-enhancing techniques for documenting the spider brain. *Journal of Comparative Neurology*. <https://doi.org/10.1002/cne.25343>
- Schmid, A. (1998). Different functions of different eye types in the spider *Cupiennius salei*. *The Journal of Experimental Biology*, 201, 221–225.
- Schmid, A., & Becherer, C. (1999). Distribution of histamine in the CNS of different spiders. *Microscopy Research and Technique*, 44(2–3), 81–93. [https://doi.org/10.1002/\(SICI\)1097-0029\(19990115/01\)44:2/3<81::AID-JEMT3>3.0.CO;2-O](https://doi.org/10.1002/(SICI)1097-0029(19990115/01)44:2/3<81::AID-JEMT3>3.0.CO;2-O)
- Schmid, A., & Duncker, M. (1993). Histamine immunoreactivity in the central nervous system of the spider *Cupiennius salei*. *Cell and Tissue Research*, 273, 533–545.
- Scholtz, G., & Edgecombe, G. D. (2006). The evolution of arthropod heads: Reconciling morphological, developmental and palaeontological evidence. *Development Genes and Evolution*, 216(7–8), 395–415. <https://doi.org/10.1007/s00427-006-0085-4>
- Steinhoff, P. O. M., Sombke, A., Liedtke, J., Schneider, J. M., Harzsch, S., & Uhl, G. (2017). The synganglion of the jumping spider *Marpissa muscosa* (Arachnida: Salticidae): Insights from histology, immunohistochemistry and microCT analysis. *Arthropod Structure and Development*, 46(2), 156–170. <https://doi.org/10.1016/j.asd.2016.11.003>
- Steinhoff, P. O. M., Uhl, G., Harzsch, S., & Sombke, A. (2020). Visual pathways in the brain of the jumping spider *Marpissa muscosa*. *Journal of Comparative Neurology*, cne.24861. <https://doi.org/10.1002/cne.24861>
- Strausfeld, N. J. (2012). *Arthropod Brains: Evolution, Functional Elegance, and Historical Significance*. Harvard University Press.
- Strausfeld, N. J., & Barth, F. G. (1993). Two visual systems in one brain: Neuropils serving the secondary eyes of the spider *Cupiennius salei*. *The Journal of Comparative Neurology*, 328(1), 43–62. <https://doi.org/10.1002/cne.903280104>

- Strausfeld, N. J., Sinakevitch, I., Brown, S. M., & Farris, S. M. (2009). Ground plan of the insect mushroom body: Functional and evolutionary implications. *The Journal of Comparative Neurology*, *513*(3), 265–291. <https://doi.org/10.1002/cne.21948>
- Strausfeld, N. J., Weltzien, P., & Barth, F. G. (1993). Two visual systems in one brain: Neuropils serving the principal eyes of the spider *Cupiennius salei*. *The Journal of Comparative Neurology*, *328*(1), 63–75. <https://doi.org/10.1002/cne.903280105>
- Weltzien, P., & Barth, F. G. (1991). Volumetric measurements do not demonstrate that the spider brain “central body” has a special role in web building. *Journal of Morphology*, *208*(1), 91–98. <https://doi.org/10.1002/jmor.1052080104>
- Wolff, G. H., & Strausfeld, N. J. (2015). Genealogical Correspondence of Mushroom Bodies across Invertebrate Phyla. *Current Biology*, *25*(1), 38–44. <https://doi.org/10.1016/j.cub.2014.10.049>
- Yamashita, S., & Tateda, H. (1976). Spectral sensitivities of jumping spider eyes. *Journal of Comparative Physiology A*, *105*(1), 29–41. <https://doi.org/10.1007/BF01380051>
- Yamashita, S., & Tateda, H. (1978). Spectral sensitivities of the anterior median eyes of the orb web spiders, *Argiope bruennichii* and *A. amoena*. *Journal of Experimental Biology*, *74*(1), 47–57.
- Zurek, D. B., & Nelson, X. J. (2012). Hyperacute motion detection by the lateral eyes of jumping spiders. *Vision Research*, *66*, 26–30. <https://doi.org/10.1016/j.visres.2012.06.011>
- Zurek, D. B., Taylor, A. J., Evans, C. S., & Nelson, X. J. (2010). The role of the anterior lateral eyes in the vision-based behaviour of jumping spiders. *Journal of Experimental Biology*, *213*(14), 2372–2378. <https://doi.org/10.1242/jeb.042382>



## Tables

**Table 1** Primary and secondary antibodies

Labeling reagent	Dilution and specifications
<b>Primary</b>	
Monoclonal anti-synapsin antibody produced in mouse (AB_528479)	1:1000, DSHB 3C11 Steinhoff et al. (2017, 2020), this study
Polyclonal anti-acetylated $\alpha$ -tubulin antibody produced in rabbit (AB_2637882)	1:1000, 1:250, ThermoFisher PA5-58711
<b>Secondary</b>	
Polyclonal Cy3 anti-mouse IgG secondary antibody produced in goat (AB_2338680)	1:500, Jackson Immuno Research, 115–165-003
Polyclonal Alexa 488 anti-rabbit IgG secondary antibody produced in goat (AB_2534074)	1:500, Invitrogen, A11006
Hoechst 33258	1:1000, Sigma 14530

**Table 2** Methods and antisera combinations

Methods	Antisera combinations/ staining	Coupled with	Specimens
Wholemout	anti-synapsin (mouse) anti-acetylated- $\alpha$ -tubulin (rabbit)	Cy3 anti-mouse (goat) Alexa Fluor 488 anti-rabbit (goat)	2
Vibratome sections (60 & 80 $\mu$ m)	anti-synapsin (mouse) anti-acetylated- $\alpha$ -tubulin (rabbit)	Cy3 anti-mouse (goat) Alexa Fluor 488 anti-rabbit (goat) Nuclear labeling: Hoechst 33258	12
Wholemout	micro-emerald dye anti-synapsin (mouse)	/ Cy3 anti-mouse (goat)	5
Paraffin sections (15 $\mu$ m)	Bodian silver impregnation	/	20
microCT scans	1% iodine (in 99% ethanol)	/	12

**Table 3** Neuropils and major longitudinal and commissural tracts in the CNS of *Cupiennius salei*, *Pardosa amentata*, *Marpissa muscosa*, *Argiope bruennichi* and *Parasteatoda tepidariorum*. Based on this study and (for *C. salei*) on Babu and Barth (1984, 1989).

CNS structures	<i>C. salei</i>	<i>M. muscosa</i>	<i>P. amentata</i>	<i>A. bruennichi</i>	<i>P. tepidariorum</i>
<i>VNC neuropilar structures</i>					
<b>BN</b>	+	+?	+?	-	-
<b>SLT (1-5)</b>	+ 5 tracts	+ single tract	+ single tract	+ single tract	+ single tract
<b>LegN</b>	+	+	+	+	+
<b>LSAT</b>	+	+	+	+	+
<b>OpN</b>	+	+	+	+	+
<i>Dcb &amp; Tcb neuropils</i>					
<b>ChN</b>	+	+	+	+	+
<b>PdN</b>	+	+	+	+	+
<i>Pcb neuropilar structures</i>					
<b>AB</b>	+	+	+	+	+
<b>MB</b>	+	+	+	+	-
<b>MBh</b>	+	+	+	+ medially	-
<b>Princ_VN2</b>	+	+	+	+	+
<b>PN</b>	+	+	+	+	+
<b>Princ_VN1</b>	+	+	+	+	+
<b>Sec_VN1</b>	+	+	+	+	+ shared
<b>Sec_VN2</b>	+	+	+	-	-
<b>Stb</b>	+	+	+	+	+
<i>Pcb longitudinal tracts</i>					
<b>BVT</b>	?	+	+	+	+
<b>LCT</b>	+	+	+	+	-
<b>MCT</b>	+	+	+	+	+
<b>PCDT</b>	+	+	+	+	+
<b>PCMT</b>	+	?	?	?	?
<b>PCVT</b>	+	+	+	+	+
<b>VMT</b>	+	+	+	+	+
<i>Pcb commissural tracts</i>					
<b>ASc</b>	?	+	+	+	+
<b>Bc3</b>	?	+	+	+	+
<b>Bc4</b>	?	+	+	-	+
<b>Bc5</b>	?	+	-	-	-
<b>MBb</b>	+	+	+	+	+
<b>MBb2</b>	?	+	+	-	-
<b>Pcc</b>	+	+	+	+	+
<b>PSc</b>	?	+	+	+	+
<i>Dcb &amp; Tcb tracts</i>					

<b>Chc</b>	+	+	+	+ connected to Pdc	+ connected to Pdc
<b>Chc2</b>	?	+	+	-	-
<b>Pdc</b>	+	+	+	+ connected to Chc	+ connected to Chc
<b>Pdc2</b>	?	+	+	+	+
<b>Pdp</b>	?	+	+	+	+
<i>VNC longitudinal tracts</i>					
<b>CL</b>	+	+	+	+	+
<b>CT</b>	+	+	+	+	+
<b>MC</b>	+	+	+	+	+
<b>MD</b>	+	+	+	+	+
<b>MV</b>	+	+	+	+	+
<b>VL</b>	+	+	+	+	+
<i>VNC commissural tracts</i>					
<b>Cc</b>	+	+	+	+	+
<b>Dc</b>	+	+	+ connected to MDc	+ connected to MDc	+ connected to MDc
<b>MCc</b>	+	+	+	-	-
<b>MDc</b>	+	+	+ connected to Dc	+ connected to Dc	+ connected to Dc
<b>Vc</b>	+	+	+	+	+

## Figures

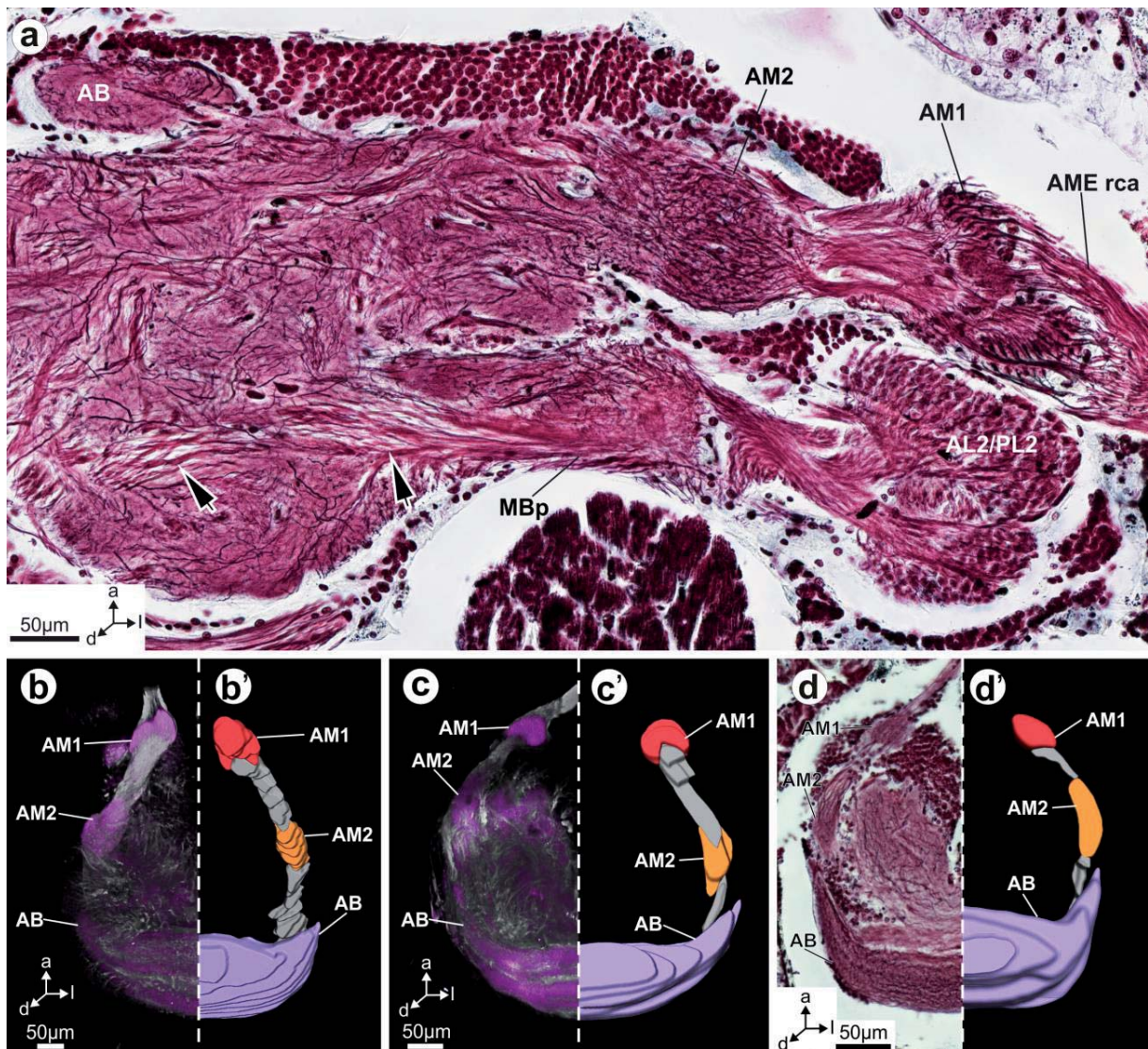


**Figure 1** The principal eye pathway. (a) Sagittal Bodian-stained section of the protocerebrum in *Marpissa muscosa* showing neurites connecting the AM1 with the AM2, as well as a chiasm of neurites connecting the AL2/PL2 to the MBp. Arrowheads point to neurites connecting the MB with the VNC. (b, c) Maximum projections of image stacks (clsm) showing synapsin-immunoreactivity (magenta) and tubulin-immunoreactivity (grey). (b) In *Pardosa amentata* the AM1 is connected to the AM2 via thick neurites, other neurites project from the AM2 to the AB. (b', c', d') three-dimensional reconstructions based on serial Bodian-stained sections. (b') Visual pathway of the principle eyes in *P. amentata*. (c) In *Argiophe bruennichi* the AM1 is connected to the AM2, while the AM2 sends neurites towards the outer tips of the AB. (c') Visual pathway of the principle eyes in *Argiophe bruennichi*. (d) In *Parasteatoda tepidariorum*, Bodian-stained sections reveal thin neurites connecting the AM1 with the AM2 and the latter with the AB. (d') Visual pathway of the principle eyes in *P. tepidariorum*. Abbreviations: a,

anterior; AL2/PL2, second-order visual neuropil of anterior lateral and posterior lateral eyes; AB, arcuate body; AME rca, retinula cell axons of the anterior median eyes; AM1, first-order visual neuropil of the anterior median eyes; AM2, second-order visual neuropil of the anterior median eyes; d, dorsal; l, lateral; MBp, mushroom body pedunculus.

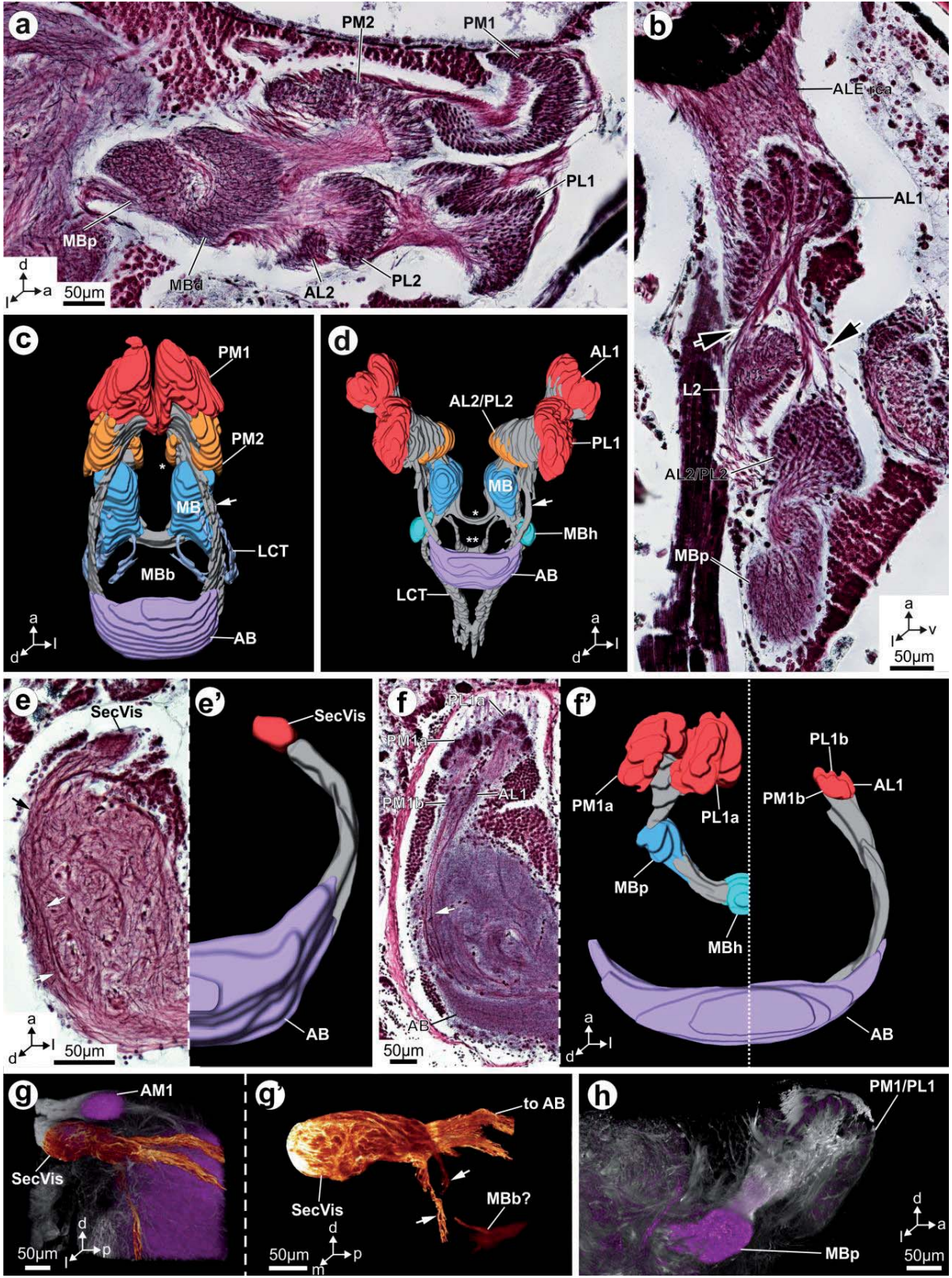


**Figure 2** The secondary eye pathway. (a, b, e, f) Bodian-stained sections. (c, d, e', f') Three-dimensional reconstructions based on serial Bodian-stained sections. (g-h) Maximum projections of image stacks (clsm) showing synapsin-immunoreactivity (magenta) and tubulin-immunoreactivity (grey and gold). (a) Sagittal section showing the secondary eye visual system of *P. amentata*. Every eye serves its own first- and second-order neuropil and the second-order neuropils connect to the MBd. The MBd is closely connected to the MBp. (b) Sagittal section showing the secondary eye visual system of *M. muscosa*. The ALE (and PLE, not shown) connect to their own first-, but two shared second-order visual neuropils. Arrows show connections between AL1 and L2 and between AL1 and AL2/PL2. AL2/PL2 further connects to the MBp. (c) Three-dimensional reconstruction of the secondary eye visual system of *P. amentata*. All first-order visual neuropils of the secondary eyes (PL1 and AL1 obscured by PM1 which is most dorsal), connect to their second-order neuropils and directly to the AB. \* shows the AL2. The LCT connects the MB to the VNC. (d) Three-dimensional reconstruction of the secondary eye visual system of *M. muscosa*. \* shows the MBb, \*\* the MBb2. Arrow points to direct connection between first-order visual neuropils and the AB. The LCT connects the MB to the VNC. (e) Horizontal section showing the secondary eye visual system of *P. tepidariorum*. Arrows point to neurites connecting the SecVis with the AB. (e') Three-dimensional reconstruction of the secondary eye visual system of *P. tepidariorum*. (f) Horizontal section showing the secondary eye visual system of *A. bruennichi*. Arrowhead points to neurites connecting PM1b, PL1b and AL1 with the AB. (f') Three-dimensional reconstruction of the secondary eye visual system of *A. bruennichi*, left half shows connections of PM1a and PL1a to the MBp, right half shows connections of PM1b, PL1b and AL1 to the AB. The MBh is located medially. (g) Secondary eye visual neuropil and tracts in *P. tepidariorum*. SecVis is located just ventral of the AM1, bundles of neurites connecting it to other brain regions are highlighted. (g') Isolated visual tracts and potential MBb in *P. tepidariorum*. (h) PM1 and PL1 connect directly to the MBp in *A. bruennichi*. Abbreviations: a, anterior; AB, arcuate body; ALE rca, retinula cell axons of the anterior lateral eyes; AL1, first-order visual neuropil of the anterior lateral eyes; AL2, second-order visual neuropil of the anterior lateral eyes; AL2/PL2, second-order visual neuropil of anterior lateral and posterior lateral eyes; AM1, first-order visual neuropil of the anterior median eyes; d, dorsal; l, lateral; L2, shared second-order visual neuropil of the anterior lateral and posterior lateral eyes; LCT, lateral cerebral tract; MB, mushroom body; MBb, mushroom body bridge; MBb2, mushroom body bridge 2; MBd, mushroom body head; MBh, mushroom body haft; MBp, mushroom body pedunculus; PL1, first-order visual neuropil of the posterior lateral eyes; PL1a, first-order visual neuropil of the posterior lateral eyes a; PL1b, first-order visual neuropil of the posterior lateral eyes b; PL2, second-order visual neuropil of the posterior lateral eyes; PM1, first-order visual neuropil of the posterior median eyes; PM1a, first-order visual neuropil of the posterior median eyes a; PM1b, first-order visual neuropil of the posterior median eyes b; PM2, second-order visual neuropil of the posterior median eyes; SecVis, first order visual neuropil of the secondary eyes; v, ventral.

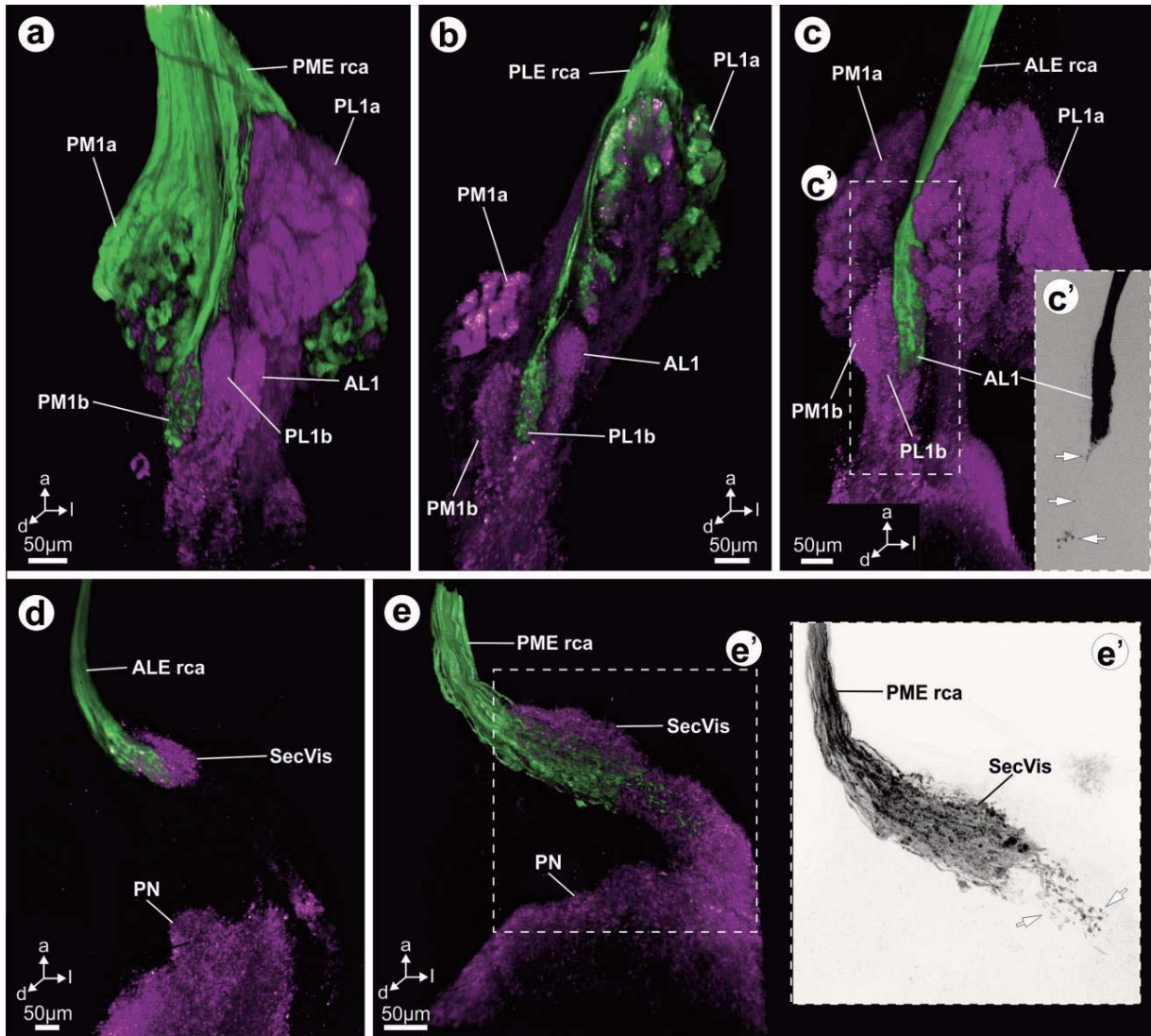


**Figure 3** Maximum projections of image stacks (clsm) showing synapsin-immunoreactivity (magenta), and anterograde tracing of retinula cell axons (green) in the secondary eye visual pathway of *Argiope bruennichi* (a-c) and *Parasteatoda tepidariorum* (d-e). (a) Most rca's of the PME terminate in the PM1a, while some terminate in the PM1b instead. (b) Most rca's of the PLE terminate in the PL1a, while some terminate in the PL1b instead. (c) Rca's of the ALE terminate in the AL1. (c') Maximum intensity projection of the anterograde tracing of ALE rca's alone, reveals that some terminate posterior and just outside of the AL1. Termination sites highlighted by arrows. (d) Rca's of the ALE terminate in the medial part of the roundish SecVis. (e) Rca's of the PME terminate in the SecVis. (e') Maximum intensity projection of the anterograde tracing of PME rca's alone, reveals that some terminate posterior and just outside of the SecVis. Termination sites highlighted by arrows. Abbreviations: a, anterior; ALE, anterior lateral eyes; AL1, first-order visual neuropil of the anterior lateral eyes; d, dorsal; l, lateral; PLE, posterior lateral eyes; PL1a, first-order visual neuropil of the posterior lateral eyes a; PL1b, first-order visual neuropil of the posterior lateral eyes b; PME, posterior medial eyes; PM1a, first-order visual neuropil of the posterior median eyes a; PM1b, first-order visual



neuropil of the posterior median eyes b; PN, protocerebral neuropil; rca, retinula cell axon; SecVis, first order visual neuropil of the secondary eyes.

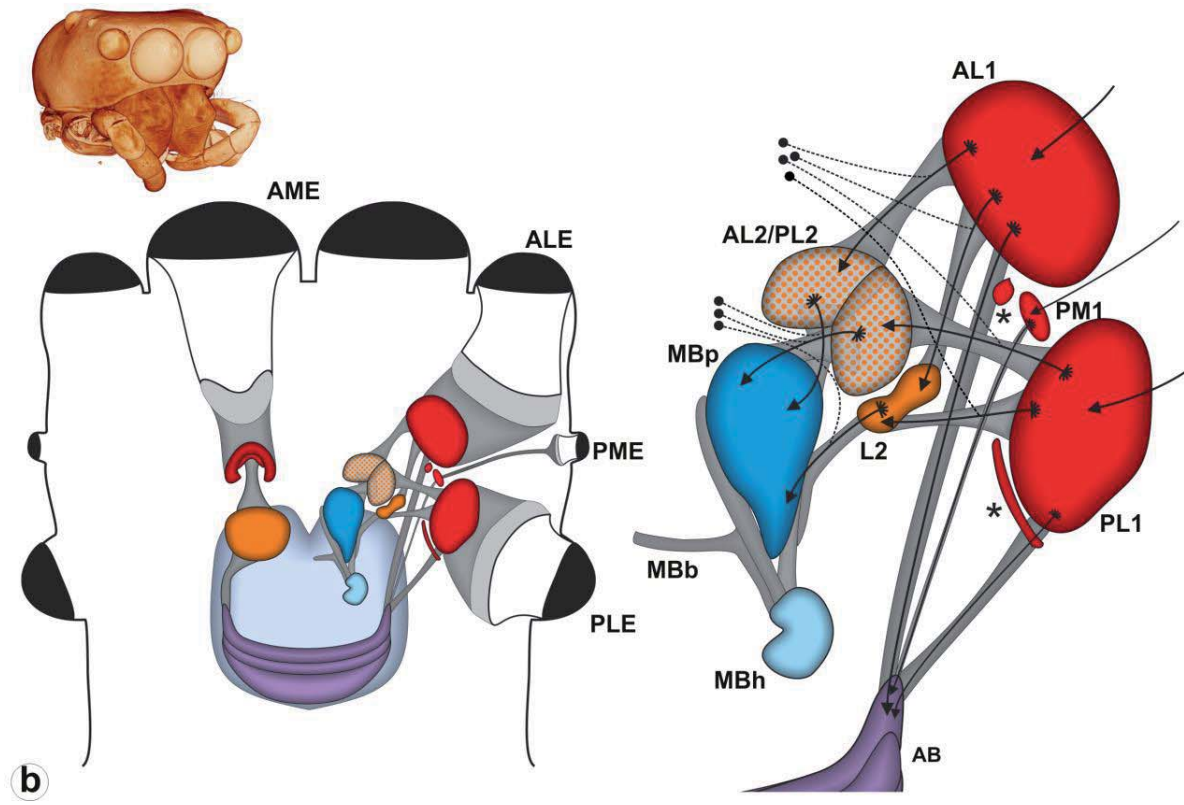
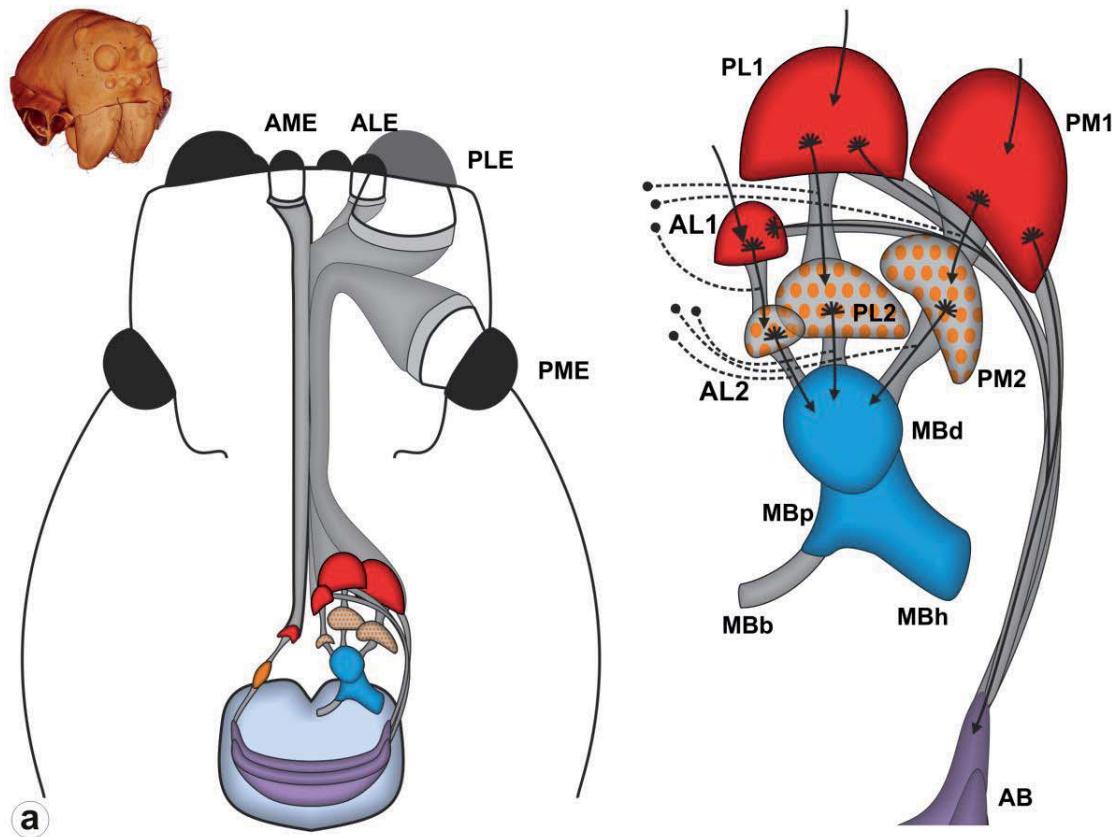


**Figure 4** Schematic representations of the principal and secondary eye visual pathways in the brains of (a) *P. amentata* and (b) *M. muscosa*. Insets top left: Three-dimensional volume rendering of the prosomata of (a) *P. amentata* and (b) *M. muscosa*, based on microCT analysis. Filled black circles indicate somata with known positions, dotted lines represent primary neurites, and arrows indicate the assumed direction of information flow. Asterisks mark neuropilar subregions of first-order neuropils (AL1x and PL1x) in *M. muscosa*. Abbreviations: AB, arcuate body; AL1, first-order visual neuropil of the anterior lateral eyes; AL2, second-order visual neuropil of the anterior lateral eyes; AL2/PL2, second-order visual neuropil of anterior lateral and posterior lateral eyes; ALE, anterior lateral eye; AME, anterior median eye; L2, shared second-order visual neuropil of the anterior lateral and posterior lateral eyes; MBb, mushroom body bridge; MBd, mushroom body head; MBh, mushroom body haft; MBp, mushroom body pedunculus; PL1, first-order visual neuropil of the posterior lateral eyes; PL2, second-order visual neuropil of the posterior lateral eyes; PLE, posterior lateral eye; PME, posterior median eye; PM1, first-order visual neuropil of the posterior median eyes; PM2, second-order visual neuropil of the posterior median eyes. (b) Altered from (Steinhoff et al., 2020).

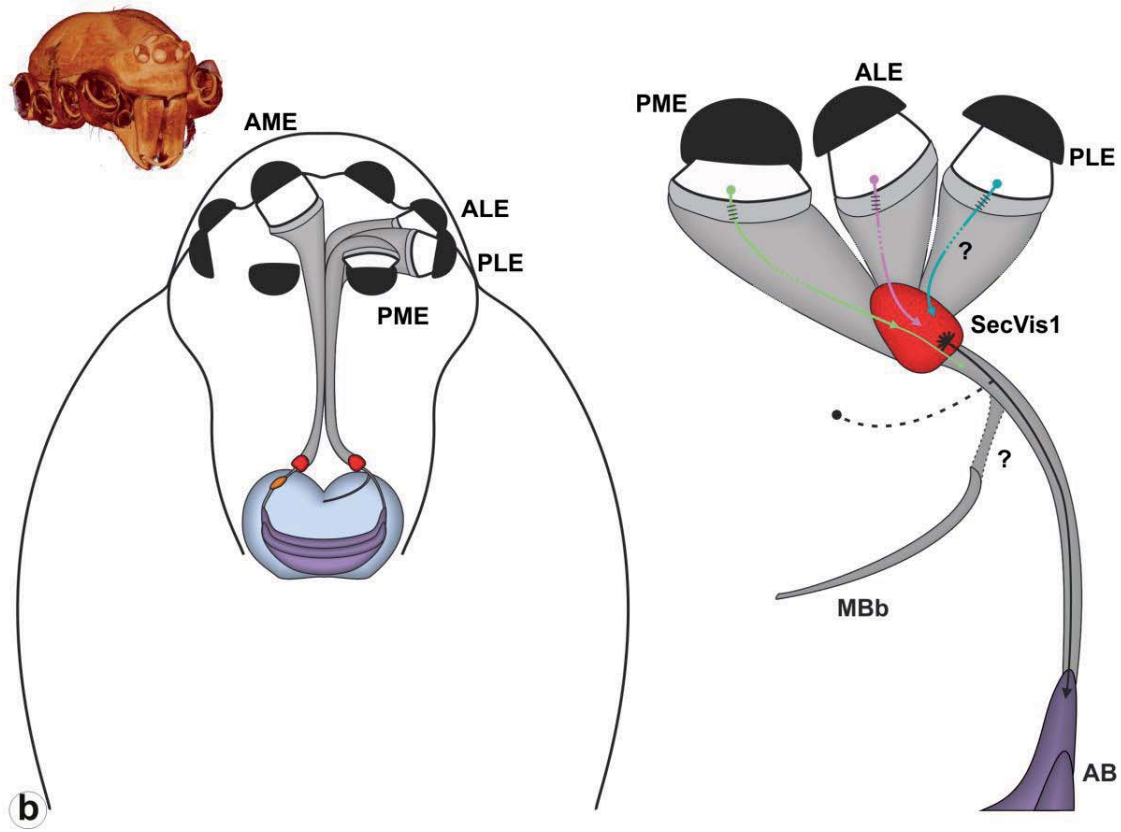
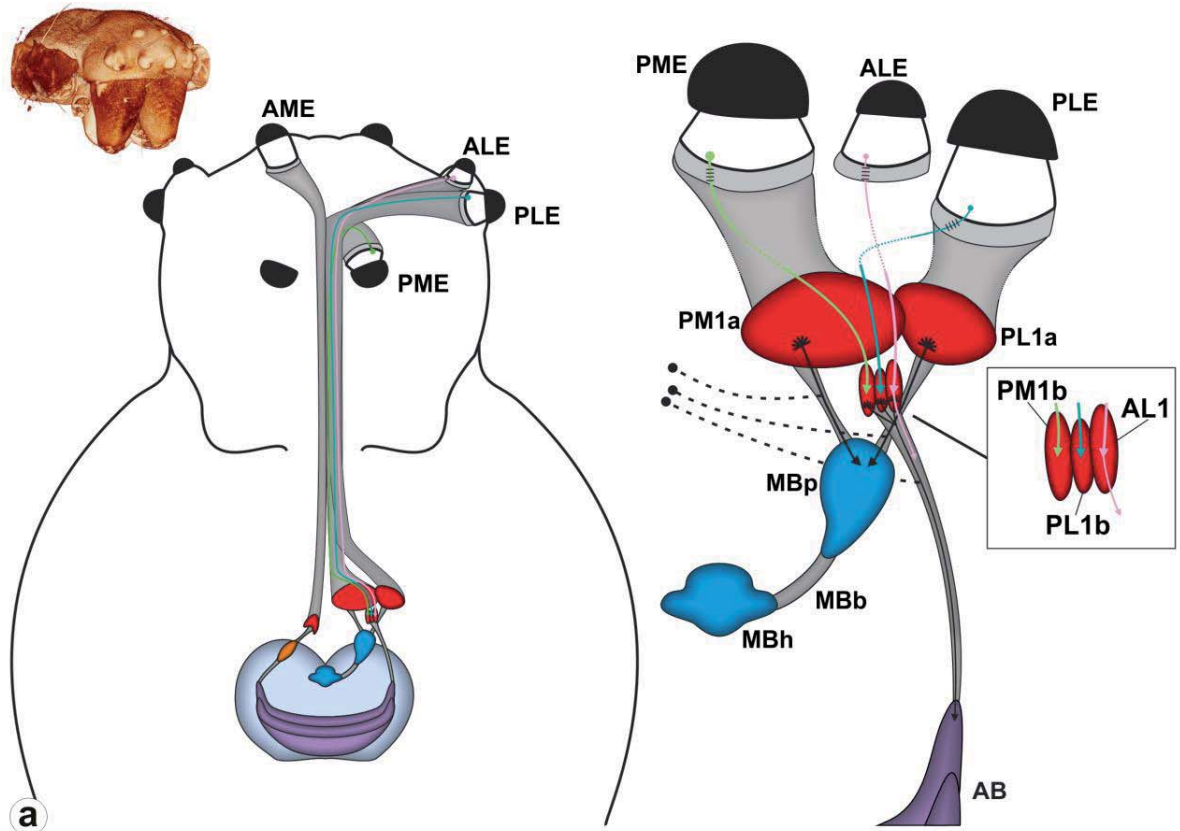


**Figure 5** Schematic representations of the principal and secondary eye visual pathways in the brains of (a) *A. bruennichi* and (b) *P. tepidariorum*. Insets top left: Three-dimensional volume rendering of the prosomata of (a) *A. bruennichi* and (b) *P. tepidariorum*, based on microCT analysis. Filled black circles indicate somata with known positions, dotted lines represent primary neurites, and arrows indicate the assumed direction of information flow. Abbreviations: AB, arcuate body; AL1, first-order visual neuropil of the anterior lateral eyes; ALE, anterior lateral eye; AME, anterior median eye; MBb, mushroom body bridge; MBh, mushroom body haft; MBp, mushroom body pedunculus; PL1a, first-order visual neuropil of the posterior lateral eyes a; PL1b, first-order visual neuropil of the posterior lateral eyes b; PLE, posterior lateral eye; PME, posterior median eye; PM1a, first-order visual neuropil of the posterior median eyes a; PM1b, first-order visual neuropil of the posterior median eyes b; SecVis, first order visual neuropil of the secondary eyes.

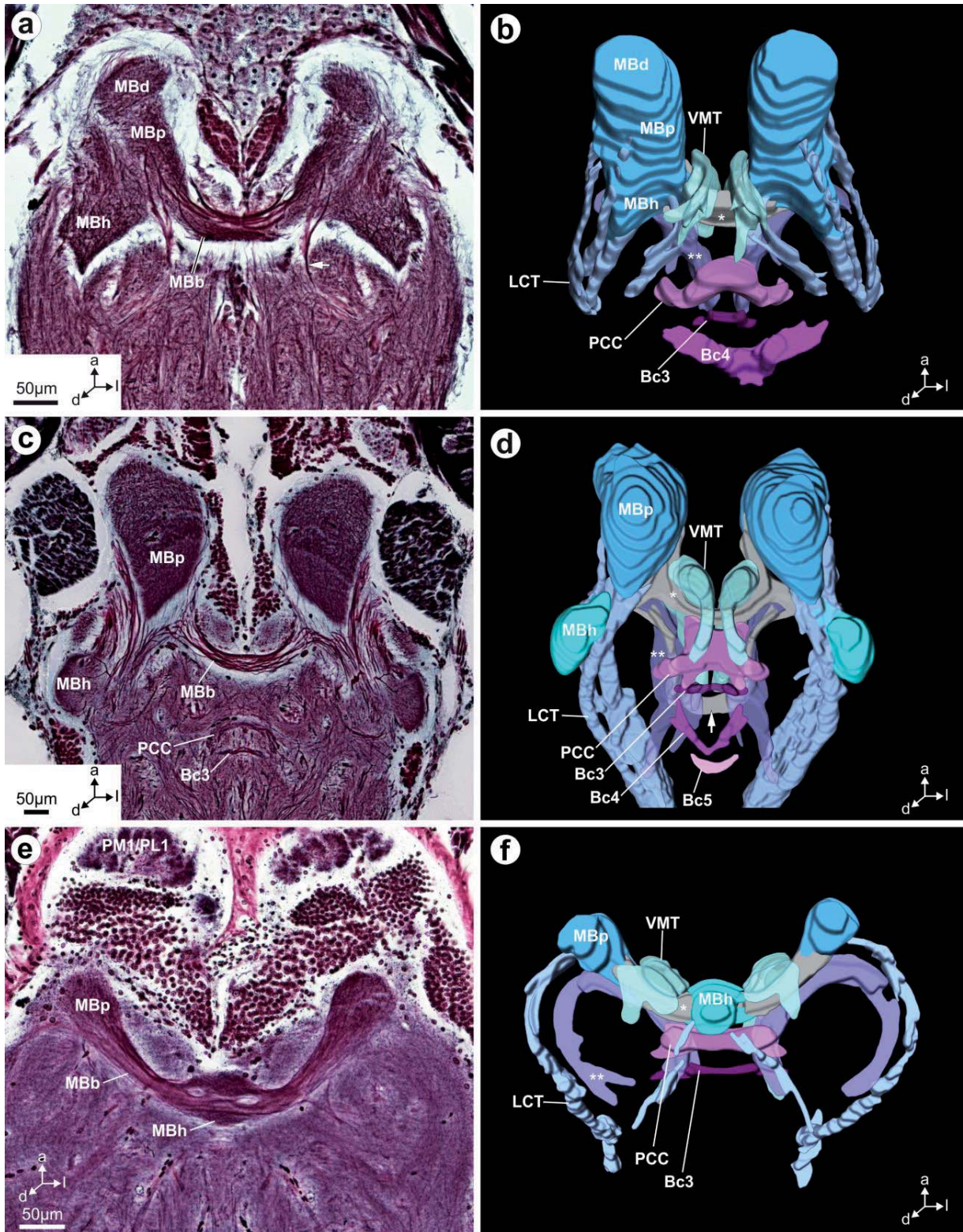


**Figure 6** Mushroom bodies and brain tracts. (a, c, e) Bodian-stained sections. (b, d, f) Three-dimensional reconstructions based on serial Bodian-stained sections. (a-b) In *P. amentata* the MB

consist of a MBd, MBp and MBh and are connected to their bilateral counterpart via a thick MBb (\*). While the LCT connects the MB to the VNC, the PCVT (\*\*) forms an arch beneath the MB. The VMT crosses over the MBb. Further commissures in the PN are the PCC, Bc3 and Bc4, which are all situated posterior of the MB. (c-b) In *M. muscosa* the MB consist of the MBp and the MBh. There is an additional protocerebral commissure, the Bc5. Arrow points to the MBb2. (e-f) In *A. bruennichi* the MBh is situated medially. A Bc4 is not present. Abbreviations: (...) a, anterior; AB, arcuate body; Bc3, brain commissure 3; Bc4, brain commissure 4; Bc5, brain commissure 5; d, dorsal; l, lateral; LCT, lateral cerebral tract; \*=MBb, mushroom body bridge; MBb2, mushroom body bridge 2; MBd, mushroom body head; MBh, mushroom body haft; MBp, mushroom body pedunculus; PCC, protocerebral commissure; \*\*=PCVT, protocerebro-ventral tract; PM1/PL1, first-order visual neuropil of the posterior median and posterior lateral eyes; VMT, ventral median tract

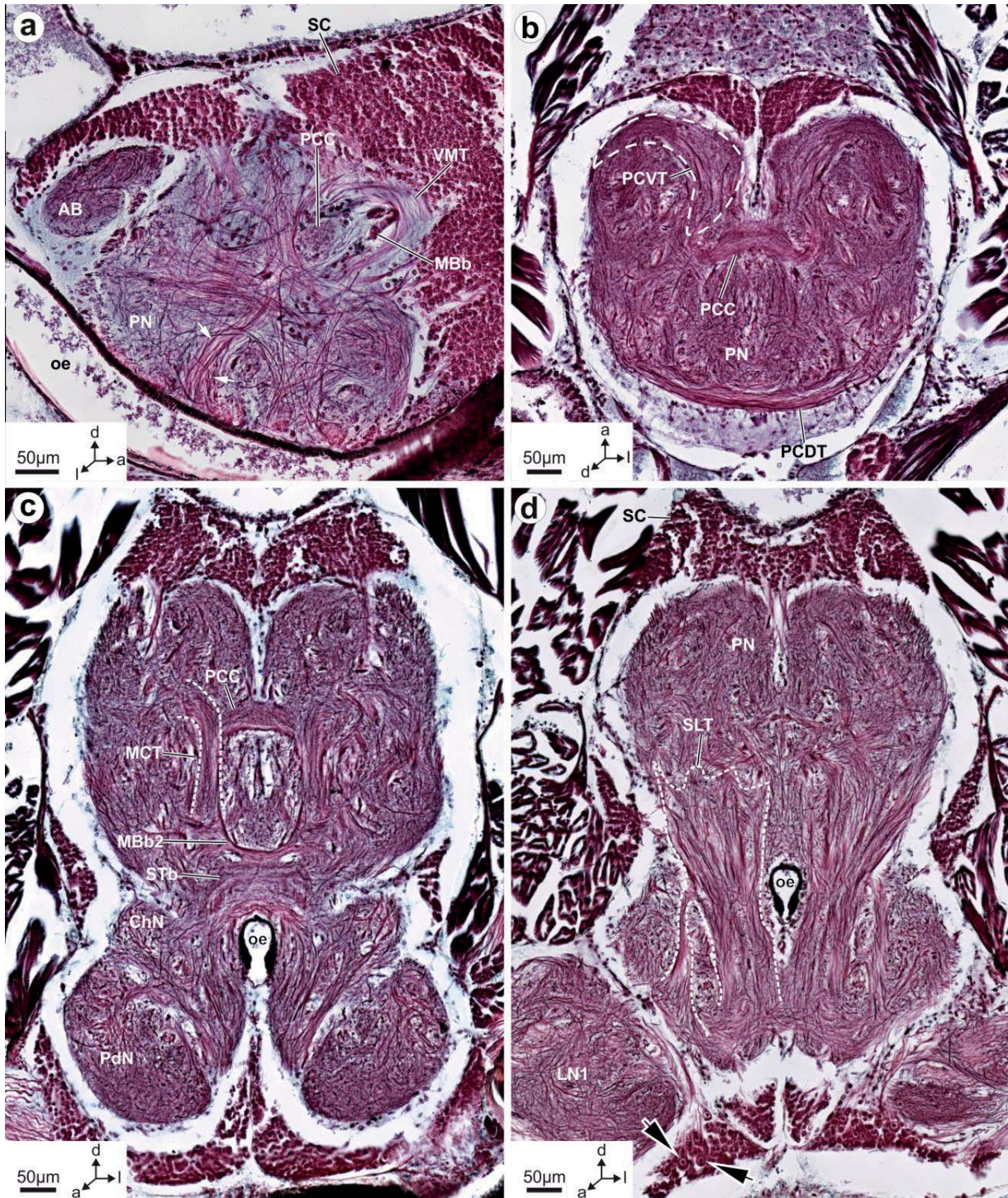


**Figure 7** Bodian-stained sections reveal protocerebral tracts and connections between protocerebrum and VNC in *P. amentata*. (a) The VMT curves around the MBb and the PCC. Arrows point to long neurites within the PN, likely contributing to the MCT. (b) PCVT forms an arch below the MB, the PCC consist of thin neurites and a central neuropilar structure. The PCDT is situated just below the AB. (c) Neurites that contribute to the thin MBb2 are embedded in the MCT, which extends



dorsally into the PN, passing the PCC. The STb neuropil forms an arch above the oe. Oe is bordered by the ChN, below which is the PdN. (d) The SLT forms a massive tract connecting the VNC with the brain. Arrows point to giant somata that send their neurites into the VNC. Abbreviations: AB, arcuate body; a, anterior; ChN, cheliceral neuropil; d, dorsal; l, lateral; LN, leg neuropil; MBb, mushroom body bridge; MBb2, mushroom body bridge 2; MCT, median cerebral tract; PCC, protocerebral commissure; PCDT, protocerebro-dorsal tract; PCVT, protocerebro-ventral tract; PdN, pedipalpal neuropil; PN, protocerebral neuropil; STb, stomodeal bridge; VMT, ventral median tract.

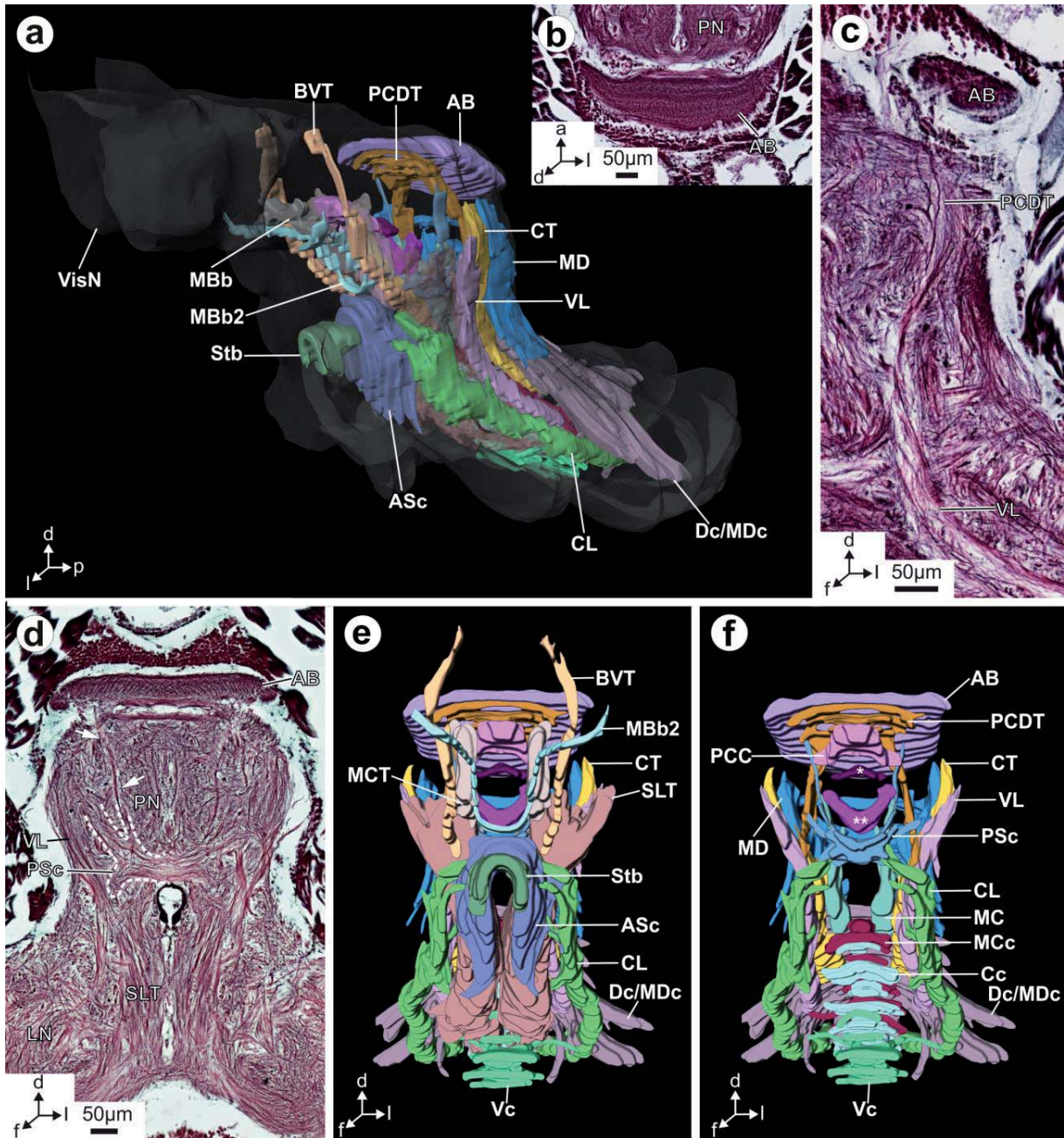


**Figure 8** Tract system connecting the brain with the VNC in *P. amentata*. (a, e, f) Three-dimensional reconstructions based on serial Bodian-stained sections. (b, c, d) Bodian-stained sections. (a) CNS (transparent grey) with tracts, reconstruction of visual and VNC neuropils removed for clarity, SLT and MCT transparent for clarity. (b) Intricate web of fine neurites in the AB. (c) PCDT connects to the AB and directly to the tract system of the VNC (specifically the VL). (d) Long neurites connect the AB to the PSc (arrows). SLT passes next to the oe into the brain. (e) The ASc connects to the VNC; BVT sends neurites through the brain into the SLT. The MBb2 forms a commissure dorsal of the Stb and ASc. VNC commissures Dc/MDc and Vc are visible ventrally. (f) Same as (e), but Stb, ASc, MBb2, MCT, BVT and

SLT omitted to reveal more posterior located tracts. VNC commissures Vc, Dc/MDc, Cc and MCc are visible, VNC longitudinal tracts MD, CT, VL, CL and MC curve upwards into the brain. The PCDT connects the AB to the VNC and the PCC forms a thick dorsal commissure. Below the PCC are the Bc3 (\*) and the Bc4 (\*\*). In the postero-ventral PN is the PSc with neurites extending into the dorsal PN. Abbreviations: a, anterior; AB, arcuate body; ASc, anterior stomodeal commissure; \*=Bc3, brain commissure 3; \*\*=Bc4, brain commissure 4; BVT, brain vertical tract; Cc, central commissure; CL, centro-lateral tract; CT, central tract; d, dorsal; Dc/MDc, dorsal and mid-dorsal commissures; f, frontal; l, lateral; LN, leg neuropil; MCT, median cerebral tract; MBb, mushroom body bridge; MBb2, mushroom body bridge 2; MC, mid-central tract; MCc, mid-central commissure; MCT, median cerebral tract; MD, mid-dorsal tract; p, posterior; PCC, protocerebral commissure; PCDT, protocerebro-dorsal tract; PN, protocerebral neuropil; PSc, posterior stomodeal commissure; SLT, sensory longitudinal tract; Stb, stomodeal bridge; Vc, ventral commissure; VisN, visual neuropils; VL, ventro-lateral tract.

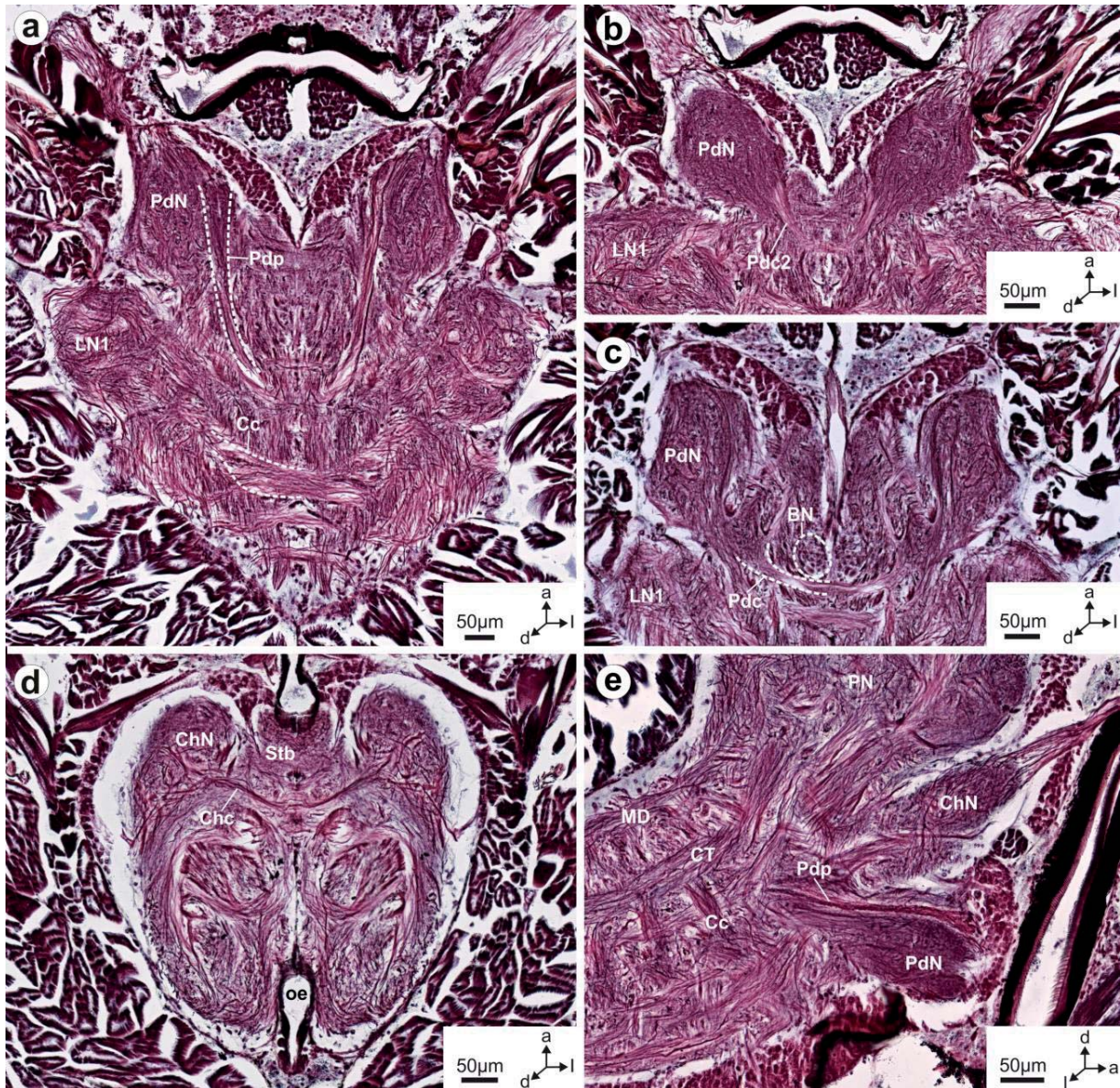


**Figure 9** Bodian-stained sections of cheliceral and pedipalpal neuropils and tracts in *P. amentata*. (a) Pdp connects PdN with the SLT, the first LN is visible and part of the Cc. (b) The Pdc2 is located in a ventral position, connecting the two bilaterally paired PdN. (c) The BN consists of conspicuous columns that are arranged from dorsal to ventral and border the Pdc, which is situated dorsal of the Pdc2. (d) The Chc connects the two bilaterally paired ChN. The Stb surrounds the oe dorsally. (e) Neurites connect the PdN and ChN with VNC tracts. Prominent longitudinal VNC tracts are the MD and CT, part of the Cc is also visible. Abbreviations: a, anterior; BN, Blumenthals neuropil; Cc, central commissure; Chc, cheliceral commissure; ChN, cheliceral neuropil; CT, central tract; d, dorsal; l, lateral; LN1, leg neuropil of the first pair of legs; MD, mid-dorsal tract; PdN, pedipalpal neuropil; Pdc, pedipalpal commissure; Pdc2, pedipalpal commissure 2; Pdp, pedipalpal projection; PN, protocerebral neuropil.

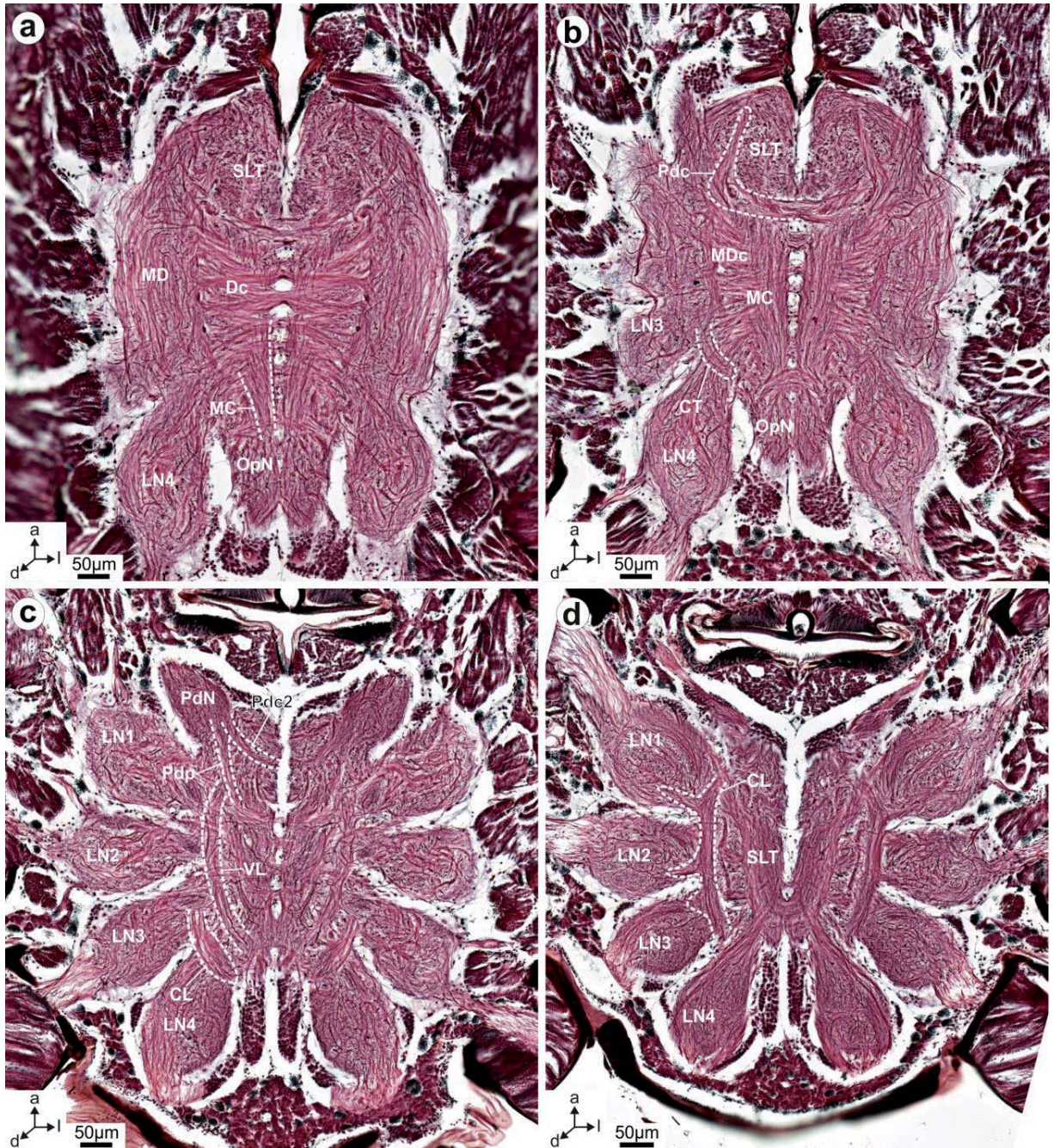


**Figure 10** Bodian-stained sections showing major tracts in the VNC of *P. tepidariorum*, shown exemplary for all species studied here. (a) The MD is the dorsalmost and largest longitudinal tract in the VNC. The SLT, which runs ventrally, can be seen anterior where it curves upward to enter the brain. The Dc connects the two halves of the VNC, the posterior part of the MC is also visible. The posterior part of the VNC is formed by the LN4 and the OpN. (b) The MC is the centralmost longitudinal tract in the VNC, part of the CT is also visible. The Pdc is situated just beneath the MC. (c) CL and VL

are located more ventral in the VNC. The 4 LN send neurites into the central part of the VNC. The Pdp and Pdc2 arise in the PdN. (d) The SLT consists of thin neurites and stains darker than the other longitudinal tracts, connections between LN1-3 and the CL and between LN4 and the SLT are visible. Abbreviations: a, anterior; CL, centro-lateral tract; CT, central tract; d, dorsal; Dc, dorsal commissure; l, lateral; LN1-4, leg neuropil 1-4; MC, mid-central tract; MD, mid-dorsal tract; MDc, mid-dorsal commissure; OpN, opisthosomal neuropil; Pdc, pedipalpal commissure; Pdc2, pedipalpal commissure 2; Pdp, pedipalpal projection; SLT, sensory longitudinal tract; VL, ventro-lateral tract.

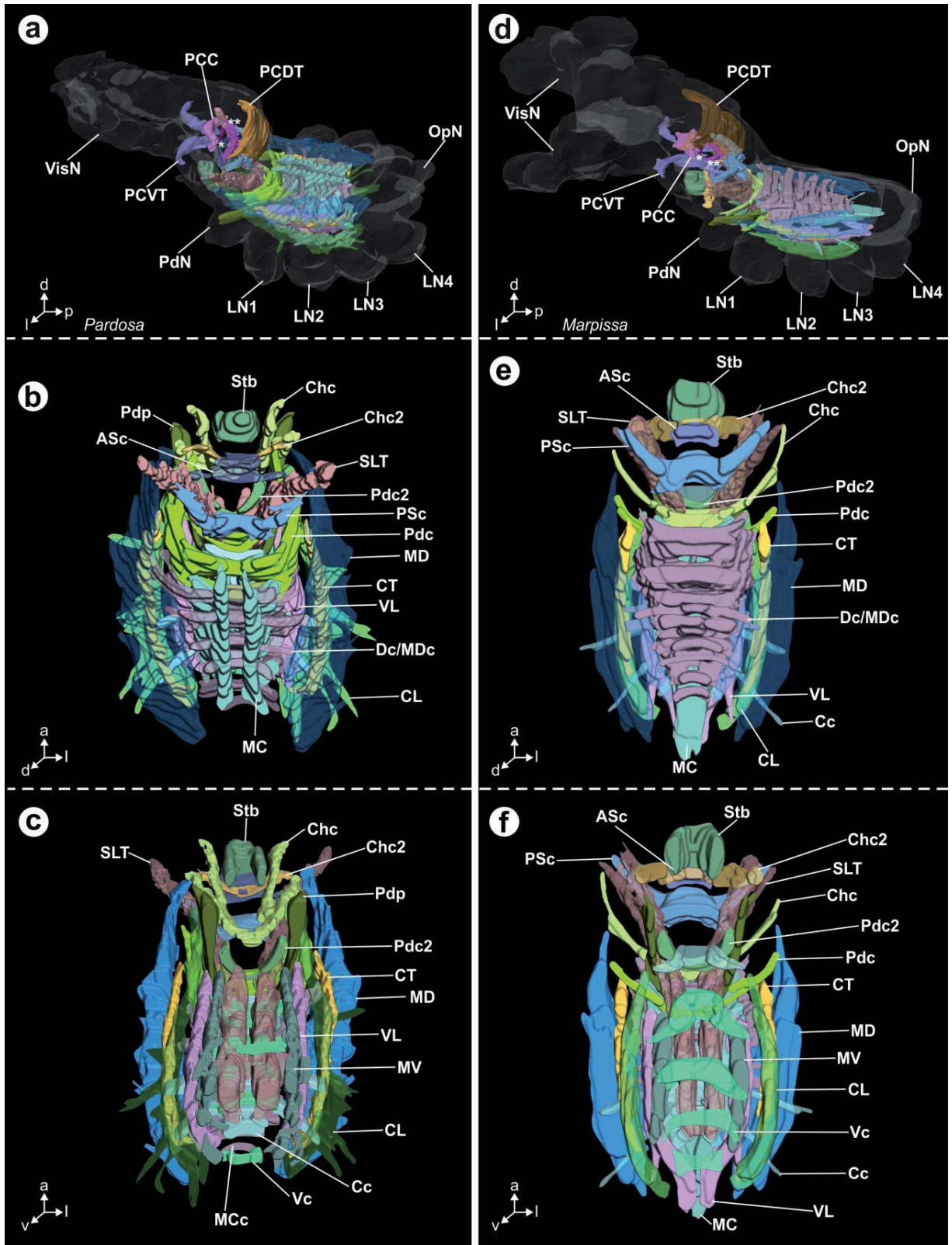


**Figure 11** CNS tracts in *P. amentata* (a-c) and *M. muscosa* (d-f). (a-f) Three-dimensional reconstructions based on serial Bodian-stained sections. (a, d) CNS (transparent grey) with tracts, reconstruction of visual neuropils, most protocerebral tracts and VNC neuropils removed for clarity. (b-c,e-f) Ventral protocerebral, all deuto- and tritocerebral and all VNC tracts in dorsal (b,e) and ventral (c,f) view. Abbreviations: a, anterior; ASc, anterior stomodeal commissure; \*=Bc3, brain commissure 3; \*\*=Bc4, brain commissure 4; BVT, brain vertical tract; Cc, central commissure; Chc, cheliceral commissure; Chc2, cheliceral commissure 2; CL, centro-lateral tract; CT, central tract; d, dorsal; Dc/MDc, dorsal and mid-dorsal commissures; f, frontal; l, lateral; LN1-4, leg neuropil 1-4; MCT, median cerebral tract; MC, mid-central tract; MCc, mid-central commissure; MD, mid-dorsal tract; MV, mid-ventral tract; OpN, opisthosomal neuropil; p, posterior; PCC, protocerebral commissure; PCDT, protocerebro-dorsal tract; PCVT, protocerebro-ventral tract; Pdc, pedipalpal commissure; Pdc2, pedipalpal commissure 2; PdN, pedipalpal neuropil; Pdp, pedipalpal projection; PSc, posterior stomodeal commissure; SLT, sensory longitudinal tract; Stb, stomodeal bridge; Vc, ventral commissure; VisN, visual neuropils; VL, ventro-lateral tract.



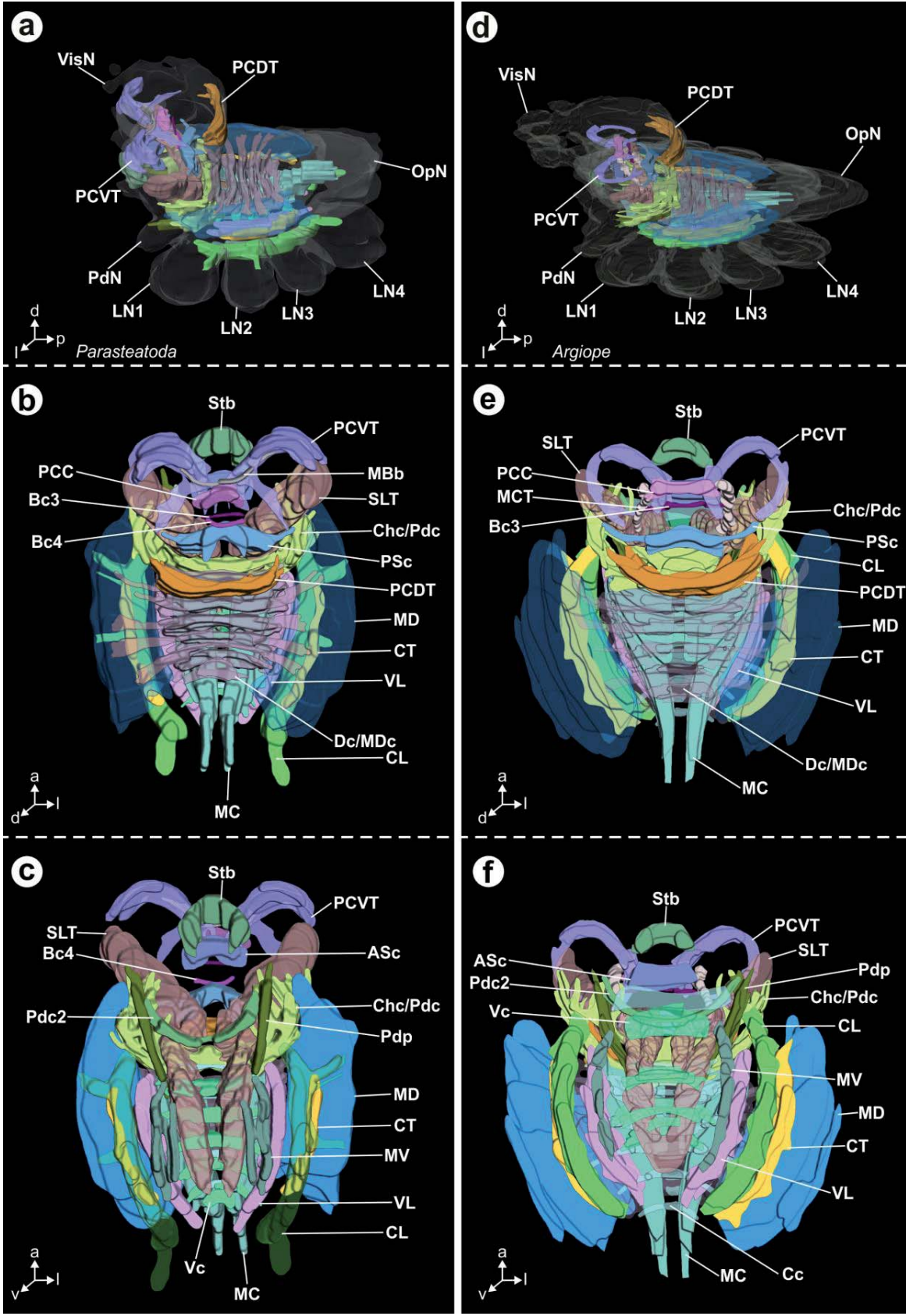


**Figure 12** CNS tracts in *P. tepidariorum* (a-c) and *A. bruennichi* (d-f). (a-f) Three-dimensional reconstructions based on serial Bodian-stained sections. (a, d) CNS (transparent grey) with tracts, reconstruction of visual neuropils, most protocerebral tracts and VNC neuropils removed for clarity. (b-c,e-f) Most protocerebral, all deuto- and tritocerebral and all VNC tracts in dorsal (b,e) and ventral (c,f) view. Abbreviations: a, anterior; ASc, anterior stomodeal commissure; Bc3, brain commissure 3; Bc4, brain commissure 4; BVT, brain vertical tract; Cc, central commissure; Chc/Pdc, cheliceral and pedipalpal commissure; CL, centro-lateral tract; CT, central tract; d, dorsal; Dc/MDC, dorsal- and mid-dorsal commissure; f, frontal; l, lateral; LN1-4, leg neuropil 1-4; MCT, median cerebral tract; MBb, mushroom body bridge; MC, mid-central tract; MCC, mid-central commissure; MCT, median cerebral tract; MD, mid-dorsal tract; MV, mid-ventral tract; OpN, opisthosomal neuropil; p, posterior; PCC, protocerebral commissure; PCDT, protocerebro-dorsal tract; PCVT, protocerebro-ventral tract; PdN, pedipalpal neuropil; Pdp, pedipalpal projection; PSc, posterior stomodeal commissure; SLT, sensory longitudinal tract; Stb, stomodeal bridge; Vc, ventral commissure; VisN, visual neuropils; VL, ventro-lateral tract.

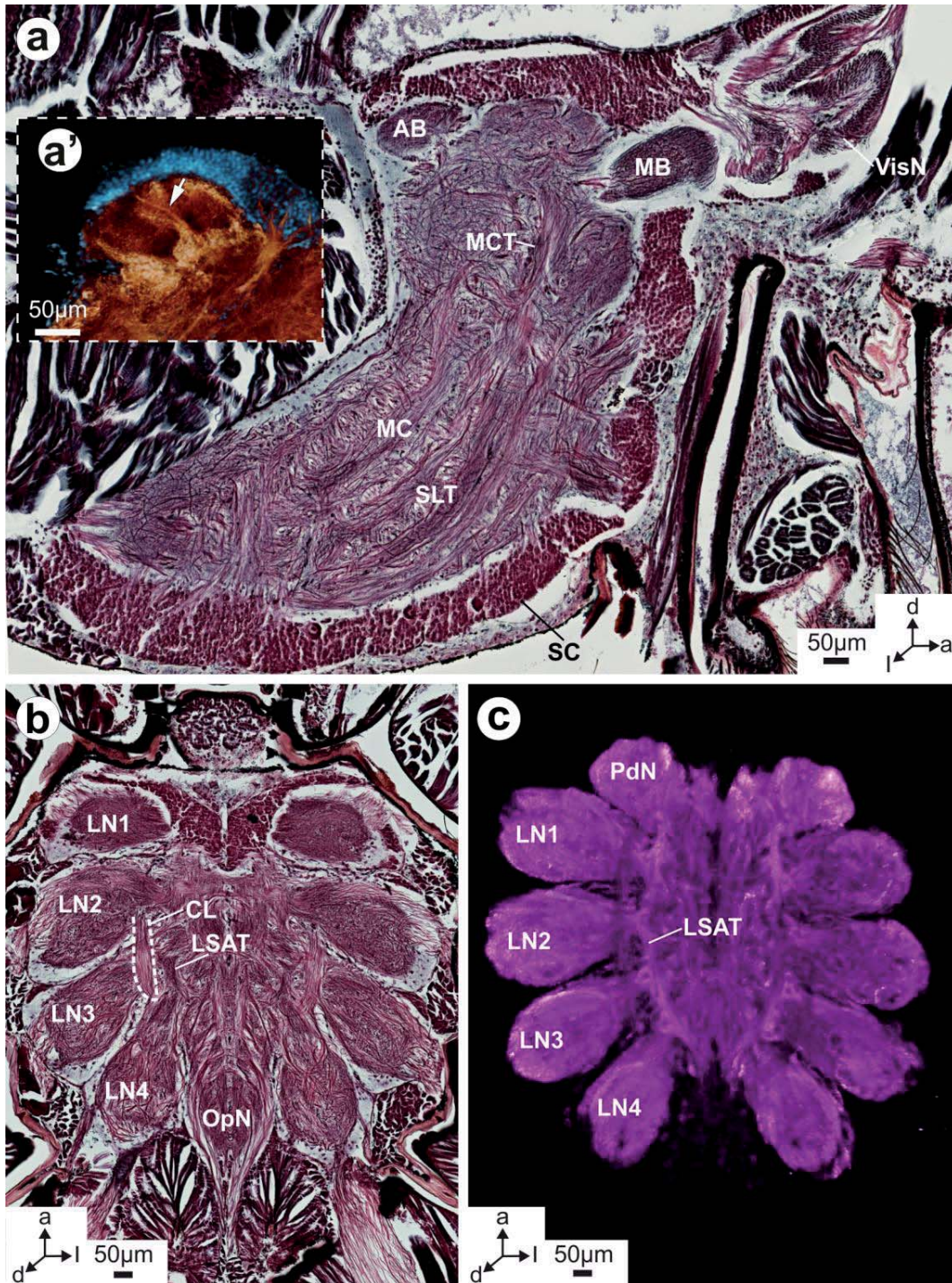


**Figure 13** Tracts and neuropilar structures in the VNC of *P. amentata*. (a, b) Bodian-stained sections. (a) The MCT connects the dorsal protocerebrum to the VNC. The SLT is visible as a thick tract with thin and dark-stained neurites, ventral of the MC. (a') Maximum projection of image stacks (clsm) showing tubulin-immunoreactivity (gold) and nuclear marker (blue). Arrow points to neurites passing through the AB into the PN. (b) The OpN is heavily innervated by neurites projecting from and to the

opisthosoma. Part of the CL is visible and the LSAT is a neuropilar structure in the central part of the VNC. (c) Maximum projection of image stacks (clsm) showing synapsin-immunoreactivity (magenta). The LSAT spans the VNC from posterior to anterior. Abbreviations: a, anterior; AB, arcuate body; d, dorsal; l, lateral; LN1-4; leg neuropils 1-4; LSAT, longitudinal sensory association tract; MB, mushroom bodies; MC, mid-central tract; MCT, median cerebral tract; PdN, pedipalpal neuropil; SC, soma cortex; SLT, sensory longitudinal tract; VisN, visual neuropils.

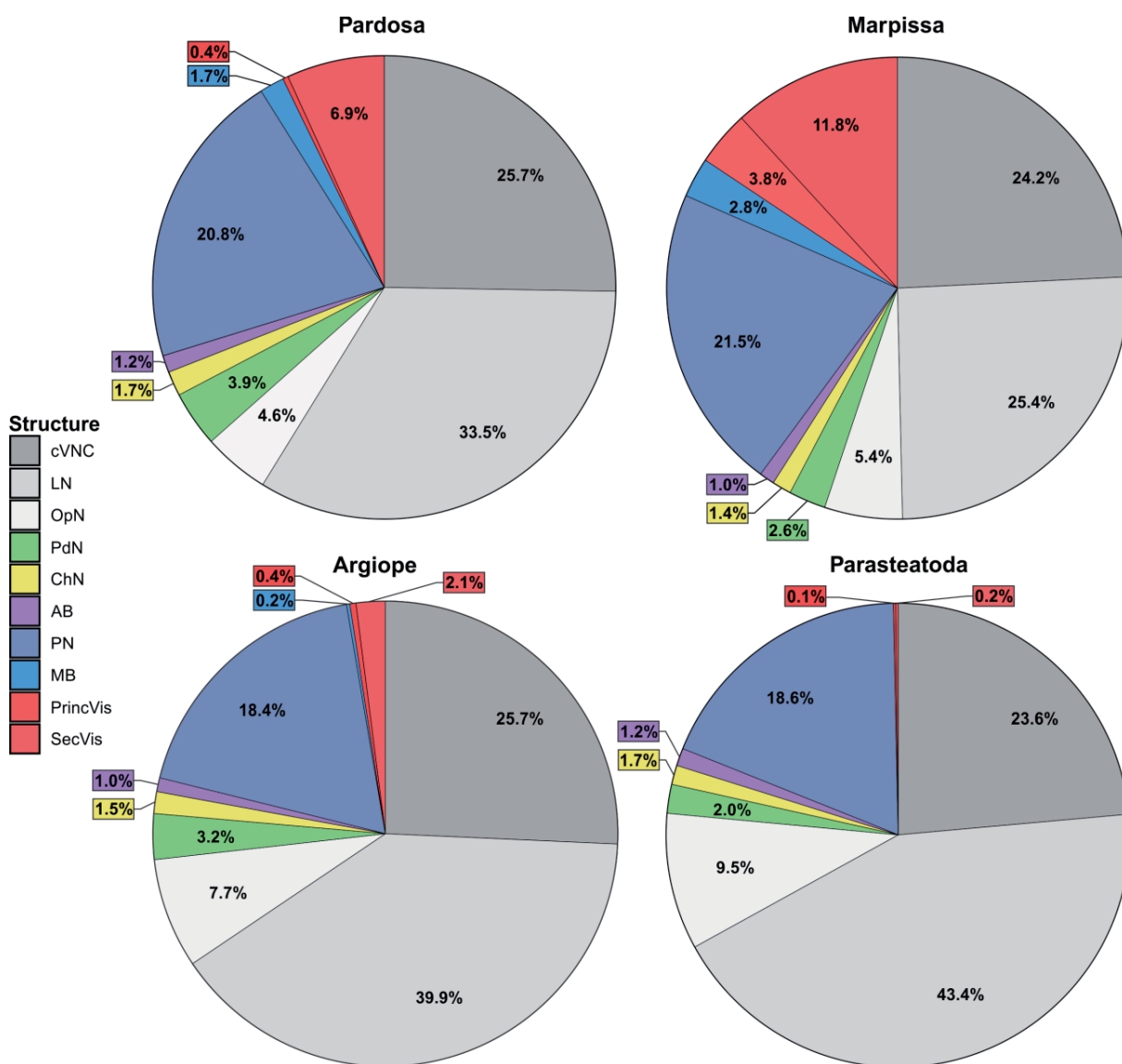


**Figure 14** Pie charts showing the relative volumes of brain areas in proportion to the volume of the entire CNS in the studied species. Abbreviations: AB, arcuate body; ChN, cheliceral neuropils; cVNC, central ventral nerve cord; LN, leg neuropils; MB, mushroom bodies; OpN, opisthosomal neuropil; PdN, pedipalpal neuropil; PN, protocerebral neuropil; PrincVis, visual neuropils of the principal eyes; SecVis, visual neuropils of the secondary eyes.

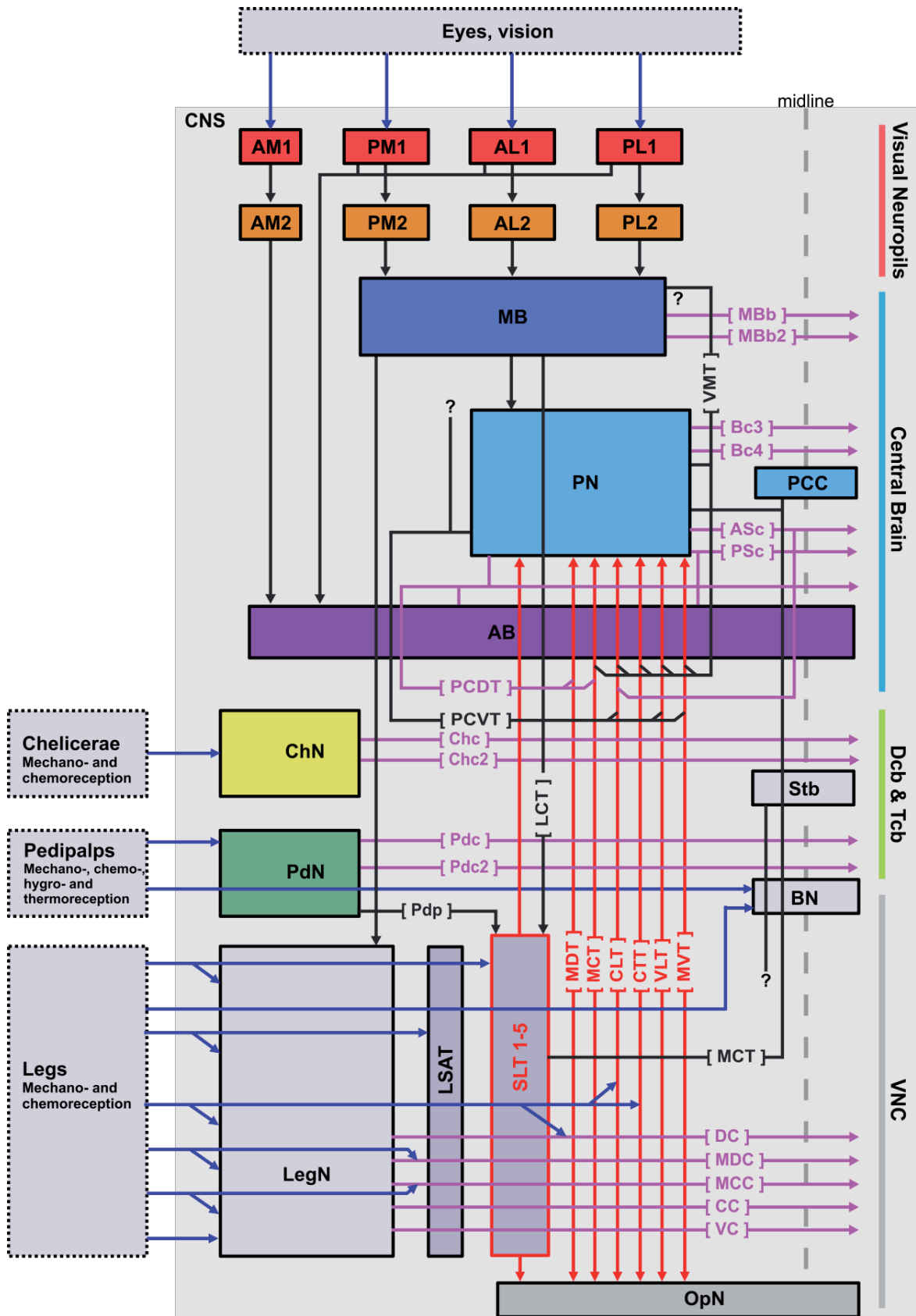


**Figure 15** Schematic wiring diagram of the spider CNS. Visual system as in *C. salei* and *P. amentata*, for variation see Figures 4 and 5. Wiring of interneurons based on Babu & Barth (1984), Gronenberg (1989, 1990) and this study; innervation, central projection and termination pattern of sensory neurons based on Babu & Barth (1989), Anton & Tichy (1994) and this study. Blue lines represent sensory neurons, red lines represent longitudinal interneurons of the VNC, black lines represent interneurons of the brain and pink lines represent commissural interneurons that cross the midline of the CNS. Abbreviations: see list of abbreviations in the main text.

**Chapter 4: Neuroplasticity in response to sensory enrichment and deprivation in a cursorial and a stationary hunting spider**

Philip O.M. Steinhoff<sup>1\*</sup>, Pierick Mougnot<sup>2</sup> & Gabriele Uhl<sup>1</sup>

<sup>1</sup> Zoological Institute and Museum, General and Systematic Zoology, University of Greifswald, Loitzer Straße 26, 17489 Greifswald, Germany. *E-Mail: gabriele.uhl@uni-greifswald.de*

<sup>2</sup> 48 rue de la fargue, la vallée heureuse, 66690, Sorède

*\*Corresponding Author. E-Mail: philipsteinhoff@gmail.com*

*Manuscript in preparation for publication*





# **Neuroplasticity in response to sensory enrichment and deprivation in a cursorial and a stationary hunting spider**

Philip O.M. Steinhoff<sup>1\*</sup>, Pierick Mougnot<sup>2</sup> & Gabriele Uhl<sup>1</sup>

<sup>1</sup>Zoological Institute and Museum, General and Systematic Zoology, University of Greifswald, Loitzer Straße 26, 17489 Greifswald, Germany. *E-Mail: gabriele.uhl@uni-greifswald.de*

<sup>2</sup>48 rue de la fargue, la vallée heureuse, 66690, Sorède

*\*Corresponding Author. E-Mail: philipsteinhoff@gmail.com*

## **ACKNOWLEDGEMENTS**

We cordially thank Shou-Wang Lin for his help with 3D-reconstructions and Monika Eberhard for assistance and advice on recording vibrations with the laser vibrometer. Brian Schulze wrote the R script to create a mosaic view of all visual stimuli, helped with the setup of the Raspberry Pi computers and gave helpful advice on the statistics. We thank Max Farnworth and Stephen Montgomery for advice on the analysis and interpretation of allometric scaling relationships. Georg Brenneis was always available for discussions on spider neuroplasticity that helped to improve the manuscript. Heidi Land, Amrei Gründer and Cynthia Leuckhardt helped with animal caretaking.

## **DATA AVAILABILITY STATEMENT**

The data that support the findings of this study are available from the corresponding author upon reasonable request.

## Abstract

Neuroplasticity is a ubiquitous feature of animals with nervous systems. Plastic changes of brain structures have been found in various species in response to changing environmental conditions or internal processes, such as learning. Spiders are a large group of predators that have evolved a diverse range of lifestyles, which include species that hunt stationary using a capture web and species that hunt cursorial without a web. Consequently, the importance of sensory modalities varies among species, which is associated with marked differences in the neuroanatomy of stationary and cursorial hunting spiders. While an earlier study has shown that neuroplasticity in response to different early environmental conditions occurs in cursorial hunting jumping spiders, we lack evidence on the direct causes of these plastic changes. Here, we tested how different sensory input affects the central nervous systems (CNS) and elucidate whether the CNS of stationary and cursorial hunting spiders differ in their plastic responses. We used an experimental sensory deprivation and enrichment approach and reared spiders under four different conditions: sensory deprived (CON), vibratory enriched (VIB), visually enriched (VIS) and vibratory and visually enriched (VISVIB). We used the stationary hunter *Parasteatoda tepidariorum* and the cursorial hunter *M. muscosa* as focal species. We predicted that sensory enrichment would lead to an increase in volume in neuropils that process primary sensory information such as the first order visual neuropils, which process information from the eyes, and the leg neuropils, which process mechanosensory information. We expected the effects of vibratory enrichment to be stronger in *P. tepidariorum* and the effects of visual enrichment to be stronger in *M. muscosa*. Contrary to our predictions, we find that sensory enrichment does not lead to an increase in volume of the respective CNS neuropils in both species. We find, however, that in *M. muscosa* spiders from the sensory deprived treatment some neuropils are significantly enlarged compared to the other treatment groups. We furthermore find a shift in the allometric scaling slope of the leg neuropil volumes for spiders from the VIB treatment in both species. This indicates, that although the vibratory enrichment did not induce a change in volume, it led to some developmental differences in the leg neuropils. Furthermore, neuropil volumes in *P. tepidariorum* were generally less constrained by total CNS size than in *M. muscosa*. We conclude that the degree of plasticity is larger in the cursorial than in the stationary hunting spider, which may be related to differences in heterogeneity of their natural habitats. Future studies should explore cellular and genetic mechanisms of neuroplasticity in cursorial and stationary hunting spiders.

## Keywords

Neuroplasticity, brain plasticity, spiders, cursorial, stationary, allometric scaling, neuropil

# 1 Introduction

Changing environmental conditions may have selected for adaptive flexibility of the brain in animals and indeed, neuroplasticity is a ubiquitous feature of all nervous systems. Neuroplasticity can occur both during an individual's development (i.e. experience-expectant plasticity) as well as during the adult phase (i.e. experience-dependent plasticity) (Kolb & Gibb, 2014). Neuroplasticity as a response to learning and memory formation has been explored most intensively in vertebrates (Burns et al., 2009; Gogolla et al., 2007; Guay & Iwaniuk, 2008; Joyce & Brown, 2022; Kihlslinger, 2006; Orije & Van der Linden, 2022; Rosenzweig & Bennett, 1996) but has also been found in adult individuals of different insect species (Anton & Rössler, 2020 review on olfactory circuit plasticity; M. Barth et al., 1997; Fabian & Sachse, 2023 review on experience-dependent plasticity in insects; Fahrbach et al., 1998, 2003; Fahrbach & Van Nest, 2016; Withers et al., 1993, 2008; Yilmaz et al., 2016). Changes in the structure of the brain under different environmental conditions during development was found in insects and spiders (Groh et al., 2004, 2006; Montgomery et al., 2016; Steinhoff et al., 2018). What causes the structural changes in the nervous system is often not well understood. However, Eriksson et al. (2019) recently showed, using an experimental sensory deprivation approach, that the expansion of specific higher-order brain centers in butterflies is not caused by olfactory input per se. In this study, the olfactory receptors of one group of butterflies were experimentally blocked, after which they were allowed to move freely. Eriksson et al. (2019) found that the first-order olfactory neuropils of butterflies with blocked receptors were smaller than in the control group. However, the higher-order neuropils involved in the further processing of olfactory information were not affected by the deprivation suggesting that volume changes in higher-order brain centers are not directly caused by sensory enrichment but might occur in response to cognitive processes such as learning (Eriksson et al., 2019).

Spiders are a large group of mesopredators with diverse sensory ecologies (Foelix, 2011). While many spiders have evolved capture webs for foraging and rely heavily on vibratory cues, other species live cursorial and mostly use visual cues to capture prey (F. G. Barth, 1985; Foelix, 2011). Neuroplasticity has not yet been studied in much detail in spiders. In an observational study, Stafstrom (2017) found a change in eye-size and associated primary and higher-order neuropil volume in response to a significant change in lifestyle in the net-casting spider *Deinopis spinosa*, in which males cease foraging after their final molt. Steinhoff et al. (2018) experimentally altered the early environmental conditions under which the spiders grew up and found volume changes in both higher-order neuropils and total brain. Spiders were reared in three different conditions: deprived, physically enriched and socially enriched (multiple spiders together in a large box), and were compared to spiders caught in the wild (Steinhoff et al., 2018). Spiders from all treatment groups had larger higher-order neuropils and total brains than wild-caught spiders, possibly due to the regular feeding regime. However, spiders from the physically enriched group had larger higher-order neuropils and larger total brain volumes than spiders from the deprived group (Steinhoff et al., 2018), suggesting that some environmental components can influence brain development. To date, it is not known whether and how spider brains respond to sensory input of different modalities, and whether plastic responses differ between species with different sensory ecologies.

Arguably the most striking differences between spiders with different lifestyles are in the size of the eyes (Morehouse, 2020). Eye size has been shown to correlate with differences in the visual pathways of the brain (Hanström, 1921; Long, 2021; Steinhoff et al., 2020, 2023). Most spiders possess four pairs of eyes, of which one pair (the principle eyes or anterior median eyes, AME) is structurally and functionally distinct from the other three pairs (secondary eyes; posterior median eyes, PME, anterior lateral eyes, ALE, and posterior lateral eyes, PLE) (Morehouse, 2020). While the AME have a movable retina and are used for object recognition, the secondary eyes have a fixed retina and are used for movement detection (Morehouse, 2020). The central nervous system of spiders is a highly fused mass of nervous tissue situated in the prosoma and consists of an anterior brain and a posterior ventral nerve cord (VNC) (Steinhoff et al., 2017). The brain contains the first- and second order visual neuropils of the AME, which connect to the arcuate body (AB), a crescent-shaped higher-order neuropil at the posterior rim of the brain (Steinhoff et al., 2020; Strausfeld et al., 1993) and a variable number of visual neuropils that serve the secondary eyes (Steinhoff et al., 2020; Strausfeld & Barth, 1993). The visual neuropils of the secondary eyes are also connected to the AB, and (in some species) to the mushroom bodies (MB), a paired higher-order neuropil in the center of the brain (Steinhoff et al., 2020; Strausfeld & Barth, 1993). The central part of the brain is composed mostly of tracts (protocerebral neuropil, ProtoN) (Babu & Barth, 1984). The posterior part of the brain is formed by the cheliceral and the pedipalpal neuropils, while the VNC is made up by the opisthosomal neuropil, four paired leg neuropils and a central part consisting mainly of tracts (Babu & Barth, 1984; Steinhoff et al., 2017). While the first-order visual neuropils are the brain areas that process primary sensory information from the eyes (Steinhoff et al., 2020), the leg neuropils receive and process mechanosensory (i.e. vibrational) information (Babu & Barth, 1989).

In the present study, we employed selective sensory enrichment - visual and vibratory - to answer the following questions: Which CNS neuropils are directly influenced by an increase in visual information, and which by an increase in vibratory information? Is the different importance of visual and vibratory cues mirrored by the degree of neuroplasticity? The sensory enriched treatments were complemented by a deprivation treatment in which there was neither visual nor vibratory stimulation. In order to assess if spiders of different life styles show a differential response to specific sensory stimulation, we used the cursorial hunter *Marpissa muscosa* and the stationary hunter *Parasteatoda tepidariorum*. Spiders of both species were reared in one of four different environments: A visually enriched environment (VIS), a vibratory enriched environment (VIB) a combination of both (VISVIB) and a deprived control (CON) without any enrichment and maximally reduced sensory input. We predicted that first-order neuropils, which process primary sensory information, would show increases in volume in the respective treatment group and that the magnitude of the change would mirror the sensory ecology of the species. Specifically, we expected first-order visual neuropils of principal and secondary eyes (AM1 and SecVis1) to be enlarged in the VIS and VISVIB treatment in *M. muscosa* but not in *P. tepidariorum*, since this species probably does not rely on visual cues (Steinhoff et al., 2023). On the other hand, we expected the volume of the leg neuropils to be enlarged in the VIB and VISVIB treatments in both species, since both use mechanosensory information (Steinhoff et al., 2023). Since *P. tepidariorum* likely relies almost solely on vibratory information for prey capture,

we expected the changes in leg neuropil volume to be relatively stronger in this species than in *M. muscosa*.

## 2 Material and Methods

### Experimental animals and housing

Adult females of *Marpissa muscosa* (Clerck, 1757) were collected in and near Greifswald (Germany). *M. muscosa* is a common species in Europe that typically occurs on wood, such as old trees or fence-poles, where it builds retreats in crevices or under the bark (Bellmann, 2016). The species is rather long-lived and might overwinter twice before reproduction (Bellmann, 2016). Spiders were kept in plastic boxes (145 x 110 x 68 mm), enriched with paper tissue. Usually, females produced egg sacs about one week after they were collected. Spiderlings hatched within 3 weeks and were transferred to individual plastic boxes (145 x 110 x 68 mm) after leaving the nest. The bottom and long sides of the plastic boxes were painted in brown colour. A window was cut into one of the short sides, covered with gauze and the spiders ID was noted on a white sticker. This side is termed “front side”, contrary to the other short side (“back side”) which was left intact so that the spiders could see through the transparent plastic (see below). Each spider was randomly assigned to one of four treatment groups: visual treatment (VIS), vibratory treatment (VIB), visual and vibratory treatment (VISVIB) and control treatment (CON).

Individuals of the species *Parasteatoda tepidariorum* were collected in the greenhouses of the botanical garden of the University Greifswald. *P. tepidariorum* is a synanthropic species that prefers warm and stable climates and is typically found in heated houses or greenhouses (Roberts, 1996). Spiders were reared in climate chambers (26°C, 80% humidity, 12/12 hrs light cycle). Spiders were kept alone in plastic boxes (145 x 110 x 68 mm) that were enriched with paper tissue. If females did not produce an egg sac within one week, they were paired overnight with a male. Once spiderlings had left the egg sac, they were moved into individual boxes and assigned randomly to one of the four treatments (see above).

### General experimental procedure

The rearing boxes of *M. muscosa* were placed in wooden shelves. We build 8 shelves that each housed 30 rearing boxes (five rows with six boxes each). Initially, 60 spiderlings were assigned to each treatment group (VIS, VIB, VISVIB, CON), so that there were two shelves per group. The shelves were designed in such a way, that the monitor which played the visual stimuli (see below) exactly fit within the frame, directly in front of the short back side (without gaze) of the boxes. For *P. tepidariorum*, initially 30 spiderlings were assigned to each treatment. Boxes of *P. tepidariorum* were oriented vertically, so that spiders could build their capture webs. Rearing boxes with spiders from the same treatment were kept next to each other, separated by cardboard spacers and fixed with straps.

Spiders received cues of prey (videos and vibrations) once a week on the day they were fed. The other visual and vibratory stimuli (see below) were presented in random order, but spiders received visual

and vibratory playback on 4 days of the week for a minimum of 4 and a maximum of 14 hours, depending on the season. Playback was always started after sunrise and always terminated before sunset. For *M. muscosa*, the experimental setup ran from beginning of July 2019 to mid-May 2020 (10.5 months), while in *P. tepidariorum* the experiment lasted from 1<sup>st</sup> of March 2020 to end of May 2020 (3 months). The difference in duration of the experiments mirrors the different maturation time and life-expectancy of the two species. After termination of the experiments, spiders were chemically fixed for the analysis of the neuropil volumes (see below).

### **Video playback**

The use of video playback is a well-established method for behavioral research in cursorial hunting spiders (Clark & Uetz, 1990; Menda et al., 2014; Peckmezian & Taylor, 2015; Uetz et al., 2017). Because habituation has been shown to affect behavior and synaptic activity of the brain and in order to avoid response decrement (Carew et al., 1972, 1972; Engel & Wu, 2009; Humphrey et al., 2018; Melrose et al., 2019), we created different types of visual stimuli and presented them to the spiders in a semi-random order. Visual stimuli consisted of still images of aspects of the environment (soil, grass, sky etc., Fig. S1b) that were shown consecutively to the spiders in 10 sec. or 1 min. intervals. Further visual stimuli were videos of moving prey (drawings of flies prepared using CorelDraw according to Menda et al. (2014); Fig. S1a) or videos of moving jumping spiders with different body postures (drawings prepared using CorelDraw according to Menda et al.; Fig. S1a). Videos were created as GIF-files by stitching together single images that served as individual frames, using GIMP 2.1.0. The package magick in R 3.5.3 was used to stitch individual videos to a single mosaic video with 6x5 mosaic tiles (one tile per spider), with each tile showing the same video (Fig. S1c). Visual stimuli were played back in loop mode on 27" monitors (Acer) in full screen-mode, so that every tile had exactly the same dimensions as the transparent back of the rearing boxes. A VLC media player on Raspberry Pi 3 computers was used to run the videos. Pre-tests with *M. muscosa* spiders collected in the wild showed that they reacted to the video playback of moving flies with typical behaviors that precede a prey attack (i.e. stalking).

### **Vibratory playback**

The setup for the vibratory playback closely follows the methods described and used by Uetz et al. (2017). Spiders in the group VIB and VISVIB received vibratory input via piezo-ceramic elements (KEPO FT-35T-2.9AL-888; voltage: 30V; 35mm diameter) that were attached to the shelf boards, contacting the bottom of the rearing boxes. Vibratory input consisted of recordings of different prey items (*Drosophila sp.*, *Lucilia sp.* and *Calliphora sp.* walking and buzzing) and environmental noise. Vibrations were recorded using a laser vibrometer (PDV-100, PolytecGmbH), and played back using an amplifier (Pyle Mini 2x40W Stereo Power Amplifier) that was connected to the piezo-ceramic elements with speaker wire. VLC media player on Raspberry Pi 3 computers was used to play the vibrations in loop mode. The output was split to all 30 boxes in one shelf using luster terminals. Played-back vibrations were validated by recording them from the spider rearing box with the laser vibrometer and comparing the waveforms (amplitude and pattern) to the original recordings using Audacity 2.1.1 (Fig. S2).

## Sample preparation and MicroCT analysis

Prosomata were fixed overnight at 4°C in 2% PFA. Samples were moved into a mixture of 80% methanol and 20% DMSO on a shaker for 12 hours and then stored at -16°C in 99.8% methanol. Before scanning, samples were transferred to an iodine solution (iodine, resublimated [Carl Roth, X864.1] in 99.8% methanol) for 24 h to enhance tissue contrast. Samples were washed three times in 99.8% methanol, mounted in fresh 99.8% methanol and scanned. Wet scans were used to avoid tissue shrinkage (Rivera Quiroz & Miller, 2022) and methanol provides much better contrast than ethanol. MicroCT scans were carried out with an optical laboratory-scale X-ray microscope (Zeiss XradiaXCT-200). Scans were performed with a 4x or 10x objective lens unit using the following settings: 40 kV, 8 W, 200 µA and exposure times between 1 and 3s. Scans took between 1 and 2 h and resulted in pixel sizes between 2.13 µm and 2.4 µm. Reconstruction of tomographic projections was done using the XMReconstructor software (Zeiss), resulting in image stacks (TIFF format). All scans were performed using Binning 2 for noise reduction (summarizing 4 pixels) and were reconstructed with full resolution (using Binning 1).

## Volume calculation and statistical analysis

The prosoma, cortex and all discernable neuropils in the CNS were reconstructed and their volumes calculated using AMIRA 5.4.5 and 6.0.0 (Visualization Science Group, FEI) (Fig. 1). All statistical analyses were performed in R 4.2.2. Before the statistical tests, all continuous variables were  $\log_{10}$ -transformed. In order to compare volumes of neuropils between the four treatments, we ran GEE models (general estimation equations; geepack in R 4.2.2), which are extensions of GLMs and robust when analyzing correlated data (Højsgaard et al., 2006; Zuur et al., 2009). To investigate the effect of treatment on the different neuropil volumes, we estimated the mean volume of each treatment group by correcting for the individual body size (measured as prosoma volume). To do so, we built a GEE model for each neuropil, including the neuropil volume as response variable and treatment and body size as fixed effects. To take into account the similarity due to a family effect, we also included the ID of the mothers as a random effect with "exchangeable" correlation structure. We estimated group means and 95% confidence interval (CI) for a mean prosoma size using the package "emmeans" (Lenth, 2022). This allowed us to compare the volumes among treatment groups for the same body size. Mean volumes are interpreted as significantly different when confidence intervals do not overlap. For each model, we report the mean and 95% CI for each treatment group, the body size coefficient, its standard error, Wald test and p-value, and the  $r^2$  value for GEE models (Zheng, 2000).

We further analyzed the data by estimating the allometric scaling relationships between all neuropils and a measure for total CNS size (rest of the CNS, ROCNS). ROCNS is a combination of the central part of the protocerebrum (ProtoN) and the central part of the ventral nerve cord (VNC), which both consist mainly of tracts and are thus likely not strongly influenced by the treatments. In both species, ROCNS correlates strongly with total CNS size (*M. muscosa*: spearman's rank correlation  $\rho = 0.92$ ; *P. tepidariorum*: spearman's rank correlation  $\rho = 0.85$ ). To estimate allometric relationships, we used standardized major axis regressions in the SMATR package in R 4.2.2 (Taskinen & Warton, 2013; Warton et al., 2012). The allometric scaling relationship can be described as:  $\log(y) = \beta \log(x) + \log$



( $\alpha$ ), with  $y$ ,  $x$  as neuropil volume and ROCNS volume,  $\beta$  describing the slope of the equation and  $\alpha$  is the  $y$ -axis intercept (Montgomery et al., 2016; Ott & Rogers, 2010; Stöckl et al., 2016; Tsuboi, 2021; Warton et al., 2006). Differences in the volume of neuropils should be visible by changes in  $\log(\alpha)$ , which is referred to as elevation or grade-shift (Farnworth & Montgomery, 2022; Montgomery et al., 2016; Ott & Rogers, 2010; Stöckl et al., 2016; Warton et al., 2012). Difference in slope  $\beta$  would indicate differences in developmental pathways of the structure in question (Riska & Atchley, 1985), while a major axis shift (shift on  $x$  axis) would mean most differences can be explained by differences in CNS size and not individual neuropil volume (Wainwright & Montgomery, 2022).

### Microscopy, image processing and nomenclature

Drawings and figure plates were produced using CorelDRAW 20.1. Images were processed in Corel Paint Shop Pro using global contrast and brightness adjustment features. The terminology used for CNS structures follows Richter et al. (2010). Spider-specific CNS structures are named according to terminologies used by (Babu & Barth, 1984; Steinhoff et al., 2020, 2023; Strausfeld et al., 1993).

## 3 Results

### Neuroanatomy of *M. muscosa* and *P. tepidariorum*

Here, we give an overview of the neuropils that were reconstructed and used for the volumetric analysis. A detailed description and comparative analysis of the neuroanatomy of *M. muscosa* and *P. tepidariorum* has recently been conducted elsewhere (Steinhoff et al., 2023). The brain of *M. muscosa* is dominated by large visual neuropils, that are located anteriorly (Fig. 1a). The first-order visual neuropils of the principal eyes (AM1) are thick and slightly crescent-shaped (Fig. 1b). Just posterior of the AM1 is the AM2 (second-order visual neuropil of the principal eyes), which is large, roundish and elongated towards the posterior part of the brain (Fig. 1a,b). The three secondary eyes supply three first-order visual neuropils (SecVis1) that are situated anterior-laterally and enclose two second-order visual neuropils (SecVis2), which are located more towards the center of the brain (Fig. 1a,b). Proximal of SecVis2 are the mushroom bodies (MB), a higher-order neuropil that consists of two tightly adjoining substructures (Fig. 1b). At the posterior rim of the brain and ensheathed by a layer of cell bodies is the arcuate body (AB), another higher-order neuropil (Fig. 1a,b). The rest of the brain is the large, protocerebral neuropil (ProtoN), which mostly consists of tracts and commissures (Fig. 1a,b). Ventral of the brain are the cheliceral neuropil (ChN) and the pedipalpal neuropil (PdN), followed by the four leg neuropils (LegN) and the opisthosomal neuropil (OpN) (Fig. 1a, b). The latter two enclose the central ventral nerve cord (VNC), which similar to the ProtoN consists mostly of tracts and commissures (Fig. 1a,b). The CNS is surrounded by a layer of cell bodies of varying thickness (cortex; Fig. 1a,b). While Cortex, OpN, LegN, VNC, PdN and ChN appear to be very similar in *P. tepidariorum* (Fig. 1c,d), there are some major differences in the brain compared to *M. muscosa*. *P. tepidariorum* possesses two subsequent neuropils that serve the principal eyes (PrincVis), but only a single small visual neuropil that serves all secondary eyes (SecVis; Fig. 1c,d). We did not detect MB in *P. tepidariorum*, but a prominent AB (Fig. 1c,d). ProtoN and VNC were added together in both species

(cf. Figure 1) and used as allometric control (rest of the central nervous system, ROCNS) in the analyses of allometric scaling relationships (see below).

### **Neuropil volume and allometric scaling in *M. muscosa***

When comparing neuropil volumes between treatments corrected for body size, we find significant differences in AM1, ChN, OpN and total CNS volume (Table 1, Figure 2a,3a,d,f). Specifically, spiders from treatment CON had significantly larger AM1 than spiders from treatment VIB (Table 1, Figure 2a) and significantly larger ChN than spiders from treatments VIB and VIS (Table 1, Figure 3a). Additionally, spiders from treatment CON had significantly larger OpN than spiders from treatment VIS (Table 1, Figure 3d). The total CNS volume was significantly larger in spiders from treatment VISVIB than in spiders from treatment VIB (Table 1, Figure 3f). The GEE models furthermore revealed that body size had a significant effect on the volume of all neuropils (Table 2). Models generally explained a large part of the variance, only the models for AM1 ( $R^2$  0.363), SecVis1 ( $R^2$  0.469) and ChN ( $R^2$  0.497) had an  $R^2$  value lower than 0.5 (Table 2).

The analysis of the allometric scaling relationships between treatment groups uncovered a significant grade-shift ( $\alpha$  shift) in AM1 of spiders from treatment CON (Table 5, Figure 2a'). This indicates that spiders from treatment CON had larger AM1 relative to the ROCNS than spiders from all other treatments (Table 5, Figure 2a'). Further grade-shifts occurred in the MB between treatment CON and VISVIB, indicating that the relative volume of MB is larger in CON than in VISVIB (Table 5, Figure 2f'), in the OpN with treatment CON having larger relative volumes than the treatments VIS and VISVIB (Table 5, Figure 3d'), in the Cortex, where spiders from VISVIB are shifted up compared to spiders from VIS (Table 5, Figure 3e') and in the total CNS, which was larger relative to body size in treatment CON than in treatments VIB and VIS (Table 5, Figure 3f'). We also observed occasional differences in  $\beta$  slope, specifically for spiders from treatment VIB (in ChN compared to treatment VISVIB, in LegN compared to treatment VIS, in OpN compared to treatments CON and VIS; Table 5). There was a major axis shift between treatment VIS and CON in several neuropils: AM2, SecVis1, SecVis2, AB, MB, PdN, LegN, CNS and Cortex (Table 5, Figures 2b'-f', 3b',c',e',f'). In some treatment groups, the neuropil volume did not correlate significantly with the allometric control (AM1: VIB; SecVis1: CON and VIB; AB: VIS; ChN: VIS; Figures 2, 3).

### **Neuropil volume and allometric scaling in *P. tepidariorum***

The volumes of all neuropils do not differ significantly among treatment groups in *P. tepidariorum* (Table 3, Figures 4, 5). The model output shows, that body size had a significant influence on the volumes of PrincVis, SecVis, ChN, LegN, OpN, ROCNS, Cortex and CNS, but not on AB and PdN (Table 4). Most models explained only a small proportion of the variance, with  $R^2$  values between 0.043 (Cortex) and 0.325 (ChN) (Table 4). The models for total CNS volume ( $R^2$  0.517) and LegN ( $R^2$  0.692) are an exception in that they explain a rather large amount of the observed variance (Table 4).

Allometric scaling analyses revealed two neuropils in which grade-shifts occurred (Table 2, Figures 4, 5). These were the AB, in which spiders from treatment VIB had smaller relative neuropil volumes than spiders from the treatments VIS and VISVIB (Table 2, Figure 4c'), and the OpN, in which spiders

from the treatment VISVIB had larger relative neuropil volumes than spiders from the treatment VIS (Table 2, Figure 5a'). We found a shift in  $\beta$  slope for LegN, with spiders from treatment VIB displaying a  $\beta$  slope that was significantly different from that in the treatments CON and VISVIB (Table 2, Figure 4f'). There was also a major axis shift in LegN, with spiders from treatment VIB having larger ROCNS than spiders from the treatment VIS (Table 2, Figure 4f'). Another major axis shift was observed in PrincVis, with spiders from treatment CON having larger ROCNS than spiders from treatment VIS (Table 2, Figure 4a'). The allometric scaling analyses further revealed that the volumes of some neuropils did not correlate significantly with the allometric control ROCNS (PrincVis, ChN, PdN, Cortex; Figures 4, 5), while for the other neuropils an absence of significant correlation was noted for some of the treatments but not for all (SecVis: treatments CON, VIS and VISVIB, AB: treatments CON and VIS, LegN: treatment VISVIB, OpN: treatments CON, VIS and VISVIB; Figures 4, 5). In the treatment groups CON, VIS and VISVIB the total CNS volume did not correlate significantly with body size (Figure 5c').

## 4 Discussion

Our results show species specific effects of sensory enrichment and deprivation on the neuroanatomy of spiders. Some of these effects are moderate and occur in other treatment groups than expected. We also show that there is generally a greater degree of plasticity in *M. muscosa* than in *P. tepidariorum*, and that in *M. muscosa* the volumes of individual neuropils seem more constrained by total CNS size than in *P. tepidariorum*.

### Differences in allometric slope $\beta$

We found in both species that some treatments differed from each other in their allometric slope ( $\beta$ -shift). Differences in the slope of an allometric curve are generally difficult to explain and are typically interpreted as indicative of differences in genetic and developmental constraints (Riska & Atchley, 1985; Tsuboi, 2021). While differences in the slope of the allometric scaling curve have frequently been found when comparing neuropil volumes of closely related species (Montgomery et al., 2016; Stöckl et al., 2016; Wainwright & Montgomery, 2022), it is unclear how our experimental setup induced these differences within a single species. Slopes of allometric scaling curves are sensitive to outliers, which is why we used robust SMATR that leads to accurate inferences in datasets with small sample-sizes (Taskinen & Warton, 2013). Despite these precautions, it cannot be ruled out entirely that the differences in allometric slope observed here, arise due to the sample sizes. However, since differences in  $\beta$  slope were exclusively observed in spiders of the treatment group VIB and only in neuropils receiving mechanosensory information (ChN, LegN and OpN in *M. muscosa* and LegN in *P. tepidariorum*), we assume that these differences are biologically determined and do not present mere noise. Since only spiders that received pure vibratory enrichment (treatment group VIB), but not spiders that received mixed vibratory and visual input (treatment group VISVIB) show the differences in slope, we must assume that the effects that led to a differential development of a number of neuropils in treatment group VIB are somehow attenuated by additional visual input. While it is

tempting to hypothesize a potential trade-off between enlarged mechanosensory neuropils and visual neuropils, this is not supported by our results, since we do not find enlarged primary visual processing neuropils in the VISVIB and VIS treatment groups.

### **Sensory enrichment-induced plasticity in *Marpissa muscosa***

In *M. muscosa* we found an effect of treatments on the volume of three neuropils, the AM1, ChN and OpN (Table 1). All of these neuropils are primary sensory processing neuropils. It is to be expected that they would be larger when exposed to additional sensory input (Chittka & Niven, 2009). Contrary to our expectations, treatment group CON had the largest neuropil volumes in all three cases (AM1, ChN and OpN). While we consider CON as a control group for the other treatments, it also is a sensory deprivation treatment, since these animals received no sensory input, which is much unlike the natural condition. We therefore assume that the observed differences are due to experience-independent plasticity (Kolb & Gibb, 2014), in which initially more neurons or synapses are produced that get later pruned (Campbell & Shatz, 1992; Hooks & Chen, 2020; Jenks et al., 2021; Sakata et al., 2022). Since the animals were not yet adults at the end of the experiment, it could be that the pruning had not yet occurred or had a lower magnitude than in spiders from the other treatments that experienced regular sensory input. The findings of our volumetric comparisons are partially consistent with the results from the allometric scaling analyses, in which grade shifts of treatment group CON occur in AM1 and OpN (Table 5, Figures 2,3). We find an additional grade-shift of MB volume in spiders from the treatment group CON compared to spiders from the treatment group VISVIB, but this is not supported by our volumetric analysis (cf. Table 1). The spider MB is a higher-order neuropil that mainly receives visual input from the secondary eyes (Long, 2021; Steinhoff et al., 2023), and the visual neuropils of these eyes are not enlarged in treatment group CON (Table 1, 5). A tendency towards enlarged MB in the CON group might be more related to complex neurobiological processes (cf. Eriksson et al., 2019). We also found an additional grade-shift in the Cortex, with spiders from treatment VISVIB having a larger Cortex volume than spiders from treatment VIS. The Cortex consists of neuron cell bodies and glial cells; all neuronal projections (axons, dendrites) that make up the CNS arise from it (Richter et al., 2010). Due to energetic constraints, cell size is generally more limited than cell number (Riska & Atchley, 1985), which implies that a larger cortex contains either more neurons or more glial cells. In order to distinguish both cell types, a neuronal marker is needed (cf. Herculano-Houzel, 2005, 2017), which does not yet exist for spiders. However, since glial cells also play an active role in CNS development and activity (Duan et al., 2020; Pinto-Lord et al., 1982), an increase in cortex volume has interesting implications regardless of whether neuronal cell bodies or glia are involved. The differences found here are small and not supported by our GEE models, but a possible interpretation could be that a combination of sensory inputs requires more cells for processing. Since this difference is not mirrored by volumetric differences of individual neuropils, one might speculate that the resulting differences are rather on a circuitry level (Chittka & Niven, 2009). Apart from these grade-shifts we found consistent major axis shifts between the CON and VIS treatment groups for all neuropils except AM1, ChN and OpN (Table 5; Figure 2, 3). These shifts indicate that the allometric control ROCNS is larger in the treatment group VIS, which in turn implies that their total CNS is larger. Since there is also a major axis shift in total CNS volume with body size as an allometric control, we

consider it safe to assume that a larger body size is driving these differences in major axis shift. Indeed, body size had a significant influence on the volumes of all neuropils in our GEE models (Table 2).

### **Sensory enrichment-induced plasticity in *Parasteatoda tepidariorum***

While we found no significant volume differences between treatment groups in *P. tepidariorum* using GEE models (Table 3), the allometric slope analysis indicates that spiders from the visually enriched treatments VIS and VISVIB tend to have relatively larger AB than spiders from the purely vibratory enriched treatment VIB (Figure 4c'). This is unexpected, as it indicates that visual enrichment affects the brain anatomy of *P. tepidariorum* although we did not detect any effect on the first-order visual neuropils. Since the AB is the main higher integrating neuropil in the spider brain (Babu & Barth, 1984; Steinhoff et al., 2023), it is reasonable to assume that direct sensory input has a limited effect compared to cognitive processes such as learning. In accordance with this, in the jumping spider *M. muscosa*, the volume of the AB was found to be plastic in response to early environmental conditions. The conditions differed in the physical landscape and thus in the need to master cognitively demanding tasks such as navigating a complex environment (Steinhoff et al., 2018). Similarly, the olfactory processing mushroom body of the butterfly does not change in volume with increased sensory input alone, but a change in volume likely requires cognitive processes such as learning (Eriksson et al., 2019). We can therefore speculate that the visual enrichment in the treatment groups VIS and VISVIB somehow led to a need for increased higher-order processing (e.g. learning or memory formation) in *P. tepidariorum*. However, since the grade-shift in AB volume is not supported by significant differences in the GEE models, this speculation should be treated with caution.

### **Interspecific comparison of sensory enrichment-induced plasticity**

Generally, we find stronger effects of the treatments on neuropil volumes in *M. muscosa* than in *P. tepidariorum*. While we had expected the CNS of the cursorial hunter *M. muscosa* to be more strongly affected by visual input, it is surprising that vibratory input does not seem to influence the volume of CNS neuropils in the stationary hunter *P. tepidariorum*. These findings suggest that the potential of neuroplasticity is larger in *M. muscosa* than in *P. tepidariorum*. Several studies found differences between species in the degree of neuroplasticity (Kamhi et al., 2017; Lai et al., 2017) or other phenotypic traits (Einum & Burton, 2023; Murren et al., 2015). Phenotypic plasticity is usually considered to be energetically costly (although difficult to measure), resulting in an evolutionary tradeoff with the benefits arising from plasticity (Auld et al., 2009; Coquillard et al., 2012; DeWitt, 1998; Murren et al., 2015). Phenotypic plasticity is selectively favoured in heterogeneous environments, in which the costs of not being plastic can be high (Coquillard et al., 2012; Murren et al., 2015). A potential explanation for the differences in the degree of neuroplasticity observed here between *M. muscosa* and *P. tepidariorum* could therefore be that *M. muscosa* lives under frequently changing environmental conditions, which might require a greater genetic potential for neuroplastic responses than in *P. tepidariorum*. Furthermore, *P. tepidariorum* was reared under constant light cycle and temperature, whereas *M. muscosa* was reared under changing daylight and room temperature which simulates to a certain extent the biology and ecology of both species, with greater heterogeneity in the environment that *M. muscosa* experienced. We also found in *P. tepidariorum*

that the goodness of fit measure ( $R^2$ ) of the models were much lower than in *M. muscosa*, suggesting that the variation in neuropil volume in *P. tepidariorum* is likely determined by a parameter that was not investigated here, consistent with the finding that in *P. tepidariorum* the volumes of most neuropils do not correlate with the allometric control, suggesting that they are less strongly constrained by total CNS size than in *M. muscosa*.

## Conclusions

We have shown here that sensory enrichment and deprivation induce plastic changes in the neuroanatomy of cursorial and stationary hunting spiders. Theory predicted a clear link between visual and vibratory enrichment and an increase in volume of primary sensory processing neuropils (Chittka & Niven, 2009; Sterling & Laughlin, 2017). However, we find an increase in volumes of some visual (AM1) and mechanosensory processing neuropils (ChN, OpN) in the sensory deprived group CON of the cursorial hunting *M. muscosa*, but no volume differences in the stationary hunting *P. tepidariorum*. Furthermore, the analysis of allometric scaling relationships reveals complex patterns in both species with grade shifts indicating changes in neuropil size, which in *M. muscosa* occur mainly in the sensory deprived treatment group CON. Shifts in slope  $\beta$  occur only in the vibratory enriched treatment groups of both species, indicating possible differences in developmental pathways, that need to be investigated at a cellular and genetic level.

Our results indicate that the degree of plasticity is greater in the cursorial hunting spider *M. muscosa* than in the stationary hunting spider *P. tepidariorum*, which might be related to a different degree of heterogeneity in the environments typically encountered by the respective species. However, scaling analyses also reveal that neuropil volumes in *P. tepidariorum* are less determined by total CNS size than in *M. muscosa*. Such species-specific effects point towards major differences in developmental constraints, that are as yet unexplored. We tentatively attribute these differences to the biology and ecology of the species, however, phylogenetic signals might also play a role.

## References

- Anton, S., & Rössler, W. (2020). Plasticity and modulation of olfactory circuits in insects. *Cell and Tissue Research*. <https://doi.org/10.1007/s00441-020-03329-z>
- Auld, J. R., Agrawal, A. A., & Relyea, R. A. (2009). Re-evaluating the costs and limits of adaptive phenotypic plasticity. *Proceedings of the Royal Society B: Biological Sciences*, 277(1681), 503–511. <https://doi.org/10.1098/rspb.2009.1355>
- Babu, K. S., & Barth, F. G. (1984). Neuroanatomy of the central nervous system of the wandering spider, *Cupiennius salei* (Arachnida, Araneida). *Zoomorphology*, 104, 344–359. <https://doi.org/10.1007/BF00312185>
- Babu, K. S., & Barth, F. G. (1989). Central nervous projections of mechanoreceptors in the spider *Cupiennius salei* Keys. *Cell and Tissue Research*, 258(1). <https://doi.org/10.1007/BF00223146>
- Barth, F. G. (Ed.). (1985). *Neurobiology of Arachnids*. Springer Berlin Heidelberg. <https://doi.org/10.1007/978-3-642-70348-5>

- Barth, M., Hirsch, H. V., Meinertzhagen, I. A., & Heisenberg, M. (1997). Experience-dependent developmental plasticity in the optic lobe of *Drosophila melanogaster*. *The Journal of Neuroscience*, *17*(4), 1493–1504.
- Bellmann, H. (2016). *Der Kosmos Spinnenführer*. Kosmos.
- Burns, J. G., Saravanan, A., & Helen Rodd, F. (2009). Rearing Environment Affects the Brain Size of Guppies: Lab-Reared Guppies have Smaller Brains than Wild-Caught Guppies. *Ethology*, *115*(2), 122–133. <https://doi.org/10.1111/j.1439-0310.2008.01585.x>
- Campbell, G., & Shatz, C. J. (1992). Synapses formed by identified retinogeniculate axons during the segregation of eye input. *Journal of Neuroscience*, *12*(5), 1847–1858. <https://doi.org/10.1523/JNEUROSCI.12-05-01847.1992>
- Carew, T. J., Pinsker, H. M., & Kandel, E. R. (1972). Long-Term Habituation of a Defensive Withdrawal Reflex in *Aplysia*. *Science*, *175*(4020), 451–454. <https://doi.org/10.1126/science.175.4020.451>
- Chittka, L., & Niven, J. (2009). Are Bigger Brains Better? *Current Biology*, *19*(21), R995–R1008. <https://doi.org/10.1016/j.cub.2009.08.023>
- Clark, D. L., & Uetz, G. W. (1990). Video image recognition by the jumping spider, *Maevia inclemens* (Araneae: Salticidae). *Animal Behaviour*, *40*(5), 884–890. [https://doi.org/10.1016/S0003-3472\(05\)80990-X](https://doi.org/10.1016/S0003-3472(05)80990-X)
- Coquillard, P., Muzy, A., & Diener, F. (2012). Optimal phenotypic plasticity in a stochastic environment minimises the cost/benefit ratio. *Ecological Modelling*, *242*, 28–36. <https://doi.org/10.1016/j.ecolmodel.2012.05.019>
- DeWitt, T. J. (1998). Costs and limits of phenotypic plasticity: Tests with predator-induced morphology and life history in a freshwater snail. *Journal of Evolutionary Biology*, *11*(4), 465–480. <https://doi.org/10.1046/j.1420-9101.1998.11040465.x>
- Duan, D., Zhang, H., Yue, X., Fan, Y., Xue, Y., Shao, J., Ding, G., Chen, D., Li, S., Cheng, H., Zhang, X., Zou, W., Liu, J., Zhao, J., Wang, L., Zhao, B., Wang, Z., Xu, S., Wen, Q., ... Kang, L. (2020). Sensory Glia Detect Repulsive Odorants and Drive Olfactory Adaptation. *Neuron*, *108*(4), 707–721.e8. <https://doi.org/10.1016/j.neuron.2020.08.026>
- Einum, S., & Burton, T. (2023). Divergence in rates of phenotypic plasticity among ectotherms. *Ecology Letters*, *26*(1), 147–156. <https://doi.org/10.1111/ele.14147>
- Engel, J. E., & Wu, C.-F. (2009). Neurogenetic approaches to habituation and dishabituation in *Drosophila*. *Neurobiology of Learning and Memory*, *92*(2), 166–175. <https://doi.org/10.1016/j.nlm.2008.08.003>
- Eriksson, M., Nylin, S., & Carlsson, M. A. (2019). Insect brain plasticity: Effects of olfactory input on neuropil size. *Royal Society Open Science*, *6*(8), 190875. <https://doi.org/10.1098/rsos.190875>
- Fabian, B., & Sachse, S. (2023). Experience-dependent plasticity in the olfactory system of *Drosophila melanogaster* and other insects. *Frontiers in Cellular Neuroscience*, *17*, 1130091. <https://doi.org/10.3389/fncel.2023.1130091>
- Fahrbach, S. E., Farris, S. M., Sullivan, J. P., & Robinson, G. E. (2003). Limits on volume changes in the mushroom bodies of the honey bee brain. *Journal of Neurobiology*, *57*(2), 141–151. <https://doi.org/10.1002/neu.10256>

- Fahrbach, S. E., Moore, D., Capaldi, E. A., Farris, S. M., & Robinson, G. E. (1998). Experience-Expectant Plasticity in the Mushroom Bodies of the Honeybee. *Learning & Memory*, *5*, 10115–10123.
- Fahrbach, S. E., & Van Nest, B. N. (2016). Synapsin-based approaches to brain plasticity in adult social insects. *Current Opinion in Insect Science*, *18*, 27–34. <https://doi.org/10.1016/j.cois.2016.08.009>
- Farnworth, M. S., & Montgomery, S. H. (2022). Complexity of biological scaling suggests an absence of systematic trade-offs between sensory modalities in *Drosophila*. *Nature Communications*, *13*(1), 2944. <https://doi.org/10.1038/s41467-022-30579-y>
- Foelix, R. (2011). *Biology of Spiders*. Oxford University Press, USA.
- Gogolla, N., Galimberti, I., & Caroni, P. (2007). Structural plasticity of axon terminals in the adult. *Current Opinion in Neurobiology*, *17*(5), 516–524. <https://doi.org/10.1016/j.conb.2007.09.002>
- Groh, C., Ahrens, D., & Rössler, W. (2006). Environment- and age-dependent plasticity of synaptic complexes in the mushroom bodies of honeybee queens. *Brain, Behavior and Evolution*, *68*(1), 1–14. <https://doi.org/10.1159/000092309>
- Groh, C., Tautz, J., & Rössler, W. (2004). Synaptic organization in the adult honey bee brain is influenced by brood-temperature control during pupal development. *Proceedings of the National Academy of Sciences of the United States of America*, *101*(12), 4268–4273. <https://doi.org/10.1073/pnas.0400773101>
- Guay, P.-J., & Iwaniuk, A. N. (2008). CAPTIVE BREEDING REDUCES BRAIN VOLUME IN WATERFOWL (ANSERIFORMES). *The Condor*, *110*(2), 276–284. <https://doi.org/10.1525/cond.2008.8424>
- Hanström, B. (1921). Über die Histologie und vergleichende Anatomie der Sehganglien und Globuli der Araneen. *Kungliga Svenska Vetenskapsakademiens Handlingar*, *61*(12), 1–39.
- Herculano-Houzel, S. (2005). Isotropic Fractionator: A Simple, Rapid Method for the Quantification of Total Cell and Neuron Numbers in the Brain. *Journal of Neuroscience*, *25*(10), 2518–2521. <https://doi.org/10.1523/JNEUROSCI.4526-04.2005>
- Herculano-Houzel, S. (2017). Numbers of neurons as biological correlates of cognitive capability. *Current Opinion in Behavioral Sciences*, *16*, 1–7. <https://doi.org/10.1016/j.cobeha.2017.02.004>
- Højsgaard, S., Halekoh, U., & Yan, J. (2006). The R Package geepack for Generalized Estimating Equations. *Journal of Statistical Software*, *15*, 1–11. <https://doi.org/10.18637/jss.v015.i02>
- Hooks, B. M., & Chen, C. (2020). Circuitry Underlying Experience-Dependent Plasticity in the Mouse Visual System. *Neuron*, *106*(1), 21–36. <https://doi.org/10.1016/j.neuron.2020.01.031>
- Humphrey, B., Helton, W. S., Bedoya, C., Dolev, Y., & Nelson, X. J. (2018). Psychophysical investigation of vigilance decrement in jumping spiders: Overstimulation or understimulation? *Animal Cognition*, *21*(6), 787–794. <https://doi.org/10.1007/s10071-018-1210-2>
- Jenks, K. R., Tsimring, K., Ip, J. P. K., Zepeda, J. C., & Sur, M. (2021). Heterosynaptic Plasticity and the Experience-Dependent Refinement of Developing Neuronal Circuits. *Frontiers in Neural Circuits*, *15*. <https://www.frontiersin.org/articles/10.3389/fncir.2021.803401>



- Joyce, B. J., & Brown, G. E. (2022). Olfaction and reaction: The role of olfactory and hypothalamic investment in the antipredator responses to chemical alarm cues by northern redbelly dace. *Current Zoology*, zoac086. <https://doi.org/10.1093/cz/zoac086>
- Kamhi, J. F., Sandridge-Gresko, A., Walker, C., Robson, S. K. A., & Traniello, J. F. A. (2017). Worker brain development and colony organization in ants: Does division of labor influence neuroplasticity?: Division of Labor and Ant Brain Development. *Developmental Neurobiology*, 77(9), 1072–1085. <https://doi.org/10.1002/dneu.22496>
- Kihlslinger, R. L. (2006). Early rearing environment impacts cerebellar growth in juvenile salmon. *Journal of Experimental Biology*, 209(3), 504–509. <https://doi.org/10.1242/jeb.02019>
- Kolb, B., & Gibb, R. (2014). Searching for the principles of brain plasticity and behavior. *Cortex*, 58, 251–260. <https://doi.org/10.1016/j.cortex.2013.11.012>
- Lai, F., Fagernes, C. E., Bernier, N. J., Miller, G. M., Munday, P. L., Jutfelt, F., & Nilsson, G. E. (2017). Responses of neurogenesis and neuroplasticity related genes to elevated CO<sub>2</sub> levels in the brain of three teleost species. *Biology Letters*, 13(8), 20170240. <https://doi.org/10.1098/rsbl.2017.0240>
- Lenth, R. (2022). *emmeans: Estimated marginal means, aka least-squares means. R package version 1.4.7. 2020.*
- Long, S. M. (2021). Variations on a theme: Morphological variation in the secondary eye visual pathway across the order of Araneae. *Journal of Comparative Neurology*, 529(2), 259–280. <https://doi.org/10.1002/cne.24945>
- Melrose, A., Nelson, X. J., Dolev, Y., & Helton, W. S. (2019). Vigilance all the way down: Vigilance decrement in jumping spiders resembles that of humans. *Quarterly Journal of Experimental Psychology*, 72(6), 1530–1538. <https://doi.org/10.1177/1747021818798743>
- Menda, G., Shamble, P. S., Nitzany, E. I., Golden, J. R., & Hoy, R. R. (2014). Visual Perception in the Brain of a Jumping Spider. *Current Biology*, 24(21), 2580–2585. <https://doi.org/10.1016/j.cub.2014.09.029>
- Montgomery, S. H., Merrill, R. M., & Ott, S. R. (2016). Brain composition in *Heliconius* butterflies, posteclosion growth and experience-dependent neuropil plasticity: Anatomy and plasticity of *heliconius* brains. *Journal of Comparative Neurology*, 524(9), 1747–1769. <https://doi.org/10.1002/cne.23993>
- Morehouse, N. (2020). Spider vision. *Current Biology*, 30(17), R975–R980. <https://doi.org/10.1016/j.cub.2020.07.042>
- Murren, C. J., Auld, J. R., Callahan, H., Ghalambor, C. K., Handelsman, C. A., Heskell, M. A., Kingsolver, J. G., Maclean, H. J., Masel, J., Maughan, H., Pfennig, D. W., Relyea, R. A., Seiter, S., Snell-Rood, E., Steiner, U. K., & Schlichting, C. D. (2015). Constraints on the evolution of phenotypic plasticity: Limits and costs of phenotype and plasticity. *Heredity*, 115(4), Article 4. <https://doi.org/10.1038/hdy.2015.8>
- Orije, J. E. M. J., & Van der Linden, A. (2022). A brain for all seasons: An in vivo MRI perspective on songbirds. *Journal of Experimental Zoology Part A: Ecological and Integrative Physiology*, 337(9–10), 967–984. <https://doi.org/10.1002/jez.2650>

- Ott, S. R., & Rogers, S. M. (2010). Gregarious desert locusts have substantially larger brains with altered proportions compared with the solitary phase. *Proceedings of the Royal Society B*, 277(1697), 3087–3096. <https://doi.org/10.1098/rspb.2010.0694>
- Peckmezian, T., & Taylor, P. W. (2015). A virtual reality paradigm for the study of visually mediated behaviour and cognition in spiders. *Animal Behaviour*, 107, 87–95. <https://doi.org/10.1016/j.anbehav.2015.06.018>
- Pinto-Lord, M. C., Evrard, P., & Caviness, V. S. (1982). Obstructed neuronal migration along radial glial fibers in the neocortex of the reeler mouse: A golgi-EM analysis. *Developmental Brain Research*, 4(4), 379–393. [https://doi.org/10.1016/0165-3806\(82\)90181-X](https://doi.org/10.1016/0165-3806(82)90181-X)
- Richter, S., Loesel, R., Purschke, G., Schmidt-Rhaesa, A., Scholtz, G., Stach, T., Vogt, L., Wanninger, A., Brenneis, G., Döring, C., Faller, S., Fritsch, M., Grobe, P., Heuer, C. M., Kaul, S., Møller, O. S., Müller, C. H., Rieger, V., Rothe, B. H., ... Harzsch, S. (2010). Invertebrate neurophylogeny: Suggested terms and definitions for a neuroanatomical glossary. *Frontiers in Zoology*, 7(1), 29. <https://doi.org/10.1186/1742-9994-7-29>
- Riska, B., & Atchley, W. R. (1985). Genetics of Growth Predict Patterns of Brain-Size Evolution. *Science*, 229(4714), 668–671. <https://doi.org/10.1126/science.229.4714.668>
- Rivera Quiroz, F. A., & Miller, J. (2022). Micro-CT visualization of the CNS: Performance of different contrast-enhancing techniques for documenting the spider brain. *Journal of Comparative Neurology*. <https://doi.org/10.1002/cne.25343>
- Roberts, M. J. (1996). *Spiders of Britain and Northern Europe*. HarperCollins Publishers Ltd.
- Rosenzweig, M. R., & Bennett, E. L. (1996). Psychobiology of plasticity: Effects of training and experience on brain and behavior. *Behavioural Brain Research*, 78(1), 57–65. [https://doi.org/10.1016/0166-4328\(95\)00216-2](https://doi.org/10.1016/0166-4328(95)00216-2)
- Sakata, J. T., Catalano, I., & Woolley, S. C. (2022). Mechanisms, development, and comparative perspectives on experience-dependent plasticity in social behavior. *Journal of Experimental Zoology Part A: Ecological and Integrative Physiology*, 337(1), 35–49. <https://doi.org/10.1002/jez.2539>
- Stafstrom, J. A., Michalik, P., & Hebets, E. A. (2017). Sensory system plasticity in a visually specialized, nocturnal spider. *Scientific Reports*, 7(March), 1–11. <https://doi.org/10.1038/srep46627>
- Steinhoff, P. O. M., Harzsch, S., & Uhl, G. (2023). *Comparative neuroanatomy of the central nervous system in stationary and cursorial hunting spiders [Manuscript submitted for publication]*.
- Steinhoff, P. O. M., Liedtke, J., Sombke, A., Schneider, J. M., & Uhl, G. (2018). Early environmental conditions affect the volume of higher-order brain centers in a jumping spider. *Journal of Zoology*, 304(3), 182–192. <https://doi.org/10.1111/jzo.12512>
- Steinhoff, P. O. M., Sombke, A., Liedtke, J., Schneider, J. M., Harzsch, S., & Uhl, G. (2017). The synganglion of the jumping spider *Marpissa muscosa* (Arachnida: Salticidae): Insights from histology, immunohistochemistry and microCT analysis. *Arthropod Structure & Development*, 46(2), 156–170. <https://doi.org/10.1016/j.asd.2016.11.003>
- Steinhoff, P. O. M., Uhl, G., Harzsch, S., & Sombke, A. (2020). Visual pathways in the brain of the jumping spider *Marpissa muscosa*. *Journal of Comparative Neurology*, 528(11), 1883–1902. <https://doi.org/10.1002/cne.24861>

- Sterling, P., & Laughlin, S. (2017). *Principles of Neural Design*. MIT Press.
- Stöckl, A., Heinze, S., Charalabidis, A., el Jundi, B., Warrant, E., & Kelber, A. (2016). Differential investment in visual and olfactory brain areas reflects behavioural choices in hawk moths. *Scientific Reports*, *6*(1), 26041. <https://doi.org/10.1038/srep26041>
- Strausfeld, N. J., & Barth, F. G. (1993). Two visual systems in one brain: Neuropils serving the secondary eyes of the spider *Cupiennius salei*. *Journal of Comparative Neurology*, *328*(1), 43–62.
- Strausfeld, N. J., Weltzien, P., & Barth, F. G. (1993). Two visual systems in one brain: Neuropils serving the principal eyes of the spider *Cupiennius salei*. *Journal of Comparative Neurology*, *328*(1), 63–75.
- Taskinen, S., & Warton, D. I. (2013). Robust tests for one or more allometric lines. *Journal of Theoretical Biology*, *333*, 38–46. <https://doi.org/10.1016/j.jtbi.2013.05.010>
- Tsuboi, M. (2021). Exceptionally Steep Brain-Body Evolutionary Allometry Underlies the Unique Encephalization of Osteoglossiformes. *Brain, Behavior and Evolution*, *96*(2), 49–63. <https://doi.org/10.1159/000519067>
- Uetz, G. W., Stoffer, B., Lallo, M. M., & Clark, D. L. (2017). Complex signals and comparative mate assessment in wolf spiders: Results from multimodal playback studies. *Animal Behaviour*, *134*, 283–299. <https://doi.org/10.1016/j.anbehav.2017.02.007>
- Wainwright, J. B., & Montgomery, S. H. (2022). Neuroanatomical shifts mirror patterns of ecological divergence in three diverse clades of mimetic butterflies. *Evolution*, *76*(8), 1806–1820. <https://doi.org/10.1111/evo.14547>
- Warton, D. I., Duursma, R. A., Falster, D. S., & Taskinen, S. (2012). Smatr 3— an R package for estimation and inference about allometric lines. *Methods in Ecology and Evolution*, *3*(2), 257–259. <https://doi.org/10.1111/j.2041-210X.2011.00153.x>
- Warton, D. I., Wright, I. J., Falster, D. S., & Westoby, M. (2006). Bivariate line-fitting methods for allometry. *Biological Reviews*, *81*(2), 259–291. <https://doi.org/10.1017/S1464793106007007>
- Withers, G. S., Day, N. F., Talbot, E. F., Dobson, H. E. M., & Wallace, C. S. (2008). Experience-dependent plasticity in the mushroom bodies of the solitary bee *Osmia lignaria* (Megachilidae). *Developmental Neurobiology*, *68*(1), 73–82. <https://doi.org/10.1002/dneu.20574>
- Withers, G. S., Fahrbach, S. E., & Robinson, G. E. (1993). Selective neuroanatomical plasticity and division of labour in the honeybee. *Nature*, *364*(6434), 238–240. <https://doi.org/10.1038/364238a0>
- Yilmaz, A., Lindenberg, A., Albert, S., Grübel, K., Spaethe, J., Rössler, W., & Groh, C. (2016). Age-related and light-induced plasticity in opsin gene expression and in primary and secondary visual centers of the nectar-feeding ant *Camponotus rufipes*. *Developmental Neurobiology*, *76*(9), 1041–1057. <https://doi.org/10.1002/dneu.22374>
- Zheng, B. (2000). Summarizing the goodness of fit of generalized linear models for longitudinal data. *Statistics in Medicine*, *19*(10), 1265–1275. [https://doi.org/10.1002/\(SICI\)1097-0258\(20000530\)19:10<1265::AID-SIM486>3.0.CO;2-U](https://doi.org/10.1002/(SICI)1097-0258(20000530)19:10<1265::AID-SIM486>3.0.CO;2-U)
- Zuur, A., Ieno, E. N., Walker, N., Saveliev, A. A., & Smith, G. M. (2009). *Mixed effects models and extensions in ecology with R*. Springer Science & Business Media.

## Tables

**Table 1.** Mean and 95% confidence interval (CI) of CNS areas (neuropils, cortex and CNS) for each group in *M. muscosa*. est, mean CI; CII, confidence interval lower limit; Clu, confidence interval upper limit.

CNS area(log)	est CON	CII CON	Clu CON	est VIB	CII VIB	Clu VIB	est VIS	CII VIS	Clu VIS	est VISVIB	CII VISVIB	Clu VISVIB
<b>AM1</b>	6.936	<b>6.914</b>	<b>6.959</b>	6.793	<b>6.704</b>	<b>6.882</b>	6.803	6.667	6.938	6.875	6.796	6.953
<b>AM2</b>	6.762	6.725	6.798	6.699	6.636	6.763	6.729	6.654	6.804	6.778	6.730	6.826
<b>SecVis1</b>	7.297	7.205	7.388	7.265	7.170	7.360	7.262	7.166	7.359	7.336	7.274	7.399
<b>SecVis2</b>	6.889	6.843	6.936	6.887	6.851	6.923	6.844	6.776	6.912	6.925	6.884	6.965
<b>AB</b>	6.513	6.467	6.559	6.501	6.467	6.536	6.500	6.470	6.531	6.533	6.508	6.557
<b>MB</b>	6.878	6.857	6.900	6.893	6.868	6.918	6.862	6.821	6.902	6.905	6.886	6.925
<b>PdN</b>	6.733	6.679	6.787	6.703	6.612	6.793	6.709	6.620	6.797	6.736	6.696	6.776
<b>ChN</b>	6.599	<b>6.553</b>	<b>6.645</b>	6.454	<b>6.398</b>	<b>6.509</b>	6.451	<b>6.401</b>	<b>6.500</b>	6.533	6.461	6.605
<b>LegN</b>	7.793	7.762	7.823	7.745	7.713	7.776	7.775	7.740	7.810	7.804	7.775	7.833
<b>OpN</b>	7.271	<b>7.229</b>	<b>7.314</b>	7.229	7.177	7.282	7.169	<b>7.132</b>	<b>7.207</b>	7.220	7.186	7.254
<b>ROCNS</b>	8.053	8.012	8.094	8.031	8.003	8.059	8.035	8.002	8.067	8.092	8.076	8.109
<b>Cortex</b>	8.023	7.996	8.050	8.025	7.998	8.052	7.981	7.938	8.023	8.054	8.017	8.091
<b>CNS</b>	8.411	8.386	8.436	8.373	<b>8.347</b>	<b>8.399</b>	8.379	8.344	8.414	8.431	<b>8.409</b>	<b>8.452</b>

**Table 2.** Coefficient (est), standard error (S.E.), Wald statistics, p-value and R<sup>2</sup>-value for body size (prosoma volume) of *M. muscosa*.

<b>CNS area(log)</b>	<b>est body size sl.</b>	<b>S.E. body size sl.</b>	<b>Wald stats body size sl.</b>	<b>p-value body size sl.</b>	<b>R<sup>2</sup></b>
<b>AM1</b>	0.624	0.101	38.454	<b>&lt;0.001</b>	0.363
<b>AM2</b>	0.559	0.076	54.817	<b>&lt;0.001</b>	0.644
<b>SecVis1</b>	0.532	0.092	33.472	<b>&lt;0.001</b>	0.469
<b>SecVis2</b>	0.708	0.067	110.714	<b>&lt;0.001</b>	0.729
<b>AB</b>	0.373	0.066	32.283	<b>&lt;0.001</b>	0.543
<b>MB</b>	0.438	0.028	242.913	<b>&lt;0.001</b>	0.662
<b>PdN</b>	0.710	0.095	55.568	<b>&lt;0.001</b>	0.737
<b>ChN</b>	0.735	0.097	57.688	<b>&lt;0.001</b>	0.497
<b>LegN</b>	0.643	0.052	155.094	<b>&lt;0.001</b>	0.863
<b>OpN</b>	0.503	0.079	40.365	<b>&lt;0.001</b>	0.594
<b>ROCNS</b>	0.553	0.042	170.755	<b>&lt;0.001</b>	0.844
<b>Cortex</b>	0.670	0.064	110.090	<b>&lt;0.001</b>	0.754
<b>CNS</b>	0.579	0.034	298.745	<b>&lt;0.001</b>	0.863

**Table 3.** Mean and 95% confidence interval (CI) of CNS areas (neuropils, cortex and CNS) for each group in *P. tepidariorum*. est, mean CI; CIl, confidence interval lower limit; Clu, confidence interval upper limit.

CNS area(log)	est CON	Cil CON	Clu CON	est VIB	Cil VIB	Clu VIB	est VIS	Cil VIS	Clu VIS	est VISVIB	Cil VISVIB	Clu VISVIB
PrincVis	5.669	5.630	5.707	5.575	5.494	5.657	5.612	5.546	5.678	5.657	5.604	5.710
SecVis	5.279	5.164	5.395	5.288	5.251	5.324	5.338	5.229	5.448	5.397	5.299	5.494
AB	6.207	6.187	6.228	6.194	6.163	6.225	6.218	6.200	6.235	6.230	6.200	6.261
PdN	6.416	6.348	6.484	6.460	6.420	6.500	6.439	6.389	6.489	6.421	6.384	6.458
ChN	6.085	6.000	6.170	6.046	5.966	6.125	6.132	6.071	6.193	6.041	5.934	6.148
LegN	7.744	7.734	7.753	7.756	7.731	7.781	7.745	7.729	7.761	7.743	7.726	7.761
OpN	7.104	7.070	7.139	7.099	7.061	7.136	7.106	7.080	7.132	7.143	7.116	7.170
ROCNS	7.791	7.779	7.803	7.787	7.770	7.804	7.781	7.762	7.801	7.794	7.767	7.822
Cortex	7.518	7.472	7.564	7.536	7.514	7.558	7.556	7.518	7.595	7.536	7.504	7.569
CNS	8.226	8.215	8.237	8.234	8.216	8.253	8.233	8.218	8.248	8.238	8.220	8.255

**Table 4.** Coefficient (est), standard error (S.E.), Wald statistics, p-value and R<sup>2</sup>-value for body size (prosoma volume) of *P. tepidariorum*.

CNS area(log)	est body size sl.	S.E. body size sl.	Wald stats body size sl.	p-value body size sl.	R <sup>2</sup>
PrincVis	0.366	0.179	4.179	<b>0.041</b>	0.185
SecVis	0.988	0.260	14.398	<b>&lt;0.001</b>	0.159
AB	0.127	0.090	1.978	0.160	0.161
PdN	0.179	0.117	2.341	0.126	0.079
ChN	1.145	0.205	31.350	<b>&lt;0.001</b>	0.325
LegN	0.465	0.056	68.801	<b>&lt;0.001</b>	0.692
OpN	0.287	0.080	12.986	<b>&lt;0.001</b>	0.273
ROCNS	0.225	0.053	17.790	<b>&lt;0.001</b>	0.396
Cortex	0.188	0.068	7.658	<b>0.006</b>	0.043
CNS	0.281	0.050	31.677	<b>&lt;0.001</b>	0.517

**Table 5.** Allometric scaling relationships of neuropils in *Marpissa muscosa*. Bold numbers indicate significant differences. LR, likelihood ratio statistic; Tstats, Test Statistics; Wald, Wald statistics.

<b>AM1 (ROCNS)</b>						
Treatments	Scaling slope $\beta$		Intercept $\alpha$		Major axis shift	
	LR	P	Wald	P	Wald	P
	1.685	0.640	12.11	<b>0.007</b>	3.781	0.286
	T stats	P	T stats	P	T stats	P
CON-VIB	0.042	0.838	4.253	<b>0.039</b>	0.197	0.657
CON-VIS	1.423	0.233	9.423	<b>0.002</b>	3.594	0.058
CON-VISVIB	0.849	0.356	8.442	<b>0.004</b>	0.841	0.359
VIB-VIS	0.448	0.503	0.200	0.655	1.978	0.159
VIB-VISVIB	0.215	0.643	0.028	0.868	0.118	0.731
VIS-VISVIB	0.170	0.680	1.140	0.286	1.292	0.256

<b>AM2 (ROCNS)</b>						
Treatments	Scaling slope $\beta$		Intercept $\alpha$		Major axis shift	
	LR	P	Wald	P	Wald	P
	1.523	0.677	0.817	0.845	4.285	0.232
	T stats	P	T stats	P	T stats	P
CON-VIB	0.188	0.664	0.086	0.770	1.426	0.232
CON-VIS	1.434	0.231	0.773	0.380	3.942	<b>0.047</b>
CON-VISVIB	0.894	0.344	0.083	0.773	2.142	0.143
VIB-VIS	0.357	0.550	0.263	0.608	1.014	0.314
VIB-VISVIB	0.157	0.692	0.022	0.881	0.055	0.814
VIS-VISVIB	0.134	0.714	0.511	0.475	0.720	0.396

<b>SecVis1 (ROCNS)</b>						
Treatments	Scaling slope $\beta$		Intercept $\alpha$		Major axis shift	
	LR	P	Wald	P	Wald	P
	1.867	0.600	2.496	0.476	5.574	0.134
	T stats	P	T stats	P	T stats	P
CON-VIB	0.205	0.651	0.054	0.815	2.548	0.110
CON-VIS	0.787	0.375	1.848	0.174	4.202	<b>0.040</b>
CON-VISVIB	0.050	0.823	0.004	0.951	3.366	0.066
VIB-VIS	0.101	0.750	1.729	0.188	0.751	0.386
VIB-VISVIB	0.158	0.691	0.015	0.902	0.044	0.834
VIS-VISVIB	1.623	0.203	2.350	0.125	0.426	0.513



<b>SecVis2 (ROCNS)</b>						
Treatments	Scaling slope $\beta$		Intercept $\alpha$		Major axis shift	
	LR	P	Wald	P	Wald	P
	1.963	0.580	3.223	0.358	5.666	0.129
Treatments	T stats	P	T stats	P	T stats	P
CON-VIB	0.327	0.567	0.164	0.685	2.758	0.097
CON-VIS	0.001	0.980	0.767	0.381	5.386	<b>0.020</b>
CON-VISVIB	0.359	0.549	0.565	0.452	2.101	0.147
VIB-VIS	0.390	0.532	2.082	0.149	0.941	0.332
VIB-VISVIB	1.432	0.231	0.548	0.459	0.066	0.797
VIS-VISVIB	0.898	0.343	1.690	0.194	1.523	0.217

<b>AB (ROCNS)</b>						
Treatments	Scaling slope $\beta$		Intercept $\alpha$		Major axis shift	
	LR	P	Wald	P	Wald	P
	2.088	0.554	2.669	0.445	5.277	0.152
Treatments	T stats	P	T stats	P	T stats	P
CON-VIB	1.412	0.235	0.459	0.498	2.603	0.107
CON-VIS	0.327	0.567	0.568	0.451	4.613	<b>0.032</b>
CON-VISVIB	0.001	0.988	1.116	0.291	1.574	0.210
VIB-VIS	0.285	0.593	1.356	0.244	1.248	0.264
VIB-VISVIB	1.440	0.230	1.156	0.282	0.232	0.630
VIS-VISVIB	0.316	0.574	0.002	0.963	2.166	0.141

<b>MB (ROCNS)</b>						
Treatments	Scaling slope $\beta$		Intercept $\alpha$		Major axis shift	
	LR	P	Wald	P	Wald	P
	2.805	0.423	6.738	0.081	5.534	0.137
Treatments	T stats	P	T stats	P	T stats	P
CON-VIB	0.028	0.866	0.000	0.989	3.407	0.065
CON-VIS	0.146	0.702	1.161	0.281	4.376	<b>0.036</b>
CON-VISVIB	1.083	0.298	4.974	<b>0.026</b>	2.361	0.124
VIB-VIS	0.392	0.531	1.166	0.280	0.592	0.442
VIB-VISVIB	2.017	0.155	3.460	0.063	0.113	0.737
VIS-VISVIB	0.676	0.411	0.169	0.681	1.113	0.291

<b>ChN (ROCNS)</b>						
Treatments	Scaling slope $\beta$		Intercept $\alpha$		Major axis shift	
	LR	P	Wald	P	Wald	P
	9.061	<b>0.028</b>	—	—	—	—
Treatments	T stats	P	T stats	P	T stats	P
CON-VIB	0.173	0.677	—	—	—	—
CON-VIS	0.508	0.476	—	—	—	—
CON-VISVIB	3.175	0.075	—	—	—	—
VIB-VIS	1.634	0.201	—	—	—	—
VIB-VISVIB	5.920	<b>0.015</b>	—	—	—	—
VIS-VISVIB	1.758	0.185	—	—	—	—

<b>PdN (ROCNS)</b>						
	Scaling slope $\beta$		Intercept $\alpha$		Major axis shift	
	LR	P	Wald	P	Wald	P
	3.645	0.302	4.347	0.226	6.286	0.098
Treatments	T stats	P	T stats	P	T stats	P
CON-VIB	1.077	0.299	0.284	0.594	2.641	0.104
CON-VIS	2.809	0.094	0.002	0.968	5.403	<b>0.020</b>
CON-VISVIB	3.619	0.057	2.376	0.123	1.934	0.164
VIB-VIS	0.128	0.720	0.279	0.597	0.843	0.358
VIB-VISVIB	0.317	0.573	2.193	0.139	0.170	0.679
VIS-VISVIB	0.192	0.661	0.217	0.641	1.863	0.172

<b>LegN (ROCNS)</b>						
	Scaling slope $\beta$		Intercept $\alpha$		Major axis shift	
	LR	P	Wald	P	Wald	P
	6.62	0.085	3.076	0.380	5.248	0.154
Treatments	T stats	P	T stats	P	T stats	P
CON-VIB	0.963	0.326	0.045	0.831	1.572	0.210
CON-VIS	1.936	0.164	1.216	0.270	5.235	<b>0.022</b>
CON-VISVIB	1.236	0.266	2.160	0.142	1.400	0.237
VIB-VIS	4.824	<b>0.028</b>	—	—	—	—
VIB-VISVIB	3.662	0.056	0.556	0.456	0.013	0.909
VIS-VISVIB	0.012	0.912	1.047	0.306	1.936	0.164

<b>OpN (ROCNS)</b>						
	Scaling slope $\beta$		Intercept $\alpha$		Major axis shift	
	LR	P	Wald	P	Wald	P
	5.818	0.121	8.189	<b>0.042</b>	2.098	0.552
Treatments	T stats	P	T stats	P	T stats	P
CON-VIB	5.503	<b>0.019</b>	—	—	—	—
CON-VIS	0.957	0.328	7.286	<b>0.006</b>	1.894	0.169
CON-VISVIB	1.318	0.251	4.262	<b>0.039</b>	0.410	0.522
VIB-VIS	4.226	<b>0.040</b>	—	—	—	—
VIB-VISVIB	2.741	0.098	3.194	0.074	0.567	0.451
VIS-VISVIB	0.171	0.679	0.838	0.360	0.991	0.319

<b>Cortex (body size)</b>						
	Scaling slope $\beta$		Intercept $\alpha$		Major axis shift	
	LR	P	Wald	P	Wald	P
	3.472	0.324	5.251	0.154	7.931	<b>0.047</b>
Treatments	T stats	P	T stats	P	T stats	P
CON-VIB	0.027	0.869	0.500	0.479	2.701	0.100
CON-VIS	1.489	0.222	0.787	0.375	6.917	<b>0.008</b>
CON-VISVIB	0.249	0.618	0.151	0.698	1.441	0.230
VIB-VIS	1.972	0.160	0.704	0.401	0.558	0.454
VIB-VISVIB	0.095	0.758	1.902	0.168	0.505	0.477
VIS-VISVIB	3.483	0.062	4.451	<b>0.035</b>	2.949	0.086

<b>CNS (body size)</b>						
Treatments	Scaling slope $\beta$		Intercept $\alpha$		Major axis shift	
	LR	P	Wald	P	Wald	P
	1.893	0.595	8.459	<b>0.037</b>	6.946	0.074
	T stats	P	T stats	P	T stats	P
CON-VIB	1.517	0.218	4.427	<b>0.035</b>	2.899	0.089
CON-VIS	0.680	0.410	5.322	<b>0.021</b>	6.341	<b>0.012</b>
CON-VISVIB	0.093	0.760	0.084	0.772	1.145	0.284
VIB-VIS	0.372	0.542	0.007	0.934	1.290	0.256
VIB-VISVIB	0.794	0.373	3.388	0.066	0.541	0.462
VIS-VISVIB	0.138	0.710	3.486	0.062	3.193	0.074

**Table 6.** Allometric scaling relationships of neuropils in *Parasteatoda tepidariorum*. LR, likelihood ratio statistic; Tstats, Test Statistics; Wald, Wald statistics.

<b>PrincVis (ROCNS)</b>						
Treatments	Scaling slope $\beta$		Intercept $\alpha$		Major axis shift	
	LR	P	Wald	P	Wald	P
	3.029	0.387	2.035	0.565	4.693	0.196
	T stats	P	T stats	P	T stats	P
CON-VIB	0.003	0.959	0.377	0.539	0.505	0.477
CON-VIS	0.047	0.828	0.259	0.611	4.468	<b>0.034</b>
CON-VISVIB	1.425	0.233	0.009	0.923	0.129	0.719
VIB-VIS	0.065	0.798	2.228	0.135	0.833	0.361
VIB-VISVIB	1.328	0.249	0.797	0.372	0.151	0.697
VIS-VISVIB	2.464	0.116	0.210	0.646	1.827	0.176

<b>SecVis (ROCNS)</b>						
Treatments	Scaling slope $\beta$		Intercept $\alpha$		Major axis shift	
	LR	P	Wald	P	Wald	P
	1.603	0.659	1.565	0.667	1.809	0.613
	T stats	P	T stats	P	T stats	P
CON-VIB	0.022	0.883	0.061	0.804	0.008	0.928
CON-VIS	1.192	0.275	1.040	0.308	0.950	0.330
CON-VISVIB	0.019	0.888	0.593	0.441	0.869	0.351
VIB-VIS	1.277	0.258	0.871	0.350	0.688	0.407
VIB-VISVIB	0.000	0.994	0.725	0.394	0.233	0.629
VIS-VISVIB	1.044	0.307	0.102	0.749	1.853	0.173

<b>AB (ROCNS)</b>						
Treatments	Scaling slope $\beta$		Intercept $\alpha$		Major axis shift	
	LR	P	Wald	P	Wald	P
	0.963	0.810	7.092	0.069	1.148	0.765
	T stats	P	T stats	P	T stats	P
CON-VIB	0.601	0.438	0.736	0.391	0.159	0.690
CON-VIS	0.033	0.855	0.902	0.342	0.738	0.390
CON-VISVIB	0.187	0.665	0.713	0.398	0.013	0.910
VIB-VIS	0.342	0.558	4.625	<b>0.031</b>	0.125	0.723
VIB-VISVIB	0.304	0.581	4.654	<b>0.031</b>	0.161	0.688
VIS-VISVIB	0.053	0.818	0.255	0.614	0.694	0.405

<b>ChN (ROCNS)</b>						
	Scaling slope $\beta$		Intercept $\alpha$		Major axis shift	
	LR	P	Wald	P	Wald	P
	0.651	0.884	2.223	0.527	0.918	0.821
Treatments	T stats	P	T stats	P	T stats	P
CON-VIB	0.337	0.561	0.019	0.890	0.032	0.858
CON-VIS	0.540	0.462	1.005	0.316	0.811	0.368
CON-VISVIB	0.529	0.467	0.144	0.704	0.242	0.623
VIB-VIS	0.032	0.857	1.777	0.182	0.427	0.513
VIB-VISVIB	0.039	0.843	0.085	0.771	0.039	0.843
VIS-VISVIB	0.001	0.976	1.219	0.270	0.321	0.571

<b>PdN (ROCNS)</b>						
	Scaling slope $\beta$		Intercept $\alpha$		Major axis shift	
	LR	P	Wald	P	Wald	P
	1.912	0.591	1.518	0.678	1.716	0.633
Treatments	T stats	P	T stats	P	T stats	P
CON-VIB	0.819	0.365	0.601	0.438	0.317	0.573
CON-VIS	0.212	0.645	1.088	0.297	0.576	0.448
CON-VISVIB	1.774	0.183	0.033	0.855	0.012	0.913
VIB-VIS	0.138	0.710	0.001	0.974	1.616	0.204
VIB-VISVIB	0.142	0.707	1.159	0.282	0.861	0.353
VIS-VISVIB	0.540	0.462	0.363	0.547	0.708	0.340

<b>LegN (ROCNS)</b>						
	Scaling slope $\beta$		Intercept $\alpha$		Major axis shift	
	LR	P	Wald	P	Wald	P
	7.775	0.051	5.45	0.142	5.596	0.132
Treatments	T stats	P	T stats	P	T stats	P
CON-VIB	5.832	<b>0.016</b>	—	—	—	—
CON-VIS	0.111	0.739	0.132	0.716	2.578	0.108
CON-VISVIB	0.856	0.355	0.018	0.893	0.035	0.851
VIB-VIS	2.008	0.156	0.251	0.616	4.551	<b>0.033</b>
VIB-VISVIB	7.019	<b>0.008</b>	—	—	—	—
VIS-VISVIB	1.006	0.316	0.000	0.998	1.975	0.160

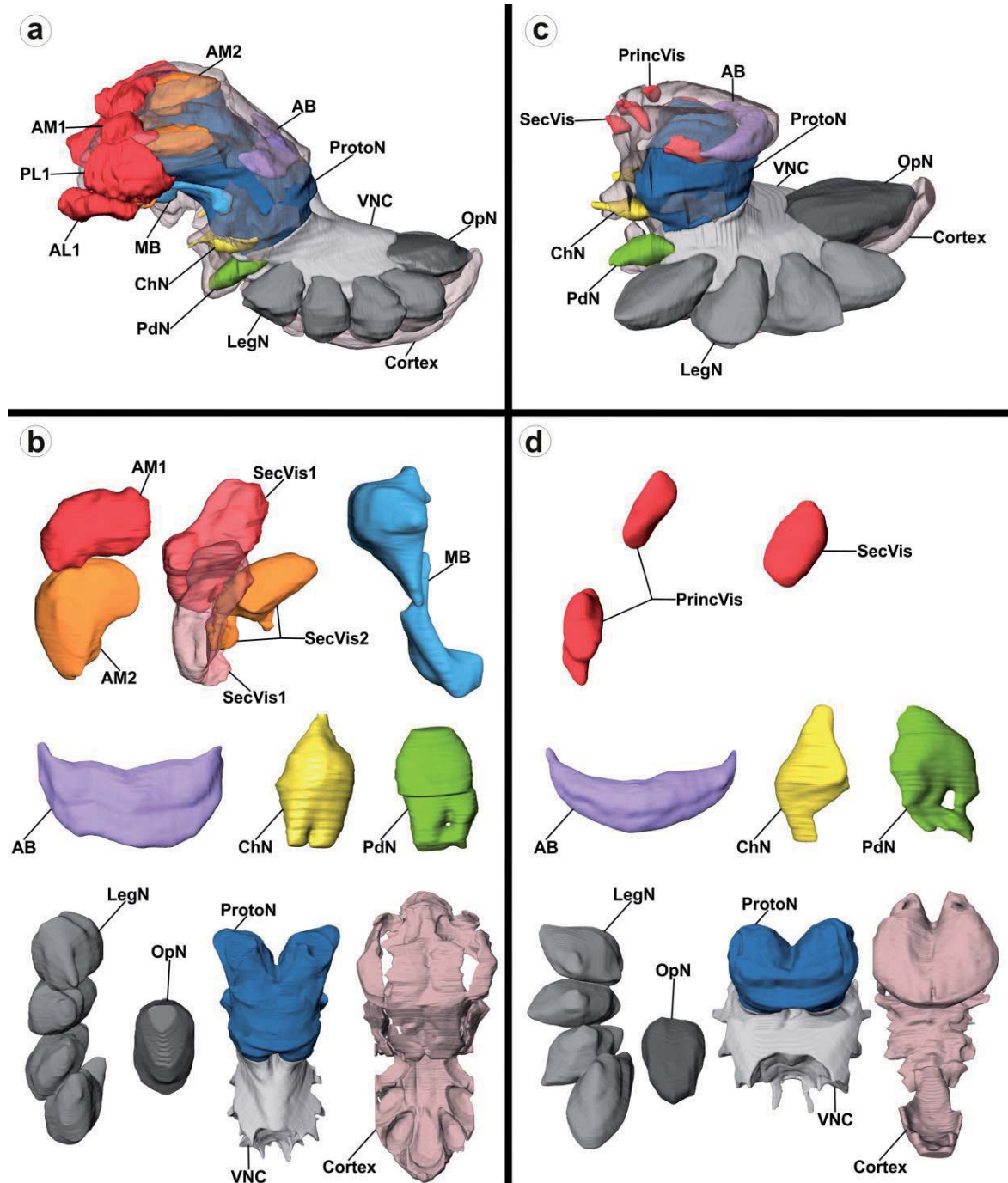
<b>OpN (ROCNS)</b>						
	Scaling slope $\beta$		Intercept $\alpha$		Major axis shift	
	LR	P	Wald	P	Wald	P
	2.969	0.396	2.576	0.462	7.667	0.053
Treatments	T stats	P	T stats	P	T stats	P
CON-VIB	0.216	0.642	0.006	0.935	0.001	0.971
CON-VIS	1.235	0.266	3.119	0.077	0.133	0.715
CON-VISVIB	0.101	0.750	1.343	0.246	0.518	0.472
VIB-VIS	2.953	0.086	0.289	0.591	1.224	0.269
VIB-VISVIB	1.009	0.315	1.822	0.177	0.295	0.587
VIS-VISVIB	1.244	0.265	4.820	<b>0.028</b>	0.949	0.330

<b>Cortex (body size)</b>						
Treatments	Scaling slope $\beta$		Intercept $\alpha$		Major axis shift	
	LR	P	Wald	P	Wald	P
	4.35	0.226	1.704	0.636	0.622	0.891
	T stats	P	T stats	P	T stats	P
CON-VIB	1.996	0.158	0.024	0.877	0.085	0.771
CON-VIS	0.367	0.544	0.710	0.400	0.190	0.663
CON-VISVIB	0.236	0.627	0.111	0.739	0.003	0.956
VIB-VIS	0.913	0.339	0.716	0.397	0.288	0.591
VIB-VISVIB	3.830	0.051	0.019	0.890	0.005	0.942
VIS-VISVIB	1.334	0.248	1.406	0.236	0.673	0.412

<b>CNS (body size)</b>						
Treatments	Scaling slope $\beta$		Intercept $\alpha$		Major axis shift	
	LR	P	Wald	P	Wald	P
	2.046	0.563	0.092	0.993	2.205	0.531
	T stats	P	T stats	P	T stats	P
CON-VIB	1.303	0.254	0.007	0.932	0.005	0.942
CON-VIS	0.198	0.656	0.045	0.832	1.722	0.189
CON-VISVIB	1.131	0.287	0.012	0.912	0.000	0.986
VIB-VIS	0.778	0.378	0.098	0.754	0.729	0.393
VIB-VISVIB	0.050	0.824	0.001	0.977	0.004	0.950
VIS-VISVIB	0.618	0.432	0.038	0.846	1.931	0.164

# Figures



**Figure 1** MicroCT reconstructions of the cortex and all CNS neuropils in *M. muscosa* (a,b) and *P. tepidariorum* (c,d). (a,c) Overview of the CNS with all reconstructed structures highlighted in different colors. Cortex transparent for clarity. (b,d) All individual neuropils in dorsal view, only the left neuropil is shown for bilaterally paired neuropils. Abbreviations: AB, arcuate body; AM1, first-order visual neuropil of the anterior median eyes; AM2, second-order visual neuropil of the anterior median eyes; ChN, cheliceral neuropil; CNS, central nervous system (sum of all reconstructed neuropils); LegN, leg neuropils; MB, mushroom bodies; OpN, opisthosomal neuropil; PdN, pedipalpal neuropil; PrincVis, visual neuropil of the principal eyes; SecVis, visual neuropil of the secondary eyes; SecVis1, first-order visual neuropils of all secondary eyes; SecVis2, second-order visual neuropils of all secondary eyes.



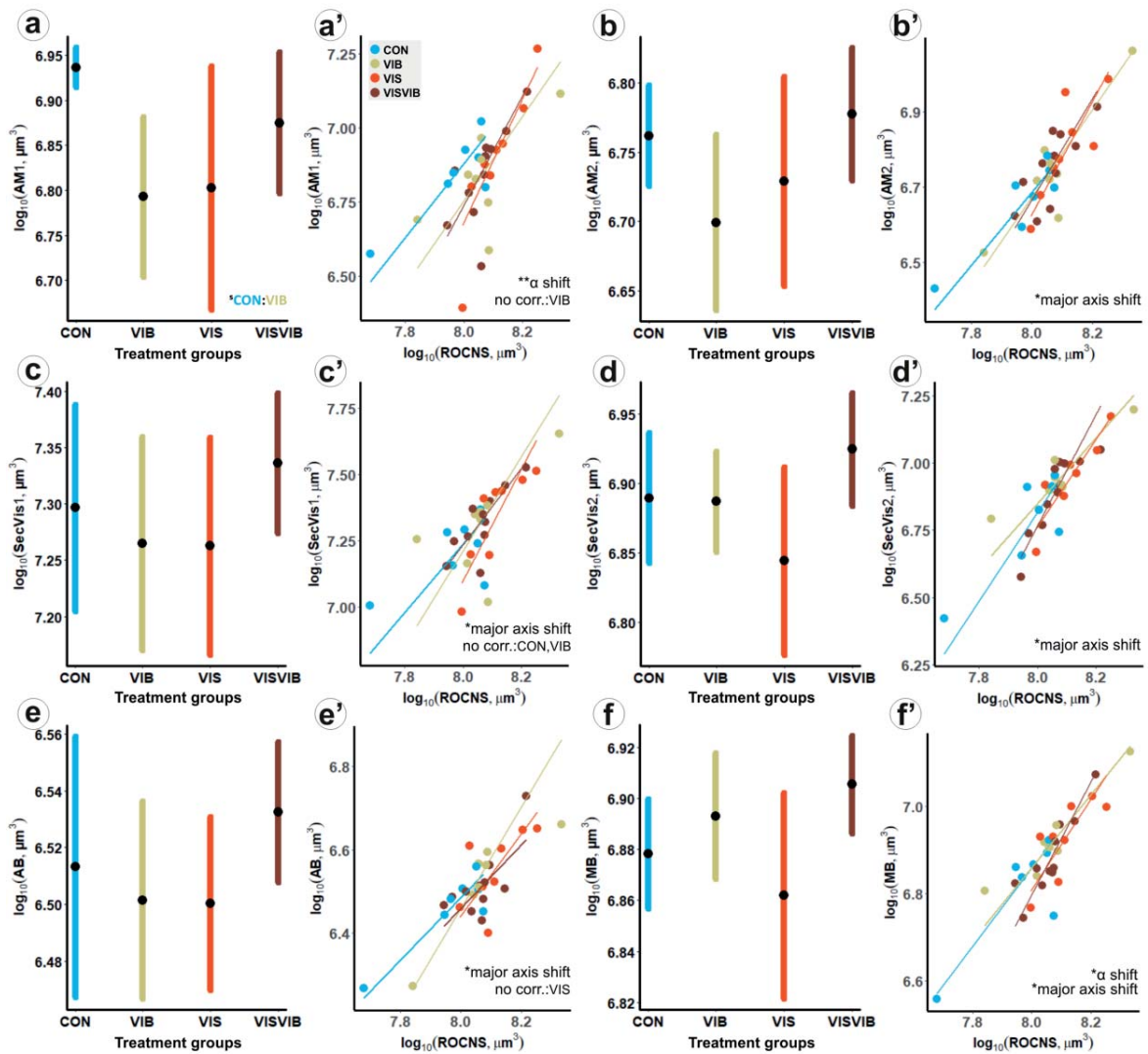


**Figure 2** Confidence intervals (a, b, c, d, e, f) and allometric scaling relationship (a', b', c', d', e', f') of neuropil volumes across treatments in *M. muscosa*. Significant differences in neuropil volume between treatment groups are indicated by an <sup>§</sup>. Significant differences in slope ( $\beta$  shift), intercept ( $\alpha$  shift) and major axis shift are indicated with asterisks (\* $<0.05$ , \*\* $<0.01$ , \*\*\* $<0.001$ ). Cases in which correlations between volume of neuropil and allometric control were not significant ( $R^2 < 0.5$ ) are highlighted (no corr.). Abbreviations: AB, arcuate body; AM1, first-order visual neuropil of the anterior median eyes; AM2, second-order visual neuropil of the anterior median eyes; ChN, cheliceral neuropil; CNS, central nervous system (sum of all reconstructed neuropils); LegN, leg neuropils; MB, mushroom bodies; OpN, opisthosomal neuropil; PdN, pedipalpal neuropil; SecVis1, first-order visual neuropils of all secondary eyes; SecVis2, second-order visual neuropils of all secondary eyes.

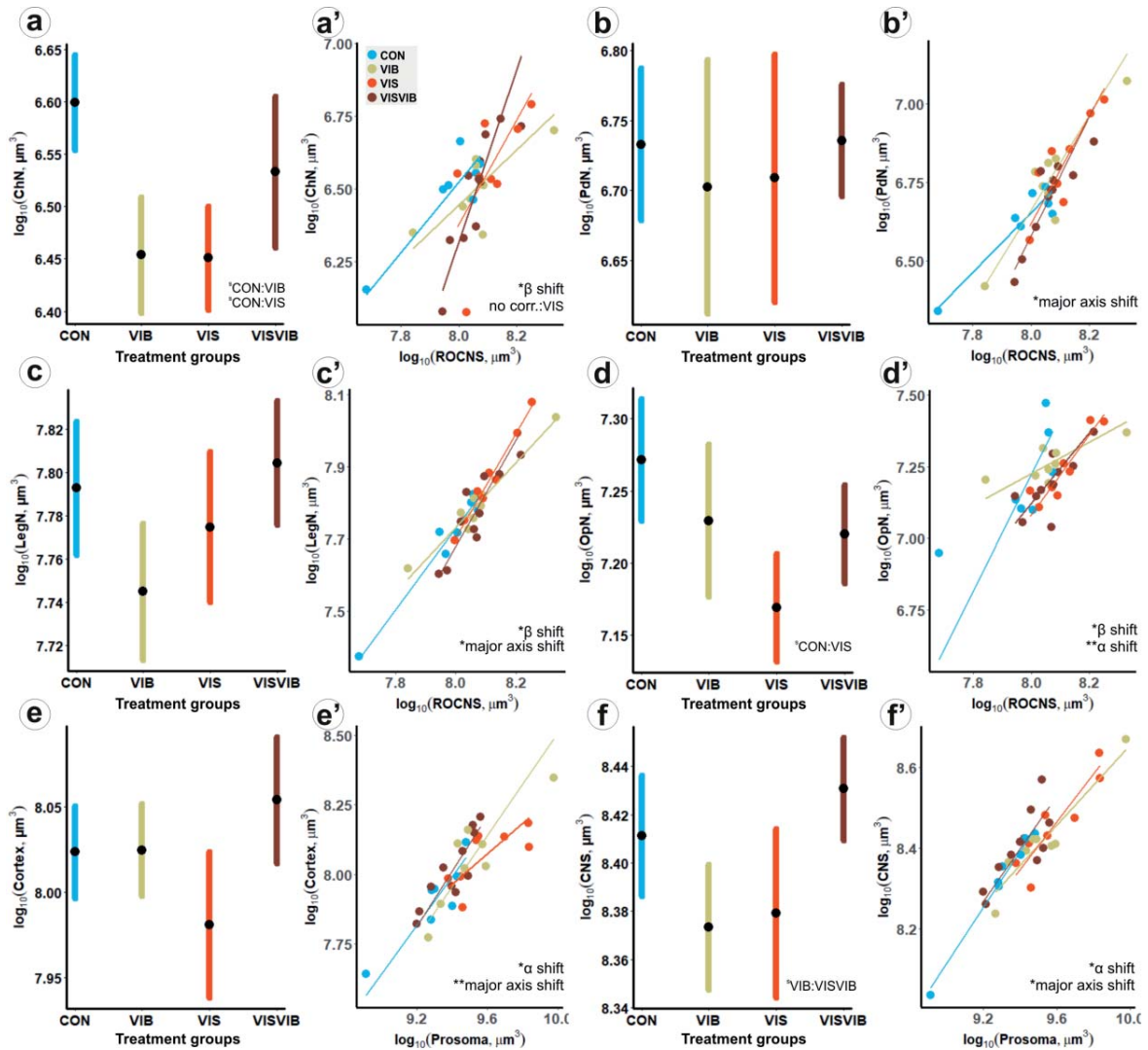


**Figure 3** Confidence intervals (a, b, c, d, e, f) and allometric scaling relationship (a', b', c', d', e', f') of neuropil volumes across treatments in *M. muscosa*. Significant differences in neuropil volume between treatment groups are indicated by an <sup>5</sup>. Significant differences in slope ( $\beta$  shift), intercept ( $\alpha$  shift) and major axis shift are indicated with asterisks (\* $<0.05$ , \*\* $<0.01$ , \*\*\* $<0.001$ ). Cases in which correlations between volume of neuropil and allometric control were not significant ( $R^2 < 0.5$ ) are highlighted (no corr.). Abbreviations: AB, arcuate body; AM1, first-order visual neuropil of the anterior median eyes; AM2, second-order visual neuropil of the anterior median eyes; ChN, cheliceral neuropil; CNS, central nervous system (sum of all reconstructed neuropils); LegN, leg neuropils; MB, mushroom bodies; OpN, opisthosomal neuropil; PdN, pedipalpal neuropil; SecVis1, first-order visual neuropils of all secondary eyes; SecVis2, second-order visual neuropils of all secondary eyes.

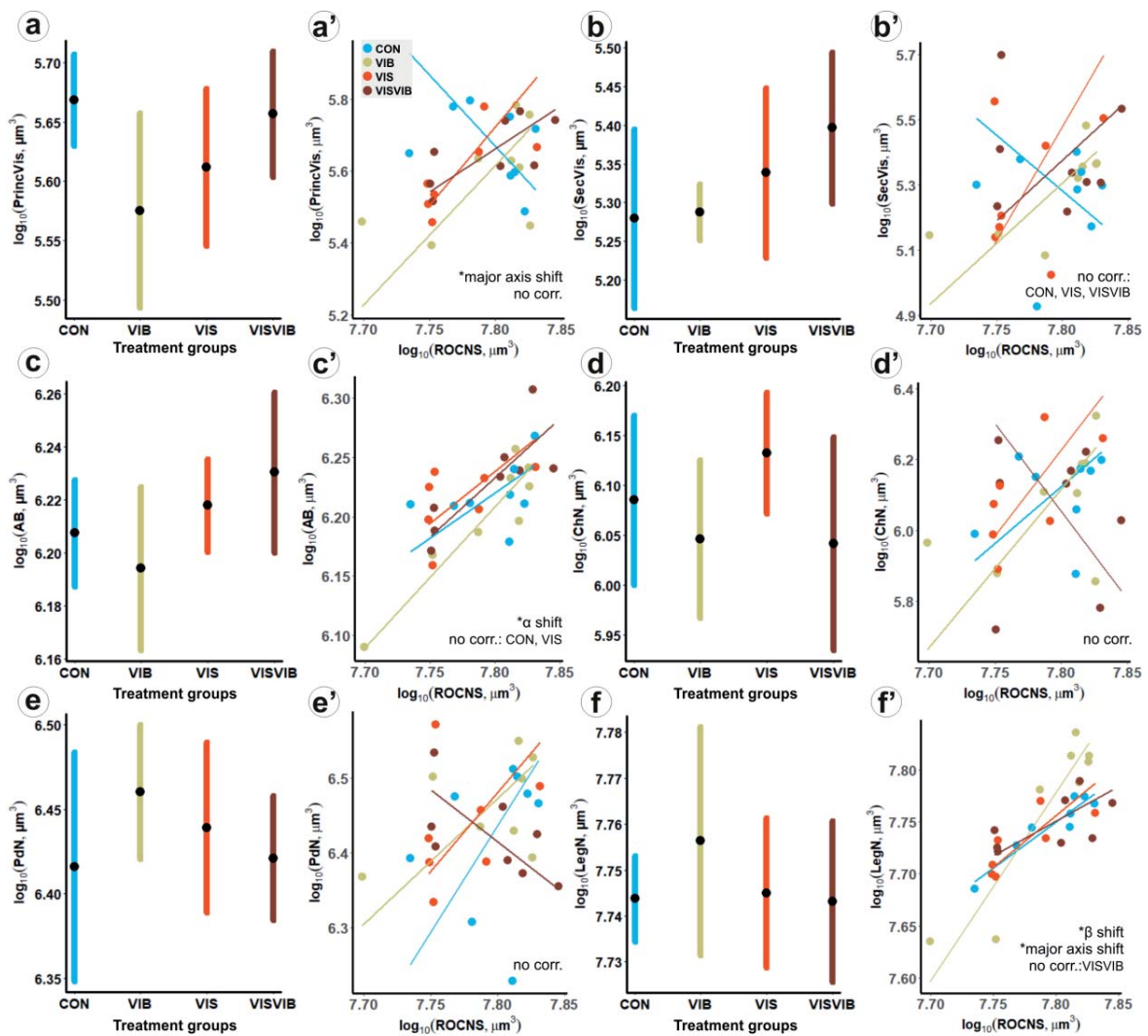


**Figure 4** Confidence intervals (a, b, c, d, e, f) and allometric scaling relationship (a', b', c', d', e', f') of neuropil volumes across treatments in *P. tepidariorum*. Significant differences in neuropil volume between treatment groups are indicated by an <sup>5</sup>. Significant differences in slope ( $\beta$  shift), intercept ( $\alpha$  shift) and major axis shift are indicated with asterisks (\* $<0.05$ , \*\* $<0.01$ , \*\*\* $<0.001$ ). Cases in which correlations between volume of neuropil and allometric control were not significant ( $R^2 < 0.5$ ) are highlighted (no corr.). Abbreviations: AB, arcuate body; ChN, cheliceral neuropil; CNS, central nervous system (sum of all reconstructed neuropils); LegN, leg neuropils; MB, mushroom bodies; OpN, opisthosomal neuropil; PdN, pedipalpal neuropil; PrincVis, visual neuropil of the principal eyes; SecVis, visual neuropil of the secondary eyes.

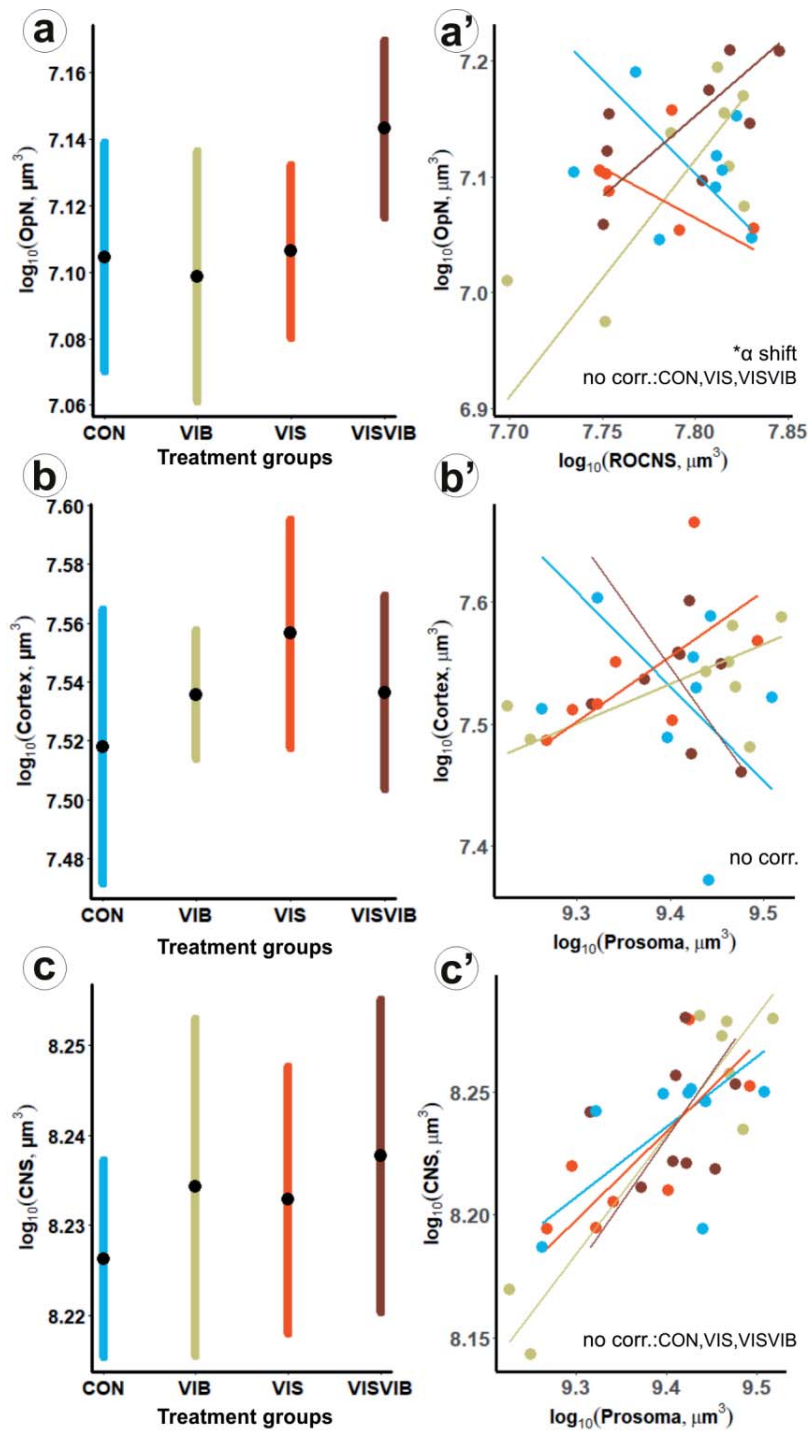


**Figure 5** Confidence intervals (a, b, c) and allometric scaling relationship (a', b', c') of neuropil volumes across treatments in *P. tepidariorum*. Significant differences in neuropil volume between treatment groups are indicated by an <sup>§</sup>. Significant differences in slope ( $\beta$  shift), intercept ( $\alpha$  shift) and major axis shift are indicated with asterisks (\* $<0.05$ , \*\* $<0.01$ , \*\*\* $<0.001$ ). Cases in which correlations between volume of neuropil and allometric control were not significant ( $R^2 < 0.5$ ) are highlighted (no corr.).

Abbreviations: AB, arcuate body; ChN, cheliceral neuropil; CNS, central nervous system (sum of all reconstructed neuropils); LegN, leg neuropils; MB, mushroom bodies; OpN, opisthosomal neuropil; PdN, pedipalpal neuropil; PrincVis, visual neuropil of the principal eyes; SecVis, visual neuropil of the secondary eyes.

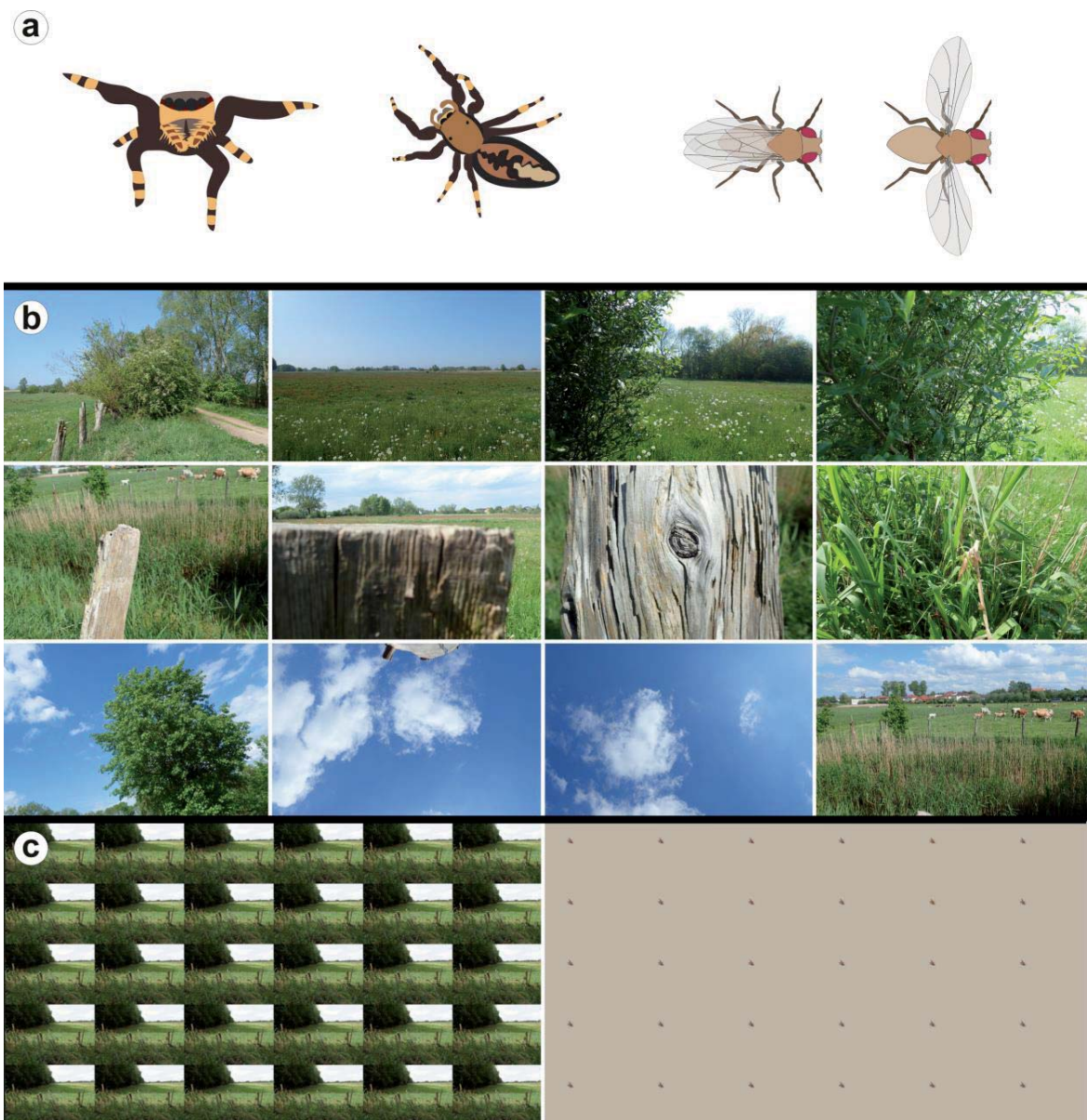


**Figure S1** Examples of visual stimuli used for video playback. (a) Drawings of jumping spiders and flies were prepared according to Menda et al. (2014) and used as individual frames in videos. (b) Examples of environmental images used for playback of still images with either 10 sec. or 1 min. intervals. (c) Examples of mosaic arrangement of videos as played to 30 individual spiders synchronously on 17'' monitors.

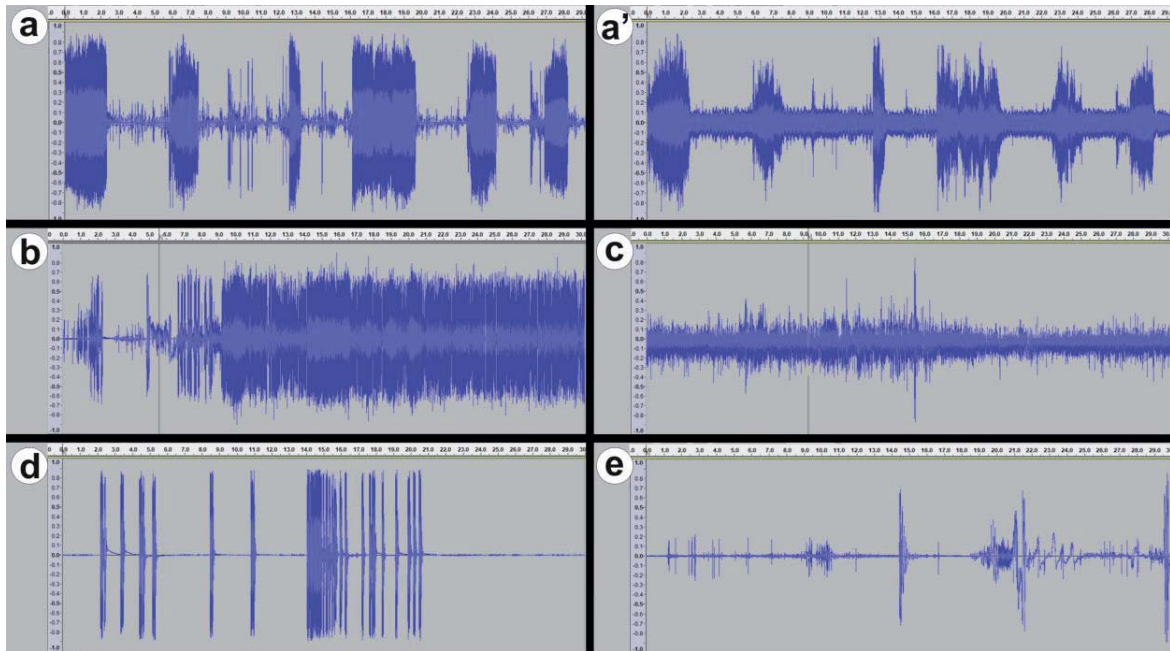


**Figure S2** Examples of vibratory stimuli used for vibration playback, waveform visualization with x axis showing the time in seconds and y axis the amplitude (0=silent, -1,+1 maximum noise). For better visibility, only the first 30 seconds of each recording are shown. (a) Waveform showing “*Calliphora* buzz” as recorded directly from the fly. (a’) “*Calliphora* buzz” control recorded from the base of the spider rearing box when played via a piezo-ceramic element shows similar pattern and amplitude to original recording. (b) Waveform showing “*Lucilia* buzz” vibration. (c) Waveform showing “*Drosophila* walking” vibration. (d) Waveform showing “Noise with regular amplitude” vibration. (e) Waveform showing “Noise with irregular amplitude” vibration.

### 3. Eigenständigkeitserklärung

Hiermit erkläre ich, dass diese Arbeit bisher von mir weder an der Mathematisch-Naturwissenschaftlichen Fakultät der Universität Greifswald noch einer anderen wissenschaftlichen Einrichtung zum Zwecke der Promotion eingereicht wurde.

Ferner erkläre ich, dass ich diese Arbeit selbstständig verfasst und keine anderen als die darin angegebenen Hilfsmittel und Hilfen benutzt und keine Textabschnitte eines Dritten ohne Kennzeichnung übernommen habe.

---

Philip O.M. Steinhoff

---

Datum (*Date*)



### 3.1 Anteile der Autoren an den zugrundeliegenden Publikationen

Hiermit erkläre ich, dass die in der folgenden Inhaltsübersicht mit meinem Namen gekennzeichneten Kapitel von mir selbständig verfasst worden sind:

<b>Abstract</b>	<b>Steinhoff, P.O.M.</b>
<b>1. Summary</b>	<b>Steinhoff, P.O.M.</b>
<b>2. Publications</b>	
<b>2.1 Individual differences in risk-taking affect foraging across different landscapes of fear</b>	<b>Steinhoff, P.O.M.;</b> Warfen, B., Voigt, S., Uhl, G., & Dammhahn, M.
<b>2.2 Visual pathways in the brain of the jumping spider <i>Marpissa muscosa</i></b>	<b>Steinhoff, P. O. M.,</b> Uhl, G., Harzsch, S., & Sombke, A.
<b>2.3 Comparative neuroanatomy of the central nervous system in stationary and cursorial hunting spiders</b>	<b>Steinhoff, P. O. M.,</b> Harzsch, S. & Uhl, G.
<b>2.4 Neuroplasticity in response to sensory enrichment and deprivation in a cursorial and a stationary hunting spider</b>	<b>Steinhoff, P. O. M.,</b> Mougnot, P. & Uhl, G.

Ich erkläre weiterhin, dass ich („POMS“) die im folgenden beschriebenen Teile derjenigen Kapitel, bei denen ich nicht Alleinautor bin, selbstständig verfasst habe:

#### 2.1 Individual differences in risk-taking affect foraging across different landscapes of fear

MD and **POMS** conceived and designed the study. **POMS**, SV and BW performed the behavioural tests and the video analysis. MD and **POMS** analysed the data, all authors interpreted the results. MD and **POMS** wrote the first draft. All authors contributed to the writing of the final manuscript. **POMS**, GU and MD obtained funding.

#### 2.2 Visual pathways in the brain of the jumping spider *Marpissa muscosa*

**POMS**, AS, and GU study concept and design. **POMS** acquisition of data. **POMS** and AS analysis and interpretation of data. **POMS** and AS wrote the manuscript. GU and SH contributed to the writing of the manuscript. GU, SH, and **POMS** obtained funding.

#### 2.3 Comparative neuroanatomy of the central nervous system in stationary and cursorial hunting spiders

**POMS** and GU study concept and design. **POMS** acquisition of data. **POMS** analysis and interpretation of data. **POMS** wrote the manuscript. GU and SH contributed to the writing of the manuscript. GU, SH, and **POMS** obtained funding.

#### **2.4 Complex patterns of neuroplasticity in response to sensory enrichment and deprivation in a cursorial and a stationary hunting spider**

**POMS** and GU study concept and design. **POMS** acquisition of data. **POMS** and PM analysis and interpretation of data. **POMS** wrote the manuscript. GU and PM contributed to the writing of the manuscript. GU and **POMS** obtained funding.

---

Philip O.M. Steinhoff

---

Datum (*Date*)

---

Prof. Dr. Gabriele Uhl

---

Datum (*Date*)

## 4. Curriculum Vitae

### Philip Otto Maria Steinhoff

Contact address: Hugo-Helfritz Straße 1, 17493 Greifswald  
 (+49) 01577/4712207  
 philipsteinhoff@gmail.com

Date & place of birth: 14.07.1990, Cologne

Nationality: German

### Professional experiences

---

04/2019 – aktuell      Doctoral researcher, General and Systematic Zoology, Zoological Institute and Museum, University of Greifswald

06/2015 – 11/2017      Research assistant at the Zoological Institute and Museum, University of Greifswald

### Education

---

04/2018 – aktuell      PhD Student at the Zoological Institute and Museum, University of Greifswald, Germany. Dissertation topic: *Foraging behavior, neuroanatomy and neuroplasticity in cursorial and stationary hunting spiders*

01/2018                  M.Sc.-Thesis *Anatomy and plasticity of higher integrating neuropils in a jumping spider (Salticidae, Arachnida)*

04/2015 – 01/2018      Master of Science, Biodiversity and Ecology at the University of Greifswald

04/2015                  B.Sc.-Thesis *Morphological investigations of the brain of the jumping spider *Marpissa muscosa* (Salticidae, Arachnida) by means of microCT analysis*

10/2011 – 04/2015      Bachelor of Science, Landscape Ecology and Nature Conservation at the University of Greifswald

### Work experience

---

since 2020	Reviewer for the citizen science project <i>Ebird</i> (section Germany)
since 2018	Reviewer for the journals <i>Frontiers in Zoology</i> and <i>Journal of Zoology</i>
2017-2021	Curation of the homepage and the social media accounts of the <i>General and Systematic Zoology</i> at the Zoological Institute of the University of Greifswald
since 2016	Reviewer for the journals <i>Zootaxa</i> and <i>International Dragonfly Fand Report</i>
11/2016 – 12/2016	Odonatological fieldwork in the Pulong Tau National Park and in the Gunong Mulu National Park in Borneo. Emphasis: Verbreitung, Taxonomy and Larval ecology of montane species.
06/2014 – 08/2014	Ornithological expedition of the Louisiana State University and Museum in the Gunong Mulu National Park in Borneo. Emphasis: Systematic recording and mapping of bird species along a latitudinal gradient.
03/2014 – 09/2014	Odonatological fieldwork in plantations of the province Bintulu, in the Kubah National Park and in the Gunong Mulu National Park in Borneo. Emphasis: Distribution, Taxonomy and Ecology unknown and little known Odonata species.
2010-2011	Work as a volunteer in the Phong Nha–Ke Bang Nature Conservation Project of the Cologne Zoo and the Frankfurt Zoological Society in Phong Nha, Vietnam
07/2009 – 08/2009	Work experience in the <i>Office for Ecological Research and Mapping Norbert Menke</i> in North Rhine-Westphalia. Emphasis: Ecological Mapping in the FFH-area Emsaue, Kreise Gütersloh and Warendorf.
2007 – 2009	Odonatological mappings for the <i>Libellenatlas NRW</i>

### Teaching experience

---

2021	Taking part in the production of DigiTib (Lernplattform Digitale Tierbestimmungsübungen, <a href="http://www.digitib.de">www.digitib.de</a> )
2020 & 2021	Teaching assistance in the Bachelor-course <i>Tierbestimmungsübungen</i>
07/2020 – 09/2021	Co-supervision of a Bachelor-thesis on the topic „Effects of different types of reward on the learning performance in the jumping spider

*Marpissa muscosa*

2019 & 2020	Teaching assistance in the Bachelor course <i>Großpraktikum Zoologie</i>
08/2018	Teaching assistance in the master-course <i>Animal Ecology</i>
04/2018 – 05/2019	Co-supervision of two bachelor theses on the topic “Behaviour in a landscape of fear and personality in the jumping spider <i>Marpissa muscosa</i> ”
2017 – 2019	Teaching assistance in the master-courses <i>Reproduction Biology &amp; Evolutionary Ecology</i>

**Scholarships, grants and awards**

---

07/2022	Lothar-Kämpfe publication price of the Zoological Institute and Museum of the University Greifswald
02/2020	RISE Scholarship of the German Academic Exchange Service (DAAD) for a self-developed scientific project, to be conducted by a student from Canada ( <i>practical was cancelled due to the Corona pandemic</i> )
10/2019	Price for the best article of the year 2018 in the <i>Journal of Zoology</i>
02/2019	Congress travel grant for the 21st International Congress of Arachnology (ICA) in Christchurch, New Zealand from <i>Laudier Histology</i>
10/2018	DZG-Award for an excellent master thesis with zoological focus at the University Greifswald (awarded by the German Zoological Society, DZG)
04/2018 – 04/2019	Bogislaw-Scholarship (PhD funding)
08/2017	Price for the 2nd best student talk at the 30th European Congress of Arachnology in Nottingham, UK
08/2017	Congress travel grant for the 30th European Congress of Arachnology in Nottingham, UK from the German Academic Scholarship Foundation ( <i>Studienstiftung des deutschen Volkes e.V.</i> )
03/2017	GdO Lopi-Award for the best student talk at the 36th annual meeting of the <i>Gesellschaft deutschsprachiger Odonatologen</i> (Society of German speaking odonatologists; GdO) in Berlin, Germany
11/2016	Research travel grant for odonatological fieldwork in Borneo from the German Academic Scholarship Foundation ( <i>Studienstiftung des</i>

	deutschen Volkes e.V.)
07/2016	Congress travel grant for the 20th International Congress of Arachnology (ICA) in Golden, USA from Laudier Histology
12/2015 – 09/2017 des	Scholarship, German Academic Scholarship Foundation (Studienstiftung des deutschen Volkes e.V.)
06/2015	Student grant from the organizing committee of the 29th European Congress of Arachnology in Brno, Czech Republic
03/2015	GdO Lopi-Award for the best student talk at the 34th annual meeting of the Gesellschaft deutschsprachiger Odonatologen (Society of german speaking odonatologists; GdO) in Braunschweig, Germany
03/2014 – 06/2014	Scholarship, German Academic Exchange Service (DAAD), PROMOS-Stipendium for conducting odonatological fieldwork in Borneo

### Special skills

---

Fremdsprachen:	Englisch (verhandlungssicher), Malaysisch & Vietnamesisch (Grandkenntnisse)
IT expertise:	Adobe Creative Suite, Corel, Geographic Information Systems (ArcGIS, QGIS), GIMP, Microsoft Office (Word, Excel, Powerpoint), R, Programming (TYPO3, Wordpress)
Memberships:	AK Libellen NRW, Biologische Station <i>Haus der Natur</i> im Rhein-Kreis Neuss, European Society of Arachnology, Gesellschaft deutschsprachiger Odonatologen, International Dragonfly Fund, International Society of Arachnology, Societas Internationalis Odonatologica, Zugvögel Grenzen überwinden e.V.
Interests:	Entomology, bird watching, nature conservation, writing texts, photography

### Publikationen

---

Dow, R. A.; Ahmad, R.; Butler, S. G.; Choong, C. Y.; Grinang, J.; Ng, Y. F.; Ngiam, R. W. J.; Reels, G. T.; **Steinhoff, P. O. M.** & Unggang, J. (2021): Previously unpublished Odonata records from Sarawak, Borneo, part VI: Miri Division including checklists for Niah, Lambir Hills, Loagan Bunut and Pulong Tau National Parks. *Faunistic Studies in Southeast Asian and Pacific Island Odonata* 36: 1-94.

**Steinhoff, P. O. M.**; Warfen, B.; Voigt, S.; Uhl, G.; Dammhahn, M. (2020): Individual differences in

risk-taking affect foraging across different landscapes of fear. *Oikos* 129 (12): 1891-1902.

**Steinhoff, P. O. M.**; Uhl, G.; Harzsch, S. & Sombke, A. (2020): Visual pathways in the brain of the jumping spider *Marpissa muscosa*. *Journal of Comparative Neurology* 528: 1883–1902.

Kompier, T.; Dow, R. A. & **Steinhoff, P. O. M.** (2020): Five new species of *Coelliccia* Kirby, 1890 from Vietnam (Odonata: Platycnemididae), and information on several other species of the genus. *Zootaxa* 4766: 501–538.

**Steinhoff, P. O. M.**; Ahmad, R.; Butler, S. G.; Choong, C. Y.; Dow, R. A. & Reels, G. T. (2019): Odonata of Gunung Mulu National Park in Sarawak, Malaysian Borneo. *International Dragonfly Fand Report* 141: 1-50.

Dow, R. A.; Butler, S. G.; Reels, G. T.; **Steinhoff, P. O. M.**; Stokvis, F. R. & Unggang, J. (2019): Previously unpublished Odonata records from Sarawak, Borneo, part IV: Bintulu Division including the Planted Forest Project and Similajau National Park. *Faunistic Studies in Southeast Asian and Pacific Island Odonata* 27: 1-66.

Reim, E.; Eichhorn, D.; Roy, J. D.; **Steinhoff, P. O. M.** & Fischer, K. (2019): Nutritional stress reduces flight performance and exploratory behavior in a butterfly. *Insect Science*

**Steinhoff P.O.M.**, Liedtke J., Sombke A., Schneider J.M., Uhl G. (2018): Early environmental conditions affect the volume of higher-order brain centers in a jumping spider. *Journal of Zoology* 304: 182–192

**Steinhoff P.O.M.** & Uhl G. Populärwissenschaftlicher Blog-Eintrag zum Artikel: <https://jzoblog.wordpress.com/2017/11/22/early-environmental-conditions-affect-the-volume-of-higher-order-brain-centers-in-a-jumping-spider/>

**Steinhoff P.O.M.**, Sombke A., Liedtke J., Schneider J.M., Harzsch S., Uhl G. (2017): The synganglion of the jumping spider *Marpissa muscosa* (Arachnida: Salticidae): insights from histology, immunohistochemistry and microCT analysis. *Arthropod Structure & Development* 46: 156-170

Böhm F., Brückner J., Eichhorn D., Geiger R., Johl B., Kahl S., Kleudgen I., Köhler K., Kreifelts V., Metschke K., Meyer M., Richter A.-C., Schulze B., Stecker R.-M., **Steinhoff P.O.M.**, Winter M. & Fischer K. (2016): Cloud cover but not artificial light pollution affect the morning activity of wood pigeons. *Ornis Fennica* 93: 246–252

Butler, S., **Steinhoff, P.O.M.**, & Dow, R.A. (2016): Description of the final instar larva of *Acrogomphus jubilaris* Lieftinck, 1964 (Odonata, Gomphidae), with information on the distribution of *Acrogomphus* in Borneo. *Zootaxa* 4184(2): 367–375

Burner, R. C., Chua, V. L., Brady, M. L., Van Els, P., **Steinhoff, P. O.M.**, Rahman, M. A., Sheldon, F. A. (2016): An Ornithological Survey of Gunung Mulu National Park, Sarawak, Malaysian Borneo. *The Wilson Journal of Ornithology* 128(2): 242–254

**Steinhoff, P.O.M.**, Butler, S. & Dow, R.A. (2016): Description of the final instar larva of *Orthetrum borneense* Kimmins 1936 (Odonata, Libellulidae), using rearing and molecular methods. *Zootaxa* 4083 (1): 099–108

**Steinhoff, P.O.M.** & Uhl, G. (2015): Taxonomy and nomenclature of some mainland South-East Asian *Coeliccia*-species (Odonata, Platycnemididae), using microCT analysis. *Zootaxa* 4059 (2): 257–276

Mouginot, P., Prügel, J., Thom, U., **Steinhoff, P.O.M.**, Kupryjanovicz, J., Uhl, G. (2015): Securing paternity by mutilating female genitalia in spiders. *Current Biology* 25: 1–5

**Steinhoff, P. O.M.** (2015): Results of Odonata larval rearing in the Gunung Mulu National Park, Sarawak, Malaysia from April to August 2014. *IDF Report* 78: 1-11

**Steinhoff, P. O.M.** & Do, M. C. (2013): Notes on some *Coeliccia* species from Vietnam. *Odonatologica* 42(4): 337-347

**Steinhoff, P.** (2012): Records of Odonata from Phong Nha-Ke Bang National Park. *Entomologie Heute* 24: 37-49

#### Talks and Posters

---

- 2022 Biopsychology Research Colloquium of the Biopsychology Department at the University Bochum, Germany. Invited Talk “Comparative brain anatomy and neuroplasticity in spiders“
- 2022 ANN (Arthropod-Neuro-Network) satellite symposium of the 114. annual meeting of the German Zoological Society (DZG), Bonn, Germany. Talk “Anatomy of the visual system for motion processing in the brains of cursorial and stationary hunting spiders“
- 2022 Zoological Symposium, University Greifswald, Germany. Talk on the occasion of the Kämpfe-publication price "Visual pathways in the jumping spider brain"
- 2021 113. annual meeting of the der German Zoological Society (DZG), Würzburg, Germany (online meeting). Talk “Analysis of the neural substrate for visual motion processing in cursorial and stationary hunting spiders“
- 2021 32. European Congress of Arachnology, Greifswald, Germany (online meeting). Talk “Comparative anatomy of the visual system for motion processing in the brains of cursorial and stationary hunting spiders“
- 2020 Seminar Evolution and Ecology (Evolution and Ecology Seminar), University Tübingen, Germany. Invited talk "Lifestyle matters: Functional role and plasticity of brain areas in spiders"



- 2019 Neuroethologisches Satellitenmeeting der 112. Jahrestagung der Deutschen Zoologischen Gesellschaft (DZG), Jena, Germany. Talk "Lifestyle matters: Brain morphology in cursorial and stationary hunting spiders"
- 2019 TierEcology Seminar Universität Potsdam, Germany. Eingeladener Talk "Function and plasticity of brain areas in spiders"
- 2019 Perspektiven der Invertebratenmorphologie (Perspectives in Invertebrate Morphology), Hiddensee Symposium, Hiddensee, Germany. Talk "Function and plasticity of brain areas in spiders"
- 2019 21. Internationaler Kongress für Arachnologie (International Congress of Arachnology (ICA)), Christchurch, Neuseeland. Talk "Complex integration of visual information: The secondary eye pathway of the jumping spider brain"
- 2019 21. Internationaler Kongress für Arachnologie (International Congress of Arachnology (ICA)), Christchurch, Neuseeland. Poster presentation "Lifestyle matters: Brain morphology in stationary and cursorial hunting spiders"
- 2019 Workshop "Spider trait network" beim 21. Internationalen Kongress für Arachnologie (International Congress of Arachnology (ICA)), Christchurch, Neuseeland. Talk "Building a chelicerate brain database"
- 2018 Zoologisches Kolloquium, Universität Greifswald, Germany. Talk zur Verleihung des Master-Arbeits Preises "Anatomy and plasticity of higher integrating neuropils in a jumping spider"
- 2018 6. GOEvol Tagung "Biology of Sensation", Göttingen, Germany. Poster presentation "Lifestyle matters: Brain morphology in cursorial and stationary hunting spiders"
- 2018 111. Jahrestagung der Deutschen Zoologischen Gesellschaft (DZG), Greifswald, Germany. Talk "Complex integration of visual information: The secondary eye pathway of the jumping spider brain"
- 2018 Arthropoden Neuro-Netzwerk (Arthropod Neuro-Network (ANN)) Tagung, Altleiningen, Germany. Talk "Anatomy and plasticity of higher-order neuropils in a jumping spider"
- 2017 110. Jahrestagung der Deutschen Zoologischen Gesellschaft (DZG), Bielefeld, Germany. Talk "Living in caves: A comparative morphological analysis of the central nervous system in *Pinelema* spiders (Telemidae)"
- 2017 30. Europäischer Kongress für Arachnologie (European Congress of Arachnology), Nottingham, UK. Talk "Living in caves: A comparative morphological analysis of the central nervous system in *Pinelema* spiders (Telemidae)"

- 2017 36. Jahrestagung der Gesellschaft deutschsprachiger Odonatologen (GdO), Berlin, Germany. Talk "Chasing the Unknown: Die Rolle von Larven in der SO-Asiatischen LibellenTaxonomy"
- 2016 Ranger & Angestellten Meeting, Gunong Mulu Nationalpark, Sarawak, Malaysia. Talk „Tying up loose ends: Odonatology in South-East Asia“
- 2016 109. Jahrestagung der Deutschen Zoologischen Gesellschaft (DZG), Kiel, Germany. Poster presentation "Neuroanatomy of the jumping spider *Marpissa muscosa*"
- 2016 20. Internationaler Kongress für Arachnologie (International Congress of Arachnology (ICA)), Golden, USA. Talk "Neuroplasticity in a jumping spider"
- 2016 20. Internationaler Kongress für Arachnologie (International Congress of Arachnology (ICA)), Golden, USA. Poster presentation "Neuroanatomy of the jumping spider *Marpissa muscosa*"
- 2016 17. Jahrestagung der Gesellschaft für Biologische Systematik (GfBS), München, Germany. Poster presentation "MicroCT Analysis as a tool for taxonomic research on Odonata"
- 2016 17. Jahrestagung der Gesellschaft für Biologische Systematik (GfBS), München, Germany. Poster presentation "Chasing the Unknown: The role of larvae in SE-Asian Odonata taxonomy, with case studies of larva descriptions from Borneo"
- 2015 108. Jahrestagung der Deutschen Zoologischen Gesellschaft (DZG), Graz, Österreich. Poster presentation "Micro-CT Analysis as a tool for taxonomic research on Odonata"
- 2015 108. Jahrestagung der Deutschen Zoologischen Gesellschaft (DZG), Graz, Österreich. Talk "Neuroplasticity in a jumping spider"
- 2015 29. Europäischer Kongress für Arachnologie (European Congress of Arachnology), Brno, Tschechien. Talk "Neuroplasticity in a jumping spider"
- 2015 Zoologisches Symposium, Universität Greifswald, Germany. Talk "Neuroplasticity in a jumping spider"
- 2015 34. Jahrestagung der Gesellschaft deutschsprachiger Odonatologen (GdO), Braunschweig, Germany. Talk "Die MicroCT-Analyse als Werkzeug in der LibellenTaxonomy"
- 2014 Ranger & Angestellten Meeting, Gunong Mulu Nationalpark, Sarawak, Malaysia. Talk „Dragonflies and Odonatology in South-East Asia“
- 2013 Internationaler Kongress für Odonatologie (International Conference on Odonatology (ICO)), Freising, Germany. Poster presentation "Zygoteran genital structure: an insight"

2011 Westdeutscher Entomologentag, Düsseldorf, Germany. Talk “Libellen in Vietnam“

## 5. Acknowledgements

I am very grateful for the past years and all the people I met and interacted with during the pursuit of my PhD. They are too many to name them all individually, but whoever reads this section rather likely received an individual mention.

First and foremost, I want to express my gratitude to my supervisor, Gabriele Uhl. Thank you for being such a great mentor and for showing me what science is about. I will keep the years in the “AG Uhl” in my fondest memories. Thank you to all the wonderful members of the Uhl group, past and present, that I had the pleasure to meet. Thank you Monica Sheffer for being the best office mate I could have wished for. It was fantastic to start the PhD together with you and be inspired by your drive and enthusiasm. I want to thank Pierick Mougnot, for philosophy, sport and a little bit of stats; Anja Junghanns for much laughter and your help with everything spider-faunistic-taxonomic; Shou-Wang Lin for invaluable help with microCT reconstructions and for being such a friendly and supportive colleague; Lenka Sentenska for helping out whenever I needed it, gaming, traveling and generally making the whole thing more fun. I also want to thank my new office mates Carolina Ortiz Movliav and Morgan Oberweiser for joining me for the last stretch, enduring my complaints and creating such a friendly, sugar-rich atmosphere. Thank you Monika Eberhard for being a wonderful colleague and for your expert help with the recordings of vibrations. I want to thank Tim Dederichs for a great time- our expeditions into different music genres were always mood-lightening. My gratitude also to Michael “Theo” Schmitt, Peter Michalik and Carsten Müller for always having an open ear and being open for critical discussions. I also want to express my gratitude to Heidi Land: I don’t know where to start really, you helped me out with so many things from office to the lab to the spiders. Thank you for being patient with me and my chair-behavior.

I had the great pleasure to not only be associated with one working group, but with two. Thank you very much Steffen Harzsch, for being a great Co-supervisor and hosting me in your lab. Thanks to all the members of the Harzsch group that I met over the past few years for a great time. I want to mention in particular Georg Brenneis, Marie Hörnig, Jakob Krieger, Matthes Kenning, Katja Kümmerlen and Frederice Hilgendorf.

It may be unusual, but I have to express special thanks to a botanist: Brian Schulze, you are the most “ready to help” person I know. Thank you for helping with your technical expertise whenever needed and for not raising your eyebrows to my frequent questions. Many thanks also to Stefan Bock, for help with MicroCT scanning. Thanks also to Kerstin Wulf for helping me with many tricky documents. I also want to thank my students, Bennet Warfen, Sissy Voigt and Clara Haas, for putting up with my ideas and being so enthusiastic about their projects.

I want to express my gratitude to Melanie Dammhahn: You opened a new field of science for me and helped to shape a substantial part of this thesis. I am very grateful to Andy Sombke for training me in neuroanatomical methods, assisting me whenever I needed help and for countless

discussions on the details of spider neuroanatomy. A special shoutout to Georg Brenneis (second mention): This thesis would have been very different without your continuous critical view (or should I say nagging?) on everything, but also your support and advice. I learned a lot from you, Pinky.

Jonas Linke and Georg Brenneis read and commented on the first draft of the text, thank you very much for fighting through it.

Lastly I want to thank my family. To my parents, who always trusted me with my decisions and have supported me throughout this endeavor. To my wife Katalin, for doing the difficult work and still being so incredibly supportive. You are the reason why things are trotzdem easy. To my son Friedrich: You may not know it now, but because of you, the last year was the best of all of them. You enabled me to think differently and reconsider many things. That's a great achievement for such a small person.